

https://dspace.org/

Purification of platinum group metals process stream using saccharomyces cerevisiae waste yeast biomass

Oke, Doris Oluwafunmilayo

2015-04-28
http://hdl.handle.net/10539/17534

Downloaded from a DSpace repository. https://dspace.org/



PURIFICATION OF PLATINUM GROUP METALS PROCESS STREAM USING SACCHAROMYCES CEREVISIAE WASTE YEAST BIOMASS

Doris Oluwafunmilayo Oke

A dissertation submitted to the Faculty of Engineering and the Built Environment, University of Witwatersrand, Johannesburg, in fulfillment of the requirements for the degree of Master of Science in Engineering.

Johannesburg, 2014

DECLARATION

I declare that this dissertation is my own unaided work. It is being submitted to the degree of Master of Science in Engineering to the University of the Witwatersrand, Johannesburg. It has not been submitted before for any other degree or examination in any other University.



Doris Oke

10th day of December, 2014

ABSTRACT

The removal of platinum group metals (PGMs) from dilute process streams is essential due to their economic value and the increasing need to recycle process water. This study presents the removal of Pd (II), Ir (III), Pt (II), Rh (III) and Au (III), from synthetic multicomponent aqueous solution in a batch system using untreated, NaOH treated and ethanol treated Saccharomyces cerevisiae waste biomass obtained as a byproduct of brewery fermentation industry. A two-level four factor full-factorial experimental design and analysis was successfully employed for the testwork. The effects of pH, initial metal ion concentration, temperature and biomass dosage on PGMs removal were assessed using the design of experiment (DOE) approach. Solution pH and initial metal concentration were found to be statistically significant for the adsorption of PGMs tested. Ethanol treated biomass gave the highest adsorption uptake for all the PGMs tested. The sorption uptake is in the order of $Au^{3+}>Pd^{2+}>Pt^{2+}>Ir^{3+}>Rh^{3+}$. The overall maximum sorption attained was 99.9% for Au (III), 91% for Pt (II), 99.5% for Pd (II), 81.9% for Ir (III) and 81.1% for Rh (III).

The desorption of the tested PGMs from the loaded biomass was carried out using different concentrations of hydrochloric acid, sulphuric acid, thiourea and hydrochloric – thiourea solution. Effective desorption was obtained using acidified 0.1M thiourea which can be explained as due to both stable complex formation and the electrostatic interaction between some of the PGMs species and charged species from elution. The biosorbent was successfully regenerated and reused up to 5 cycles.

Equilibrium data for metal removal in the batch study conformed well to the Langmuir isotherm except for the fitting of Pd (II) which complied with Freundlich isotherm model. Kinetic data were fitted to Lagergren first –order, pseudo second – order, Intraparticle diffusion and Elovich models. The kinetic parameters, rate constants, equilibrium adsorption capacities and related correlation coefficients for each kinetic model were calculated and discussed. Consequently, the adsorption of

Pd (II), Ir (III), Pt (II), Rh (III) and Au (III) were found to follow a pseudo- second order kinetic model suggesting chemisorption of all the tested PGMs.

In addition, column studies were conducted for the purification of real dilute process stream from Impala Platinum using ethanol treated yeast immobilized on Plaster of Paris (POP). These studies focused not only on the PGMs but base metals and other trace elements present in the dilute solution. The breakthrough curve for most of the element do not resemble those of an ideal breakthrough curve due to the complexity of the solution and the normalized concentration (C/C_o) for most of the metals in solution remained high even in the early stages of treatment when the sorbent material was most pristine. Generally, the affinity of the sorbent for the elements considered follow the order Pd^{2+}> SO_4^{2-}>Te^{2+}>Pt^{2+}>Ir^{3+}>Ni^{2+}>Cl^->.Ru^{3+}>Se^{2+}> Na^+.

The data from the column studies was fitted into Adam-Bohart and Thomas model and the data conformed well to Adam – Bohart model. In general, ethanol treated S.cerevisiae yeast biomass appeared to be a good sorbent for the effective removal of PGMs but the complexity of the industrial wastewater requires that pretreatment steps be taken to reduce chloride and sulphate concentration in the solution before this process can be applied successfully.

PUBLICATIONS AND PRESENTATIONS

Journal Publications

1. Oke, D; Ndlovu, S; Sibanda, V; 2014. Removal of Platinum group metals from dilute process streams: Identification of influential factors using DOE approach. Journal of Environmental Chemical Engineering 2, pp.1061-1069.

Conference Proceedings

1. Oke, D; Ndlovu, S; Sibanda, V; 2013. The removal of Platinum group metals from dilute process streams. SAMMRI/MMI Hydrometallurgy Symposium, University of Cape Town, South Africa, 2nd – 6th August, 2013.

DEDICATION

This dissertation is dedicated to God Almighty, you are the source and the help of my life and l will forever be grateful to you. To my loving and ever caring husband, Ibrahim and my lovely children, Ireoluwa Samuel and IranlowoOluwa Emmanuel (you are mummy's friends), thank you for your support, encouragement and for believing in me. You are the best I ever have and I will forever love you.

ACKNOWLEDGEMENTS

I wish to express my special gratitude to my supervisor Prof. S. Ndlovu for her support, insight and technical guidance throughout this work. My sincere gratitude goes to my co-supervisor Dr. V. Sibanda for his suggestions and technical support.

My special love goes to my parent, Mr. and Mrs. Remi Oke for their full support even when everything seems impossible, you are the best parent in the whole world and you will live to eat the fruit of your labor. To my mother in-law, Mrs. Mary Musayayi for her understanding and for the values you instill in my husband, l love you mummy. My deep appreciation also goes to my grandmother, Mrs. Olajiire Esther Akintaro, thank you for taking care of me from infant and the unending love you still show to me, I can never forget you maami and to my siblings, Temilade, Bisola and Babatunde, it is a privilege to have you and l cherish you all.

South African Breweries is gratefully acknowledged for the yeast used in this study.

Dr Rodrick Lamya of Impala platinum is gratefully acknowledged for the PGM dilute stream used in this study.

Many people have contributed directly or indirectly to this work, l will like to mention some of them by name: Dr Geoffrey Simate, Mr. Alan Shemi, Fortunate Moyo, Dr Phillip Oladijo, Xolani, Doctor Mbense, many thanks for your support.

To my colleagues in metal extraction and recovery group: Lizzy Seepe, Glawdis Tshofu, Dominique Kyembo and Lerato Lekhanya for the team work and for making the environment conducive throughout the research period.

Lastly, to all my family members, thank you for being there for me in one way or the other, l love you all.

Table of Contents

DECLARATION……ii

ABSTRACT……...…iii

PUBLICATIONS AND PRESENTATIONS…….v

DEDICATION……...vi

ACKNOWLEDGEMENTS……...….vii

LIST OF FIGURES……...…xiv

LIST OF TABLES…….....xix

CHAPTER ONE……..1

INTRODUCTION……...1

1.1 General Introduction……..…..….1

1.2 Problem statement……...……4

1.3 Objectives……4

1.4 Research Methodology…….…….....5

1.5 Dissertation Lay Out…….…...…....5

CHAPTER TWO…….....……7

LITERATURE REVIEW……7

2.1 Water: A Sustainable Resource……...7

2.2 Water in Industry……...10

2.3 PGM Mining and Refining Process……...….11

2.3.1 Physical and Chemical Properties of PGMs.....17

2.4 Conventional Methods of Metal Removal from Wastewater……....19

2.5 Biosorption Process……..…....25

2.5.1 Physical Adsorption/ Ion Exchange 28

2.5.2 Micro-precipitation……..…29

2.5.3 Biosorbents.....29

2.6 Factors Affecting Biosorption…….…..……..……31

2.7 Adsorbate – Adsorbent Contactors……...…….35

2.7.1 Batch Process…….…..……35

2.7.2 Column Biosorption Studies……36

2.8 Biomass Immobilization……..……..38

2.9 Biosorption Process Modelling …….....39

2.9.1 Kinetic Modelling……..……...……....39

2.9.2 Biosorption Isotherms…..…….……..……42

*2.9.3 Mathematical Models in Fixed bed Column.……..……48

2.10 Desorption and Regeneration…….....50

CHAPTER THREE……51

MATERIALS AND METHODS…….. ....…51

3.1 Introduction…….……..…….51

3.2 Materials……..……..……..…51

3.2.1 Biosorbent…….……51

3.2.2 Dilute Process Solution……51

3.2.3 Reagents……...51

3.2.4 Plaster of Paris (POP)…….…....51

3.3 Experimental methods……....52

3.3.1 Chemical Treatment of Yeast Cells……..……..…52

3.3.2 Preparation of stock solution……52

3.3.3 Batch adsorption studies……..……52

3.3.4 Design of Experiments……..……53

3.3.5 Equilibrium Studies……..……54

3.3.6 Adsorption- desorption Experiments……54

3.3.7 Yeast immobilization in Plaster of Paris…….…….55

3.3.8 Characterisation of PGMs industrial process dilute stream……...55

3.3.9 Column Experiments…….……...……56

3.3.10 Column model……58

3.3.11 Kinetic models……...…….……59

3.4 Analytical Techniques…….…….…….60

3.4.1 Determination of the surface functional group……60

3.4.2 Determination of the pH of the point of Zero Charge (PZC)……...60

3.4.3 Determination of surface area and pore structure……..…….60

3.4.4 Surface Morphology……...……...……60

3.4.5 Determination of metal ion concentration……...……....61

3.4.6 Determination of total solid (TS), total suspended solid (TSS) and total dissolved solid (TDS)…….……61

3.4.7 Determination of chemical oxygen demand (COD)…….……...62

CHAPTER FOUR……..……63

RESULTS AND DISCUSSIONS……..……63

4.1 Characterization of Biosorbent……...63

4.1.1 Fourier transform infrared spectroscopy (FTIR)……...……..63

4.1.2 BET Analysis……67

4.1.3 Determination of Point of Zero Charge……...68

4.1.4 Surface Morphology…….70

4.2 Batch Studies……..……72

4.2.1 Effect of Biomass pretreatment……72

4.2.2 Kinetics…….76

4.3 Identification of Influential Factors……..……..83

4.3.1 Introduction……..83

4.3.2 Experimental Plan for Statistical Design of Experiments (DOE)…..…..83

4.3.3 Methodology for Data Analysis……...…….85

4.3.4 Significant Factors…….……..86

4.3.5 Modeling the significant effects for adsorption prediction…..…..…..92

4.3.6 Influence of factors on Adsorption……...93

4.4 Equilibrium Isotherms…….……106

4.5 Adsorption –Desorption Cycles……..…….107

4.6 Column Studies……..……..112

4.6.1 Characterisation of PGMs dilutes process streams……..….112

4.6.2 Analysis of chemical oxygen demand (COD)……113

4.7 Column Experiment…….....……..114

4.7.1 Effects of flow rates……...…….115

4.7.2 Effect of Bed depths……127

4.7.3 Evaluation of kinetic models…….....……...139

4.7.4 Summary.....144

CHAPTER FIVE…….…….147

CONCLUSIONS AND RECOMMENDATIONS……...147

5.1 Conclusions……..……147

5.1.1 Introduction.....147

5.1.2 Effect of chemical pretreatment.....148

5.1.3 Identification of Influential Factor Tests.....148

5.1.4 Kinetic Studies.....149

5.1.5 Adsorption – Desorption Cycles.....150

5.1.6 Column Study.....151

5.2 Recommendations…….152

REFERENCES……154

APPENDICES.....170

APPENDIX A.....170

APPENDIX B.....177

APPENDIX C.....181

APPENDIX D.....191

APPENDIX E.....199

APPENDIX F.....200

LIST OF FIGURES

Figure 1.1: Dissertation Layout……. .6

Figure 2.1: Availability of water per capital in South Africa……. 9

Figure 2.2: Overview of the PGM production process: from mine to market place…….....13

Figure 2.3: Overview of PGM refining process…… 15

Figure 2.4: An overview of Impala's precious metals refinery at Springs, South Africa.....16

Figure 2.5: Schematic representation of breakthrough curve…….37

Figure 2.6: Graphical representation of Langmuir isotherm model……...44

Figure 2.7: Graphical representation of Freundlich isotherm model…….46

Figure 2.8: Graphical representation of BET isotherm model……...47

Figure 3.1: Experimental set up for column study…….57

Figure 4.1: IR spectra of untreated yeast..……..64

Figure 4.2: IR spectra of ethanol treated yeast……...……65

Figure 4.3: IR spectra of NaOH treated yeast…..……..66

Figure 4.4: Comparison of IR spectra of the three biomasses…...…….67

Figure 4.5: Mass titration results for untreated yeast……...……...69

Figure 4.6...: Mass titration results for ethanol treated yeast……..70

Figure 4.7: SEM of waste *S.cerevisiae* (a) original yeast (b) ethanol treated (c) sodium hydroxide treated (d) ethanol treated after adsorption…….....71

LIST OF FIGURES (continued)

Figure 4.8: Effect of biomass pretreatment on the adsorption of Pt (II)……..……...73

Figure 4.9: Effect of biomass pretreatment on the adsorption of Au (III)……..…....74

Figure 4.10: Effect of biomass pretreatment on the adsorption of Pd (II)……..74

Figure.4.11: Effect of biomass pretreatment on the adsorption of Rh (III)……....75

Figure.4.12: Effect of biomass pretreatment on the adsorption of Ir (III)……..75

Figure 4.13: Effect of adsorption time on the uptake of Pt (II), Pd (II), Au (III), Rh (III) and Ir (III) in a single metal ion system……..77

Figure 4.14: Pseudo-first-order kinetic plots for the adsorption of Pt (II), Pd (II), and Au (III) on S. cerevisiae waste biomass…….80

Figure 4.15: Pseudo-first-order kinetic plots for the adsorption of Ir (III) and Rh (III) on S. cerevisiae waste biomass……...80

Figure 4.16: Pseudo-second-order kinetic plots for the adsorption of Pt (II), Pd (II), and Au (III) on S. cerevisiae waste biomass……...81

Figure 4.17: Pseudo-second-order kinetic plots for the adsorption of Ir (III) and Rh (III) on S. cerevisiae waste biomass……...81

Figure 4.18: Intra particle diffusion model for the adsorption of Pt (II), Pd (II), Au (III), Ir (III) and Rh (III) on *S. cerevisiae* waste biomass……...82

Figure 4.19: Elovich model for the adsorption of Pt (II), Pd (II), Au (III), Ir (III) and Rh (III) on *S. cerevisiae* waste biomass……..82

Figure 4.20: Normal plots of effects of main factors and factors interaction for Gold from the 2^4 full factorial designs…….88

Figure 4.21: Normal plots of effects of main factors and factors interaction for Iridium from the 2^4 full factorial designs……....89

LIST OF FIGURES (continued)

Figure 4.22: Normal plots of effects of main factors and factors interaction for palladium from the 2^4 full factorial designs……...90

Figure 4.23: Normal plots of effects of main factors and factors interaction for platinum from the 2^4 full factorial designs…….91

Figure 4.24: Normal plots of effects of main factors and factors interaction for Rhodium from the 2^4 full factorial designs……91

Figure 4.25: Main effect plot of pH on Au (III)…….94

Figure 4.26: Main effect plot of initial metal ion concentration on Au (III) …….95

Figure 4.27: Interaction plot of pH and initial metal ion concentration on Au (III)

……....96

Figure 4.28: Main effect plot of initial metal ion concentration on Ir (III)……97

Figure 4.29: Main effect plot of pH on Ir (III) ……..97

Figure 4.30: Main effect plot of pH on Pd (II)……..…….98

Figure 4.31: Main effect plot of initial metal ion concentration on Pd (II)……...….99

Figure 4.32: Interaction plot of pH and initial metal ion concentration on Pd (II)…….100

Figure 4.33: Main effect plot of initial metal ion concentration on Pt (II)…...…...101

Figure 4.34: Main effect plot of pH on Pt (II)……..……...……101

Figure 4.35: Main effect plot of pH on Rh (III)…….…….102

Figure 4.36: Main effect plot of initial metal ion concentration on Rh (III)..……102

LIST OF FIGURES (continued)

Figure 4.37: Effect of pH on the adsorption of Pt (II), Pd (II), Au (III), Ir (III) and Rh (III) on S. cerevisiae waste biomass……...104

Figure 4.38: Adsorption efficiency cycle of the yeast biomass for Au (III), Pd (II), Pt (II), Ir (III) and Rh (III)…….……..110

Figure 4.39: Desorption efficiency cycle…..……...110

Figure 4.40: Breakthrough curve for platinum adsorption at different flow rates …….….117

Figure 4.41: Breakthrough curve for palladium adsorption at different flow rates…….....118

Figure 4.42: Breakthrough curve for iridium adsorption at different flow rates …….….119

Figure 4.43: Breakthrough curve for ruthenium adsorption at different flow rates……..120

Figure 4.44: Breakthrough curve for nickel adsorption at different flow rates..…..121

Figure 4.45: Breakthrough curve for selenium adsorption at different flow rates…….....122

Figure 4.46: Breakthrough curve for tellurium adsorption at different flow rates……..123

Figure 4.47: Breakthrough curve for sodium adsorption at different flow rates……..124

Figure 4.48: Breakthrough curve for sulphate adsorption at different flow rates……..125

Figure 4.49: Breakthrough curve for platinum at different bed depth……....127

Figure 4.50: Breakthrough curve for palladium at different bed depth…….…….128

Figure 4.51: Breakthrough curve for iridium at different bed depth……..…….129

Figure 4.52: Breakthrough curve for ruthenium adsorption at different bed depth.....130

Figure 4.53: Breakthrough curve for nickel adsorption at different bed depth…….131

Figure 4.54: Breakthrough curve for selenium adsorption at different bed depth…….....132

Figure 4.55: Breakthrough curve for tellurium adsorption at different bed depth…….....133

Figure 4.56: Breakthrough curve for sodium adsorption at different bed depth…….133

Figure 4.57: Breakthrough curve for sulphate adsorption at different bed depth….....134

LIST OF TABLES

Table 2.1: Physical and chemical properties of PGMs……...18

Table 2.2: Performance characteristics of some physico-chemical heavy metal removal and recovery technologies……....20

Table 3.1: Composition of PGMs sample.....56

Table 3.2: Experimental condition for column studies……...57

Table 4.1: Physicochemical properties of *Saccharomyces cerevisiae* yeast……...68

Table 4.2: Coefficient of pseudo-first- order, pseudo-second- order kinetic models and intra- particle diffusion model…….78

Table 4.3: Calculated values of α and β for the Elovich Model…..……79

Table 4.4: Experimental factors and levels for controlled factors……..85

Table 4.5: PGMs Adsorption results for the 2^4 full factorial design……..87

Table 4.6: Summary of the significant factors on the adsorption of Au (III), Pd (II), Pt (II), Rh (III) and Ir (III).....92

Table 4.7: Dominant species of Au (III), Pd (II), Pt (II), Rh (III) and Ir (III) under the experimental condition studied…….105

Table 4.8: Linear Langmuir and Freundlich isotherm parameters for Au (III), Pd (II), Pt (II), Rh (III) and Ir (III) sorption by *S. cerevisiae* waste yeast…….107

Table 4.9: desorption data for Au (III), Pd (II), Pt (II), Rh (III) and Ir (III)…….108

Table 4.10: Ionic radius and Electronegativity of the tested PGMS…….111

Table 4.11: Summary of the physico-chemical characterization of the PGMs process streams….....113

Table 4.12: Discharge limits for PGMs and some base metals in wastewater…….116

Table 4.13: Breakthrough time at different flow rates…….126

Table 4.14: Breakthrough time at different bed depths……....135

Table 4.15: Adsorption breakthrough data at different flow rates……....138

Table 4.16: Adsorption breakthrough data at different bed depth……....139

Table 4.17: Adam-Bohart model parameters at different bed depth……140

Table 4.18: Adam-Bohart model parameters at different flow rates……141

Table 4.19: Thomas model parameters at different bed depth……..143

Table 4.20: Thomas model parameters at different flow rates…….144

Table 4.21: Summary of the effect of biomass pre-treatment on the adsorption of Pt (II), Au (III), Pd (II), Ir (III) and Rh (III).....145

CHAPTER ONE

INTRODUCTION

1.1 General Introduction

Platinum, palladium rhodium, iridium, osmium, and ruthenium constitute the platinum group metals (PGMs). These metals are identified as rare elements and platinum is known to be the most common with an abundance of about 10^{-6}% whereas the others have abundances of the order of 10^{-7}% of the earth's crust (Mack et al., 2008). In all the associated ore deposits, the value of PGMs is in grams per ton. PGMs are commonly associated with major base metals as well as gold and silver. PGMs together with gold and silver form the family of precious metals (Glaister and Mudd, 2010).

Precious metals are widely used as catalyst in various industries, agriculture and pharmaceutical industry because of their specific physical and chemical properties. These metals have unique properties of corrosion resistance, heat resistance, high melting point, high mechanical strength, good ductility and catalytic activity (Mack, 2005). Economically, the precious metals are historically important as currency and remain important as investment commodities. Gold (Au), silver (Ag), platinum (Pt) and palladium (Pd) are internationally recognized as a form of currency under ISO4217 (Das, 2010).The global production of PGMs is dominated by South Africa due to its large economic PGM resources in the Bushveld region, while other countries such as Russia, Canada, Zimbabwe and the United States also play an important role (Glaister and Mudd, 2010).

The steady increase in demand for precious metals, especially platinum and palladium has resulted in the scale-up of metal extraction and refining operations worldwide (Mack et al., 2007).The discharge of PGMs wastewater is an environmental concern as well as a loss of unreclaimed water and valuable metals.

As a leading producer of PGMs with an already existing strong PGMs industrial base, it is in the interest of South Africa to recover and recycle the precious metals from secondary sources such as PGM wastewater within the country. This coupled with strict government regulations on environmental protection, the scarcity and growing demands for precious metals to be used in advanced technological applications makes it imperative to develop innovative methods for their recovery (Mack, 2005).

Conventional methods for the removal of low metal ion concentration from wastewater such as solvent extraction; chemical precipitation and ion exchange have been found to possess significant disadvantages. Prominent among the disadvantages are: incomplete metal removal, high capital costs, high reagent and/or energy requirements, and generation of toxic sludge or other waste products that require disposal (Goksungur et al., 2002; Alluri et al., 2007). A satisfactory process would be one that achieves the goal of metal recovery as well as wastewater purification at a relatively low cost and without the generation of large amounts of residual solids.

Thus, the search for new effective and economical technologies involving the removal of precious metals from waste waters has now shifted towards bio-sorption, a method that is based on the metal binding capacities of living microorganisms and biomass materials such as bacteria, fungi, yeast, algae, etc. generally termed as bio-sorbents (Aksu, 2005). Employing materials of biological origin allows the application of the knowledge available to the development of technology to treat metal and organic containing solutions. These bio-sorbents possess metal – sequestering properties capable of decreasing the concentration of metals ions in solution from parts per trillion to parts per billion (Wang and Chen, 2006). They can quickly and efficiently sequester dissolved metal ions out of dilute complex solutions. In addition to high efficiency, the advantages of bio-sorption when compared to the conventional methods include low operating cost, minimization of chemical and /or biological sludge volume to be handled (Alluri et al., 2007). Furthermore, bio-sorbents are environmentally friendly, biodegradable and cost effective when considering the possibility of bio-sorbents regeneration and water

recycle (Aksu, 2005). Moreover, various chemical or physical treatment processes can be carried out on the bio-sorbents to improve their functional group thereby increase their binding capacities.

Some biomaterials with high metal binding capacities have been identified in the past as potential alternatives to the existing metal removal technologies. Among these are bacteria (e.g. Bacillus subtillis), fungi (e.g. Rhizopus arrhizus), yeast (e.g. S.cerevisiae) and waste biomass from the fermentation and food industry (Alluri et al; 2007). For economic reasons, researchers have paid much attention to various by-products from the fermentation industry because they are produced in large quantities (Wang and Chen, 2006). Utilization of this biomass would serve both as a solution to the waste disposal problem as well as an economic source of biosorbents for industrial wastewater treatment. One such solid waste from the food and beverage industry is Saccharomyces cerevisiae. Investigations conducted by several researchers have demonstrated that Saccharomyces cersvisiae biomass can remove toxic metals, recover precious metals and clean radio-nuclides from aqueous solutions (Alluri et al., 2007; Wang and Chen, 2006; Park et al., 2008; Goksungur et al., 2003; Mack et al., 2008).

Although, Saccharomyces cerevisiae may have been considered as a mediocre biomass in the past, it is still an important biomaterial in biosorption studies because of its unique characteristics in comparison with other microorganisms used in metal removal (Nilanjana et al., 2008). However, very few studies on PGMs biosorption by this yeast are documented (Mack et al., 2008; Godlewska-Zylkiewicz and Kozlowska, 2005; Frazzoli et al., 2007; Godlewska-Zylkiewicz, 2008).In addition, information on the process optimization, scale up for industrial purposes, biomass estimation and economic analysis of the whole operation relative to other existing technologies is limited.

The focus of this research is to develop a process for the purification of wastewater from platinum industry for the purpose of metal recovery and water reclamation using ethanol and caustic treated saccharomyces cerevisiae biomass. A possible

viable system would employ fixed bed columns such as the ones used in conventional practice that use ion exchange resins or activated carbon. This would allow the treatment of large volumes of wastewater limited only by the biomass loading system. It would thus be necessary to develop a system in such a way that the regeneration of the biomass can allow for a large number of sorption cycles.

1.2 Problem statement

Although Saccharomyces Cerevisiae yeast has proven to adsorb PGMs from waste water using both batch and continuous processes and different immobilization materials have been used as support for this biomass, no published work is available on the treatment of PGMs dilute streams using saccharomyces cerevisiae immobilized on Plaster of Paris.

1.3 Objectives

The aim of this research is to develop a process for the purification of PGMs process stream using spent yeast of Saccharomyces Cerevisiae which will involve the immobilization of the yeast on Plaster of Paris. The process will also involve looking at the reaction kinetics, identification of and optimization of influential process parameters.

The specific objectives are:

- To investigate the use of saccharomyces cerevisiae biomass for the purification of PGM wastewater stream in batch and continuous process.
- To establish the process parameters and operating conditions such as temperature, pH, residence time and biomass dosage required for the optimum purification efficiency.
- To evaluate the process efficiency in terms of metal removal, chemical oxygen demand, etc. of the waste stream.
- To analyse the effect of chemical pretreatment on the adsorption capacity of the biomass
- To establish an adsorption kinetic model for the process under study.

- To establish the possibility of regeneration and re-use or beneficial disposal of the biomass.

1.4 Research Methodology

The research methodology for this study involved the following major tasks: Literature review, experimental design, laboratory testing, laboratory test data analysis, drawing conclusions from results, recommendations and documentation.

1.5 Dissertation Lay Out

This dissertation consists of five chapters including this chapter (Chapter One) that provides the motivation for the research, the problem statement, and the overall objective of this study. The layout is schematically represented in Figure 1.1.

Chapter Two is the literature review, which includes the general overview of water scarcity in the semi-arid region of the world, the general knowledge on biosorption processes and the overview of PGMs mining and refining process.

Chapter Three (experimental design) describes the materials and methods used in the study.

Chapters Four describes the laboratory tests and discussions of the findings.

Chapter Five concludes the dissertation with a summary of the findings and recommendation.

References to all articles used in the study are provided at the end of the dissertation. An appendix section provides relevant laboratory test results and other important data.

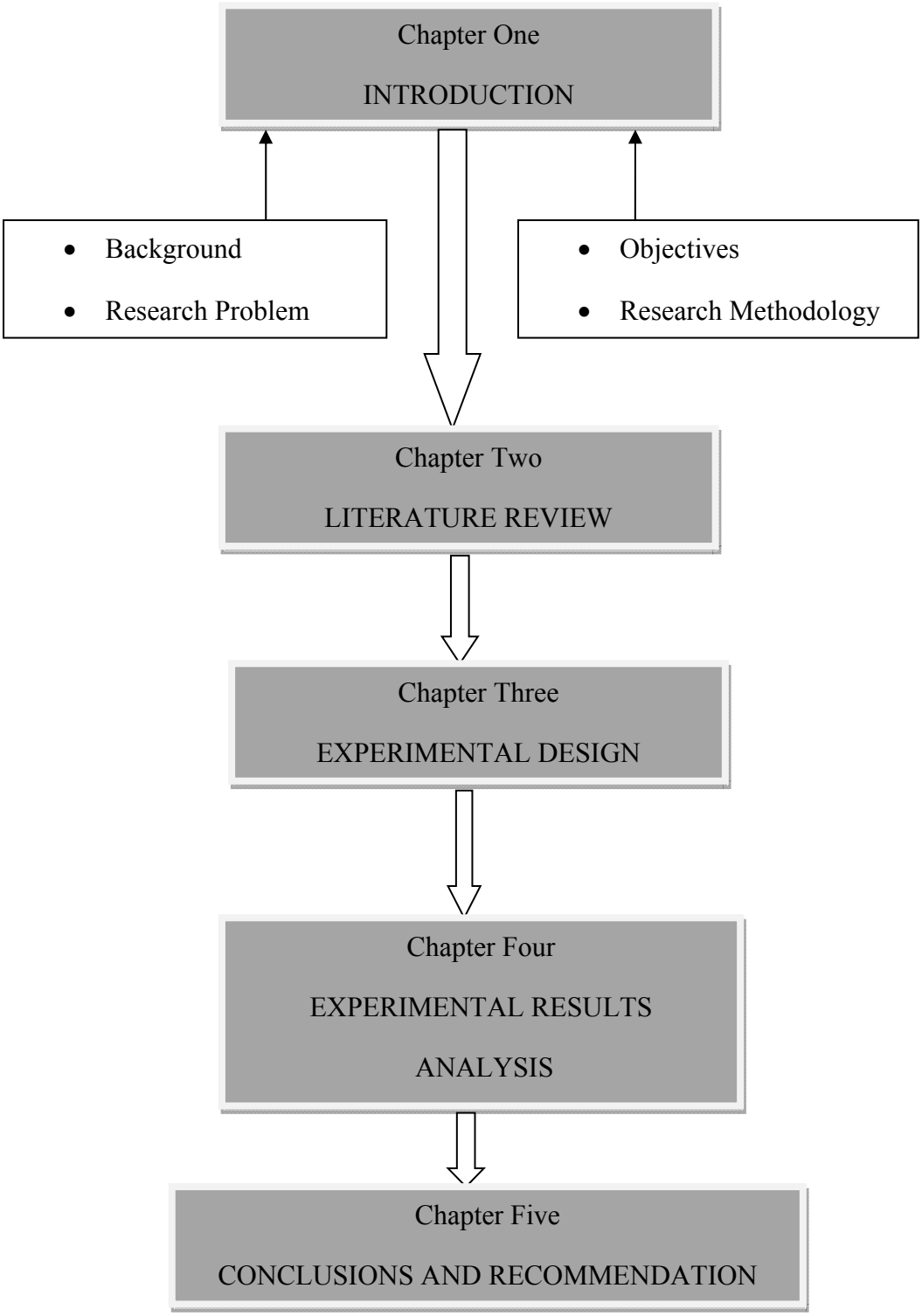


Figure 1.1: Dissertation Layout

CHAPTER TWO

LITERATURE REVIEW

2.1 Water: A Sustainable Resource

Water is the most common substance on earth covering almost three quarters of the planet's surface. The rain cycle-powered by the energy of the sun distributes water to the different areas of the planets. Water is a very vital resource for both social and economic growth therefore, it is very important to manage water according to the principle of sustainable development to counteract the combination of increasing economic development and environmental degradation. The constantly increasing degree of industrialization and urbanization, rising standard of living, increasing population growth and agricultural activities are strongly impacting on the use of available water sources and quality of water found therein. This exhaustive use of limited resources and energy by modern society implies a need for change in present and future urban water and waste water treatment (Holtzhausen, 2002).

Developing countries like South Africa are facing a greater problem because of moderate to high stresses on the fresh water resources, as large inequalities exist in the quantity and quality of water available to rural communities compared to that of the urban areas. Thus, appropriate management strategies need to be implemented to optimize the use of these water sources and efficient disposal of polluted water (Mack, 2005).

South Africa has an average rainfall of 450mm, compared with a world average of 860mm (Benhin, 2006). About 65% of the country receives less than 500mm per year, which is generally accepted as the minimum amount required for successful dry-land farming. About 21% of the country, mainly the arid west, receives less than 20mm per year (Benhin, 2006).

In South Africa, rainfall is unreliable and unpredictable. Large fluctuations in the average annual rainfall are the rule rather than the exception in most areas of the country. This uneven distribution of rainfall across the country with much of it higher in the east than in the west increases the problem of water supply. Major industries, mining and power generators account for large percentage of water usage in South Africa. These are found mainly in Mpumalanga, Limpopo and Gauteng provinces, which are highly populated due to the labour force required to run such industries and the resulting commercial and residential areas surrounding them. The result is a very high water demand by both industrial and domestic users in an area of generally low rainfall. “Equitable access to water, or to the benefits derived from using water, is critical to eradicating poverty and promoting growth. This is particularly important in South Africa, which is still facing significant inequalities in access to and use of water.” (DWAF, 2005). Numerous dams, storage facilities and inter-catchment transfer schemes have been developed to alleviate the inequalities between the eastern and western areas of the country. Thus, South Africa heavily reliant on surface water resources and with evaporation rates much higher in the west than in the east, the potential water shortage problem is evident (Mack, 2005).

Schutte and Pretorius (1997) state that of the total water resources presently available, 52% is used in agricultural activities, 12.5% by industry, mining and power generation, and 12% for domestic and municipal use. 15% of the remaining water resources are required for nature conservation and ecological purposes such as maintaining estuaries and rivers.

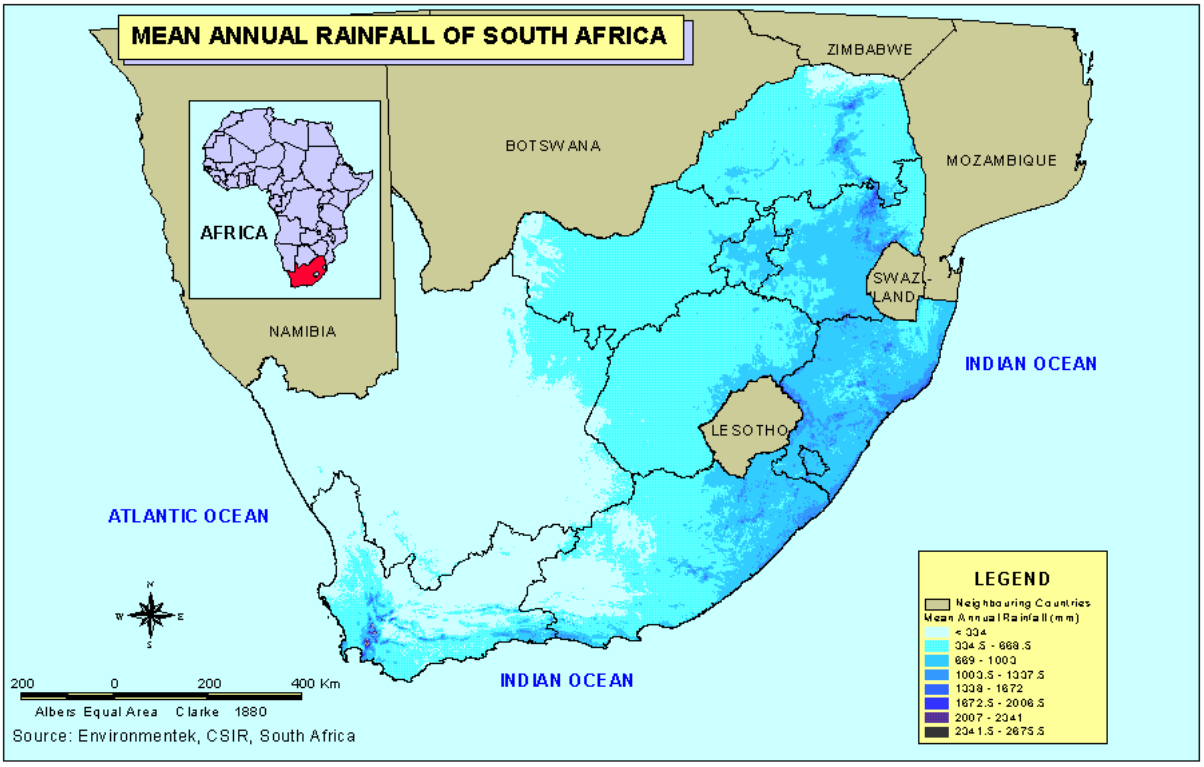


Figure 2.1: Availability of water per capital in South Africa (Environmental potential Atlas (ENPAT), 2001).

The national legislation under the National Water Acts (1998) outlined three policy principles for water resource protection strategies. These are:

- Protection of all significant water resources
- Resource sustainability, i.e. use that does not cause long-term deterioration of overall resource in term of any measurable criteria (e.g. quality and quantity) (Wright and Xu, 2000).
- Integrated water resource management of all water user groups.

It is the third principle that places pressure on all industries to reconsider their current water management strategies and look for ways to increase the amount of reuse and recycling that occurs within that industry.

2.2 Water in Industry

The most widely used raw material in process industries, as well as an abundant component of chemical, petrochemical, petroleum refining, mining and mineral extraction, food and drink, pulp and paper and many other industries is water (Mack, 2005). In light of potentially chronic water shortage facing South Africa, awareness and motivation among the larger users for optimization of water utilization is increasing. This increase is as a result of powerful economic driving forces such as increased cost of wastewater treatment, higher environmental standards and the increasing scarcity and cost of good quality water sources (Alva-Algåez et al., 1998).

Water use minimization can be achieved in three basic ways;

- Reduction in the use of fresh water by instituting changes in the process (Zhe lev and Bhaw, 2000; Alva-Argåez et al., 1998).
- Reuse of process water in areas where high quality water is not key and lower quality water will not adversely affect the process into which it is being added.
- Reduction in water treatment costs by implementing low-cost biological treatments and reusing this treated water (Alva-Algåez et al., 1998).

The third option can be further split into regeneration reuse and regeneration recycling. The first involves partial recycling to remove contaminants that may affect the process into which the water is being added. The regeneration recycling requires that the treatment removes any contaminants that may build up, as the treated water will pass through the same process from which it was taken.

Industries in South Africa are experiencing increasing international pressure to reduce the amount of fresh water used and the amount of effluent produced. A technique known as water pinch analysis is gaining popularity as a ‘cleaner production’ technique. This technique is aimed at reducing fresh water consumption and wastewater generation by analyzing current or proposed industrial complexes and pinpointing areas where changes such as those mentioned earlier can be implemented (Gianadda et al., 2002; Zhe lev and Bhaw, 2000).

Industries involving the extraction, purification and application of metals are generally highly water-intensive. Effluent streams released by these industries are characterized by contaminants such as cyanides, heavy metals, associated salts, oil and greases, cleaning aids and solvents (Cowan, 1998). These contaminants arise, in one way or another, from the processes within the industry, and depending on the process, the reclamation of components such as organic solvents and metal from these waste streams may be financially viable. The major factors used to determine the financial viability of a reclamation process include the volume of water containing metals, the concentration of those metals in the water and the potential to recirculate some of the metal salts and recovered metals as opposed to discharge fees and penalties (Cowan, 1998).

For industries such as electroplaters and refineries, the cost involved in treatment of effluents produced is sometimes prohibitively expensive, especially for the smaller installation, and far outweighs the advantage of recycling and regeneration of materials (Mack, 2005).

For mines and metal refineries, the possibility of retaining every milligram of metal value is highly attractive and the increase in profit gained by the extra metal value will soon outweigh the cost of the treatment plant installation. Present treatment strategies require costly chemical and physical operation and involve a high degree of maintenance and operating supervision. Reliable systems that are cost- effective and low maintenance would be an ideal solution for these mine and metal refiners. Precious metal refineries have the most to gain from maximizing their metal recovery efficiencies. The value of the metal retained than lost to a slime dam would rapidly repay the initial capital outlay required for the installation of a metal recovery plant (Mack, 2005).

2.3 PGM Mining and Refining Process

The PGMs consists of a family of six greyish to silver-white metals with close physical and chemical affinities and belong to the transition metals of group VIII in the periodic table. Three of the PGM family namely, platinum(Pt.), iridium(Ir) and

osmium(Os), have high melting points, are very inert and are heaviest known elements (~22g/cm^3). The remaining three PGM, palladium (Pd), rhodium (Rh) and ruthenium (Ru) are much lighter (~12g/cm^3).

PGMs are principally extracted from two types of deposits, namely the platinum rich layered mafic intrusion (e.g. Bushveld in South Africa and the great Dyke in Zimbabwe) and palladium-rich nickel sulfide deposits (e.g. Noril^{s}sk-Talnakh in Russia). In both types of deposits, there is a strong association between the PGMs. Natural PGM deposits are almost always related to basic igneous rocks and are closely associated with copper, nickel and iron sulphides. The concentration of PGM in these ores differs quite markedly depending on the origin and this has a significant bearing on the manner in which they are refined (Bernardis et al., 2005).The average concentration of these metals in the earth crust is estimated to be in the range of 0.001-0.005mg/kg for Pt., 0.015mg/kg for Pd, 0.0001mg/kg for Rh, 0.0001mg/kg for Ru, 0.005mg/kg for Os and 0.001mg/kg for Ir (Mack, 2005). Considerable treatment of the original PGM bearing ore is required before a product suitable for final refining is obtained. The Bushveld igneous complex (BIC), formed around 2000 million years ago is the world's single largest PGM resource. It consists of a series of distinct layers, three of which are of economic importance as sources of PGMs. These are the Merensky Reef, the Upper Group 2 (UG2) Reef and the Plat Reef. The Merensky Reef has been the principal source of PGMs since it was first worked in 1925 and now produces 50% of all platinum-bearing ore processed in South Africa. The UG2 Reef, in 1999, produced 42% and the Platreef only began to be exploited on a large scale in 1993 (Johnson-Matthey, 2003). Mill head grades of BIC ore (a measure of the ores PGM content on entering the first process stage) are typically between 4 and 7 g/ton. This translates to between 7 and 12 tons of ore being processed to produce a single ounce (28.35g) 0f platinum (Johnson-Matthey, 2003). Figure 2.2 gives an overview of the PGM production process.

In the concentrator, the ore is crushed and milled to reduce rock sizes and expose the minerals containing the PGMs. The rock is mixed with water and other reagents and

air is pumped through the mixture to create bubbles to which the PGM containing particles adhere.

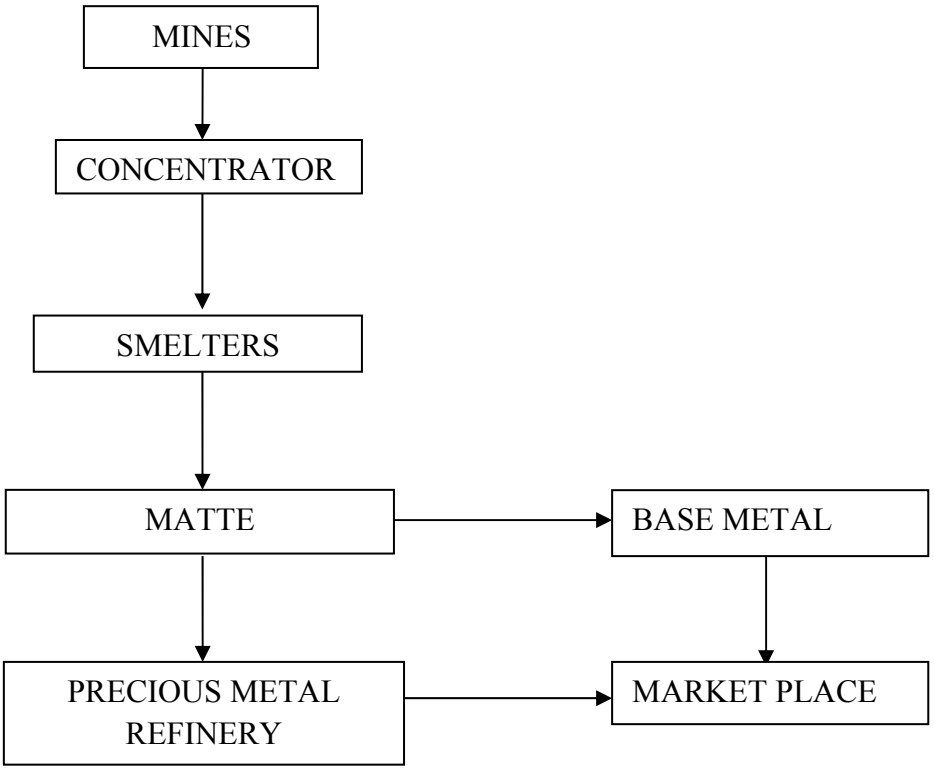


Figure 2.2: Overview of the PGM production process: from mine to market place (Robinson, 2002).

These float to the surface and are removed as a soapy froth called concentrate. This process is known as floatation. The PGM concentration of this concentrate varies between 100 and 1000 g/ton (Johnson-Matthey, 2003).The flotation concentrates are then sent to a smelter for further treatment.

In the smelter, the concentrate is dried and smelted in furnaces reaching temperatures of $1500^{\circ}C$ and higher to obtain a matte that contains principally copper, nickel, iron and PGMs. The matte is transferred to converters, where air is blown through in order to remove iron and sulphur. The PGM content of converter matte is in excess of 1400 g/ton (Johnson-Matthew, 2003). The next step is to separate base metals from the PGMs. The base metals are transferred to a base metal

refinery where copper; nickel and cobalt are recovered through various processes including pressure leaching and electro-winning. The final stage is the separation and purification of the six PGMs, plus gold, which is a byproduct of the ore body. Figures 2.3 and 2.4 illustrate some of the methods used and the order in which the metals are extracted from the matte. The soluble metals, gold, palladium and platinum are generally removed first. The insoluble metals are then removed, with rhodium usually taken out last (Robinson, 2002). The precious metal refinery feed is dissolved in hot HCl to produce a leach liquor. Solvent extraction and ion exchange are the common separation processes that are used at precious metal refineries. In solvent extraction process, PGMs are extracted from the dissolved liquor into an organic medium (e.g. dibutylcarbitol, di-n-octylsulfide, tri-n-butylphosphate etc.). The extracted PGMs contained in the organic phase are then stripped into an aqueous medium for final refining (Dobson and Burgess, 2007) as illustrated in Figure 2.3. Ion exchange process as employed by Impala Platinum, Springs, South Africa where the dilute stream targeted in this study was obtained is presented in Figure 2.4.

Recently, a newer class of separation molecules, which resemble IX resins, has been developed specifically for rhodium recovery (Benguerel et al., 1996). These molecules are based on crown ethers and are described as molecular recognition ligands. The functional molecule, which is bound to a solid silica support, is designed and synthesized in order to bind a specific metal species selectively by carefully considering its geometry, size, charge and coordination affinity (Benguerel et al., 1996).

The refined PGMs usually have a purity of over 99.95% and are produced in a number of forms including ingots, grains or fine powders known as sponges. However, a relatively large percentage of PGMs are not recovered by the conventional techniques and are stored as wastewater in slime dams (Els et al., 1997).

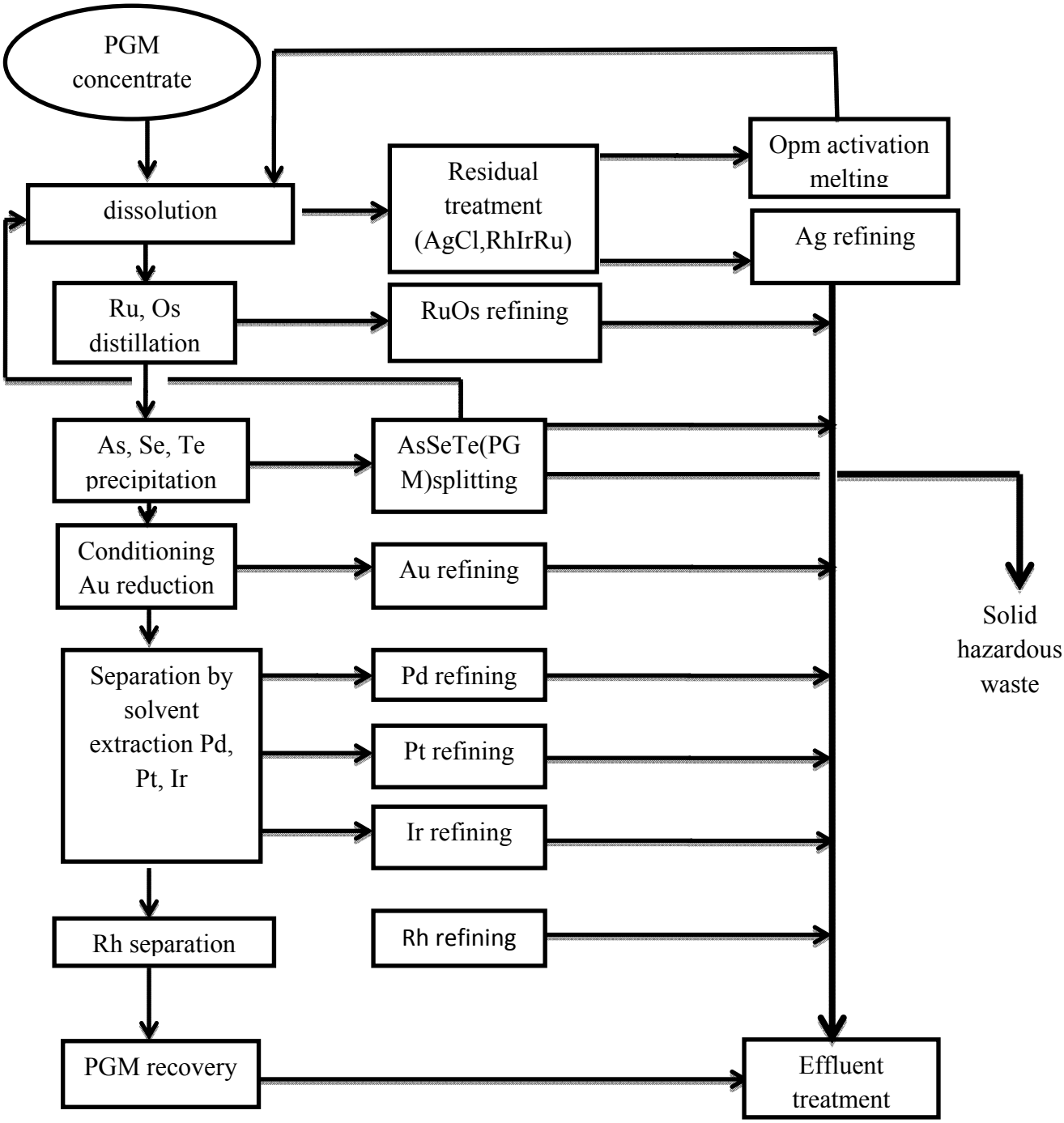


Figure 2.3: Overview of PGM refining process.

(http://www.halwachs.de/pgm-refining.htm)

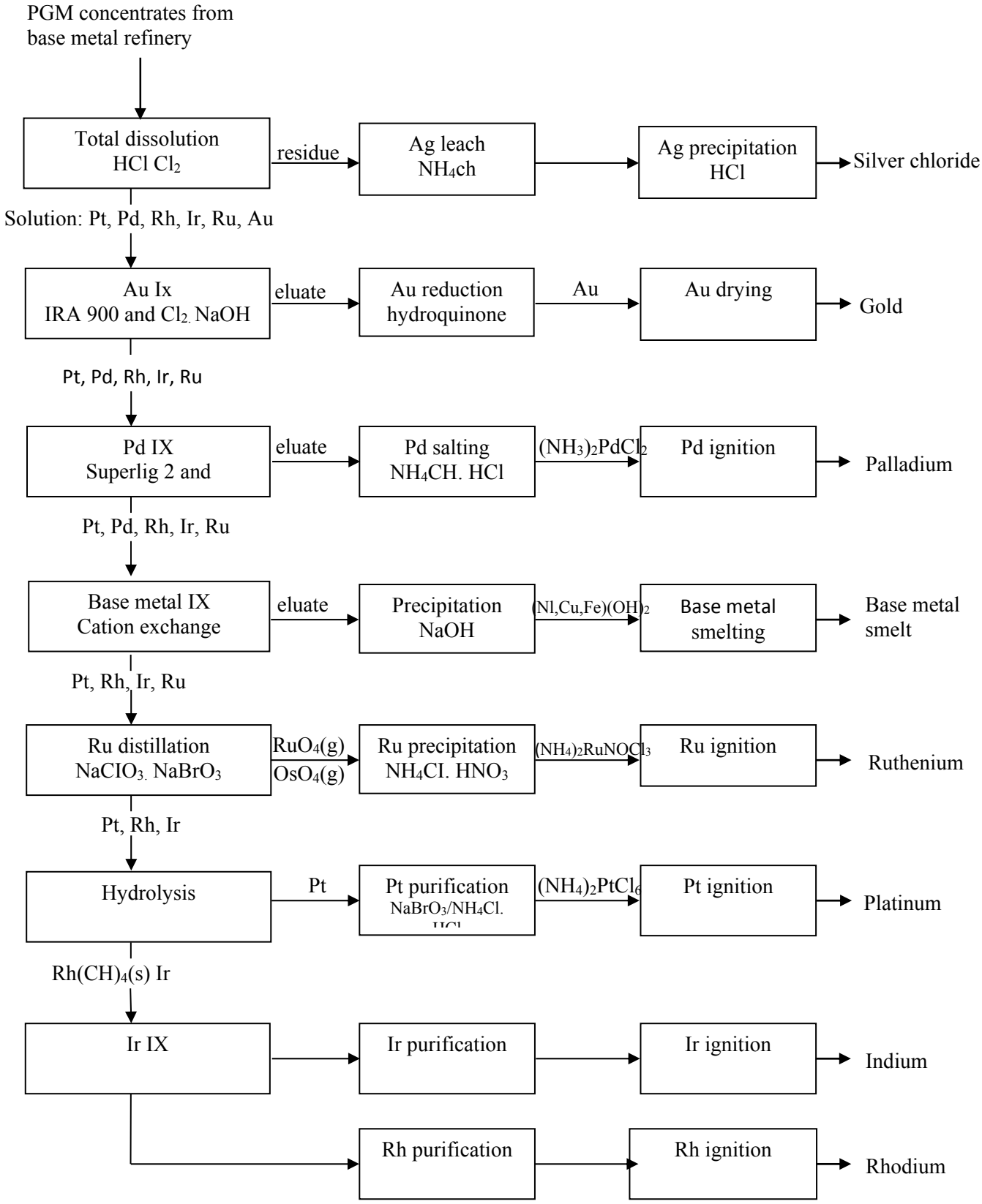


Figure 2.4: An overview of Impala's precious metals refinery at Springs, South Africa (Crundwell et al., 2011).

2.3.1 Physical and Chemical Properties of PGMs

The PGMs possess some unique physical and chemical characteristics. They generally display low reactivity. The state of sub-division of each metal is an important factor when considering reactivity. Platinum and palladium dissolve in aqua regia (AR) whereas rhodium, iridium and osmium are relatively inert. Strong alkaline oxidizing agents however, can dissolve PGMs. All PGMs dissolve in molten bases such as sodium, phosphorus, silicon, arsenic, antimony and lead (Rao and Reddi, 2000). Some useful physical and chemical properties of PGMs are listed in Table. 2.1

Table 2.1. Physical and chemical properties of PGMs.

	Platinum	Palladium	Rhodium	Ruthenium	Iridium	Osmium
Atomic Number	78	46	45	44	77	76
Atomic Weight	195.08	106.42	102.91	101.07	192.22	190.2
Density kg/m^3	21.45	12.0	12.4	12.2	22.4	22.5
Melting Point ◦C	1772	1552	1966	2310	2410	3045
Boiling Point ◦C	3827	3140	3727	3900	4130	5027
Oxidation States	**+2, +4**	**+2,+4**	+2**,+3**,+4, +6	+1**,+2,+3,+4**,+5 +6,+7,+8	+1,+2**,+3 , +4**	+3**,+4**,+6 +8
First Ionization Potential (eV)	8.88	8.3	7.7	7.7	8.7	8.7
Resistivity (microhm.cm at 20◦C)	9.85	9.93	4.33	6.71	4.71	8.12
Hardness (Mhos scale)	4.3	4.8	-	6.5	6-6.5	7.0
Reactivity towards mineral acids						
Bulk	Dissolved by Aqua regia. Not attacked by single mineral acids	Dissolved by aqua regia. Attacked by boiling H_2SO_4, hot HNO_3 and HCI	Attacked by boiling H_2SO_4 and hot HBr	Not attacked by acids	Not attacked by acids	Not attacked by acids
Sponge	-do-	Dissolved by aqua regia, H_2SO_4, HNO_3 and HCI	Dissolved slowly by boiling H_2SO_4 and hot HBr	-do-	Attacked very slowly	Dissolved slowly by hot HNO_3

Oxidation states indicated in bold are the most common ones (Rao and Reddi, 2000).

2.4 Conventional Methods of Metal Removal from Wastewater

The recovery of metals from wastewater has twofold advantage. Firstly, it minimizes contamination of aquatic environment and secondly, recovering of metals of value such as gold and platinum group metals (PGMs) would have significant commercial value (Volesky, 1990). According to convention, the majority of current metal removal and recovery technologies are physical or chemical in nature. Biological systems however, are gaining popularity, as they are being proven to be as effective as physical methods while operating at substantially lower cost (Eccles, 1999).

Metal accumulation tends to be a function of metal concentration. Where metals are in high concentrations (>500mg/l), they can be recovered by electrolysis, while at low concentrations (< 5mg/l), they can be removed by biosorption or ion exchange. At concentrations between 500 and 5 mg/l, precipitation with lime is possible, generating high volume of sludge with low metal/sludge ratios (Diels et al., 1993).

Some of the conventional methods for recovering precious metals from wastewater include: solvent extraction, ion exchange, evaporation, chemical precipitation, cementation, ion membrane technology and adsorption.

Table 2.2 summarizes the major performance characteristics of some of the physic-chemical methods used commercially.

Table 2.2: **Performance characteristics of some physico-chemical heavy metal removal and recovery technologies (Eccles, 1999)**

Technology	Performance characteristics				
	pH change	Metal selectivity	Influence of suspended solids	Tolerance to organic molecules	Working level for appropriate metals (mg/l)
Adsorption	Limited tolerance	Moderate	Fouled	Can be poisoned	< 10
Electrochemical	Tolerant	Moderate	Can be engineered to tolerate	Can be accommodated	> 10
Ion exchange	Limited tolerance	Chelate resins can be selective	Fouled	Can be poisoned	< 100
Precipitation as hydroxide	Tolerant	Nonselective	Tolerant	Tolerant	> 10
Solvent extraction	Some system tolerant	Metal selective extractant available	Fouled	Intolerant	> 100
Ion membrane technology	Limited tolerance	Moderate	Fouled	Intolerant	>10

Solvent extraction: involves extracting the metal of interest by contacting the solution with an organic reagent that will react with the metal ion and result in its conversion to a form soluble in the solvent. Solvent extraction of metals is widely employed for

selective recovery. For optimal operation, this method requires high initial metal ion concentrations. However, the environmental standards for acceptable metal levels in the discharge water cannot be met with this method alone. It is one of the most common methods used for the separation of PGMs from aqueous solution due to the simplicity of the process. The precious metal anions are usually extracted by ion-pair formation with long chain alkyl amines such as tri-n-octylamine (TOA), methyl tricaprylyl ammonium chloride (Aliquot 336), methyl isobutyl ketones(MiBK) and other amines (Mack, 2005). The other limitation of this process is that several of these solvents have been shown to be toxic to human health or to stages of food chains. For example, secondary amines in nature are generally converted to compounds known as N-nitrosamines which are strong mutagens (Dobson and Burgess, 2007).

Ion exchange: is a reversible chemical reaction where an ion from solution is exchanged for similarly charged ion attached to an immobile solid particle. These solid ion exchange particles are either naturally occurring inorganic zeolites or synthetically produced organic resins. Conventional ion exchange resins have been used in conjunction with solvent extraction in the recovery of metals. These ion exchangers are no longer sufficiently selective to remove certain metals from large volumes of accompanying metals and metal selective resins are therefore being developed (Cortina et al., 1998). Ion exchange is capable of reducing metal ion concentration to parts per million levels. The major limitation on the use of ion exchange for inorganic effluent is primarily high cost requirements for appropriate pretreatment systems. The matrix gets easily fouled by organics and other solids in waste water.

Chemical precipitation: is the most common method for removing heavy metals from water up to parts per million (ppm) levels. This is achieved by the addition of coagulants such as alum, lime, iron salts and other organic polymers. Although the process is cost effective, its efficiency is affected by low pH and the presence of other salts (ions). The process requires addition of other chemicals which finally leads to the generation of a high water content sludge, the disposal of which is cost

intensive. Precipitation with lime or bisulphide lacks specificity and is ineffective in removal of metal ions at low concentration (Ahluwalia and Goyal, 2007).

Electrolytic Metal Removal (EMR): electrolytic recovery in waste streams (also known as electro winning) involves the recovery and purification of metals using electro deposition of metals at the cathode and either metal dissolution or a competing oxidation reaction at the anode. The process of electrolysis is used to obtain very highly purified metals. It is very widely used to obtain refined copper, zinc, tin, lead, chromium, nickel, silver and gold metals. Although, the process is capable of obtaining very highly purified metal, it is only more efficient at higher concentration of metal in the waste stream. It would not work well with a flowing waste stream containing a relatively dilute amount of dissolved metals. Another caution with EMR is other "ingredients", this could be additional metal ions that will not plate in the conditions that the primary metal does, or it could be additives that interfere with the ability to plate out (e.g. oxidants). Another limitation of EMR is the high capital cost and energy consumption.

Evaporation: Presently, a common treatment of wastewater from PGM extraction is evaporation in holding ponds. The purpose of this treatment is two-fold; to reduce the volume of the wastewater and to concentrate trace amounts of metal still remaining in the water. Allowing the water to stand outdoors means that surface evaporation occurs using solar energy, resulting in the desired reduction of volume, and increased metal recovery through concentrating the wastewater. However, the solvents used in the metal extraction process are generally less dense than water and form a layer on top of the water, preventing evaporation. Vacuum evaporation, in which the water is vaporized at low temperatures, is only occasionally employed as the equipment required is complex to construct and maintain. Another limitation is that dams required for this method can occupy vast areas of land, making it a viable option only for processes where this land is available close by.

Cementation: is another type of precipitation method employing an electrochemical mechanism in which a metal having a higher oxidation potential passes into solution

to replace a metal having a lower oxidation potential. This technology has found application in recovering silver from industrial baths used for electro winning or electro refining of copper (Sulka and Jaskula, 2003).

Ion membrane technology: Important examples of membrane process applicable to inorganic wastewater treatment include reverse osmosis and electrodialysis (EPA, 1980). These processes involve ionic concentration by the use of selective membrane with a specific driving force. For reverse osmosis, pressure difference is employed to initiate the transport of solvent across a semipermeable membrane and electrodialysis relies on ion migration through selective permeable membrane in response to a current applied to electrodes (Ramachandra et al., 2005). The application of the membrane process described is limited due to pretreatment requirements, primarily, for the removal of suspended solids. The methods are expensive and sophisticated, requiring a higher level of technical expertise to operate.

The above mentioned conventional techniques although having found wide application, require the use of chemicals and synthetic resins which are expensive. Therefore, there is a need to explore other techniques. Among the technologies under development, the one generating much interest involves the use of microorganisms and non-living biomass as metal binding compounds. The use of biomass as adsorbents for the removal of metal ions from aqueous solution has been a topic of great interest for a number of years. Although, the technique is not new, the constant screening of new potential materials to be used in such processes results in a growing pool of biosorbents from which to choose. Large volumes of published data exist regarding the recovery or removal of base metals from aqueous solutions using biomaterials. The same cannot be said for precious metal recovery.

A variety of biomaterials are known to bind the precious metals including algae, fungi, bacteria actinomycetes, yeast, along with some biopolymers (Das, 2010; Alluri et al., 2007). Recently, attention has been diverted towards the application of biomaterials which are by-products or wastes from large scale industrial operations and agricultural waste materials for the treatment of industrial effluent. Biomass cell

walls, consisting mainly of polysaccharides, proteins and lipids offer many functional groups that can bind metal ions such as carboxylate, hydroxyl, sulphate, phosphate, and amino groups. In addition to these functional binding groups, polysaccharides often have ion exchange properties (Goksungur et al., 2002; Alluri et al., 2007).

Among the different types of biological materials, Saccharomyces cerevisiae has been recognized as an effective biomass for the treatment of waste containing heavy metals (Wang and Chen, 2006). Saccharomyces cerevisiae can remove toxic metals, recover precious metals, and clean radio-nuclides from aqueous solution. Saccharomyces yeast biomass is the second major by-product (after spent grain) of the brewing industry. It can be of value as a raw material with different uses, however, it is still largely underutilized, being used mostly for swine and ruminant feeds (Ferreira et al., 2010). The biomass of S.cerevisiae can be further obtained from various food and beverage industries. S.cerevisiae as a by-product is easier to get from the fermentation industry in comparison with other types of waste microbial biomass. During fermentation, the yeast biomass increases three to six fold, in a typical larger fermentation, approximately 2.6kg of surplus yeast solids are produced per cubic meter of beer produced (Soares and Soares, 2012).Thus, the supply of S.cerevisiae as waste residuals is basically stable.

S.cerevisiae has the status of generally being recognized as a safe by the U.S food and drug administration (FDA), which means that it can be handled by humans without any health risk concerns (Wang and Chen, 2006). As a waste product of brewing industry, this biomass can be obtained in large quantities at very low cost; these are two critical points (availability and price), which should be taken into account when seeking a new biomass for biosorption based technology (Machado et al., 2010).

In addition, S.cerevisiae is easy to cultivate at large scale. The yeast can be easily grown using unsophisticated fermentation techniques and inexpensive growth media and the yield of biomass is also high. The yeast is an ideal model organism to

identify the mechanism of biosorption in metal ion removal, especially to investigate the interaction of metal-microbe at molecular level because they are eukaryotic cells that can be easily cultured, manipulated and have a completely sequenced genome (Soare and Soares, 2012).

2.5 Biosorption Process

The term biosorption and bioaccumulation are often used interchangeably to describe the retention of metal ions from aqueous solution by a wide variety of biomass types. Whether or not this interchangeable use of this term is valid, depends on the state of the biomass i.e. only living biomass may bioaccumulate metal ions, while both living and dead biomass may biosorb metal ions (Mack, 2005). Thus, biosorption has been defined as the accumulation of chemicals by microbial biomass. This includes both adsorption and absorption phenomena occurring between the biomass surface and interfacial liquid (Pujol and Canler 1992). In general, adsorption seems to play a major role in chemical accumulation. The mechanisms of biosorption are generally based on physico-chemical interactions between metal ions and the functional groups present on the cell surface. These include complexation, adsorption, ion exchange, coordination, chelation, and inorganic micro-precipitation (Volesky, 1990).

Bioaccumulation, on the other hand, is an active mode of metal sequestration, reliant on the metabolic activity of the cell. A major disadvantage of this process is that the presence of these metal ions within the cell can greatly inhibit that activity (Mack, 2005).

Biosorption is a process that makes use of inexpensive, non-living biomass to remove toxic heavy and precious metals from aqueous solution by the use of biological materials, thus allowing the recovery and/ or environmentally acceptable disposal of the pollutant. Biosorbents are prepared from naturally abundant or waste biomass such as algae, fungi, plants or bacteria that have been killed either in a production processes or as a pre-treatment step in their use as biosorbent (Mack, 2005).

Conventional methods for removing metals from industrial waste solutions (which include chemical precipitation, chemical oxidation or reduction, filtration, electrochemical treatment, application of membrane technology and evaporation recovery) may be ineffective or extremely expensive, especially when the metals are dissolved in large volume of solutions at relatively low concentrations (around 1-100mg/l). The use of ion exchange resins solely for purifying wastewaters is, in most cases inappropriate because of the high price of the materials although in some instances the cost may be partially offset by the value of the metal recovered. Rare, precious or strategic metals need to be efficiently recovered both at their source (e.g.; from leach mining) and from waste solutions. The increasing demand for these metals and diminishing resources or geopolitically unstable supplies combine to provide powerful stimulus for the development of alternative (and less expensive) recovery methods.

As well as providing an alternative recovery strategy for valuable metals, naturally abundant or easily propagated biosorbents might be used where more expensive ion exchangers are not feasible, particularly in combined purification/ recovery processes for dilute metal-bearing industrial wastewaters. The initial concept, that very cheap biosorbents could be used in purifying industrial waste water solutions by non-specifically decreasing their metal content, has been revised in the light of results from applied studies which have shown not only that metal uptake capacities are high but also that uptake can be metal selective (Volesky, 1987). These advantages have resulted in vast amounts of research in this field and a number of commercialization. However, of all these commercial ventures into biosorption for wastewater treatment and metal value recovery, none has been successfully integrated into industrial use (Volesky, 1990).

Consequently, biosorbents are now also being considered as replacements for ion exchangers or other metal extraction and concentration operations in upstream metal recovery. At least four broad areas of application for new biosorbent materials have been considered:

(1) detoxification of metal bearing wastewaters,
(2) decontamination of radioactive wastewaters,
(3) recovery of metals from ore processing solutions,
(4) Concentration/ recovery of strategic/rare metals from seawater.

The efficiency of the process is governed by factors which include the type of metal, the ionic form of the metal in solution and on the binding site on the biomass responsible for uptake of the particular metal. The most important physical characteristics of a successful biosorbent are hardness, porosity, particle size and density. These characteristics ensure that the biosorbent is capable of withstanding high liquid pressures that may be experienced in biosorption environment and still maintain superior removal efficiency. A broad tolerance to a number of factors including temperature, pH and solvent content are also highly beneficial, especially in cases where the effluent to be treated is highly acidic in nature or contains organic compounds that could possibly render the biosorbent useless. Potential for the regeneration and reuse of the biosorbent is also important. This is usually much easier to accomplish when using non-viable biomass, as regeneration usually entails elution with mineral acids (Wilhemi and Duncan, 1996) or toxic complexing and chelating ligands such as thiourea (Godlewska-Zylkiewicz, 2003).

The availability of a specific biomass is also a major factor in the final choice. An enormous pool of possible biosorbent material exists in nature and many of these natural biosorbent are cheaply available as they can even be acquired as spent biomass from pre existing processes, such as spent yeast from breweries or bacterial biomass from pharmaceutical industries (Mack, 2005). Recently, attention has been diverted towards the application of biomaterials which are by-products or waste from large scale industrial operations and agricultural waste materials for the treatment of industrial effluents.

The cell wall composition of the biomass chosen also plays an important role in the efficiency of the process. The quantity and type of active sites on the cell wall may be a major factor in the binding behavior of the metal ion of interest. The complexity of the cell surface implies that there are many possible explanations for how metal

ions are sequestered by the cell. In the case of non-viable biomass, these interactions are generally physicochemical processes such as physical adsorption, ion exchange and micro precipitation (Pagnanelli et al., 2000). These interactions occur between structures on the cell walls such as; carboxylate, sulphydryl, amino, amide, and hydroxyl group (Goksungur et al., 2002; Alluri et al., 2007). Stanberg et al. (1981) and Volesky, (1987) have demonstrated the rapid uptake of uranium and postulated that the poly-phosphate group and the carboxyl groups on the cell surface of S.cerevisiae are active in metal complexation.

In a review of metal sorption by fungi, Kapoor and Viraraghavan (1995) suggests that adsorption of metal is achieved via two mechanisms. The first is uptake regulated by the functional groups listed above and the second is through physic-chemical interaction based on adsorption phenomena.

2.5.1 Physical Adsorption/ Ion Exchange

The basis for physical adsorption is the presence of Van der Waals' forces between the cell surface and metal ion of interest. The interaction energy is very weak (10-100meV) and it can only be observed in the environment of low temperature. In practice, the categorization of a particular adsorption as physisorption or chemisorption depends principally on the binding energy of the adsorbate to the substrate. Physical sorption or adsorption involves no exchange of electrons rather intermolecular attractions between sorption sites and is therefore independent of the electronic properties of the molecules involved. Ion exchange or electrostatic sorption involves columbic attractive forces between ion and charged functional group. Ion exchange interactions are characterized by a stoichiometric exchange of metal ions for protons and/or other metal ions at relevantly charged cell wall component. Ion exchange share many common characteristics with adsorption such as mass transfer from the liquid to the solid phase, which is a diffusion-driven process. However, there are some significant differences, the most important being the nature of sorbed species which are ions in ion exchange and electrically neutral substance in adsorption. In ion exchange, the ions removed from the liquid phase are

replaced by ions from the solid phase, and thus a two-way traffic (exchange) occurs in contrast to adsorption. This exchange of ions between the two phases is such that the total charged sorbed and desorbed is exactly the same as imposed by the electro neutrality principle. All these factors make the quantitative treatment of ion exchange much more complicated than adsorption. Although, the differences, adsorption and ion exchange are grouped together as sorption for the purpose of a unified treatment in practical applications. In the related literatures (Inglezakis and Zorpas, 2012), most of the mathematical theories and approaches developed originally for adsorption are used with minor modification for ion exchange.

2.5.2 Micro-precipitation

The precipitation or condensation of metal hydroxides onto biological surfaces occurs when, despite there being a metal ion concentration, in the bulk liquid, far lower than the solubility limit, that limit is exceeded at the surface. This accumulation will occur if a net negative charge exists within that microenvironment (Schneider et al., 2001). However, no matter how simple the processes involved may seem, the actual mechanism used are thought to vary depending on the biosorbent used and/or the metal to be sorbed.

2.5.3 Biosorbents

A large array of biomaterials has been investigated as biosorbents for the removal of metals or organic extensively. The biosorbent can be classified as bacteria, fungi, yeast, algae, industrial wastes and other polysaccharide materials (Dhankhar and Guriyan, 2011). Bacteria biosorption is by far the best studied. Bacterial make excellent biosorbent because of their high surface-to-volume ratios and a high content of potentially active chemosorption site such as on teichoic acid in their cell walls (Dhankhar and Guriyan, 2011). Bacteria are used as biosorbents because of their small size, their ubiquity, their ability to grow under controlled conditions, and their resilience to wide range of environmental situations. Bacteria species such as Bacillus, Pseudomonas, Streptomyces, Escherichia, Micrococcus, etc, have been tested for uptake of metals or organics (Dhankhar and Guriyan, 2011). The most

relevant work on true bacteria biosorption has been done by the Brierleys (Brierley, 1990) who took the metal biosorption concept all the way to the commercial stage. Various advantages of using dead cells can be summarized as:

- absence of toxicity limitations
- absence of requirements for growth media and nutrients in the feed solutions
- easy absorbance and recovery of biosorbed metals
- easy regeneration and reuse of biomass
- possibility of easy immobilization of dead cells
- avoidance of sudden death of the biomass population
- easy mathematical modeling of metal uptake reactors.

Bacteria can be classified as Gram-positive and Gram-negative bacteria based on the chemical composition of their cell wall. Studies of both Gram-positive and Gram-negative bacteria cell walls have shown that Gram-positive walls bind up to 10 times more metal than Gram-negative walls. This is due to their simple peptidoglycan structure and the anionic carboxyl and phosphoryl groups contained in the polymer of the cell wall (Dhankhar and Guriyan, 2011; Uruttia, 1997).

Fungi and yeast species are of significant interest as biosorbents due to their abundance as waste from fermentation processes and their relative ease of cultivation and as such, they are ready source of cheap biomass. However, the small particle size and low strength of fungal cell can cause difficulties in biosorption processes, so fungal application are preferred only if the biomass is immobilized or pelletized before use (Kapoor and Viraraghavan, 1995).

Algal biosorption capacity is generally attributed to the characteristics of cell wall such as fibre-like structure and the amorphous embedding matrix of polysaccharides. The polysaccharides include alginates and sulphated polysaccharides such as fucoidan, which are known to have high affinities for divalent and trivalent cations respectively. Alginates are found within the cell wall and as the component of intercellular substance and comprise up to 40 %(dry matters) of the cell wall (Sheng et al., 2004).

Major constituents of fungi cell walls include chitin and chitosan (Niu and Volesky, 2003). These are both natural polysaccharides and are found widely, not only in fungi, but also in animals such as crustaceans and insects. The major commercial sources however, are the exoskeletons of crabs obtained as waste from food processing (Niu and Volesky, 2003). Both of these compounds have been found capable of metal ion uptake. Chitin is a polymer of N-acetyl-d-glucosamine. Chitosan is a completely deacetylated derivative. Uptake of metals such as iron, zinc, copper, lead, mercury and uranium by chitin varies due to changes in the chitin and chitosan content of the cell wall changing during growth (Kapoor and Viraraghavan, 1995). Metal uptake by chitin and chitosan is pH dependent, with optima pH between pH 3 and pH 4. It is suggested that the uptake mechanisms is a combination of ion exchange and complexation with chitin nitrogen atoms ((Kapoor and Viraraghavan, 1995; Volesky, 1990).

A rapidly growing number of waste products have been screened for biosorptive abilities as they have been recognized as being the most cost effective solution to commercialization of biosorption processes (Mack, 2005). Agricultural wastes such as carrot residues, crab shells, olive mill residues, rice milling by-products, rice bran and wheat husks have been screened for biosorptive activity. Metals such as copper, zinc, chromium, cadmium, nickel, aluminium and lead have been shown to adsorb to some or all of these.

2.6 Factors Affecting Biosorption

Batch experiments usually focus on the study of factors influencing biosorption which are important in the evaluation of the full biosorption potential of any biomaterial (Nilanjana Das, 2010). The important factors include: temperature, solution pH, ionic strength, biomass dosage, initial solute concentration and agitation rate/period.

Temperature Effect: Temperature of the solution is an important factor during the process of biosorption. The effect of temperature on biosorption depends on the

adsorption heat (enthalpy change). The intrinsic adsorption constant k_{int} can be described thermodynamically as

$$k_{int} = \exp - \frac{\Delta H^0}{RT} = \exp - \frac{\Delta H^0}{RT} \exp - \frac{\Delta S^0}{R} \quad (2.1)$$

where ΔH^0 is the enthalpy change (adsorption heat), ΔS^0 is the entropy change, R is the Universal gas constant and T is the temperature. For physical adsorption, adsorption heat $\Delta H^0 < 0$, adsorption reaction is exothermic and preferred at lower temperature, for chemisorptions, adsorption heat $\Delta H^0 > 0$, adsorption reaction is endothermic and favored at higher temperatures (Stumm and Morgan, 1996b).

Biomass usually contain more than one type of sites for binding, the effect of temperature on each kind of sites can thus contribute to the overall metal uptake.

Solution pH: solution pH is one of the most important variables which affect the speciation of metals in solution through hydrolysis, complexation and redox reaction during metal recovery (Nilanjana Das, 2010). This factor is capable of influencing not only the binding site dissociation state but also the solution chemistry of the target metals in terms of hydrolysis, complexation by organic/inorganic ligands and redox potentials. The pH of the solution is of great importance in anion and cation biosorption. However, the optimum pH for anion biosorption is opposite to that of cation biosorption. While cation biosorption is favored at increase pH >4.5 (Kratochvil, 1997), anion biosorption is preferred in a lower pH range 1.5-4.5 (Roberts, 1992b)). Generally, biosorption carried out at low pH values (smaller than 2.0) has a non-effective metal uptake for cationic metallic species. This is because the high hydronium concentration makes the competition among these protons for the biomass active sites more prominent than that from the metal ions in solution. This means that at lower pH, H^+ ions compete with cations for the surface of the adsorbent which would hinder cations from reaching the binding sites of the sorbent caused by repulsive forces between the H^+ and the cations. Moreover, the acidic functional groups on the biosorbent at low pH become protonated according with their pk_a values and as the solution pH increases, the acidic groups become

deprotonated from their pk_a values and the metallic ion presents a chemical speciation that provides greater adsorption performance (Oliviera, 2011). Biosorption of anionic species are very less common and occur when a metallic complex is formed with a negative global charge (Atkinson et al., 1998). Anion biosorption is favored at low pH because at very low pH, the surface of sorbent would also be surrounded by the hydronium ions which enhance the anions interaction with binding sites of the biosorbent by greater attractive force (Wang and Cheng, 2006).

There are three ways in which the pH can influence metal biosorption:

- The state of chemically active sites could be changed by the solution pH. When the metal binding group are weakly acidic/basic, the availability of free sites is dependent on the pH.
- Extreme pH values as they are employed for regeneration (desorption) of the sorbent, may damage the structure of the biosorbent materials.
- The speciation of metal in solution is pH dependent, whereas metal in aqueous solution occurs as hydrolyzed ion when pH is low especially metal anions with high charge and a small size (Beveridge, 1990).

Ionic strength: Another important parameter in biosorption is ionic strength, which influences the adsorption of solute to the biomass surface. The effect of ionic strength may be ascribed to the competition between ions, changes in the metal activity, or in the properties of electrical double layer. When two phases' biomass surface and solute in aqueous solution are in contact, they are bound to be surrounded by an electrical double layer owing to electrostatic interaction. Thus, adsorption decreases with increase in ionic strength (Nilanjana Das, 2010). Some inorganic ions such as chloride may form complexes with some metals ions and therefore affects the sorption process. In high chloride environment, complication arises from the presence of large excess of chloride ions which cause strong competition between the anion of the acid (chloride) and the metal species restricting the metal sorption in industrial waste water environment(Godlewska-Zylkiewicz, 2003).

Biosorbent Dosage: The dosage of biosorbent strongly influences the extent of biosorption. An increase in the biomass concentration generally increases the amount of biosorbed solute (Nilanjana Das, 2010). This is due to the increased surface area of the biosorbent which in turn increases the number of binding sites. On the other hand, the quantity of biosorbed solute per unit weight of biosorbent decreases with increasing biosorbent dosage which may be due to a complex interaction of several factors. An important factor at high sorbent dosage is that the available solute is insufficient to completely cover the available exchangeable sites on the biosorbent, usually resulting in low solute uptake per given weight (Tangaromsuk et al., 2002). In addition, as suggested by Gadd et al. (1988), the interference between binding sites due to increased biosorbent dosages cannot be overruled, as this will result in a low specific uptake.

Agitation rate/period: The rate of biosorption process can be influenced by external film diffusion. With appropriate agitation, the mass transfer resistance can be minimized. When agitation rate is increased, the diffusion rate of a solute from the bulk liquid to the liquid boundary layer surrounding particles become high due to enhanced turbulence and the decrease in thickness of the liquid boundary layer (Shen and Duvnjak, 2005). At higher agitation rate, the boundary layer becomes thin, which usually enhances the rate at which a solute diffuses through the boundary layer (Nilanjana, Das, 2010).

Competition between metal ions: The binding of metallic ions by a biomass is influenced by other ionic species such as cations and anions present in solution (Oliveira et al., 2011). Other sorbable ions in the solution may compete with the metal ion of interest for sorption sites. The binding of this metal ion is then decreased. The amount of inhibition depends on the binding strength of the respective ion to the biomass. From the different literature sources, it can be generally concluded that the light metals (alkaline and alkaline earth metals) bind less strongly than the heavy metal ions or radioactive elements. Therefore, the former do not strongly interfere with the binding of the latter. There are indications that

among the heavy metals, Zn binds rather weakly and its binding is therefore more strongly affected by other ions.

2.7 Adsorbate – Adsorbent Contactors

There are two main modes of adsorbate-adsorbent contact patterns in adsorption process. These are batch and column contactor.

2.7.1 Batch Process

A great deal of biosorption process is performed in batch systems with single species of organic (solute). These processes are conceptually simple; a suitable microbial biomass is contacted with aqueous solution containing organic pollutants molecules or ions. The contacting process is allowed to proceed for a sufficient time for the biomass to sequester these molecules and to reach equilibrium. Then the biomass is separated from the liquid phase and the pollutant-containing biomass is either regenerated or disposed in an environmentally acceptable manner (Aksu, 2005). Despite the continuous operation in columns being the preferential mode for amplifying the biosorption process to a pilot scale (Volesky, 2003), the batch systems serve as pre-stage for an initial evaluation of adsorption phenomena and operational conditions before the application of the process on continous systems (Gadds, 2009).

The physico chemical modeling is based on the analysis of the metal uptake capacity (according to equation 2.2) as function of the assay time (biosorption kinetics) or the equilibrium concentration of adsorbed metals (biosorption isotherms).

$$q = \frac{\left(c_i - c_f\right)v}{s} \tag{2.2}$$

Where q is the metal uptake that represents amount of accumulated metal by mass unity of the biomass (mg/g), V is the volume of the metal bearing solution (ml), C_i and C_f are the initial and equilibrium concentrations of the metals in solution (mg/l), S is the amount of added biosorbent in dry basis (g).

2.7.2 Column Biosorption Studies

Continuous mode sorption studies have an important role in evaluating the technical feasibility of a process for industrial treatment systems. Among the different column configurations, packed bed columns have been established as effective, economical and most convenient for biosorption processes. The columns allow for more efficient sorption capacity of the sorbent material. Packed bed sorption columns are simple to operate, attain a high yield and can be easily scaled up from laboratory scale procedure (Akar and Divriklioglu, 2010).The top of the bed might be covered by a layer of glass beads to avoid the loss of biosorbents and to ensure a closely packed arrangement. Furthermore, a porous sheet might be attached at the bottom of the column in order to support the biosorbent bed, ensure uniform inlet flow and a good liquid distribution into the column (Das Saha et al; 2012). The time for break through appearance and shape of the break through curve are very important characteristics for determining the operation and the dynamics response of an adsorption column. A typical fixed bed breakthrough curve is given in Figure 2.5. From the perspective of design and optimization of the column processes, the behavior in fixed- bed is described by the effluent concentration profile (C/C_o, where C and C_o are the concentration of eluate and eluent, respectively) in function of the time or percolated volume (Naddaffi et al., 2007).

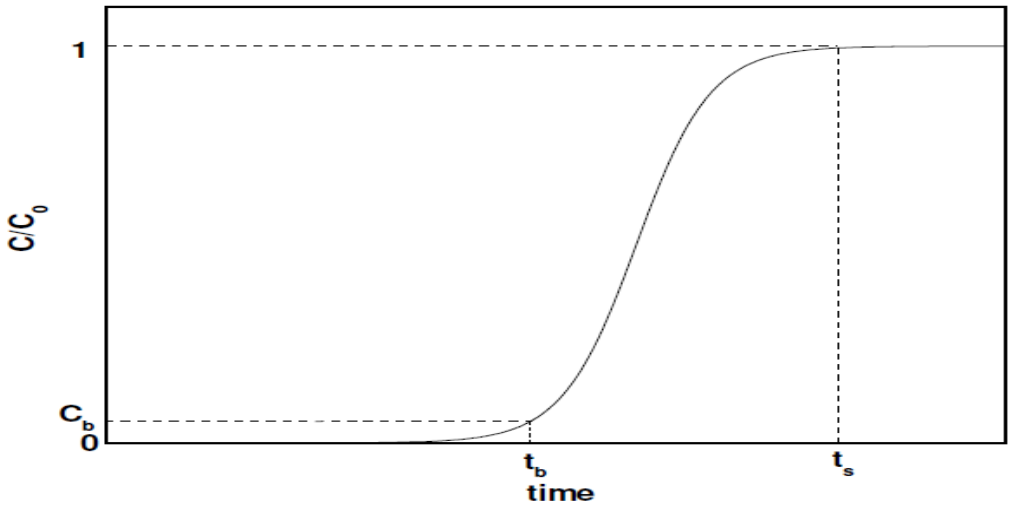


Figure 2.5: Schematic representation of breakthrough curve. Source: Oliviera et al., 2011

The curve shape is given by a sigmoid function and it is determined by the shape of the equilibrium isotherms, i.e. it is influenced by the transport processes and the adsorbent nature (Chu, 2004).

The breakthrough curves are used to determine the breakthrough and saturation times (t_b and t_s, respectively). The breakthrough time indicates the instant in which the metallic ion is effectively discharged on eluate, and the saturation time corresponds to the instant of metal mass saturation on biomass. The breakthrough time is arbitrarily inferred for C/C_o at 0.05; while the saturation time is defined ideally when C/C_o value reaches 1.0 (generally at 0.9- 0.95) **(**Oliviera et al., 2011). An optimized system in columns is based on accurate prediction of the breakthrough time under selected operational conditions because it represents the interaction between the metal and the biomass. Hence, if the breakthrough time is high, this indicates that the interaction between the metal and the biomass is also high. When the eluate concentration reaches a predefined level, the column operation is finalized; at this point the regeneration process may be achieved to activate the column for a next operation cycle (Kentish and Stevens, 2010).Some of the terms associated with column adsorption are defined below:

Breakthrough point: The breakthrough point is defined as the point when a preset concentration emerges in the effluent, and the effluent quality no longer meets predetermined treatment objectives. Usually, a breakthrough point composition is set to be the maximum amount of solute that can be acceptably lost, typically something between 1 and 5 percent.

Saturation point: Bed saturation point is defined as the point when the influent concentration is equal to the effluent concentration.

Breakthrough capacity: The breakthrough capacity is defined as the mass of sorbate removed by the sorbent at breakthrough point concentration; this is also termed as maximum acceptable concentration of the sorbates.

2.8 Biomass Immobilization

Free cell biosorbents are basically small particles with low density, poor mechanical strength, and little rigidity. Even though they have merit such as high biosorption capacity, rapid equilibrium attainment, offer lower process costs and good particle mass transfer, they often suffer several draw backs. The most important of these include solid-liquid separation problems, possible biomass swelling, impossible to regenerate/reuse and tendency to develop a high pressure drop when used in the column mode (Vijayaraghavan and Yun, 2007). Several established techniques are available for making biosorbents suitable for process applications; these include immobilization techniques such as entrapment and cross linking which have been found to be practical for biosorption (Volesky, 2001). Immobilization of free cells within a polymeric matrix has exhibited greater potential, especially in packed or fluidized bed reactors, with benefits including the control of particle size, regeneration/reuse of the biomass, easy separation of the biomass and effluent, high biomass loading and minimal clogging under continuous flow conditions (Hu and Reeves, 1997). Various synthetic, natural polymer derivatives and chitosan have been experimentally used. Important immobilization matrices used in biosorbent immobilization include sodium alginate, polysulfone, polyacrylamide and polyurethane. The choice of immobilization matrix is a key factor in the

environmental application of immobilized biomass. The polymeric matrix determines the mechanical strength and chemical resistance of the final biosorbent particle to be utilized for successive adsorption-desorption cycles (Bai and Abraham, 2003)). After immobilization, the biomass will usually be retained within the interior of the matrix used for the immobilization; hence a successful immobilization matrix should allow all the active binding sites to have access to the solute, even at a slower rate.

Biosorption is always portrayed as cost effective process and this is often highlighted as the main attraction of biosorption as compared to the other proven technologies. However, immobilizing the biomass always increases the process cost i.e. the immobilization materials and technique usually increase the cost of the overall biosorption process.

2.9 Biosorption Process Modelling

2.9.1 Kinetic Modelling

The knowledge of the kinetics of any biosorption process is crucial in order to be able to design industrial scale separation processes. The data obtained from the contact time-temperature dependent experiments can be used to study the kinetics of the biosorption process (Das. Saha et al., 2012; Mack et al., 2008). A number of models have been developed to describe kinetics of metal biosorption in batch experiments. Kinetic modelling describes the solute uptake rate which controls the residence time of adsorbate uptake at solid-solution interface. Conformity between experimental data and model predicted values is always expressed by a correlation coefficient (R^2, values close or equal to 1).

A relatively high R^2 value indicates that a model successfully describes the kinetics of adsorption (Mohamed and Krim, 2010).

Lagergren equation (pseudo-first order)

The pseudo first order equation of Lagergren (1898) is based on solid capacity and is expressed as:

$$\frac{dq_t}{dt} = K_1\left(q_e - q_t\right) \tag{2.3}$$

where K_1 is the rate constant of first order sorption (l/min), q_e is the amount of solute sorbed at equilibrium (mg/g), q_t is the amount of solute sorbed to the sorbent surface at any time t (mg/g).

After integration, by applying boundary conditions ($q_t = 0$ at $t = 0$ and $q_t = q_t$ at $t = t$), the equation can then be rearranged for linearized data plotting.

$$\log\left(q_e - q_t\right) = \log\left(q_e\right) - \frac{k_1}{2.303}t \tag{2.4}$$

In order to confirm the applicability of the model, a plot of log $\left(q_e - q_t\right)$ against t should yield a straight line. In a true first order process, experimental $\log q_e$ should be equal to the intercept of the straight line (Mack et al., 2008).

Ho and McKay Model (Pseudo second order).

The pseudo second order kinetic model (Ho, 1995) is expressed as:

$$\frac{dq_t}{dt} = K_2\left(q_e - q_t\right)^2 \tag{2.5}$$

After taking into account the boundary conditions, $q_t = 0$ $t = 0$ and $q_t = q_t$ at $t = t$, the integrated form of the equation can be rearranged and expressed as;

$$\frac{t}{q_t} = \frac{1}{k_2 q_e^{\,2}} + \frac{1}{q_e}t \tag{2.6}$$

Where k_2 is the rate constant of second order sorption (g/mg/min).

If the initial adsorption rate $\left(h\right)$ ($mgg^{-1}min^{-1}$) is

$$h = k_2 q_e^{\,2} \tag{2.7}$$

Then the equation becomes;

$$\frac{t}{q_t} = \frac{1}{h} + \frac{1}{q_e}(t) \tag{2.8}$$

The applicability of the pseudo second order is confirmed if a plot of $\frac{t}{q_t}$ against t yields a straight line. The value q_e and k_2 can be determined from the slope and the intercept of the plot respectively. In a true second order process, the theoretical q_e values will closely match the experimental values.

Elovich Model

Elovich model equation is generally expressed as:

$$\frac{dq_t}{dt} = \alpha \exp(-\beta q_t) \tag{2.9}$$

Where, α is the initial adsorption rate (mg/gmin); β is desorption constant (g/mg) during any one experiment. To simplify Elovich equation, Chien and Clayton assumed $\beta q_t >> t$ and by applying boundary conditions ($q_t = 0$ at $t = 0$ and $q_t = q_t \;\; at\; t = t$), the equation becomes

$$q_t = \beta \ln(\alpha\beta) + \beta \ln(t) \tag{2.10}$$

If adsorption fits Elovich model, the plot of q_t vs. $\ln(t)$ should yield a linear relationship with slope of (β) and an intercept of $\beta \ln(\alpha\beta)$.

Morris-Weber Model.

The intra- particle diffusion model was first proposed in 1963 by Weber and Morris, who concluded that sorption-rate, is proportional to the square root of contact time.

$$q_t = k_i t^{0.5} \quad (2.11)$$

Where k_i is the intra- particle diffusion rate (mg/g/min$^{0.5}$).

A basic assumption of this model is that film diffusion is negligible and intra-particle diffusion is the only rate controlling step. When intra- particle diffusion controls the sorption process, a graph of q_t against $t^{0.5}$ should yield a straight line passing through the origin and the rate constant can be calculated from the slope of the line.

2.9.2 Biosorption Isotherms

In the analysis and design of a biosorption process, isotherms provide the most important piece of information in understanding the biosorption process. The equation parameters and the underlying thermodynamic assumption of the isotherm models give some idea about the underlying biosorption mechanism as well as the surface properties and affinity of the biosorbent (Das Saha et al., 2012).

In determining the equilibrium isotherm in modeling experimental data, the Langmuir, Freundlich, Langmuir-Freundlich, Redlich-Peterson, Brunaver-Emmet-Teller (BET), Radke-Prausnitz are the most frequently used two-and three parameter models in the literature describing non-linear equilibrium between adsorbed organic pollutant on the cells(q_{eq}) and organic pollutant in the solution(C_{eq}) at constant temperature.

Langmuir isotherm

The Langmuir equation (Langmuir, 1916) is valid for monolayer sorption onto a surface with a finite number of identical sites and it is used for homogeneous surfaces. The model assumes:

- Monolayer coverage
- Equilibrium model
- All adsorption sites are equally probable

- A second order reaction

The equation is given by:

$$q_{eq} = \frac{Q^o b C_{eq}}{1 + bC_{eq}} \tag{2.12}$$

The linear form of the Langmuir equation can be described by:

$$\frac{C_e}{q_e} = \frac{1}{Q^o b} + \frac{C_e}{Q^o} \tag{2.13}$$

Where parameters Q^o and b are Langmuir constants related to maximum adsorption capacity and bonding energy of adsorption respectively, which are functions of the characteristics of the system as well as time.

The linear plot of specific adsorption capacity $\frac{C_e}{q_e}$ against the equilibrium concentration (C_e) shows that the adsorption obeys the Langmuir model. The Langmuir constant Q^0 and b can be determined from the slope and intercept of the plot. The general representation of Langmuir isotherm model is given in the Figure2.6 below

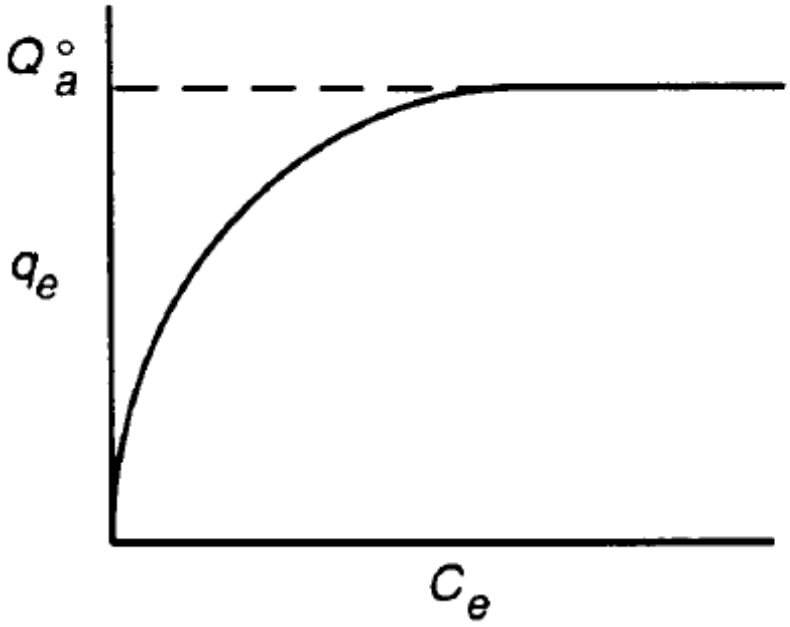


Figure 2.6: Graphical representation of Langmuir isotherm model (University of Washington, n.d)

In order to find out the feasibility of the isotherms, the essential characteristics of the Langmuir isotherms can be expressed in terms of dimensionless constant separation factor R_L which is given by the equation (Hussain et al., 2012).

$$R_L = \frac{1}{1 + bC_o} \tag{2.14}$$

Where C_o (mg/l) is the highest initial concentration of adsorbent and b (L/mg) is Langmuir isotherm constants. The parameter R_L indicates the nature of shape of the isotherm accordingly.

$R_L > 1$ Unfavorable adsorption

$0 < R_L < 1$ Favorable adsorption

$R_L = 0$ Irreversible adsorption

$R_L = 1$ Linear adsorption

Freundlich isotherm

The Freundlich isotherm model (Freundlich and Kuster, 1909) assumes neither homogeneous site energies nor limited levels of sorption. The Freundlich has the general form:

$$q_{eq} = k_f c_{eq}^{\frac{1}{n}} \tag{2.15}$$

The linear form of Freundlich isotherm is represented by equation

$$\log q_e = \log k_f + \frac{1}{n} \log c_e \tag{2.16}$$

Where K_F and n are the Freundlich constants related to adsorption capacity and adsorption intensity respectively. The general form of Freundlich model is represented in the Figure below.

The value of K_f and n are calculated from the intercept and slope of the plot of log q_e vs. log C_e respectively. The magnitude of exponent $\frac{1}{n}$ gives an indication of the favorability of adsorption. The value of n >1 represents favorable adsorption condition ((Hussain et al., 2012).

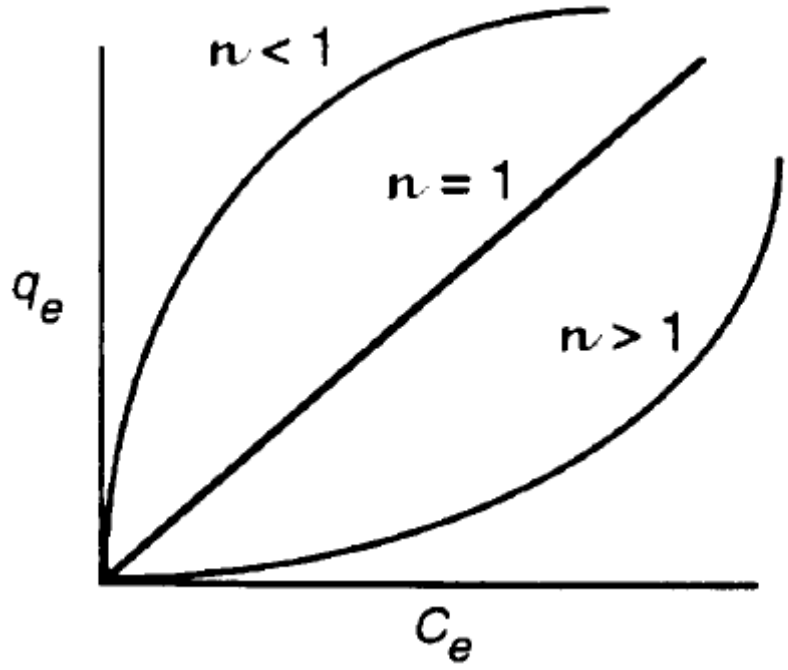


Figure 2.7: Graphical representation of Freundlich isotherm model (University of Washington, n.d)

BET (Brunauer, Emmett and Teller) Isotherm

The BET isotherm (Brunauer et al., 1938) is a more general multilayer model. It assumes that a Langmuir isotherm applies to each layer and that no transmigration occurs between layers. It also assumes that there is equal energy of adsorption for each layer except for the first layer.

BET isotherm is represented by equation

$$q_e = \frac{k_B c_e Q^o}{\left\{ c_s - c_e \left(1 + \left(k_B - 1 \right) \left(\frac{c_e}{c_s} \right) \right) \right.} \tag{2.17}$$

Where C_s is the saturation (solubility limit) concentration of the solute (mg/l), and K_B is a parameter related to the binding intensity for all layers.

NOTE: when $C_e << C_S$ and $K_B >> 1$ and $K_{ad} = \frac{K_B}{C_s}$, BET isotherm approaches Langmuir isotherm.

Figure 2.8 gives the general graphical representation of BET isotherm.

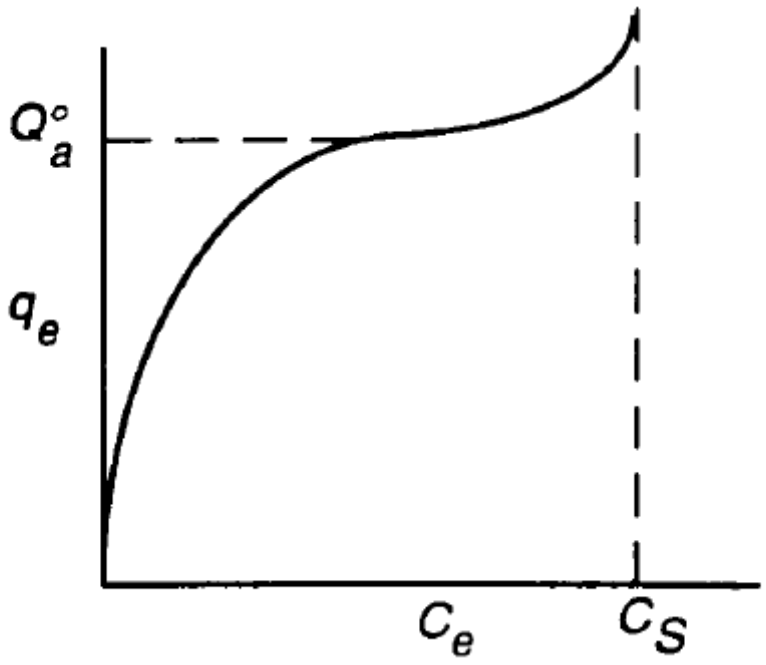


Figure 2.8: Graphical representation of BET isotherm model (University of Washington, n.d)

The linearized form of BET isotherm is given by equation:

$$\frac{c_e}{(c_e - c_s)q_e} = \frac{k_B - 1}{k_B Q^o}\frac{c_e}{c_s} + \frac{1}{k_B Q^o} \tag{2.18}$$

The Langmuir- Freundlich model is essentially a Freundlich isotherm which approaches an adsorption maximum at high concentration of adsorbate.

Redlich-Peterson (Redlich and Peterson, 1959) is a further empirical model developed to improve the fit by the Langmuir or Freundlich equation.

2.9.3 Mathematical Models in Fixed bed Columns.

The fundamental equations for a fixed-bed column depends on the mechanism responsible for the process (mass transfer from the liquid to the surface of the solid, diffusion and/or reaction on the surface of the solid) and include mass balances between the solid and the fluid and for the sorbed solute, rate of the process, etc. The equations derived to model the system with theoretical rigor are differential in nature and usually require complex numerical methods to solve (Calero et al., 2009). Because of this, various simple mathematical models such as Adam- Boharts, Thomas, Yoon and Nelson, etc. have been developed to predict the dynamic behavior of the column and allow some kinetic coefficients to be estimated.

Adams-Bohart model

Adams and Bohart in 1920 established the fundamental equation, which describes the relationship between C/C_i and t in a continuous system, and, although it was originally applied to gas-solid system, it has been extensively used to describe and quantify other types of systems (Bohart and Adams, 1920).This model is based on the assumption that the rate of adsorption is proportional to both the concentration of the adsorbing species and the residual capacity of the adsorbent. The Adams-Bohart model is only used for the description of the initial part of the breakthrough curve and is expressed as:

$$\frac{c_t}{c_o} = \exp\left(k_{AB} c_o t - \frac{k_{AB} N_o Z}{u_o} \right) \tag{2.19}$$

Where K_{AB} (l/min.mg) is rate constant of Adams- Bohart model, Z (cm) is the bed depth, N_o (mg/l) is maximum ion adsorption capacity per unit volume of adsorbent column, and U_o (cm/min) is the linear velocity of influent solutions. The linear form of Adams-Bohart model is expressed as:

$$\ln\left(\frac{c_t}{c_o} \right) = k_{AB} c_o t - \frac{k_{AB} N_o Z}{u_o} \tag{2.20}$$

Thomas model

The Thomas model (Thomas, 1944) is the most general models and is widely used to describe the behavior of the biosorption process in fixed-bed columns. Its main limitation is that its derivation is based on second order kinetics and considers that sorption is not limited by the chemical reaction but controlled by the mass transfer at the interface. This discrepancy can lead to errors when this method is used to model biosorption processes in specific conditions (Calero et al., 2009). Its derivation assumes Langmuir kinetics of adsorption-desorption and no axial dispersion.

The expression for the Thomas model is given as:

$$\frac{c_t}{c_o} = \frac{1}{1+\exp\left(\frac{k_{Th}q_e X}{Q} - k_{Th}c_o t\right)} \tag{2.21}$$

Where K_{Th} (ml/ min.mg) is the Thomas model constant, q_e (mg/g) is the predicted adsorption capacity, x is mass of adsorbent (g), Q is influent flow rate (ml/min), C_o is initial solution concentration (mg/l), and Ct is effluent solution concentration (mg/l). The linear form of Thomas model is expressed as:

$$\ln\left(\frac{c_o}{c_t} - 1\right) = \frac{k_{Th}q_e X}{Q} - K_{Th}c_o t \tag{2.22}$$

Yoon-Nelson model

Yoon and Nelson developed a relatively simple model focused on the adsorption of vapours or gases in activated coal (Yoon and Nelson, 1984). This model assumes that the rate of decrease in the probability of adsorption for each adsorbate molecule is proportional to the probability of sorbate sorption and the probability of sorbate breakthrough on sorbent. The Yoon-Nelson equation is expressed as:

$$\frac{c_t}{c_o - c_t} = \exp\left(k_{YN}t - \tau k_{YN}\right) \tag{2.23}$$

Where K_{YN} (l/min) is the rate constant and ι is the time required for 50% adsorbate breakthrough. The linear form of Yoon-Nelson model is expressed as:

$$\ln\left(\frac{c_t}{c_o - c_t}\right) = k_{YN}t - \tau k_{YN} \tag{2.24}$$

2.10 Desorption and Regeneration

If the biosorption process is to be used as an alternative to the wastewater treatment scheme, the regeneration of the biosorbent is crucially important for keeping the process costs down (Ahalya, et al., 2003). For this purpose, it is desirable to desorb the sorbed metals and to regenerate the biosorbent material for subsequent cycles of application. The desorption process should: yield the metals in a concentrated form; restore the biosorbent close to the original condition for effective reuse with undiminished metal uptake and without physical changes or damage to the biosorbent. It has been observed that for metal ions which show marked pH dependence in binding to the biomass, stripping of bound metal(s) can be accomplished by pH adjustments (Singh and Stapleton, 2002). While the regeneration of the biosorbent may be accomplished by washing the metal-laden biosorbent with an appropriate solution, the type and strength of this solution would depend on the extent of binding of the deposited metal. Dilute solutions of mineral acids like hydrochloric acid, sulphuric acid, acetic acid and nitric acid can be used for metal desorption from the biomass (de Rome and Gadd, 1987; Zhou and Kiff, 1991; Luef et al., 1991; Holan et al., 1993; Pagnanelli et al., 2002; Bai and Abraham, 2003).

CHAPTER THREE

MATERIALS AND METHODS

3.1 Introduction

This chapter presents the materials, experimental methods and analytical techniques used during this research.

3.2 Materials

3.2.1 Biosorbent

Spent waste yeast biomass was collected from the fermentor at South African Breweries (SAB) and transported to the laboratory in plastic containers. The yeast cells were washed with distilled water. After washing, the biosorbent was separated by centrifugation. The biosorbent was air dried and stored for further use.

3.2.2 Dilute Process Solution

The dilute industrial solution used for the continuous process was collected at the process outlet stream of PGMs Refinery of Impala Platinum, Springs, South Africa.

3.2.3 Reagents

All reagents used in this study were of analytical grade obtained from Merck and Sigma Aldrich, South Africa (unless otherwise stated), and were used as obtained without further purification.

3.2.4 Plaster of Paris (POP).

The Plaster of Paris used in biomass immobilization was purchased locally in a hardware shop.

3.3 Experimental methods

3.3.1 Chemical Treatment of Yeast Cells

Caustic treated cells were prepared by suspending 30g of yeast cells in 100ml 1mol/l NaOH and the resulting solution was heated to 70^0c for 20 min (Goksungur et al., 2002; Lu and Wilkins, 1996).

Ethanol treated cells were prepared by suspending 30g of yeast cells in 100ml of 700g/l ethanol solution for 20 min (Goksungur et al., 2002). After treatment, yeast cells were collected by centrifugation, washed several times with distilled water and air dried.

3.3.2 Preparation of stock solution.

The stock solutions of Pt (II), Au (III), Pd (II), Rh (III), and Ir (III) (1000ppm) were prepared by dissolving weighed quantity of K_2PtCl_4, $AuCl_3$, $PdCl_2$, $RhCl_3.3H_2O$ and $IrCl_3.XH_2O$ respectively in distilled water. The stock solutions were diluted with distilled water to obtain the desired initial metal concentrations. The composition of the synthetic aqueous solutions used in this study was simulated on the basis of the analysis of the real dilute PGMs solution composition obtained from Impala Platinum Precious Metal Refinery, Springs, South Africa. The pH of the solution was adjusted using dilute HCl or NaOH. Synthetic solution was used for all the batch test works.

3.3.3 Batch adsorption studies

Batch experiments were carried out to determine the effect of biomass pretreatment with respect to contact time on the adsorption of each metal.

0.5g of treated and untreated bio sorbents were differently added to 100ml of metal solution containing 10 mg/l Pt, Pd, Au, Rh and Ir in 250 ml Erlenmeyer flasks. The flasks were agitated on a rotary shaker (150rpm) at 30^OC for 3 hrs. Samples (1ml) were taken at different time intervals over 3hrs, the samples were then centrifuged and the supernatant liquids were analysed for metal concentration using ICP-MS

(Inductively coupled plasma mass spectrometry). The metal adsorbed by the biomass (q) in mg/g and the percentage removal (θ) in % was calculated as:

$$q = \frac{(C_i - C_f)V}{S} \tag{3.1}$$

$$\theta = \frac{(C_i - C_f)100}{C_i} \tag{3.2}$$

Where C_i is the initial sorbate concentration (mg/l), C_f is the equilibrium sorbate concentration, V is the volume of the test solution and S is the amount of added biosorbent (g).

3.3.4 Design of Experiments

One of the key objectives of this study is the screening and identification of important factors that have an influence on the adsorption of PGMs from the process solutions. Therefore, a statistical design of experiment (DOE) method was employed as a research tool to develop an experimentation strategy to execute this objective. The advantage of using DOE is that it provides a quantitative approach in which an appropriate experimental matrix can be selected (Musapatika et al., 2010). Therefore, by using DOE, one obtains more precise information about the studied system.

Screening of factors was done at the beginning so as to explore some factors and their possible influence on the adsorption of PGMs from dilute streams and to identify their appropriate ranges. A 2^4 full factorial design was employed in determining the influential factors. A statistical analysis of experimental results was employed to evaluate the significance of factors using the normal probability plots.

3.3.5 Equilibrium Studies

Following the identification of influential factors, equilibrium studies were conducted at 0.1, 0.5, 1, 5 and 10ppm initial metal ion concentration at constant temperature in order to evaluate the isotherm parameters of the tested PGMs onto the yeast biomass using a single metal ion system. 100ml metal solution of desired concentration was taken in 250ml Erlenmeyer flasks. To this solution, 0.5g of biomass was added and the mixture was agitated in a rotary shaker at 150rpm. At the end of 4hrs, samples were taken and centrifuged and the supernatant liquids were analyzed for metal concentration using ICP-MS (Perkin Elmer Nexlon 300D). The agitation speed used was based on the information from literature (Zhou et al., 2009) while the experimental time was based on the preliminary experiments carried out.

3.3.6 Adsorption- desorption Experiments.

The adsorption and desorption experiments were carried out using different concentrations of thiourea, HCl, H_2SO_4 and thiourea- HCl solution.

The yeast biomass with adsorbed metal was washed with distilled water to remove any metals loosely attached to the adsorbent.100ml of different concentrations of eluants were added to 250ml Erlenmeyer flasks containing 0.5g yeast biomass loaded with PGMs. The bottles were shaken at room temperature at 150rpm for 4hrs using an orbital shaker.

The adsorbed and desorbed metal ions were analyzed using ICP-MS and desorption efficiency was calculated as follows:

$$Desorption\,efficiency(\%) = \frac{released\,metal\,ion(mg)}{initially\,sorbed\,metal\,ion(mg)} \qquad (3.3)$$

After each desorption cycle, the yeast biomass was washed with distilled water and pre-treated again with 20ml ethanol for 10minutes for the next adsorption cycle.

3.3.7 Yeast immobilization in Plaster of Paris.

Immobilization of the yeast biomass was carried out using Plaster of Paris (POP) as supportive material by the method reported by Ghosh, 1988. The ethanol treated yeast was suspended in water to which the plaster was added to form a thick dough. The final concentration of yeast was 20% (w/v). Beads (4.5-5.5mm) were cast from this dough and kept overnight at 26-28℃. The beads were then washed in running tap water to remove any loosely adhered yeast and were again kept overnight at 26-28℃. Slight modification in the immobilization procedure was made as; radiation killing of the yeast cells was avoided (radiation killing is a form of heat treatment using ultraviolent light) and yeast cells were used as is after immobilization for purification of the PGMs effluent. Plaster of Paris was chosen as a supportive material in this study because of its cost effectiveness as compared to other supportive materials in the literature. The immobilised yeast was used for the column studies.

3.3.8 Characterisation of PGMs industrial process dilute stream.

Effluent was characterised for; total solids (TS), total dissolved solids (TDS), total suspended solids (TSS), pH, chlorides, ammonia, sulphates, salinity (conductivity), chemical oxygen demand (COD), PGMs and base metals.Table 3.1 gives the chemical composition of the PGMs stream as received.

Table 3.1: Composition of PGMs sample

Characteristics	Acidic Sample	Alkaline Sample
pH	1.8	8.5
Total conductivity(mS/m)	12,644	15,423
colour	Brown	Pale brown/yellow
COD (mg/l)	200	221
TSS (mg/l)	1080	1230
TDS (mg/l)	220	304
TS (mg/l)	1300	1534
Chlorides(mg/l)	3497	856
Sulphate (SO_4) (mg/l)	10947	70349
t (NH_3) (mg/l)	79.1	‹2.5
Ag (mg/l)	0.004	0.002
Au (mg/l)	0.015	‹0.001
Pd (mg/l)	0.248	0.215
Pt (mg/l)	1.88	2.72
Rh (mg/l)	0.065	0.029
Ir (mg/l)	8.25	3.8
Ru (mg/l)	0.937	5.12
Co (mg/l)	0.026	0.947
Cu (mg/l)	0.275	0.787
Zn (mg/l)	0.077	0.310
Te (mg/l)	1.24	10.1
Se (mg/l)	416	1113
Fe (mg/l)	1.17	1.10
Na (mg/l)	45100	103850
Ni(mg/l)	2.08	41.4

3.3.9 Column Experiments.

Column experiments were conducted in an acrylic glass tube of 2.5cm inner diameter and 45cm height packed with yeast immobilized on Plaster of Paris. Glass beads were introduced at the top and the bottom of the packed column to prevent the adsorbent from floating. The PGMs dilute process solution was conditioned to pH 3 (the optimum pH for adsorption obtained under the batch experiments) using 0.1M NaOH or HCl solution. The solution of known concentration of solutes was pumped through the column in an up flow direction using a peristaltic pump (Watson Marlow 5045) with variable speed adjustment. The up flow movement was chosen because it

minimises clogging and unintentional filtration. Samples were collected from the column at regular time intervals and analysed by ICP-MS (Perkin Elmer Nexlon 300D). Figure 3.1 shows the experimental set up for the column study.

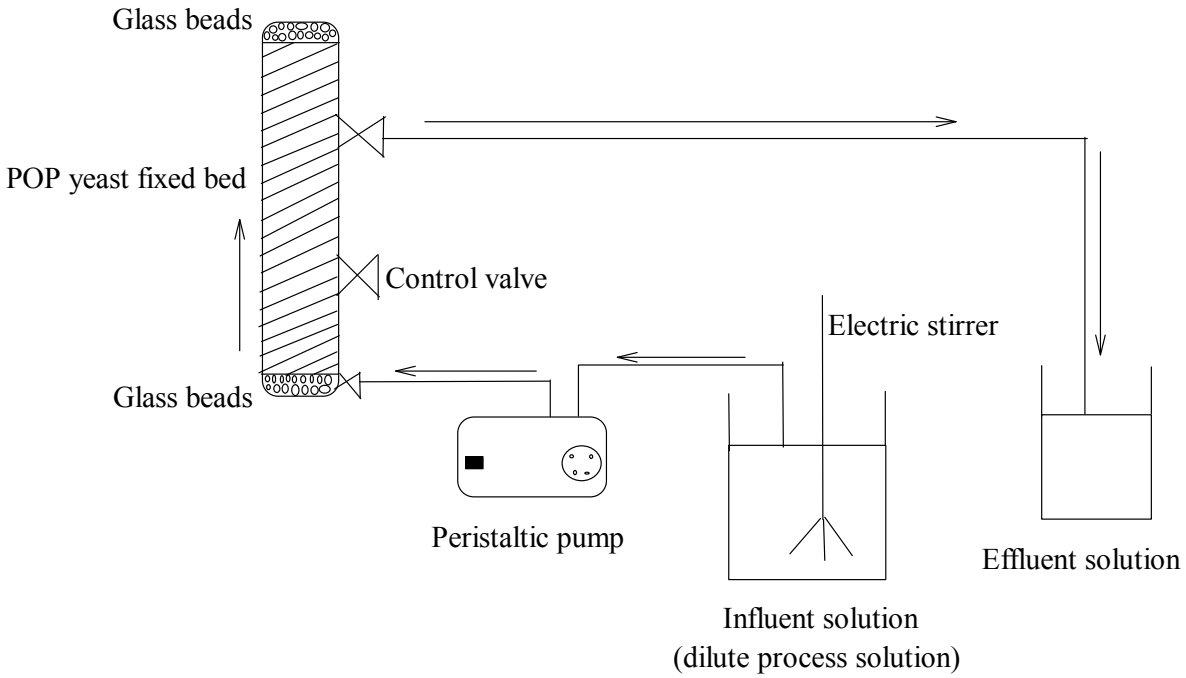


Figure 3.1: Experimental set up for column study.

The experimental conditions chosen for the sorption performance of POP yeast in a fixed bed column is presented in Table 3.2:

Table 3.2: Experimental condition for column studies

Operating Parameters	Levels
Flow Rates	0.9ml/s, 1.3ml/s, 2.1ml/s
Bed Depth	6.5cm, 8.5cm, 13cm
pH	3
Time	180minutes

The experimental conditions for column studies (the flow rates and the bed depth) were chosen based on the information from literature (Calero et al., 2009; Danny et al., 2000). The pH and the time used was based on the information gathered from the batch studies.

3.3.10 Column model

The loading behaviour of solutes to be removed from solution in a fixed bed is usually represented in term of C/C_o where (C = effluent concentration and C_o= influent concentration (mg/l). C/C_o is then plotted against time to obtain breakthrough curves. The maximum column capacity, q_{total} (mg) for a given feed concentration and flow rate is equal to the area under the plot of the adsorbed solute concentration and is calculated from the equation below:

$$q_{total} = \frac{QA}{1000} = \frac{Q}{1000}\int_{t=0}^{t=t} Cad\,dt \tag{3.4}$$

where t_{total}, Q and A are the total flow time (min), volumetric flow rate (ml/min) and the area under the breakthrough curve respectively

The equilibrium uptake q_{eq} (exp) is calculated as follows:

$$q_{eq}(\exp) = \frac{q_{total}}{m} \tag{3.5}$$

where m is the total dry weight of adsorbent in column (g).

The total amount of solute pumped to the column W_{total} (mg) is calculated from equation below:

$$W_{total} = C_o Q \frac{t_{total}}{1000} \tag{3.6}$$

where C_0 is the influent concentration (mg/l), Q is the flow rate (ml) and t_{total} is the total flow time (min).

Total percentage removal (R) is the ratio of the maximum capacity of the column (q_{total}) to the total amount of solute sent to column (W_{total}).

$$R = \frac{q_{total}}{W_{total}} \times 100 \tag{3.7}$$

The total volume of effluent treated V_{ef} (ml) is calculated from the equation below:

$$V_{ef} = Qt_{total} \tag{3.8}$$

where Q is the volumetric flow rate (ml) and t_{total} is the total flow time (min).

3.3.11 Kinetic models

In this work, two models were used namely Adam-Bohart and Thomas models for kinetic studies.

Adam –Bohart model is used for the description of the initial part of the breakthrough curve. The linear form of Adam- Bohart is expressed as:

$$\ln\left(\frac{C_t}{C_o}\right) = K_{AB}C_o t - K_{AB}N_o\frac{Z}{U_o} \tag{3.9}$$

Where K_{AB} (l/min.mg) is rate constant of Adams- Bohart model, Z (cm) is the bed depth, N_o (mg/l) is maximum ion adsorption capacity per unit volume of adsorbent column, and U_o (cm/min) is the linear velocity of influent solutions. The values of N_o and K_{AB} which describes the characteristics operation of the column were determined from the slope and the intercept of the plot.

The linear expression for the Thomas model is given as:

$$\ln\left(\frac{C_o}{C_t} - 1\right) = \frac{K_{Th}}{Q}q_e X - K_{Th}C_o t \tag{3.10}$$

Where K_{Th} (ml/ min.mg) is the Thomas model constant, q_e (mg/g) is the predicted adsorption capacity, X is mass of adsorbent (g), Q is influent flow rate (ml/min), C_o is initial solution concentration (mg/l), and C_t is effluent solution concentration (mg/l).

3.4 Analytical Techniques

3.4.1 Determination of the surface functional group

Fourier transforms infrared (FTIR) spectra analysis was carried out in the range 500cm^{-1}-4000cm^{-1} using FT-IR spectrometer (FT – IRM Bruker Tensor 27) in order to explore the number and positions of the functional groups responsible for adsorption.

3.4.2 Determination of the pH of the point of Zero Charge (PZC)

The pH of the point of zero charge of the biomass was determined using the procedure of mass titration as follows:

Three different solutions of pH 3, 6 and 11 of 0.1M $NaNO_3$ were prepared.

For each initial pH, six containers were filled with 100ml of 0.1M $NaNO_3$ solution and different amount of yeast biomass was added (0.05%, 0.1%, 0.5%, 1%, 5%, and 10% by weight/volume of solution).The resulting solutions were agitated on a rotary shaker at 150 rpm for 24hrs and the equilibrium pH after 24hrs was measured (Simate et al., 2012).

3.4.3 Determination of surface area and pore structure

The Brunauer Emmett Teller (BET) surface area and pore structural parameters of the adsorbents were determined from the adsorption-desorption isotherm of nitrogen at -196.15°C using Micrometrics (Tristar 3000) surface area and porosity analyzer. All the samples were degassed at 180°C for 4 hours, prior to adsorption- desorption experiments.

3.4.4 Surface Morphology

The surface morphology of the yeast was visualized using a scanning electron microscope (Model Quanta- 400F, FEI).

3.4.5 Determination of metal ion concentration

The inductively coupled plasma ICP-MS (Perkin Elmer Nexlon 300D) was used for the analysis of metal ion concentration in solution.

3.4.6 Determination of total solid (TS), total suspended solid (TSS) and total dissolved solid (TDS)

The determination of total solids, total suspended solids and total dissolved solids in the dilute process solution were done using gravimetric method as highlighted below:

Total Solid*:* A dry 250ml glass beaker which was kept at $103\,^{\circ}C$ in an oven for 1hr was weighed. 100ml of thoroughly mixed dilute process solution was measured in the beaker and the beaker was placed in an oven maintained at $103\,^{\circ}C$ for 24hrs. After 24hrs, the beaker was cooled and reweighed and the total solid was calculated as follows:

$$Total\ solid\ (mg/l) = \frac{mg\ of\ solid\ in\ the\ beaker}{Volume\ of\ sample} \times 1000 \quad (3.11)$$

Total dissolved solid: A dry 250ml glass beaker which was kept at $103\,^{\circ}C$ in an oven for 1hr was weighed.100ml of thoroughly mixed dilute process stream was measured and filtered through a double layered filter paper. The filtrate was collected and placed in an oven maintained at $103\,^{\circ}C$ for 24hrs. After 24hrs, the beaker was cooled and reweighed and the dissolved solid content was determined as follows:

$$Total\ dissolved\ solid\ (mg/l) = \frac{mg\ of\ solid\ in\ the\ beaker}{Volume\ of\ sample} \times 1000 \quad (3.12)$$

Total suspended solid: The total suspended solid in the sample was calculated as follows:

$$Total\ suspended\ solid\ (mg/l) = Total\ solid\ (mg/l) - Total\ dissolved\ solid\ (mg/l) \quad (3.13)$$

3.4.7 Determination of chemical oxygen demand (COD)

Chemical oxygen demand (COD) was determined with Spectroquant (Pharo 300) in accordance with the instructions of the manufacturer.

The analysis to determine chlorides, ammonia, sulphate and salinity was done by Setpoint Laboratories, Isando, South Africa and it was based on the method used by the said laboratory.

CHAPTER FOUR

RESULTS AND DISCUSSIONS

4.1 Characterization of Biosorbent

4.1.1 Fourier transform infrared spectroscopy (FTIR).

The FT-IR was used to identify the existence or absence of functional groups on the surface of the yeasts. Infrared spectrum measures the quantity of radiation absorbed versus its frequency. The IR spectra play an important role in the analysis of these organic functional groups and the mechanism of metal ions adsorbed by the adsorbents (Zhang et al., 2010). Figures 4.1- 4.4 show the FT-IR spectra of the untreated, ethanol treated and NaOH treated biomass. The availability of a particular functional group or binding site does not necessarily guarantee its accessibility as an adsorption site for a metal ion, because of the presence of steric, conformational or other types of barriers. The spectrum of the untreated yeast biomass was complex due to the numerous and multifarious functional groups on the biomass. The absorbance peaks at 3282.94, 2926.32, 1638.36, 1541.63, 1460.08, 1398.17, 1238.13, and 1042.73cm^{-1} were observed in the untreated biomass spectrum shown in Figure 4.1

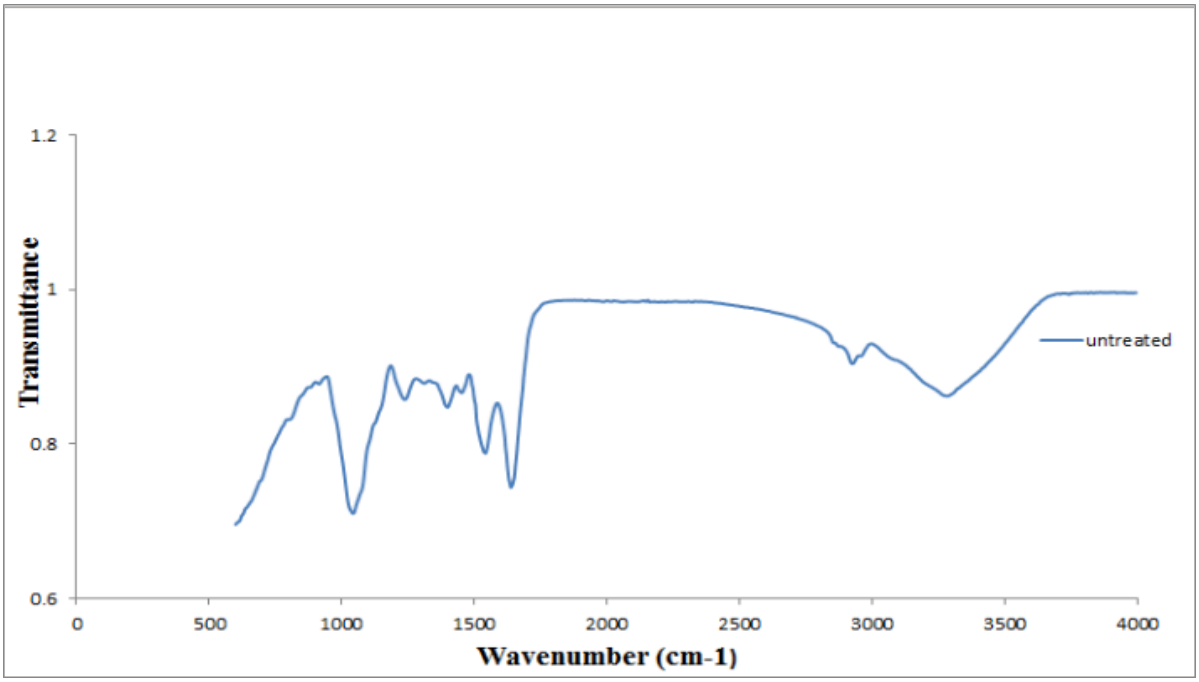


Figure 4.1: IR spectra of untreated yeast.

The broad strong band at 3282.94cm^{-1} corresponded with overlapping of –NH/-OH stretching,-COOH stretching and stretching band of C-H. The strong peak at 2926.32cm^{-1} indicates the H-C-H asymmetric and symmetric stretch. The strong peaks at 1638.36 and 1541.63cm^{-1} indicated the stretching band of C=O, C=C, N=O which can be attributed to carboxylic acid, ketones, aldehydes , alkenes, nitro group and the bending band of N-H from amide 11 functional group respectively. The weak peak at 1460.08 is attributed to the asymmetric stretching band of C=C and bending band of N-H. The band at 1398.17cm^{-1} belonged to the bending band of carboxyl and Nitro (N=O) groups. The peak at1238.13 indicated the stretching band of C-N (amine 2^0), C-O (esters or ethers) and P=O (phosphonate). The absorbance peak at 1042.73cm^{-1} is attributed to glycitols (C-OH) and the stretching band of S=O (sulfoxide), Si-OR or P-OR esters. This means that the main organic functional groups on the waste yeast cell wall were carboxyl, amino/hydroxyl, phosphoryl, sulfhydryl, nitro group, silicon group, etc. In biosorption process, these functional groups serve as binding sites for the metals or species of interest.

After ethanol pretreatment, some IR spectrum changes of the untreated biomass were observed as seen in Figure.4.2

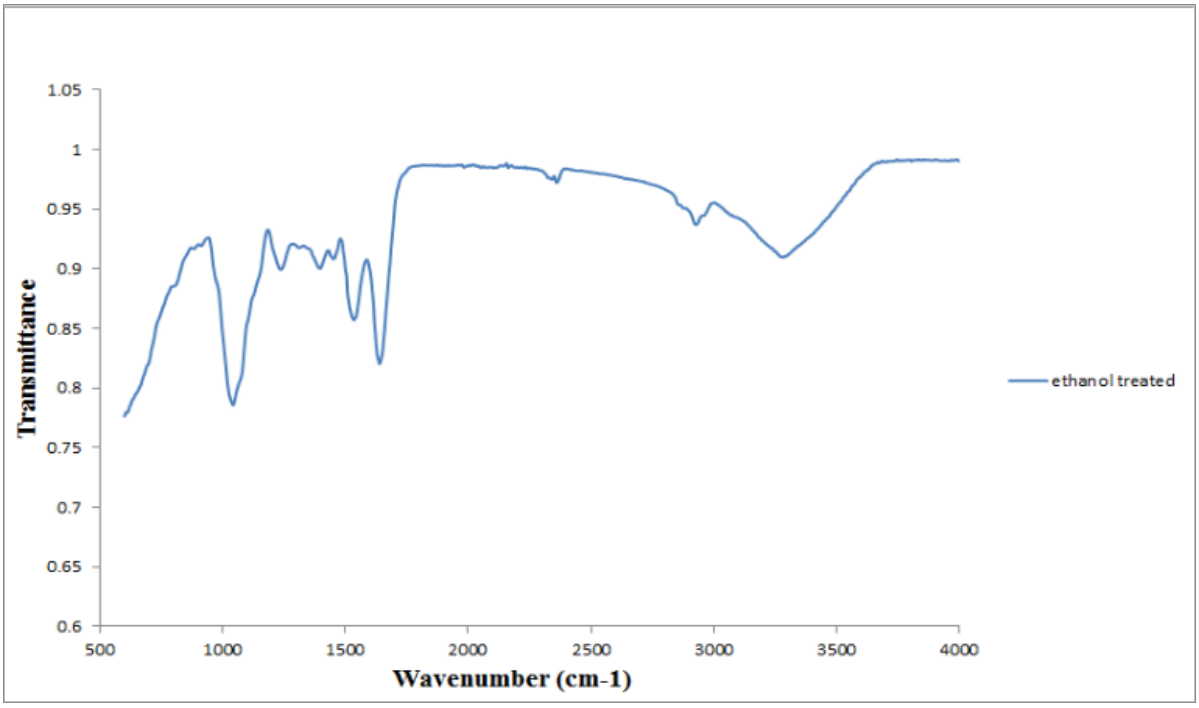


Figure 4.2: IR spectra of ethanol treated yeast.

First, the bending band of N-H from amide11and the asymmetric stretching band of C=C moved 6.3cm^{-1}, 8.5cm^{-1} to a low frequency direction respectively. Second, the bending band of carboxyl and nitro group moved from 1398.17 to1397.39cm^{-1}., the stretching band of C-N, C-O, and P=O also moved from 1238.13 to 1236.77cm^{-1} because the ethanol molecule would denature the protein on the cell walls of the biomass. The –NH/-OH increased and a large number of amine groups on the surface of the ethanol treated yeast were exposed. In addition, a new absorbance peak at 2359.08cm^{-1} representing silicon (Si-H) and phosphorous (P-H) groups appeared.

After caustic pretreatment, some IR spectrum changes of the untreated biomass were also observed as seen in Figure.4.3.

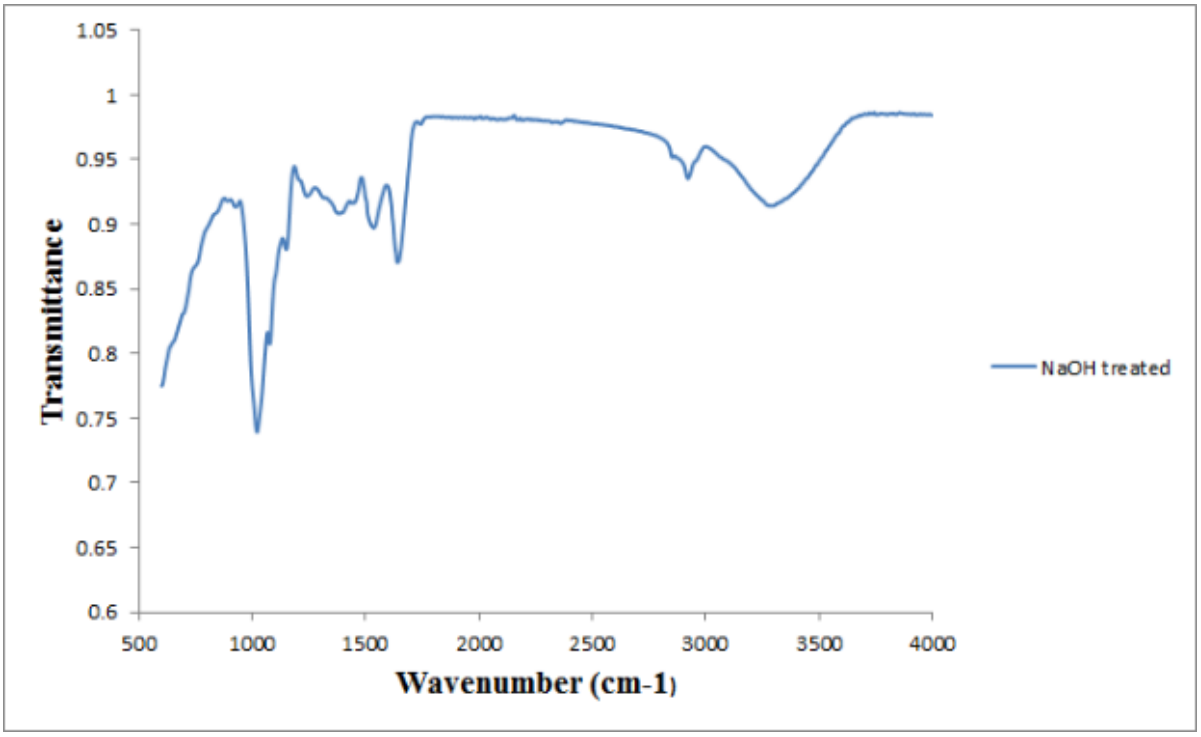


Figure 4.3: IR spectra of NaOH treated yeast.

The stretching band of –NH/-OH moved from 3282.94 to 3296.95cm^{-1}. Second, two weak absorbance peaks at 1150.24 and 1077.35cm^{-1} representing the stretching band of C-O and C-N. The absorbance peaks at1638.36, 1541.63cm^{-1} moved to1640.43 and1535.37 respectively. The characteristic peak of carboxyl and nitro group also shifted 9.61cm^{-1} to a low frequency direction and the stretching band of C-N, C-O, and P=O moved from 1238.12 to 1242.35cm^{-1}. In addition, the absorbance of glycitols (C-OH) and the stretching band of S=O (sulfoxide), Si-OR or P-OR moved almost 22cm^{-1} to a low frequency direction. All of these phenomena meant that the polysaccharide and the steric configuration of protein in the cell wall was destroyed by the hydrolysis of sodium hydroxide, and a large quantity of polypeptide, amino-acid residues was exposed. At any rate, the pretreatment of the yeast biomass resulted in the structure of the biomass changing and the amount of organic functional groups increased and being exposed (Zhang et al., 2010). The clear differences between the IR spectra of the untreated, ethanol treated and caustic treated is presented in Figure 4.4.

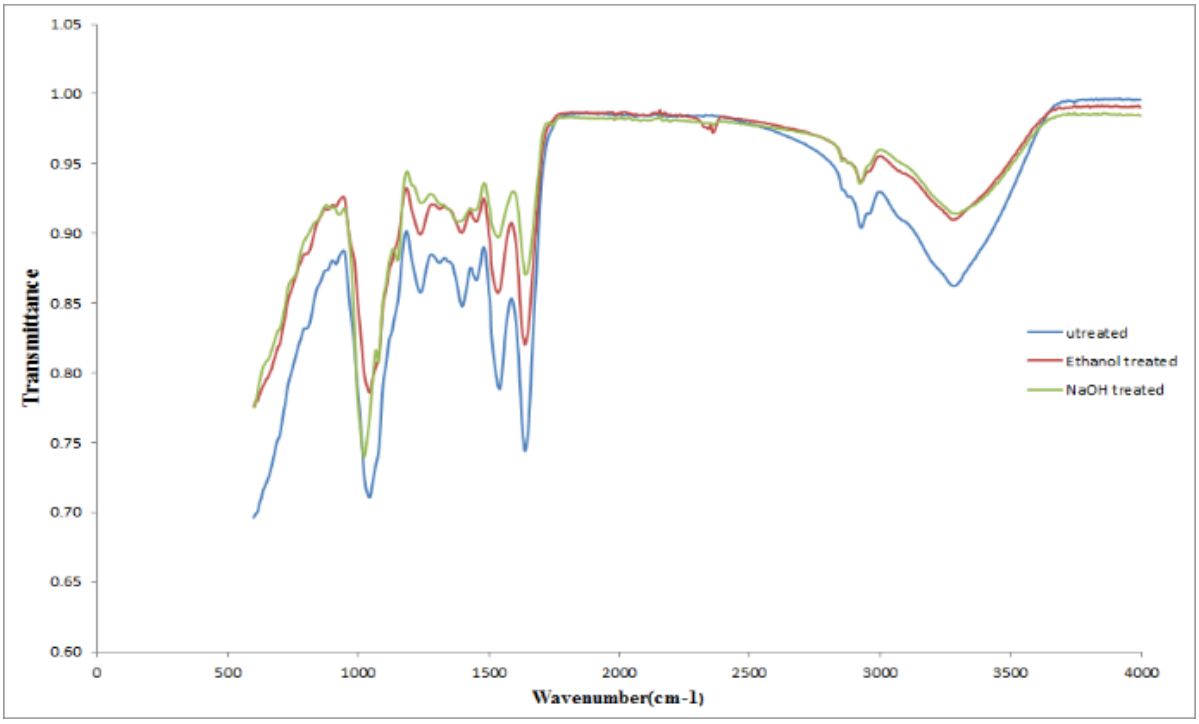


Figure 4.4: Comparison of IR spectra of the three biomasses.

4.1.2 BET Analysis

Adsorption is a surface phenomenon and the rate and extent of adsorption are functions of the specific surface area of the adsorbent used. The amount of adsorption per unit weight of adsorbent depends on its composition, texture and porosity (Musapatika et al., 2010). The specific area of an adsorbent is the ratio of its surface area to its mass. Specific surface area considers the combined effects of particle size and slenderness or thinness of the particle in a measurement that is independent and complementary to grain size distribution. There is a considerable effect of particle size on specific surface area; as the particle size decreases, the specific surface area increases (Onwu and Ogah, 2010). The physicochemical characteristics of the yeasts used in the study are presented in Table 4.1.

Table 4.1: Physicochemical properties of *Saccharomyces cerevisiae* yeast

Property	Untreated	Ethanol treated	NaOH treated
Surface area (m^2/g)	0.543200	1.634000	1.061200
Pore volume (cm^3/g)	0.001974	0.006795	0.004761
Pore size (nm)	11.633710	14.142980	15.061870

From the table, it can be seen that the specific surface area, pore volume and pore size increased after ethanol and caustic pretreatment of the yeast biomass. However, the increase in the specific surface area and pore volume are more significant in ethanol treated biomass. Since the specific surface area varies inversely with the particle size, it can therefore be concluded that the chemical treatment of the biomass resulted in a decrease in the particle size of the yeast.

4.1.3 Determination of Point of Zero Charge.

The pH value at which the Zeta potential equals to Zero is called the point of Zero charge (PZC) or the isoelectric point (IEP). It is used to assess the adsorbent surface charge qualitatively. At pH< PZC, the surface of the adsorbent is positively charged and is accessible to anions, at pH = PZC, the surface is neutral, and at pH > PZC, the surface is negatively charged and will repel the anions (Simate et al., 2012). The mass titration results for untreated and ethanol treated yeast is shown in Figures 4.5 and 4.6 respectively. A plateau is obtained in this plot of pH versus mass fraction.

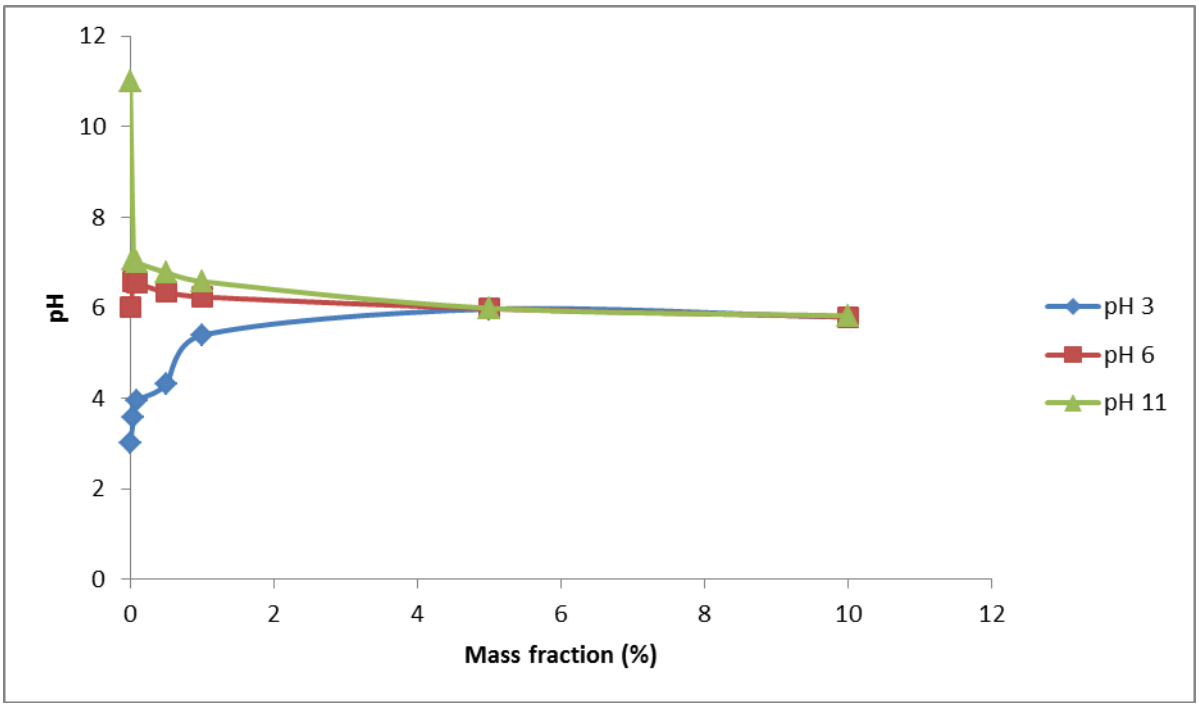


Figure 4.5: Mass titration results for untreated yeast.

By taking the average value of the asymptotic pH values (asymptotes to x-axis), the pH of the PZC for untreated yeast and ethanol treated yeast were found to be 5.89 and 6.31 respectively. It has been observed by various researchers that the pH_{pzc} of an adsorbent decreases with an increase in the acidic groups on the surface of the adsorbent. From the results, it can be observed that the pH_{pzc} of the ethanol treated yeast tends towards negative (basic) surface charge for the biomass since the pH_{pzc} for the treated was found to be higher than that of the untreated biomass. This therefore, implies that the ethanol treatment of the yeast cells led to a decrease in the acidic groups on the surface of the biomass thereby leading to an increase in pH_{pzc}.

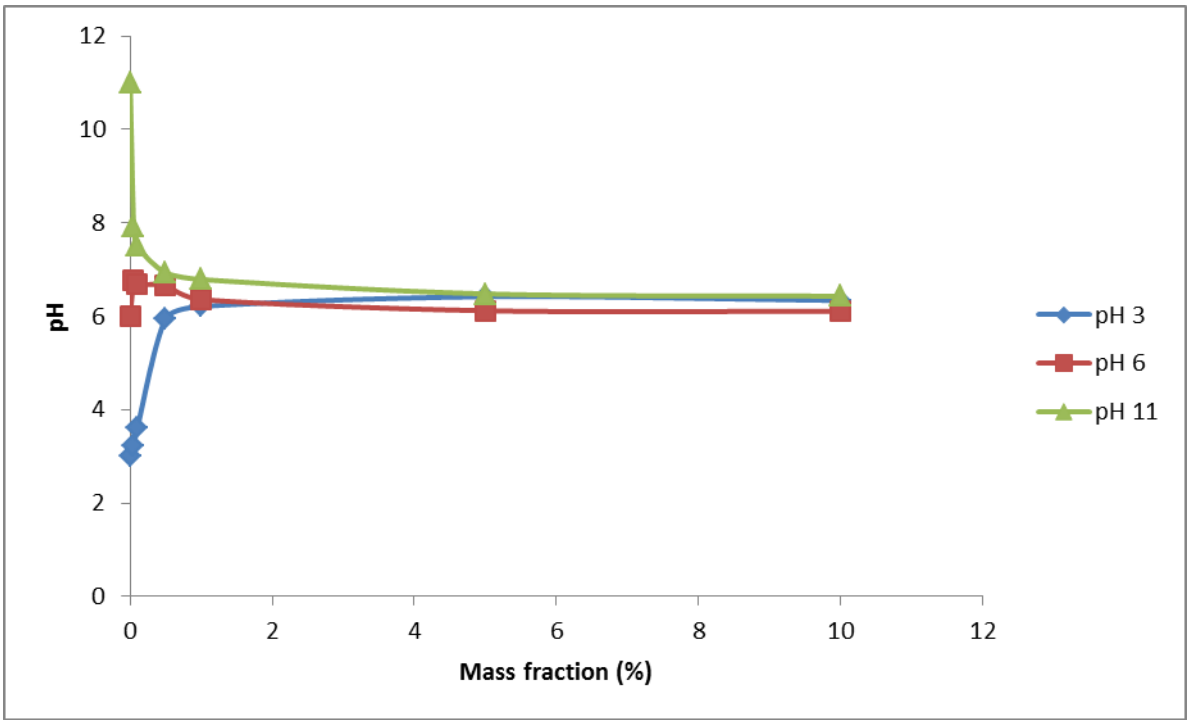


Figure 4.6: Mass titration results for ethanol treated yeast.

Thus, it can be concluded that ethanol treatment of the biomass increased the pH_{pzc} of the biomass from pH 5.89 to 6.31. The point of zero charge of the sodium hydroxide treated yeast biomass was, however, not determined. This is because it was very difficult to separate the yeast cell from sodium hydroxide solution due to very high solubility of the yeast in sodium hydroxide (a large quantity of biomass was needed for the mass titration).

4.1.4 Surface Morphology

Figure 4.7 (a-d) shows the SEM images of untreated, sodium hydroxide treated, ethanol treated and PGMs loaded *Saccharomyces cerevisiae* waste yeast after adsorption. The differences in the surface morphology of the yeast can be analyzed by comparing the images. Figure 4.7a shows that the original waste yeast biomass consists of an irregular leaf-like filament structure. Figure 4.7b shows that after chemical pretreatment with ethanol, the surface of the biomass becomes cleaner with the appearance of some micro pore structures. Generally, treatment with ethanol increased the specific surface area for adsorption which is validated by BET analysis.

Figure 4.7c shows that the appearance of the biomass changed considerably after treatment with sodium hydroxide. Treatment with sodium hydroxide resulted in dissolution and hydrolysis of the polysaccharide on the cell wall of the yeast and the yeast structure became much more compact. The surface of the ethanol treated biomass became rough after adsorption (Figure 4.7d) which confirms accumulation of PGMs within the biomass.

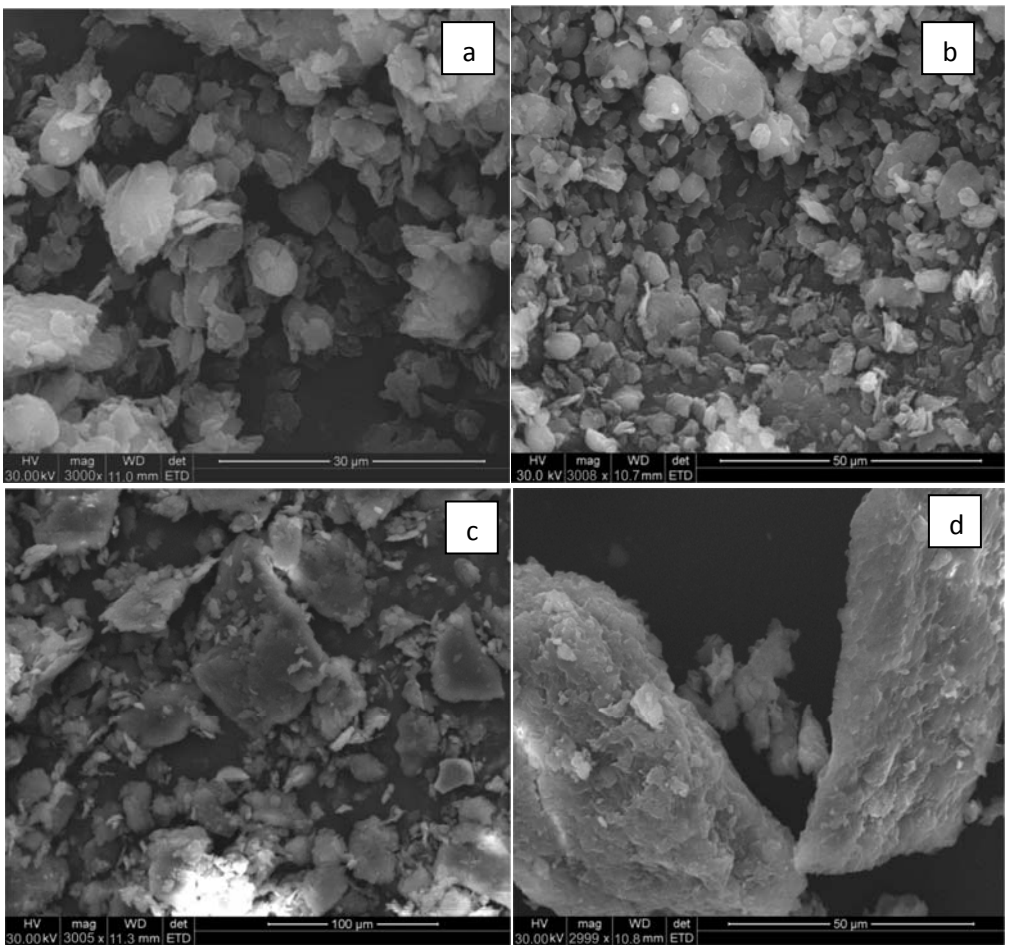


Figure 4.7: SEM of waste *S.cerevisiae* (a) original yeast (b) ethanol treated (c) sodium hydroxide treated (d) ethanol treated after adsorption all at 3000 times magnification.

4.2 Batch Studies

4.2.1 Effect of Biomass pretreatment

Batch experiments were carried out to determine the variation of percentage adsorption of differently treated yeast biomass with respect to time. Figure 4.8 – 4.12 shows the effect of biomass pretreatment on the adsorption of Pt (II), Pd (II), Au (III), Rh (III) and Ir (III) from single metal ion system. From the Figures, it can be seen that in all cases the metal ion adsorption by ethanol treated biomass was greater than the untreated and caustic treated biomass. Ethanol treated biomass gave the highest adsorption uptake of 88.4% removal for platinum, 86% for gold, 81.3% for palladium, 41.3% for rhodium and 15.7% for iridium. Ethanol treatment of the biosorbent increased the biosorption capacity of the biomass.

The higher metal uptake values obtained by ethanol treated yeast biomass may be explained by the increase in the availability of binding sites and thereby improvement in the access of metal ions to the binding sites of the yeast biomass. Furthermore, Zhang et al. (2010) reported that treatment of the yeast with ethanol possibly resulted in the biomass protein denaturing and the yeast cell walls being destroyed. Thus the permeability within the internal structure of the yeast improves, and more organic functional groups on the yeast are exposed

Based on the information given in Table 4.1, it is expected that sodium hydroxide treated yeast should give higher adsorption uptake compared to the untreated yeast because of the increase in the surface area, pore volume and pore size but the reverse is the case. This may be due to the considerable dissolution of the yeast in sodium hydroxide which led to the loss of the biomass with metal binding capacity. Alkali treatment dissolves a considerable amount of biomass which would not be retained during normal filtration, such as manno-protein from the cell wall, and these base soluble materials also have metal-binding capacity (Lu and Wilkins, 1996).This accounts for the drastic reduction in PGMs sorption by sodium hydroxide treated yeas. In addition, the FTIR diagram (Figure 4.3) for sodium hydroxide treated yeast showed that after treatment with sodium hydroxide, the absorbance peaks at 1238.14, 1398.17 and 1460 which belongs to the stretching band of C-N, C-O and P=O, the

bending band of carboxyl and nitro groups, and the asymmetric stretching band of C=C and N-H disappeared, respectively. The loss of these functional groups also contributed to the low adsorption uptake observed in sodium hydroxide treated yeast. Therefore, subsequent experiments were conducted using ethanol treated yeast biomass.

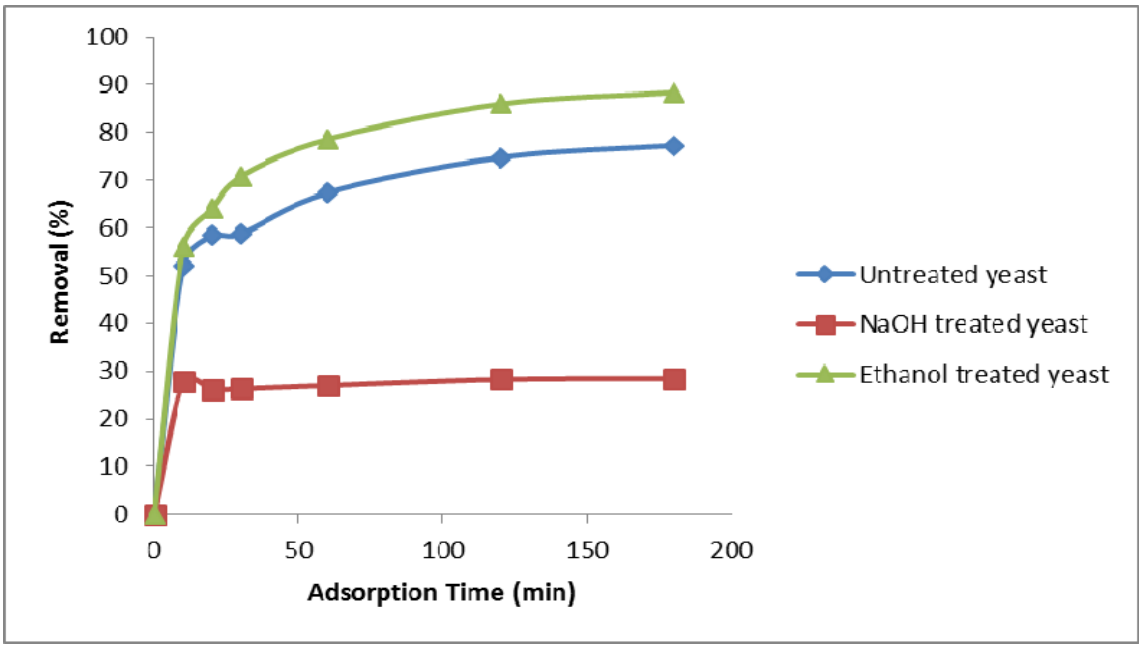


Figure 4.8: Effect of biomass pretreatment on the adsorption of Pt (II) (initial metal ion concentration = 10mg/l, biomass dosage = 0.5g, agitation speed = 150rpm, temperature = 30°C, contact time = 3hrs).

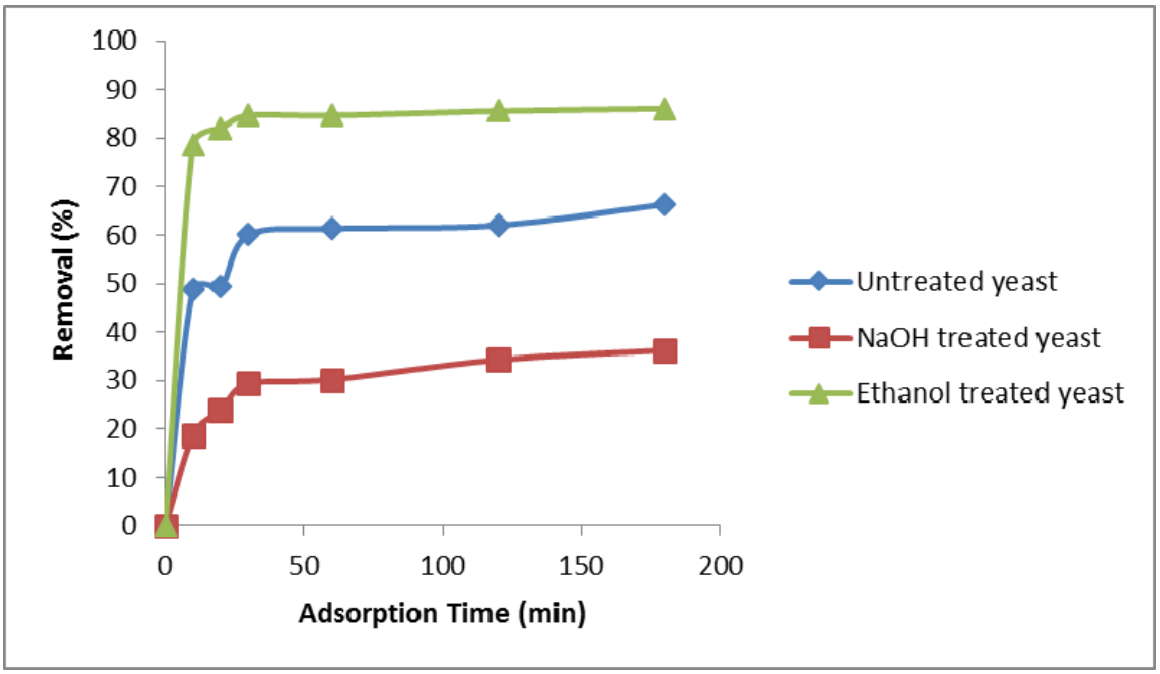


Figure 4.9: Effect of biomass pretreatment on the adsorption of Au (III) (initial metal ion concentration = 10mg/l, biomass dosage = 0.5g, agitation speed = 150rpm, temperature = 30°C, contact time=3hrs).

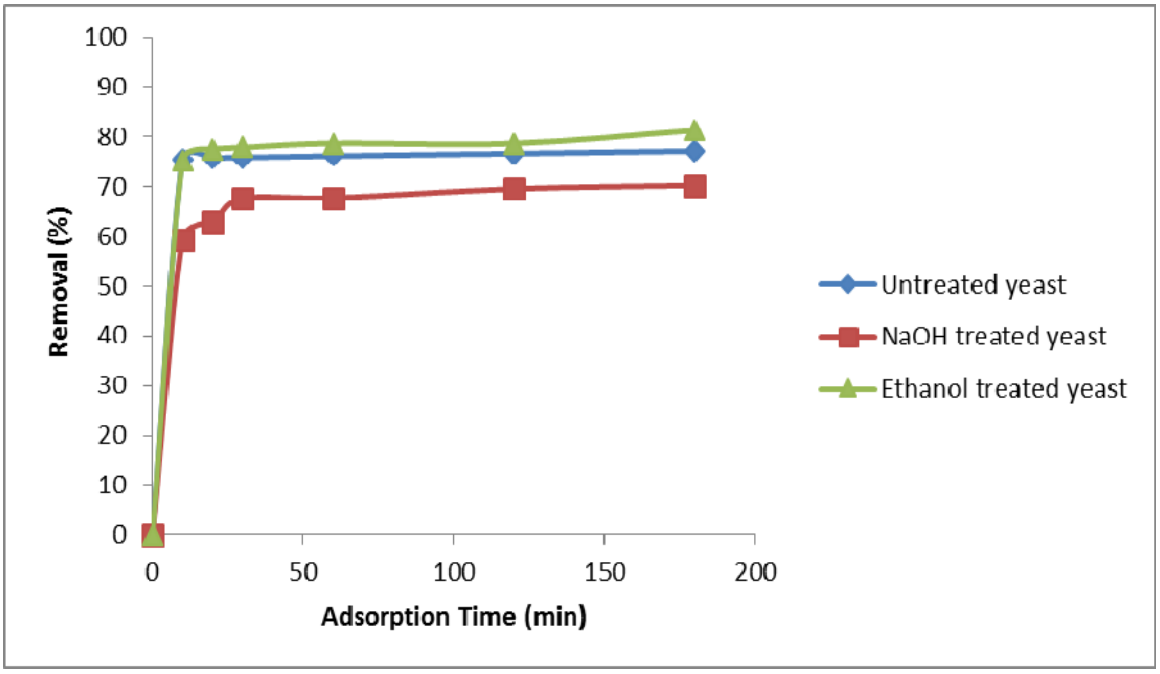


Figure 4.10: Effect of biomass pretreatment on the adsorption of Pd (II) (initial metal ion concentration =10mg/ biomass dosage = 0.5g, agitation speed = 150rpm, temperature 30°C, contact time = 3hrs).

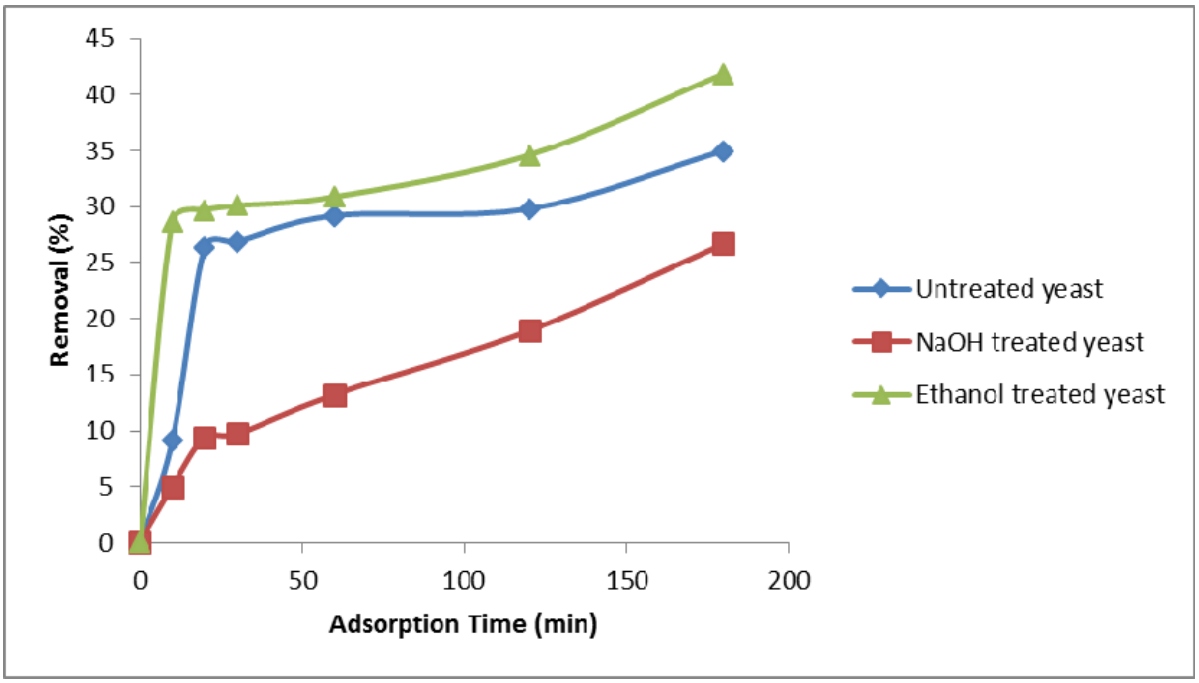


Figure 4.11: Effect of biomass pretreatment on the adsorption of Rh (III) (initial metal ion concentration =10mg/l, biomass dosage = 0.5g, agitation speed = 150rpm, temperature 30°C, contact time = 3hrs.

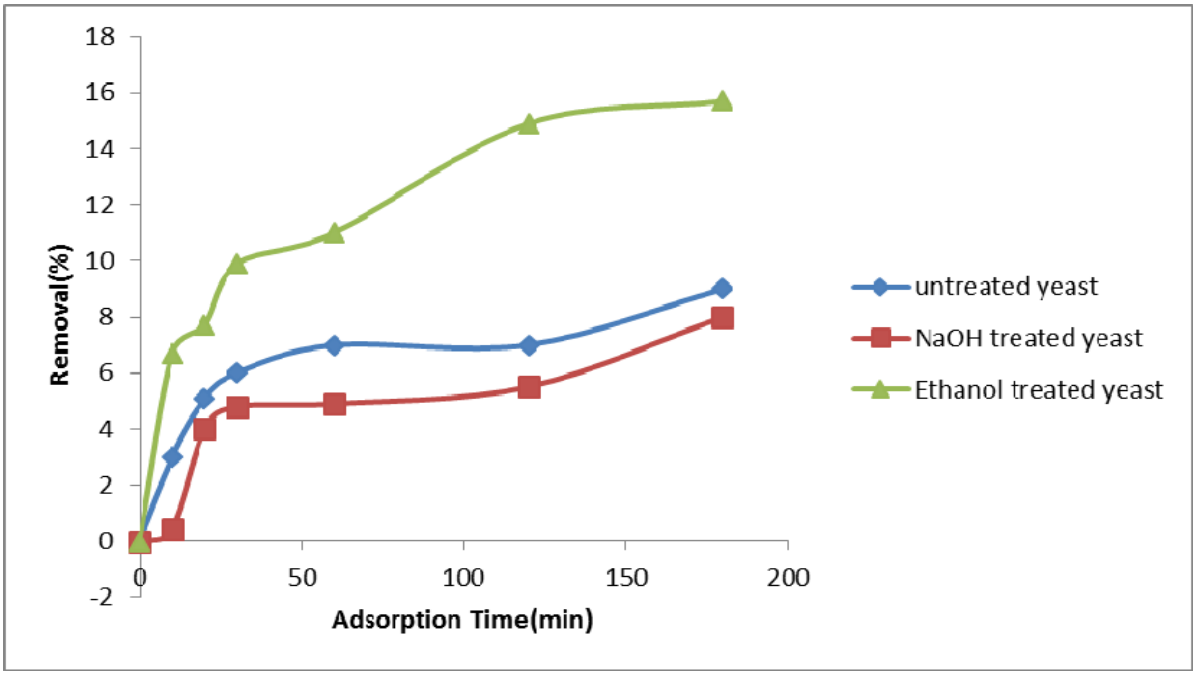


Figure 4.12: Effect of biomass pretreatment on the adsorption of Ir (III) (initial metal ion concentration =10mg/l, biomass dosage = 0.5g, agitation speed = 150rpm, temperature 30°C, contact time = 3hrs.

4.2.2 Kinetics

The relationship between percentage removal by adsorbent and contact time was plotted and presented in Figure 4.13.The kinetics curves for Pt (II), Pd (II), and Au (III) showed that the adsorption was rapid for the first 30 minutes, when percentage removal reached 70.8%, 77.9%, and 84.6% respectively. In addition, the kinetics curves for Rh (III), and Ir (III) showed that the rate of adsorption for these two metals is very slow and adsorption reached only 30.1% and 9.9% respectively in the first 30 minutes. Rhodium and iridium are transition metals and are known for their slow kinetics properties (Torapava, 2011). These two metals also have typical soft binding properties as they prefer to bind to sulphur donor ligands over oxygen donor ones.

Experimental results suggests that the amount of Pd (II), Au (III) and Ir (III) increased with increasing contact time and reached equilibrium at 20minutes for Au (III), Pd (II) and Ir(III). The kinetics curves for Pt (II) and Rh (III) suggest that even after 180minutes, there is still a significant uptake and consequently, it was decided to increase the contact time to 240 minutes for the subsequent tests. Zhou,et al., 2009 also observed that the adsorption of Pt (IV) and Pd (II) by thiourea-modified chitosan microsphere increased with increasing contact time and reached equilibrium at 300minutes for Pt (IV) and 150minutes for Pd (II).

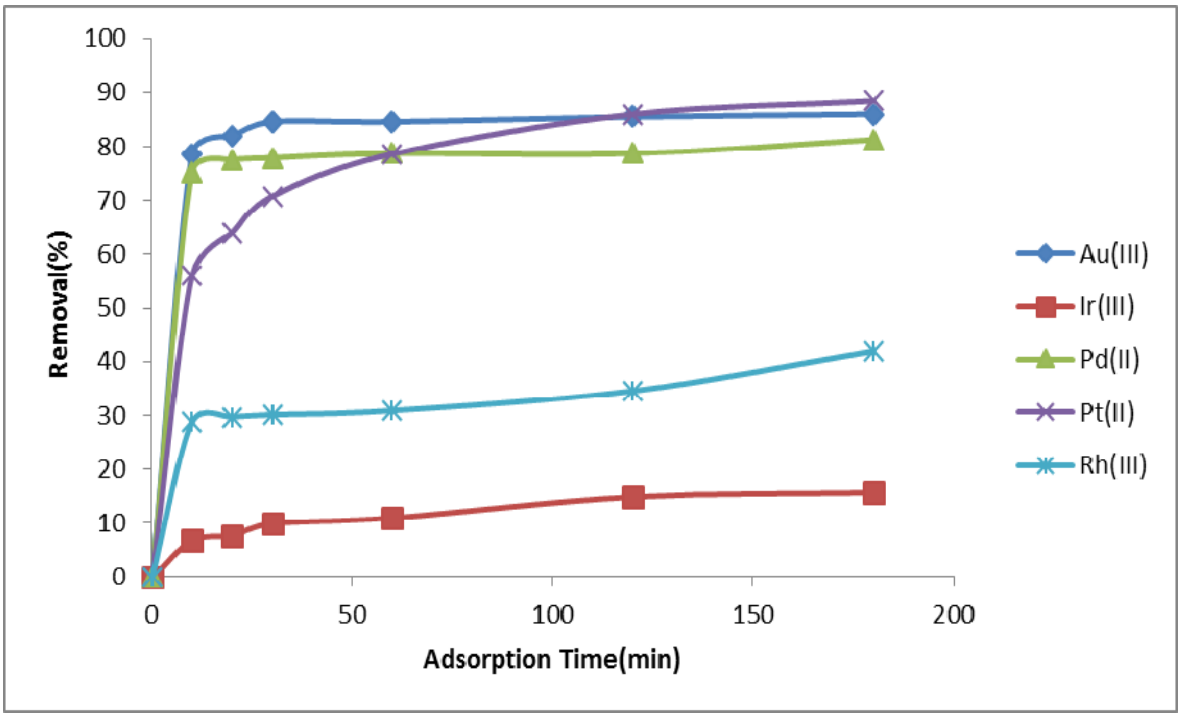


Figure 4.13: Effect of adsorption time on the uptake of Pt (II), Pd (II), Au (III), Rh (III) and Ir (III) in a single metal ion system (metal ions concentration = 10 mg/L), biomass dosage = 0.50 g; temperature = 30°C; agitation speed = 150 rpm.

In order to evaluate the kinetic mechanism that controls the adsorption process under study, pseudo-first order, pseudo-second order, Elovich model and Intra-particle diffusion models were employed to interpret the experimental data.

The kinetic models for Pt (II), Pd (II), Au (III), Rh (III) and Ir (III) in single metal component are presented in Figure 4.14 – 4.19 and the results of kinetic parameters are shown in Table 4.2 and 4.3. A good correlation of the kinetic data explains the adsorption mechanism of the metal ions on the solid phase. The validity of each model could be checked by the fitness of the straight lines (R^2 value).

Table 4.2: Coefficient of pseudo-first- order, pseudo-second- order kinetic models and intra- particle diffusion model.

Metal ions	qe (ept) mg/g	Pseudo-1st-order kinetics			Pseudo-2nd-0rder kinetics				Intraparticle diffusion	
		K_1	q_e(Cal)	R^2	k_2	h	$q_{e\,(Cal)}$	R^2	K_{id}	R^2
Pt (II)	1.768	0.030	1.080	0.957	0.091	0.299	1.815	0.997	0.113	0.74
Pd (II)	1.574	0.150	0.748	0.851	0.280	0.389	1.880	0.888	0.084	0.40
Au (III)	1.720	0.032	0.269	0.633	0.159	0.473	1.724	0.971	0.091	0.45
Ir (III)	0.314	0.021	0.267	0.963	0.177	0.020	0.336	0.978	0.022	0.93
Rh (III)	0.838	0.010	0.400	0.526	0.142	0.095	0.820	0.979	0.047	0.69

As shown in Table 4.2, the correlation coefficient values of pseudo-second order models were higher than those of the pseudo –first order model. Furthermore the calculated q_e values from pseudo-second-order model were very close to experimental values. In the case of pseudo-first order model, the values of calculated q_e differed severely from the experimental q_e values. The adsorption data was processed to determine whether Intraparticle diffusion is the rate limiting step. As seen from Figure.4.18, the straight lines did not pass through the origin and this further indicated that Intraparticle diffusion may not be the rate controlling step.

The Elovich equation was also used to describe second order kinetic assuming that the actual solid surfaces are energetically heterogeneous but the equation does not propose any definite mechanism for adsorbate-adsorbent. It has extensively been accepted that the chemisorption process can be described by this semi empirical equation.

Table 4.3: Calculated values of α and β for the Elovich Model

Metal ions	$\alpha\left(g/mg\ \min\right)$	$\beta\left(\frac{g}{mg}\right)$	R^2
Pt(II)	57.000	0.232	0.989
Pd(II)	1.280	0.034	0.862
Au (III)	2.120	0.046	0.816
Ir (III)	9.440	0.066	0.965
Rh (III)	1.260	0.078	0.747

From Table 4.3, the applicability of the simple Elovich equation for the kinetic data indicates that the Elovich equation was able to describe the kinetics of Pt (II), Pd (II), Au (III), Ir (III) and Rh (III) on *S. cerevisiae* waste biomass to some extent. The α and β values which represent the initial sorption rate and coefficient of desorption respectively may be used to estimate the reaction rates (Chien and Clayton, 1980). It has been suggested that an increase in the initial sorption rate α would increase the reaction rates, hence the higher the value of α, the higher the reaction rate. Besides Rh (III), with R^2 value of 0.7, the correlation coefficient was greater than 0.8 for all other tested PGMs.

Based on the higher correlation coefficient and the agreement of calculated q_e values with the experimental q_e values, the adsorption of Pt (II), Pd (II), Au (III), Ir (III) and Rh (III) on *S. cerevisiae* waste biomass was best described by pseudo-second-order equation. The q_e values differed slightly because of a time lag that might have been caused by a boundary layer or an external resistance that controlled the beginning of the sorption process (Mao et al., 2010). This suggests the applicability of second order kinetic model to the kinetic data. This model is based on the assumption that the rate limiting step may be chemical sorption and not involving mass transfer in solution. It is more likely to predict that the adsorption behavior may involve valency forces through sharing of electron between precious metal cations and the adsorbent.

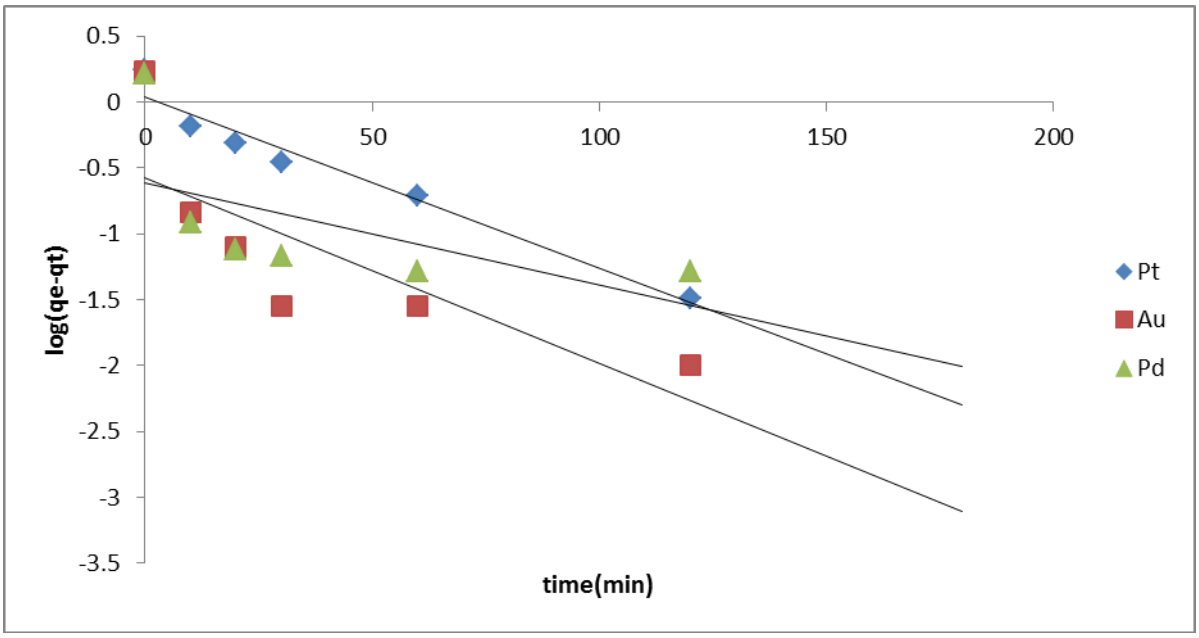


Figure 4.14: Pseudo-first-order kinetic plots for the adsorption of Pt (II), Pd (II), and Au (III) on S. cerevisiae waste biomass.

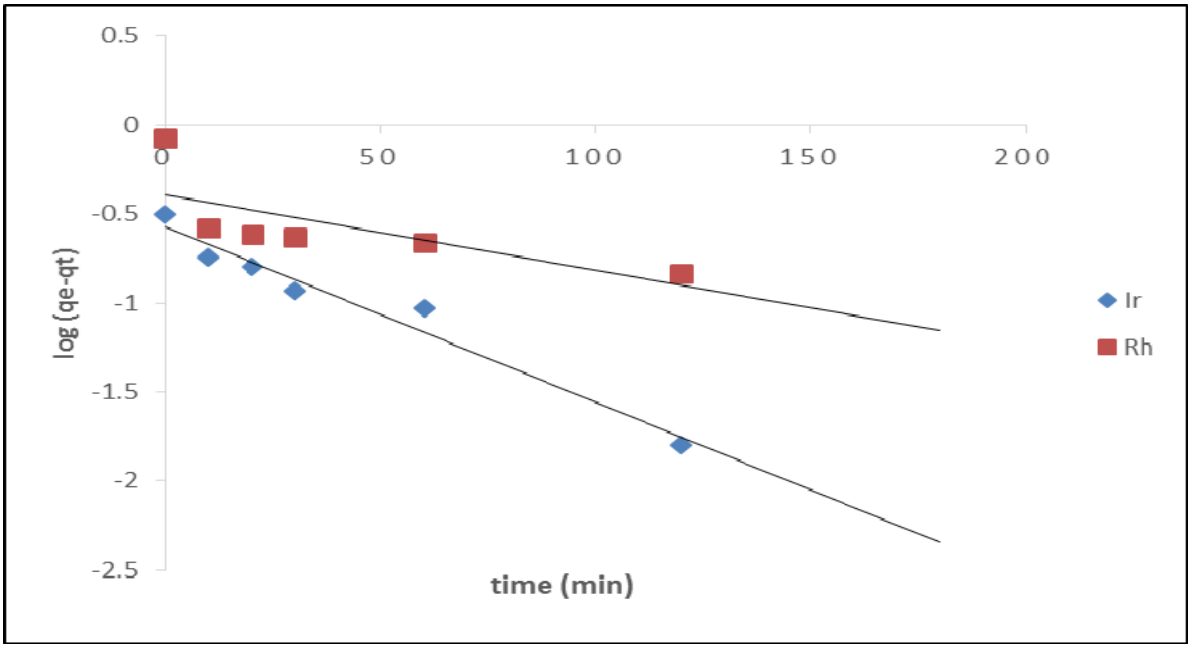


Figure 4.15: Pseudo-first-order kinetic plots for the adsorption of Ir (III) and Rh (III) on S. cerevisiae waste biomass.

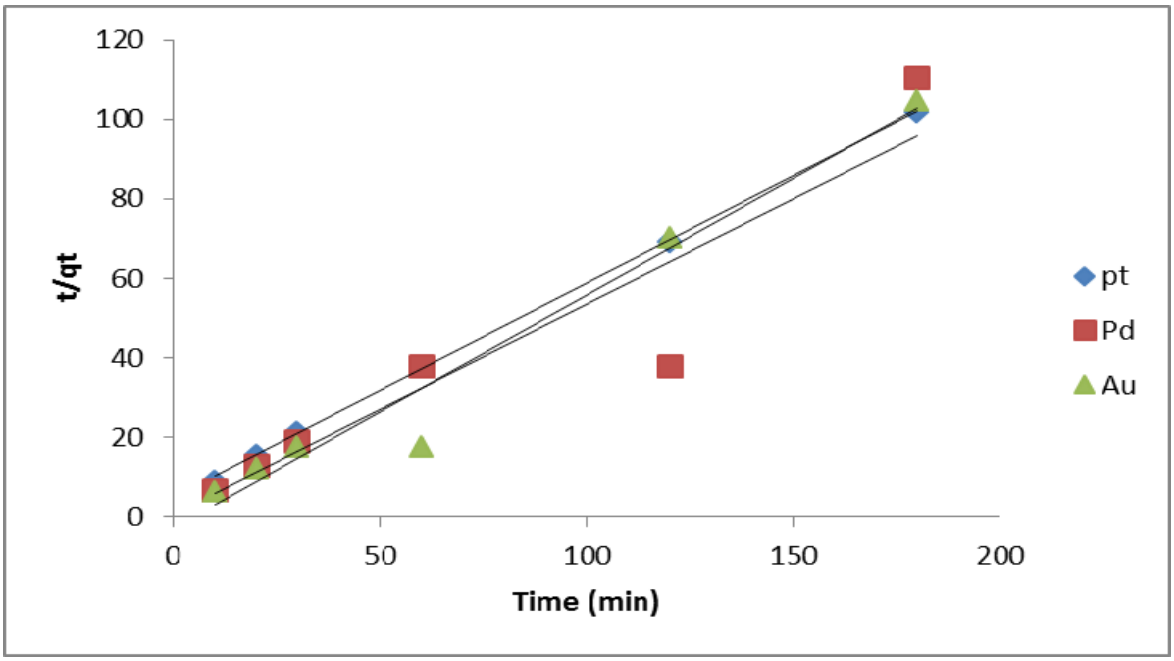


Figure 4.16: Pseudo-second-order kinetic plots for the adsorption of Pt (II), Pd (II), and Au (III) on S. cerevisiae waste biomass.

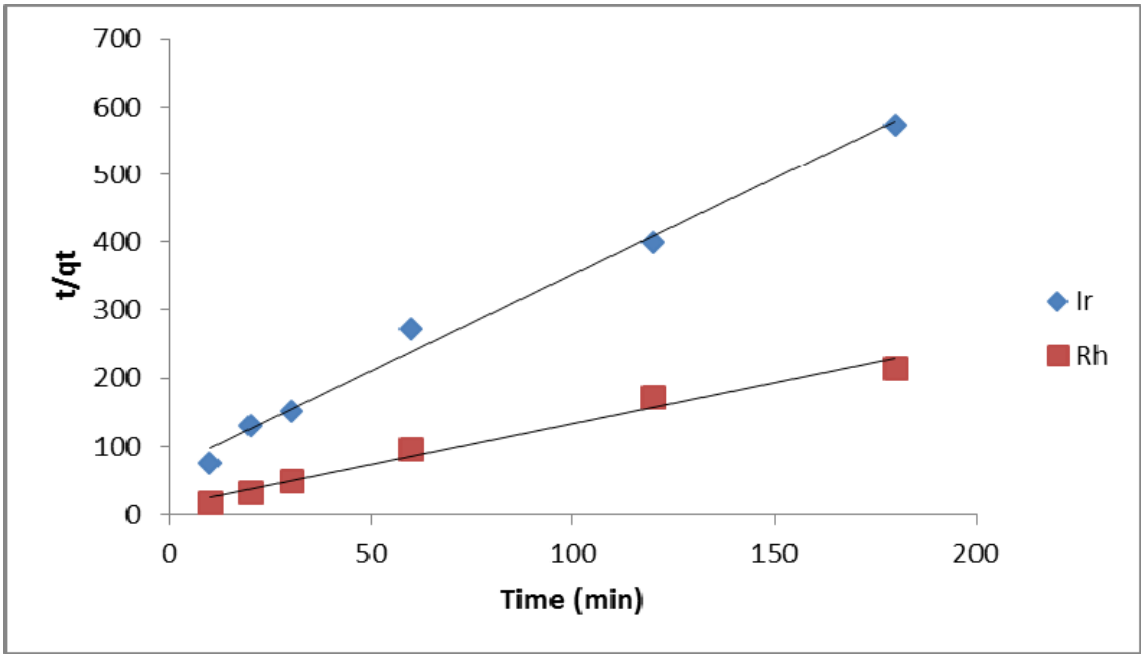


Figure 4.17: Pseudo-second-order kinetic plots for the adsorption of Ir (III) and Rh (III) on S. cerevisiae waste biomass.

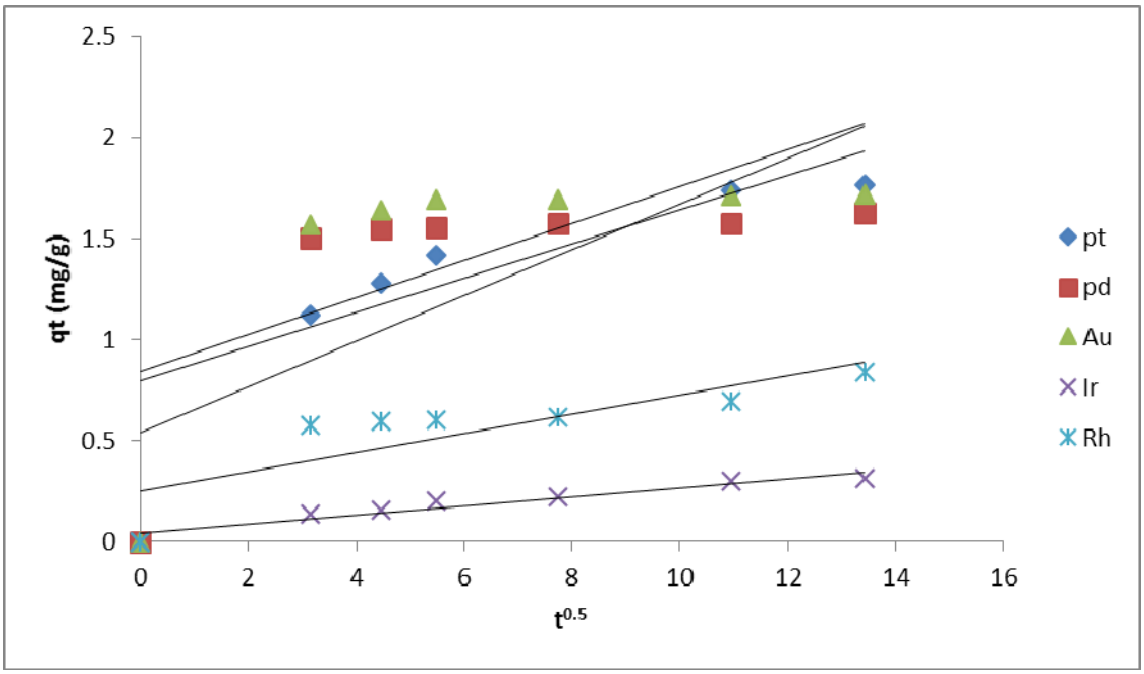


Figure 4.18: Intra particle diffusion model for the adsorption of Pt (II), Pd (II), Au (III), Ir (III) and Rh (III) on *S. cerevisiae* waste biomass.

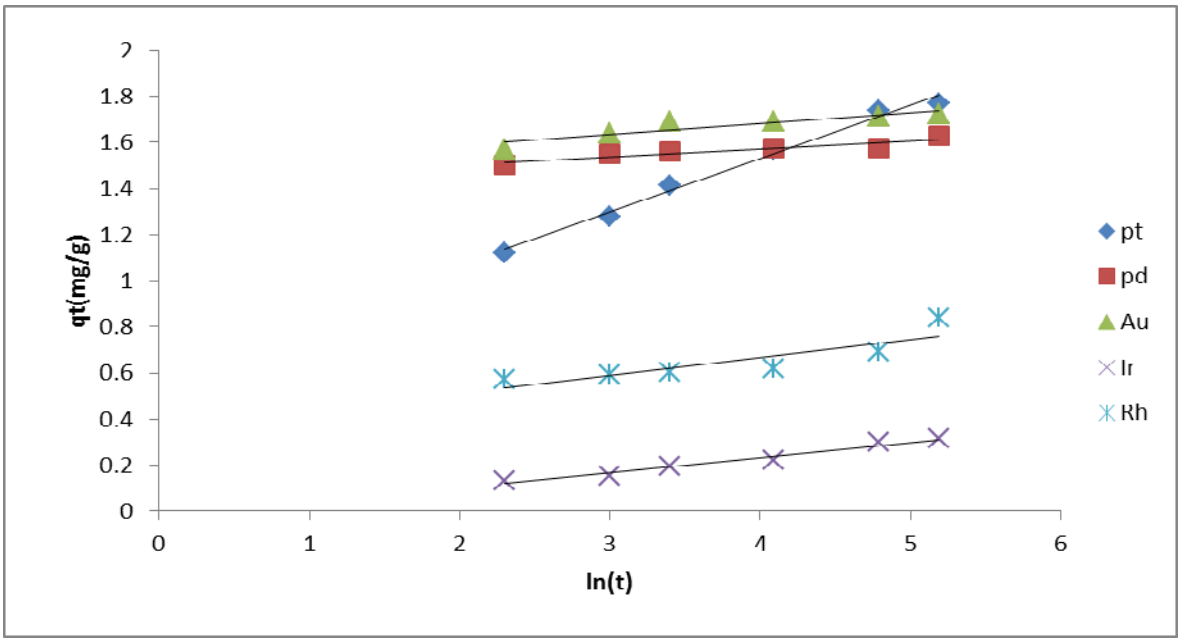


Figure 4.19: Elovich model for the adsorption of Pt (II), Pd (II), Au (III), Ir (III) and Rh (III) on *S. cerevisiae* waste biomass.

The adsorption of Pt (II), Pd (II), Au (III), Ir (III) and Rh (III) on S. cerevisiae waste biomass may consist of two processes; the first process is interpreted to be the instantaneous adsorption stage or external surface adsorption. The second process is interpreted to be the gradual adsorption stage where Intraparticle diffusion controls the adsorption rate until finally the metal uptake reaches equilibrium.

4.3 Identification of Influential Factors

4.3.1 Introduction

Design of Experiment are more efficient than one- factor- at- a- time experiment. While one- factor- at-a-time experiments are easy to undestand, they are often expensive, time consuming and do not allow the investigation of the interactive nature of other independent factors that would otherwise affect the product or process (Box et al., 1978; Montgomery, 2005). An interaction of factors is a relationship where the effect that a factor has on the product or process is altered due to the presence of one or more factors, and often time, interaction effect have more impact on the results than individual factors. The purpose of this part of the study was therefore to investigate and identify factors that significantly influence the adsorption of PGMs from dilute streams.

The study employed a statistical Design of Experiments (DOE) method as a research tool to develop an experimentation strategy for determining the significant factors affecting PGMs adsorption in dilute stream using *Saccharomyces cerevisiae yeast* biomass. The significance of each factor and associated interactive effect were evaluated using a two-level four-factor full factorial statistical design of experiment (2^4) and percentage adsorption was taken as the measured response.

4.3.2 Experimental Plan for Statistical Design of Experiments (DOE)

Design of Experiment was used in this part of the work to study the adsorption of PGMs from dilute stream using ethanol treated *Sacharomyces cerevisiae* spent yeast.

Design of Experiments is the simultaneous study of several process variables (Montgomery, 2005). A full factorial design matrix was used in order to change

several factors in a systematic way so as to ensure a reliable study of main factors and their interaction.

Previous researchers, though using different types of biomass did identify some factors that may be significant in the biosorption of PGMs from aqueous streams (Mack et al., 2008; Frazzoli et al., 2007; Golewska-Zylkiewicz and Kozlowska, 2005). Examples of such factors include; solution pH, temperature, concentration of metal ion in solution etc. Therefore, the choice of factors and levels was based on information on metal adsorption from literature as referenced above.

The main intention was to identify the key factors that affect the response and the interaction among themselves. The desired response was therefore the amount of PGMs biosorbed onto the biomass from the solution. Biosorption experiments were carried out at low and high factor represented by -1 and +1 respectively. Factors investigated included: temperature, solution pH, biomass dosage and initial metal ion concentration.

In this work, design factors were categorized as controlled factors and held constant factors. The controlled factors presented in Table 4.4**,** were the factors selected for investigation. The held constant factor such as agitation rate is a factor that may have an influence on the response (Shemi, 2012) but is of no particular interest in this work so it was held constant at 150 rpm.

Table 4.4: Experimental factors and levels for controlled factors

Controlled factors	Level 1	Level 2
Temperature (◦C) (A)	30	50
pH (B)	1	6
Metal ion concentration (ppm) (C)	0.1	10
Biomass dosage (g) (D)	0.5	1

The choice of low and high level of factors for pH, temperature and biomass dosage was based on information from literature Frazzoli et al., 2007; Golewska-Zylkiewicz and Kozlowska, 2005; Zhou et al., 2009) while the choice of low and high level for initial metal ion concentration was based on the analysis of the real dilute industrial solution from Impala Platinum.

To simplify calculations and for uniform comparison, controlled factors were studied with their codified values of +1 or -1. The levels of controlled variables in coded units were obtained using the following formula (Box et al; 1978):

$$Coded\ value = \frac{X - X_0}{0.5\left(X_2 - X_1\right)} \tag{4.1}$$

Where X = actual, X_0 = Mean, X_1 = lowest, X_2 = highest.

4.3.3 Methodology for Data Analysis.

Normal probability plot of effect

When analyzing data from unreplicate factorial design, occasionally, very high order interactions occur and therefore it is necessary to allow for selection. A method of analysis attributed to Daniel (1959) provides a simple way to overcome this problem.

Daniel suggests constructing a normal probability plot of the effect estimates. This is the plot of the actual value of the effect estimates against their cumulative normal probabilities (Daniel, 1959). The effects that are negligible are normally distributed, with mean zero and variance δ^2, and will tend to fall along a straight line on this plot, whereas significant effects will have non zero means and will not lie along the straight line.

In the probability plot, all the effects have to be graded from low to high and numbered in this order. Afterward, the numbered effects (i) get a value of percentage based on the following equation:

$$P = \left(i - 0.5\right) \times \frac{100}{m} \tag{4.2}$$

Where m = total number of effects, P = probability points, i = order number.

4.3.4 Significant Factors

PGMs adsorption results from experimental runs for the 2^4 full factorial designs with codified and actual values are given in Table 4.5:

Table 4.5: PGMs Adsorption results for the 2^4 full factorial design

Standard run order	Random run order	Control factors				Percent Adsorption (%)				
		A	B	C	D	Au	Ir	Pd	Pt	Rh
1	16	-1	-1	-1	-1	10.0	20.0	15.0	49.28	13.0
2	1	+1	-1	-1	-1	6.0	13.0	8.0	32.3	10.0
3	14	-1	+1	-1	-1	44.0	30.3	62.0	27.0	9.0
4	4	+1	+1	-1	-1	71.0	29.3	64.0	21.0	37.0
5	9	-1	-1	+1	-1	92.4	63.2	85.3	86.6	46.0
6	2	+1	-1	+1	-1	95.4	60.8	81.5	87.6	47.3
7	11	-1	+1	+1	-1	96.9	80.3	91.8	66.5	51.8
8	3	+1	+1	+1	-1	97.8	81.9	95.8	67.9	81.1
9	15	-1	-1	-1	+1	6.0	7.0	24.0	32.3	4.0
10	7	+1	-1	-1	+1	10.0	11.0	31.0	50.3	10.0
11	13	-1	+1	-1	+1	57.0	41.3	60.0	9.0	39.0
12	8	+1	+1	-1	+1	83.0	43.3	89.0	33.0	35.0
13	10	-1	-1	+1	+1	78.2	67.0	82.3	89.5	45.8
14	5	+1	-1	+1	+1	81.6	62.8	78.1	89.1	48.4
15	12	-1	+1	+1	+1	97.0	80.1	90.8	66.5	54.1
16	6	+1	+1	+1	+1	97.6	78.8	92.9	66.6	77.9

The actual factor levels coded as values of (-1) and (+1) in the table are as follows: A (Temperature): 30◦C (-1) and 50◦C (+1); B (pH): 1(-1) and 6(+1); C (metal concentration): 0.1ppm (-1) and 10ppm (+1); D (Biomass dosage): 0.5g (-1) and 1g (+1).

For the results discussed in this section, reference should be made to the experimental data in Appendix C (Table C1-C10).

The experimental data given in Table 4.5 was used to estimate the main and interaction effects presented in Figure 4.20 – 4.24.

The normal probability of effect presented in Figure 4.20 was used to determine the significant effect on Au (III) adsorption. Analysis of the individual factor on the probability plot showed that solution pH(B), initial concentration of metal ions (C) and the interaction of solution pH and metal ion concentration(BC) were statistically significant for adsorption of Au (III) since they were not distributed about a fixed zero mean. All the other main and interaction effects that lie along the line (the normal distribution line) are negligible therefore not statistically significant.

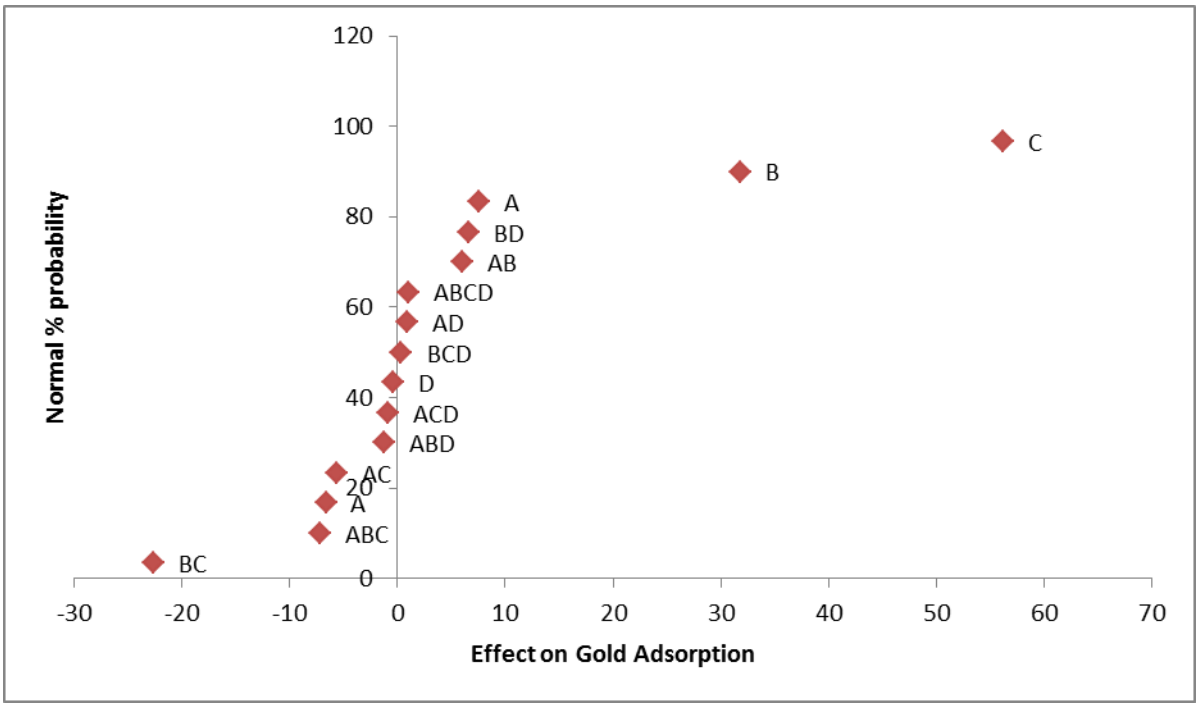


Figure 4.20: Normal plots of effects of main factors and factors interaction for Gold from the 2^4 full factorial designs. A, B, C and **D** are main factors**; A** (Temperature)**, B** (pH), **C** (metal concentration) and **D** (Biomass dosage). AB, BC, AC, BD, CD, AD, ABC, ACD, ABD, BCD and ABCD are factor interactions

From Figure 4.21**,** analysis of individual factors on the probability plot for Ir (III) adsorption also showed that the important effect for iridium adsorption is the initial concentration of metal ions in the solution (C) and the solution pH (B). All other main and interaction effect are not significant because they do not differ much from the normal distribution line.

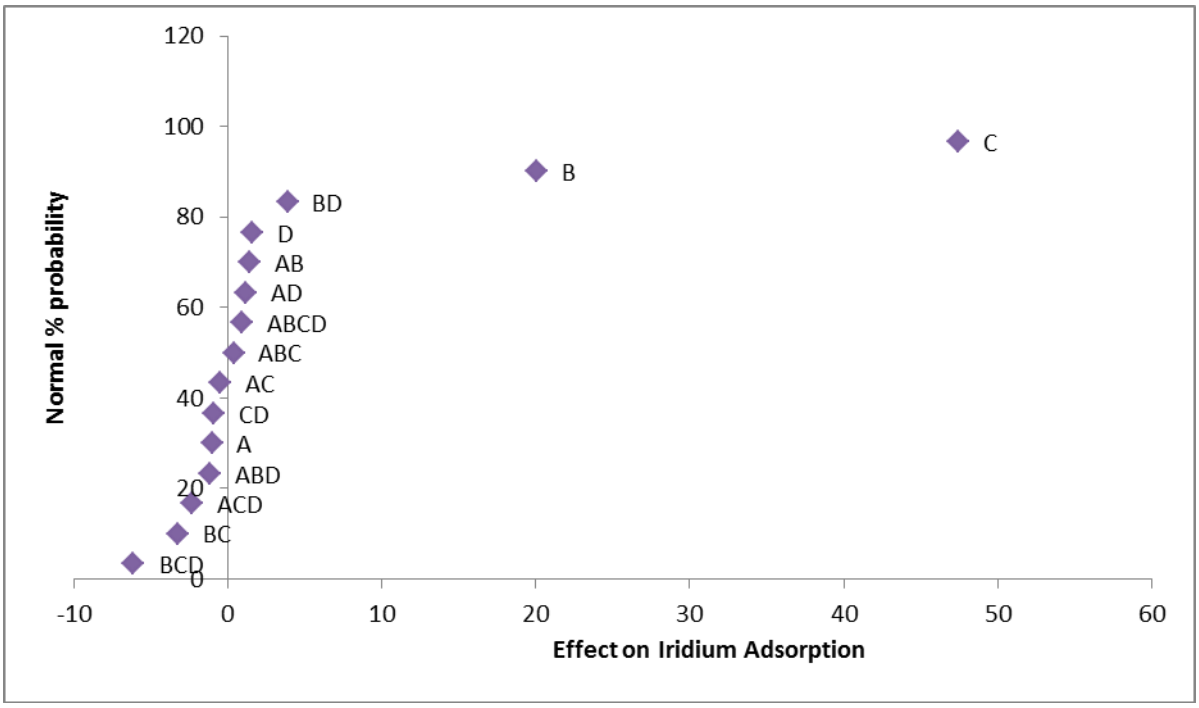


Figure 4.21: Normal plots of effects of main factors and factors interaction for Iridium from the 2^4 full factorial designs. A, B, Cand **D** are main factors**; A** (Temperature)**, B** (pH), **C** (metal concentration) and **D** (Biomass dosage). AB, BC, AC, BD, CD, AD, ABC, ACD, ABD, BCD and ABCD are factor interactions

The normal probability plot of effect for Pd (II) is shown in Figure 4.22. The important effects that emerge from this analysis are the main effects of solution pH (B), initial concentration of metal ions (C) and the interaction of solution pH and metal ion concentration (BC) while other main and interaction effect are not significant.

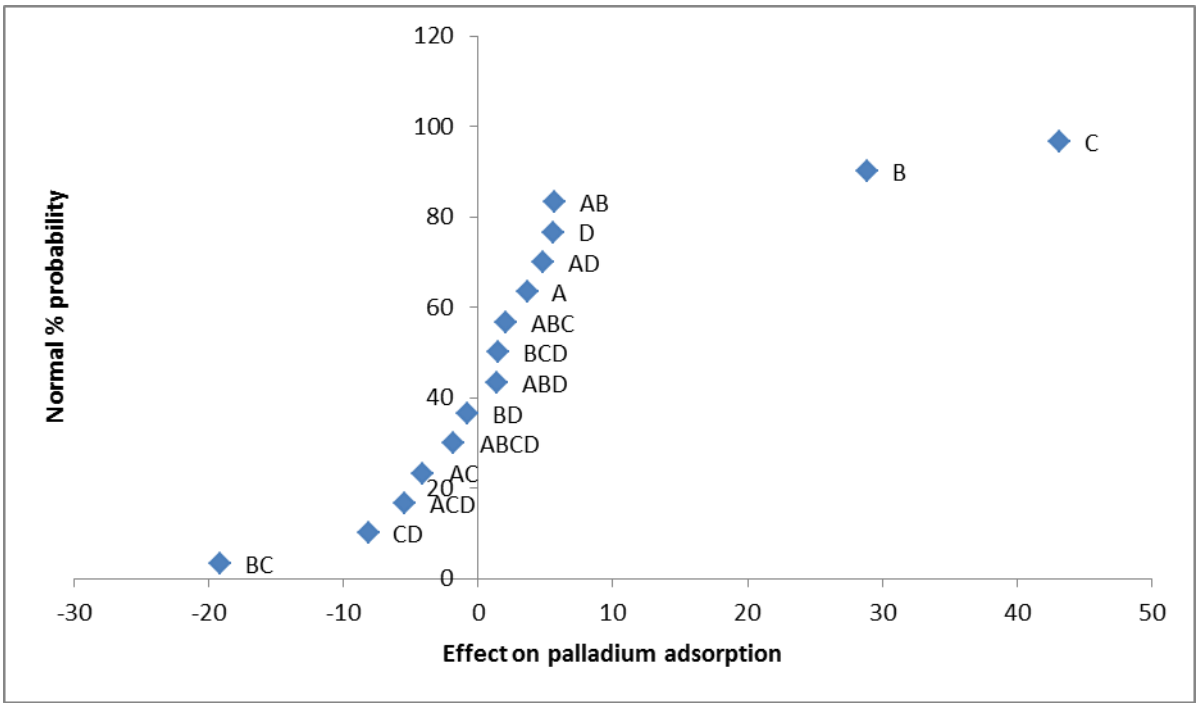


Figure 4.22: Normal plots of effects of main factors and factors interaction for palladium from the 2^4 full factorial designs. A, B, C and **D** are main factors**; A** (Temperature)**, B** (pH), **C** (metal concentration) and **D** (Biomass dosage). AB, BC, AC, BD, CD, AD, ABC, ACD, ABD, BCD and ABCD are factor interactions.

Analysis of Figure 4.23 and Figure 4.24 showed that the important effects for the adsorption of Pt (II) and Rh (III) are the initial metal ion concentration (C) and solution pH (B) while the effect of other factors is negligible.

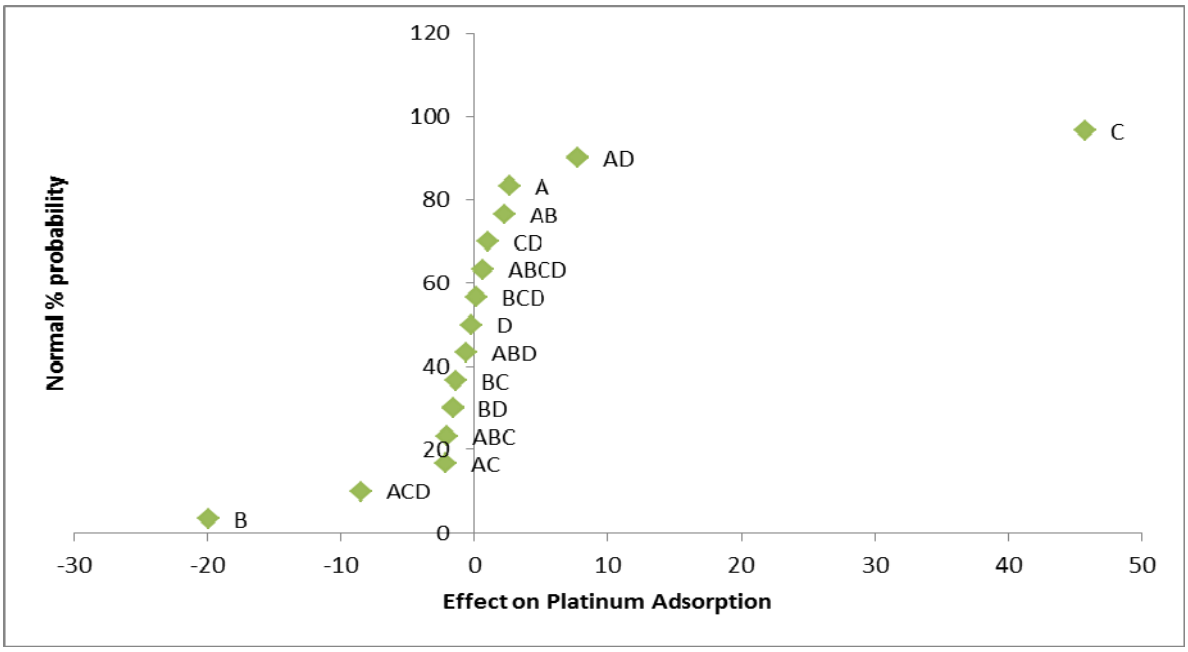


Figure 4.23: Normal plots of effects of main factors and factors interaction for platinum from the 2^4 full factorial designs. A, B, C and **D** are main factors**; A** (Temperature)**, B** (pH), **C** (metal concentration) and **D** (Biomass dosage). AB, BC, AC, BD, CD, AD, ABC, ACD, ABD, BCD and ABCD are factor interactions

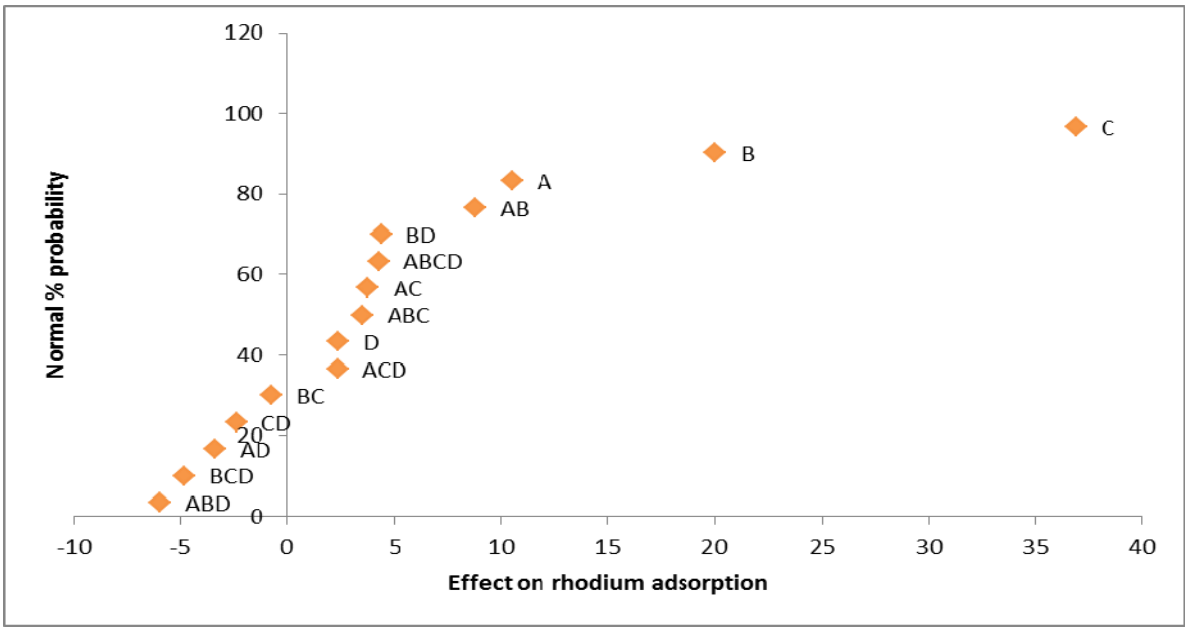


Figure 4.24: Normal plots of effects of main factors and factors interaction for Rhodium from the 2^4 full factorial designs. A, B, C and **D** are main factors**; A**

(Temperature)**, B** (pH), **C** (metal concentration) and **D** (Biomass dosage). AB, BC, AC, BD, CD, AD, ABC, ACD, ABD, BCD and ABCD are factor interactions.

The Table below gives the summary of the significant factors on the adsorption of the PGMs tested. The factors marked are those that have significant influence on the adsorption of each metal.

Table 4.6: Summary of the significant factors on the adsorption of Au (III), Pd (II), Pt (II), Rh (III) and Ir (III)

Metal Ions	A	B	C	D	AB	AC	AD	BC	CD	BD	ABC	ABD	ACD	BCD	ABCD
Au (III)		X	X					X							
Pt (II)		X	X												
Pd (II)		X	X					X							
Ir (III)		X	X												
Rh (III)		X	X												

4.3.5 Modeling the significant effects for adsorption prediction

A first order polynomial model (fitted model) between significant factors and the response was developed to illustrate the dependence of the response on the significant factors. Beginning with effects with magnitudes close to zero (using Au (III) as an example), 12 of the estimates fit well on a straight line. Those corresponding to B, C and BC do not fit on the straight line. It can therefore be concluded that the effects B, C and BC are not easily explained as chance occurrences. This suggests that all effects with the exception of the average adsorption 63.99, B = 31.8, C = 56.2 and BC = -22.6 can be explained by noise.

Therefore, Adsorption, $Y = \overline{Y} + \left(\frac{B}{2}\right)X_B + \left(\frac{C}{2}\right)X_C - \left(\frac{BC}{2}\right)X_{BC}$ (4.3)

Where, $\overline{Y}$ represents the average of all the data for the runs (i.e., average of all adsorptions) and X_B, X_C and X_{BC} are the predictor variables (i.e., +1 or -1), B and C are main effects while BC is interaction effects. Therefore, for Au (III) the model for the predicted adsorption is expressed as:

$$Y = 63.99 + 16.54X_B + 28.11X_C - 11.33X_{BC} \quad (4.4)$$

For Pt (II), the model for predicted adsorption is expressed as:

$$Y = 54.66 - 9.95X_B + 22.85X_C \quad (4.5)$$

For Pd (II), the model for predicted adsorption is expressed as:

$$Y = 65.72 + 14.4X_B + 21.55X_C - 9.55X_{BC} \quad (4.6)$$

For Ir (III), the model for predicted adsorption is expressed as:

$$Y = 48.13 + 10X_B + 23.76X_C \quad (4.7)$$

For Rh (III), the model for predicted adsorption is expressed as:

$$Y = 38.08 + 10X_B + 18.45X_C \quad (4.8)$$

In equations 4.4 - 4.9, the positive signs in some of the variables of the predicted model equation indicate that in order to maximize the adsorption of the PGMs, these factors must be kept in high levels. The negative sign means the factors must be kept at low level.

The analysis of residuals which gives the difference between the actual adsorption and the predicted adsorption is provided in detail in Appendix C.

4.3.6 Influence of factors on adsorption.

The main effects of B (pH) and C (initial metal ion concentration) on Au (III) adsorption are plotted in Figure 4.25 and 4.26 respectively. Figure 4.25 shows the

average percentage adsorption of Au (III) from dilute stream at pH1 and 6 which are low and high solution pH respectively. Higher gold adsorption was obtained at higher pH whereas low pH gave lower adsorption.

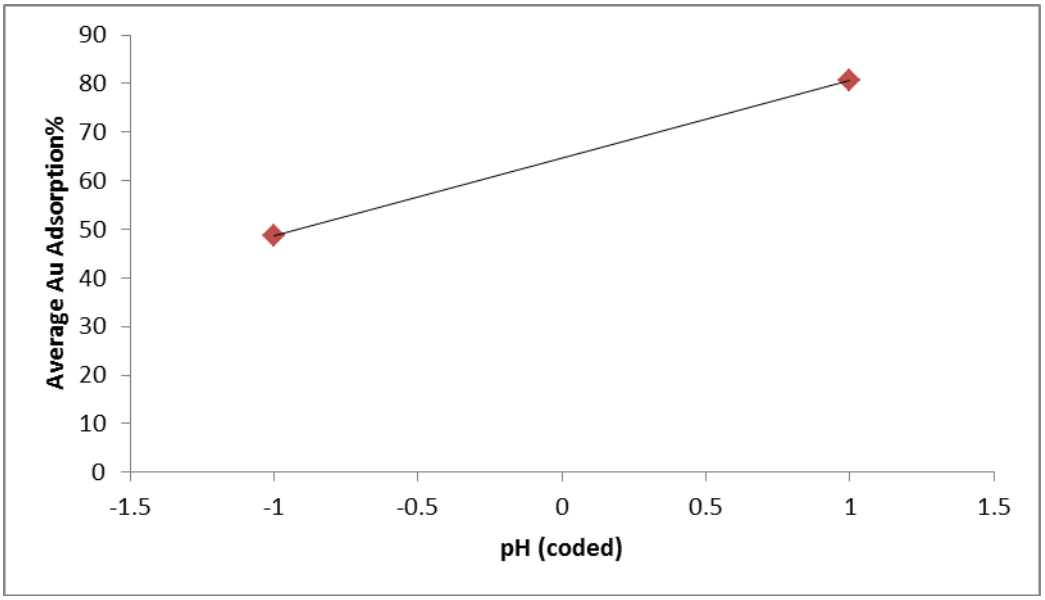


Figure 4.25: Main effect plot of pH on Au (III)

The effect of initial metal ion concentration on Au (III) adsorption is shown in Figure 4.26. Higher adsorption was obtained at higher initial metal ion concentration (10ppm) whereas low initial metal ion concentration (0.1ppm) gave lower adsorption percentage.

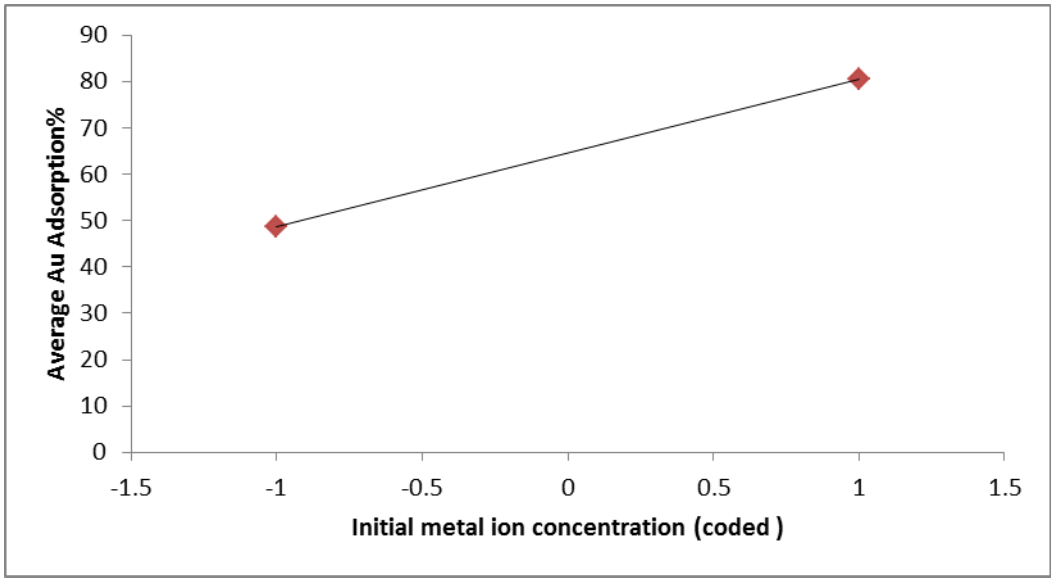


Figure 4.26: Main effect plot of initial metal ion concentration on Au (III)

Since the effect of pH (B) and metal ion concentration (C) on the adsorption of Au (III) were found to be positive, if only these main effects are considered, the two factors will be run at high level to maximize the adsorption percentage. However, it is always necessary to examine any interactions that are important since main effects do not have much meaning when they are involved in significant interactions (Daniel, 1959).

The BC interaction effect is plotted in Figure 4.27. Inspection of the interaction graph indicates that change in the solution pH produces a much larger percentage adsorption at the higher initial metal ion concentration than at the lower concentration. However, the change in solution pH also has a very significant effect on the adsorption at lower concentration because it can be observed that at lower pH and lower concentration the average percentage adsorption is 8% while at higher pH and lower concentration the response increases to 63.75%.Therefore, the best adsorption percentage of 97.32% would appear to be obtained at higher pH and higher metal concentration.

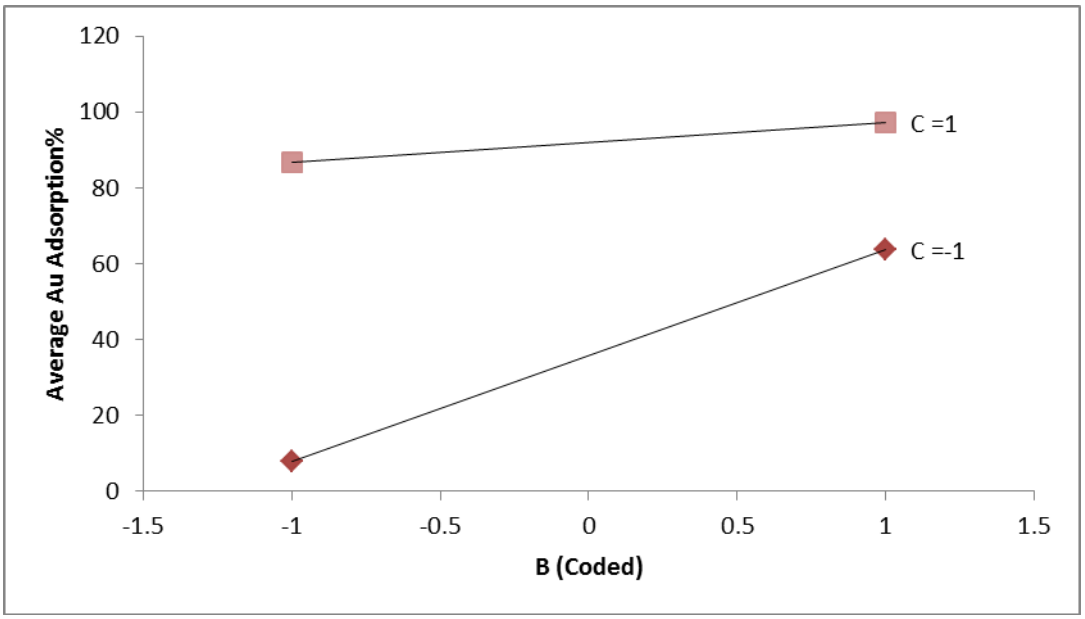


Figure 4.27: Interaction plot of pH and initial metal ion concentration on Au (III)

PGM speciation is strongly related to pH and chloride concentration. At lowest pH, the surface of the biomass is protonated which may reduce metal binding. In addition, at low pH, when the pH is controlled by HCI, the chloride concentration in the solution becomes very high which in turn may compete with the PGM chloro anionic species for the binding site on the biomass. According to Figure 4.27, at low pH and high metal concentration, the adsorption is still around 80%. It should be noted however, that there is about 17.32% difference between the adsorption at low pH, high metal ion concentration and high pH and high metal ion concentration. This indicates that the protonation of the biomass surface and chloride concentration in solution at low pH has a significant effect on the percentage adsorption.

The main effect of initial metal ion concentration on Ir (III) adsorption is shown in Figure 4.28. It is apparent that the average adsorption percentage of iridium increased from 24.4 % at lower metal ion concentration to 71.86% at higher concentration.

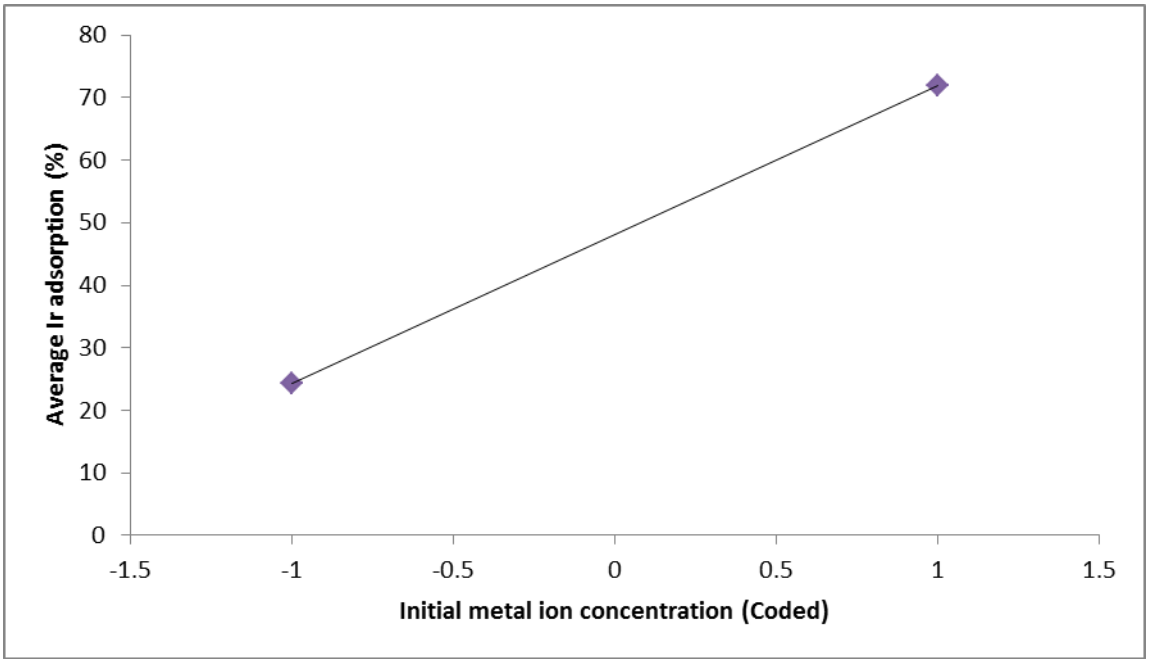


Figure 4.28: Main effect plot of initial metal ion concentration on Ir (III)

Figure 4.29 shows the main effect of pH on Ir (III) adsorption, an increase in the solution pH yielded higher adsorption (38.1% at low pH and 58.16% at high pH). All other factors have no significant effect on Ir (III) adsorption and no interaction effects were observed.

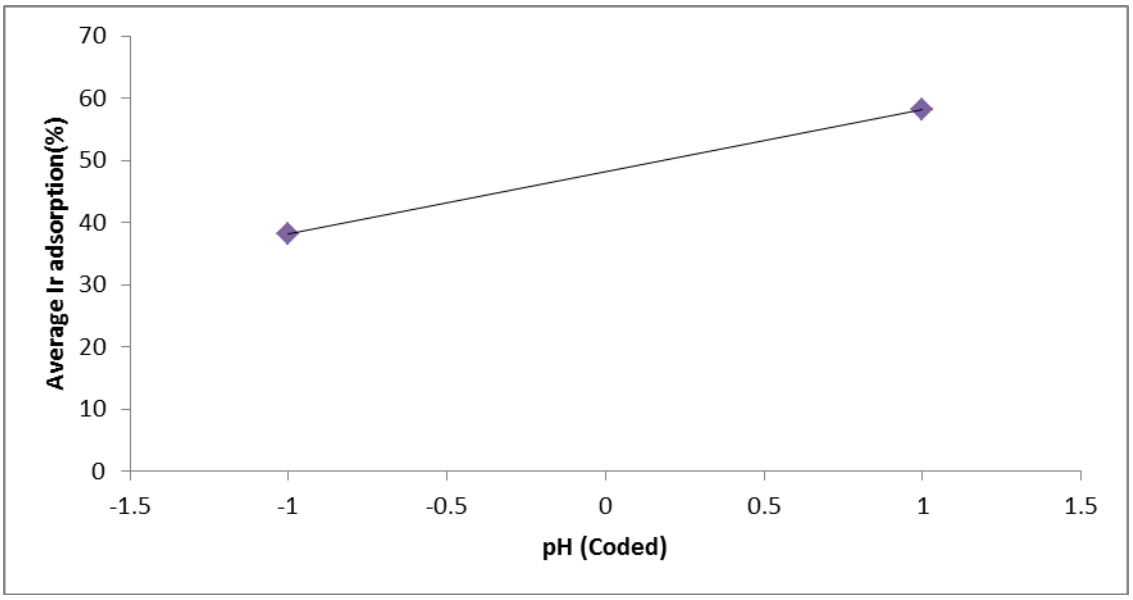


Figure 4.29: Main effect plot of pH on Ir (III)

The main effects of B (pH) and C (initial metal ion concentration) on Pd (II) adsorption are plotted in Figure 4.30 and 4.31 respectively. Figure 4.30a shows the adsorption percentage of Pd (II) from the dilute process solution at pH 1 and 6 which are low and high solution pH respectively. Higher Pd (II) adsorption was obtained at higher pH whereas low pH gave lower adsorption.

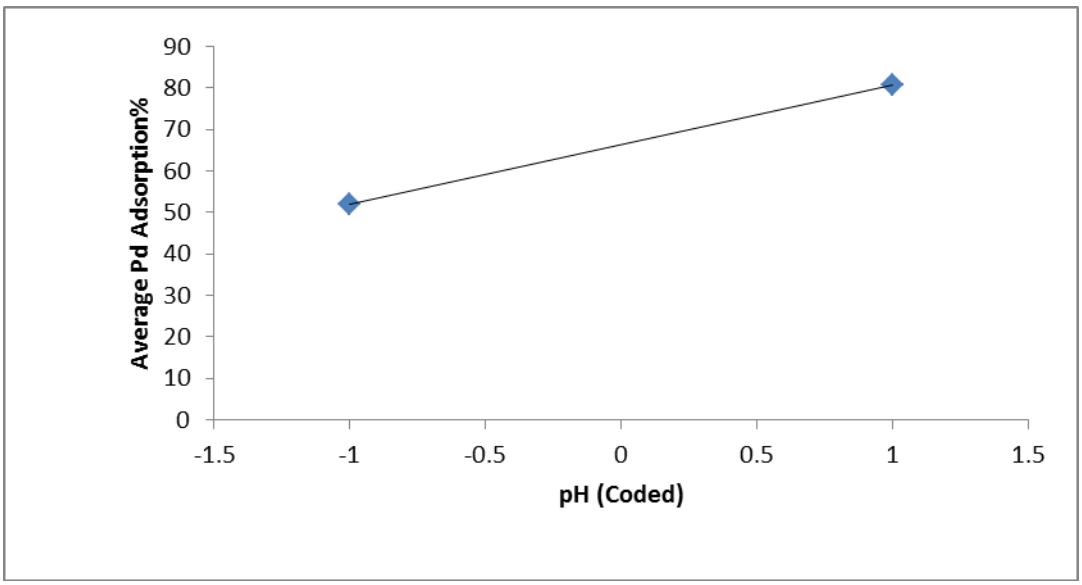


Figure 4.30: Main effect plot of pH on Pd (II).

The effect of initial metal ion concentration on Pd (II) adsorption is shown in Figure 4.31. Higher adsorption was obtained at higher initial metal ion concentration (10ppm) whereas low initial metal ion concentration (0.1ppm) gave a lower adsorption percentage.

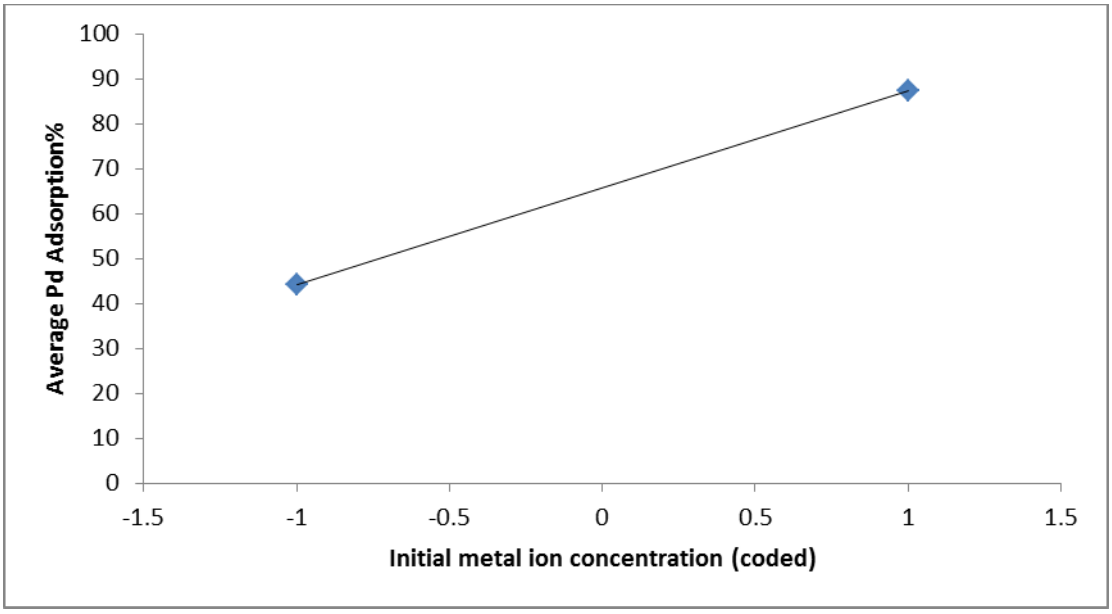


Figure 4.31: Main effect plot of initial metal ion concentration on Pd (II)

The BC interaction effect is plotted in Figure.4.32. Inspection of the interaction graph indicates that a change in the solution pH produces a much larger percentage adsorption at the higher initial metal ion concentration than at the lower concentration. However, the change in solution pH also has a very significant effect on the adsorption at lower concentration. This is because it can be observed that at a lower pH and a lower concentration the average percentage adsorption is 19.5% while at a higher pH and a lower concentration the response increases to 68.75%.Therefore, the best adsorption percentage of 92.86 % would appear to be obtained at higher pH and higher metal concentration.

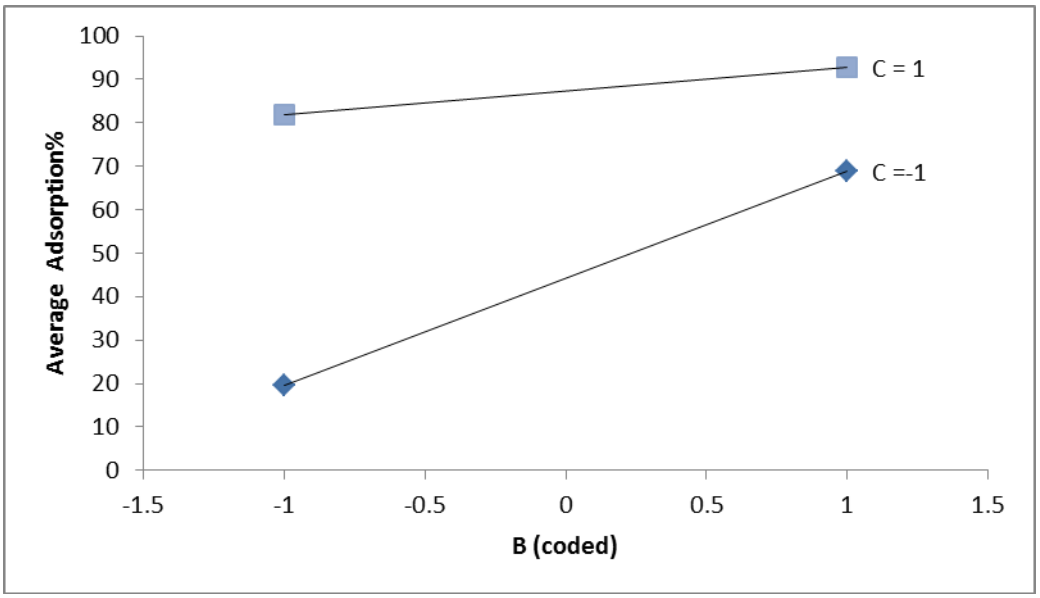


Figure 4.32: Interaction plot of pH and initial metal ion concentration on Pd (II).

The main effect of initial metal ion concentration on Pt (II) adsorption is shown in Figure 4.33. It is apparent that the average adsorption percentage of platinum increased from 31.77% at lower metal ion concentration to 77.54% at higher concentration. An analysis of Figure 4.34 shows that an increase in the solution pH decreased the rate of adsorption from 64.6% to 44.69%. This indicates that an increase in pH has a negative effect on the adsorption of Pt (II). The negative effect of pH on the adsorption of Pt (II) might be of significant use in the selective adsorption of Pt (II) from the other tested PGMs. All other main factors as well as interaction factors have no effect on the adsorption of Pt (II).

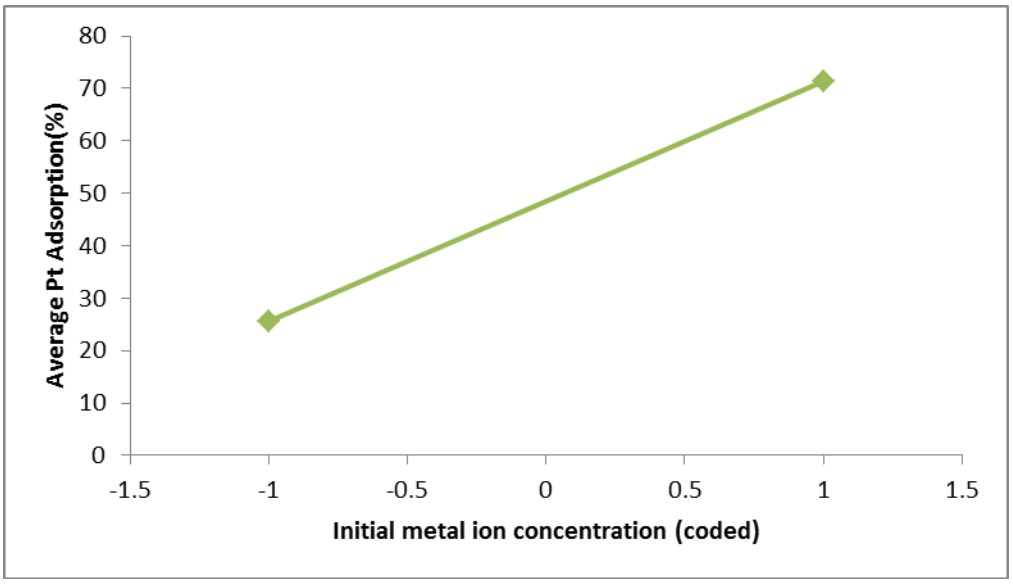


Figure 4.33: Main effect plot of initial metal ion concentration on Pt (II).

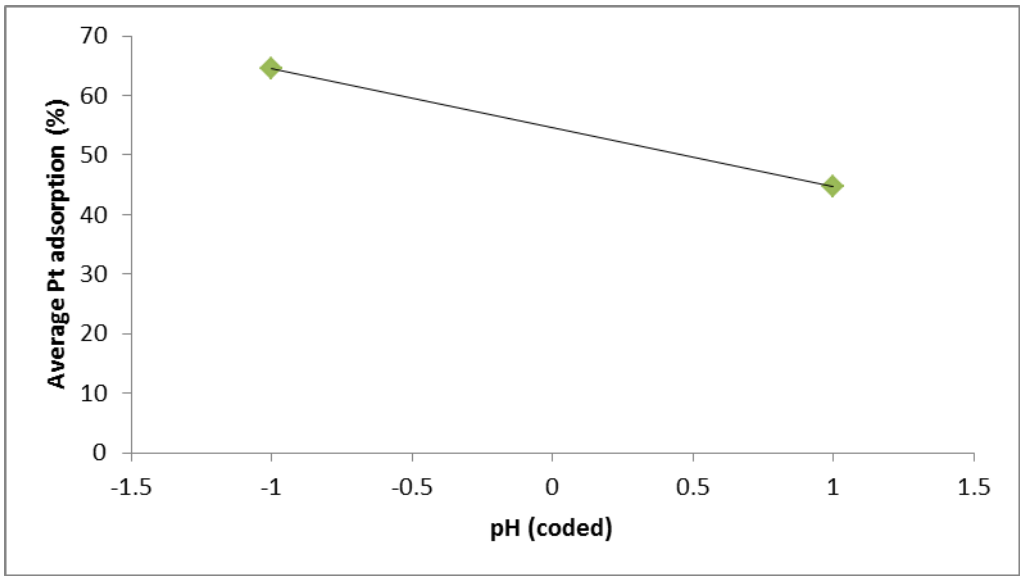


Figure 4.34: Main effect plot of pH on Pt (II).

The main effect of pH on Rh (III) adsorption is shown in Figure 4.35. Analysis of Figure 4.35 shows that an increase in the solution pH resulted in higher adsorption uptake for Rh (III) (adsorption increases from 28.06% to 48.1%). The main effect of initial metal ion concentration on Rh (III) adsorption is shown in Figure 4.36. It is apparent that the average percentage adsorption of rhodium increased from 19.63% at lower metal ion concentration to 56.55% at higher concentration. No interaction effects were observed for the adsorption of Rh (III).

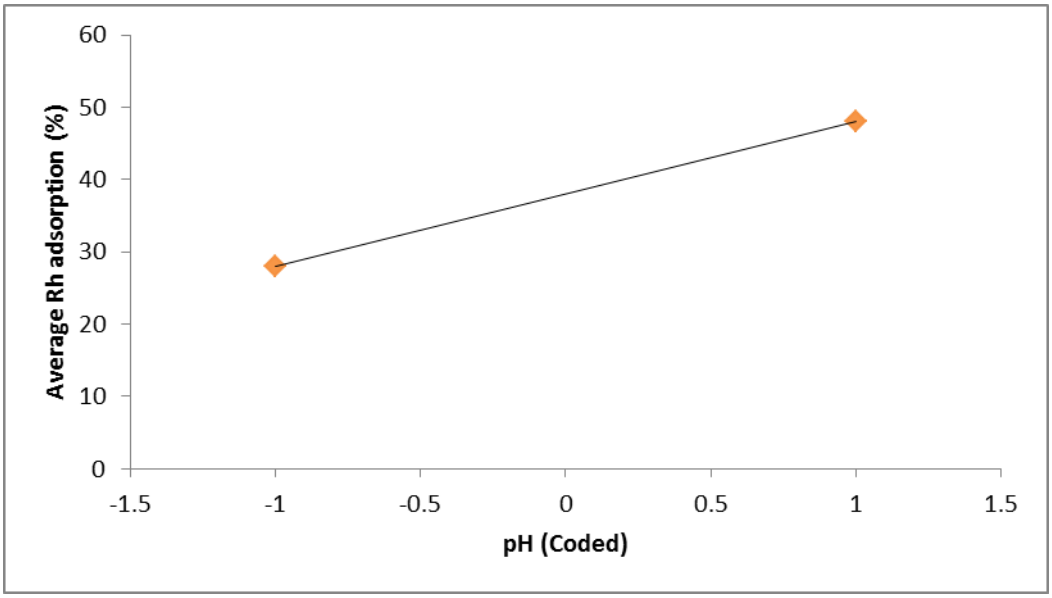


Figure 4.35: Main effect plot of pH on Rh (III).

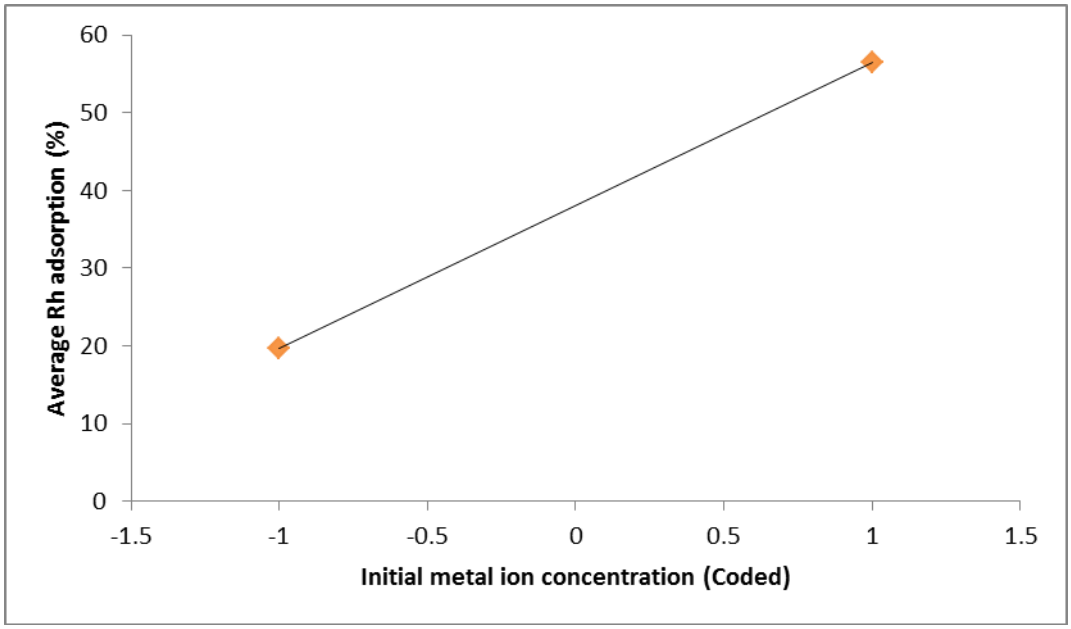


Figure 4.36: Main effect plot of initial metal ion concentration on Rh (III).

Overall Discussion

An increase in adsorption due to an increase in the initial metal concentration for all the five PGMs tested is as a result of the increase in the driving force of the concentration gradient. This is because a higher initial metal ion concentration enhances the driving force between the aqueous and solid phases and increases the number of collision between metal ions and adsorbents (Dula et al., 2014).

In order to explain the differences between the metals matrices in solution at a given pH, it is useful to consider the factors that determine possible sorption mechanisms. The main factor that influences the biosorption process is the property of the metal solution i.e. the pH, metal concentration and metal ion chemistry. According to their chemical characteristics, the metal ionic species exhibit different preferences for ligand binding sites (Vargas et al., 2004). Solution pH influences metal biosorption in two ways: Firstly, it determines the availability of the metal in soluble form i.e. the type of metal species available for biosorption. Secondly, it dictates the overall surface charge of the biosorbent material which in turn influences metal uptake behaviour (Pethkar, 1998).

Since, according to the DOE results, pH is statistically significant for the adsorption of PGMs and PGMs speciation is strongly related to pH and chloride concentration, further experiments were conducted to validate the effect of pH on the adsorption of PGMs tested. The results are presented in Figure 4.37. The results showed that the maximum adsorption capacity occurred at pH 3.0 for all the PGMs tested with 90.4% for Pt (II), 96.7% Pd (II), 98.3% for Au (III),81.7% for Ir ((III) and 79.9% for Rh (III).

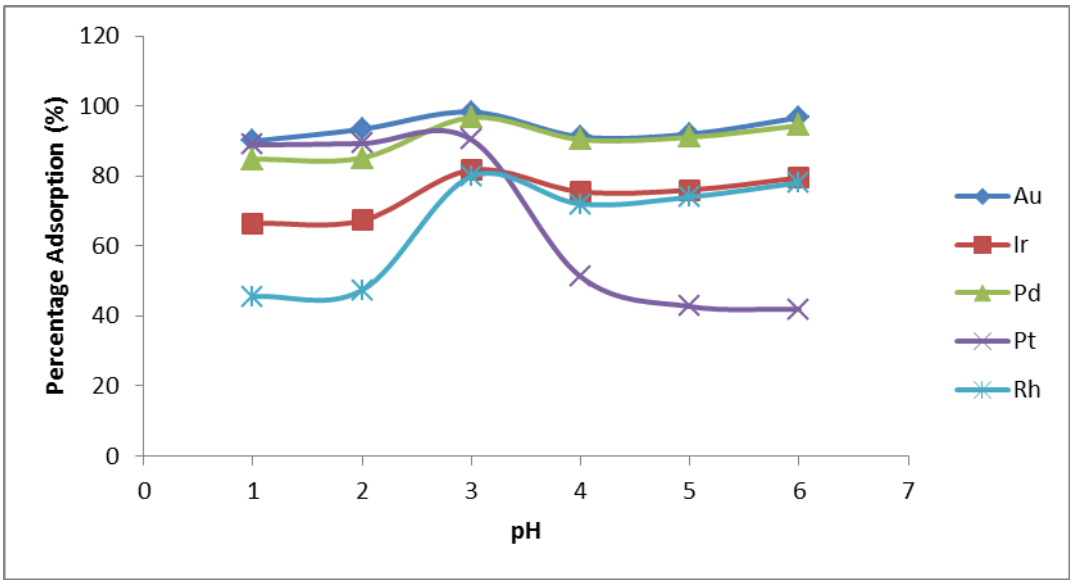


Figure 4.37: Effect of pH on the adsorption of Pt (II), Pd (II), Au (III), Ir (III) and Rh (III) on S. cerevisiae waste biomass (pH = 1-6; biomass dosage = 0.50 g; agitation speed = 150 rpm; contact time= 4hrs; temperature = 50°C; metal ions concentration = 10 mg/L).

The data indicated that the adsorption percentage increased as pH increased from 1-3 and slightly decreased again at pH higher than 3 for Pd (II), Au (III), Ir (III) and Rh (III). Although, there is a slight decrease in the adsorption of Pd (II), Au (III), Ir (III) and Rh (III) at pH higher than 3, Figure 4.37 still showed that the percentage adsorption at high pH 6 is higher than at low pH. This is in agreement with the result from DOE which showed that higher adsorption was obtained at higher pH (pH 6) while low pH (pH 1) gave lower adsorption percentage. However, at pH higher than 3, the adsorption of Pt (II) reduced drastically which confirms the result from the design of experiment which showed that an increase in pH has a negative effect on the adsorption of Pt (II). The negative effect of high pH on Pt (II) adsorption may be as a result of low chloride concentration at higher pH which might not favor the formation of platinum chloro anionic complex. In addition, Madrid and Camara (1997) found that the response of metal ions to a biosorption process has allowed for the classification of metal ions into three classes, dependent on their behavior at a specific pH. Class I metals (Al^{3+}, Cu^{2+}, Ni^{2+} etc.) are strongly bound at near-neutral pH, Class II metals ($PtCl_4^{2-}$, CrO_4^{2-} and SeO_4^{2-}) are bound strongly at low pH and only very weakly at high pH. Class III metals ($AuCl_4^-$, Ag^+, Hg^{2+}) are most strongly bound of all

metals, as their binding is pH independent. Precious metals are routinely present in anionic form, they are bound most strongly at low pH or exhibit pH independency and thus fall into class II / III. Therefore, the negative effect of pH on Pt (II) can be linked to the fact that the anionic form of platinum formed in solution falls into class II metals which are bound very weakly at high pH. Table 4.7 shows the dominant species of metal ion present in solution under the pH ranges studied.

Table 4.7: Dominant species of Au (III), Pd (II), Pt (II), Rh (III) and Ir (III) under the experimental condition studied.

Metal ion	Dominant species in solution
Au (III)	$(AuCI_4)^-$
Pd (II)	$PdCI_2(H_2O_2)$, $PdCI(H_2O)_3^+$ and $PdCI_3(H_2O)^-$
Pt (II)	$PtCI_2(H_2O_2)$, $PtCI(H_2O)_3^+$ and $PtCI_3(H_2O)^-$
Rh (III)	$RhCI_3(H_20)_3$, $Rh(H_2O)_6^{3+}$, and $RhCI(H_2O)_5^{2+}$,
Ir (III)	$IrCI_3(H_20)_3$, $Ir(H_2O)_6^{3+}$, and $IrCI(H_2O)_5^{2+}$,

These chloro complexes differ in the greater or lesser degree of ease with which they can show substitution reactions (Torapava, 2011). In general terms, these substitutions follow the sequence below;

Au (III) > Pd (II) > Pt (II) > Ir (III) > Rh (III)

Although, the effect of temperature (A) and biomass dosage (D) were found to be statistically insignificant for the adsorption of the PGMs under study, it was observed from the analysis of data in Table 4.5 that higher average adsorption percentage of all the tested PGMs was obtained at higher temperature (50°C). This is because at higher temperature, the rate of adsorbate diffusion across the external boundary layer and in the internal pores of the adsorbent increased (Ajaykumar et al., 2009), thus liquid

viscosity decreases as temperature increases. However, analysis of the data also showed that higher average adsorption was obtained at low biomass dosage (0.5g) while high biomass dosage gave lower average adsorption uptake for all the tested PGMs. The lower average adsorption obtained at high biomass dosage is as a result of decrease in adsorption intensity due to the unsaturation of the adsorption sites (Dorris et al., 2003). Therefore, it can be concluded that though the effect of factor A (temperature) and factor D (biomass dosage) are statistically insignificant, they are scientifically or logically significant for the adsorption of the tested PGMs.

4.4 Equilibrium Isotherms

The adsorption isotherm is an equation relating the amount of solute adsorbed onto the solid and the equilibrium concentration of the solute in solution at a given temperature. Isotherm data is essential in order to evaluate the adsorption potential of any adsorbent. Efficient design of an adsorption system very much depends on accurate estimation of these isotherm parameters (Pratibha et al., 2010).

The most commonly used isotherms in water and wastewater treatment are the Freundlich and Langmuir isotherms which are also selected in this study to determine the adsorption capacity of ethanol treated yeast biomass for various precious metals at 50°C**.**

Table 4.8 shows the experimental data of the adsorption isotherms for Au (III), Pd (II), Pt (II), Rh (III) and Ir (III) fitted with both Langmuir and Freundlich equations. From the Langmuir isotherm, the adsorption affinity constant, b (L/mg), and the maximum adsorption capacity,q_{max} (mg/g) of Au (III), Pd (II), Pt (II), Rh (III) and Ir (III) were estimated as 6.395L/mg and 0.006mg/g, 4.0 L/mg and 0.05mg/g, 12.41L/mg and 0.27mg/g, 2.28L/mg and 0.096mg/g and 2.29 L/mg and 0.13mg/g respectively. The high value of b which represents the affinity between sorbent and sorbate (the higher the value of b, the higher the affinity of the sorbent for the sorbate), suggests a strong binding between the ions and the biomass surface, indicating a chemisorption of metal ions at the surface of the waste yeast biomass, which is in a good agreement with the kinetics study. The Freundlich adsorption coefficient K_F and the intensity n were determined as 85.3mg/g and 0.39 for Au (III),

1.34mg/g and 1.09 for Pt (II), 2.1mg/g and 0.6 for Pd (II), 11.24mg/g and 1.16 for Rh (III) and 5.38mg/g and 0.96 for Ir (III) respectively.

Except for the fitting of the Langmuir isotherm with Pd (II), the R^2 of the Langmuir isotherms for the tested PGMs are all greater than 0.94 which validates the applicability of the Langmuir isotherm compared to the Freundlich isotherms with R^2 value between 0.82 and 0.88 for all the tested PGMs. The R_L values were between 0.4 and 0.8 indicating that the adsorption of these ions onto the waste yeast biomass was favourable.

Table 4.8: Linear Langmuir and Freundlich isotherm parameters for Au (III), Pd (II), Pt (II), Rh (III) and Ir (III) sorption by *S. cerevisiae* waste yeast.

	Langmuir isotherm $1/q_e=(1/q_{max}.b).1/C_e+ 1/q_{max}x$				Freundlich isotherm $\log q_e= \log K_F +1/n \log C_e$		
Metals	q_{max}(mg/g)	R_L	b (L/mg)	R^2	K_F(mg/g)	n	R^2
Au (III)	0.060	0.610	6.395	0.992	85.300	0.390	0.845
Pt (II)	0.270	0.450	12.410	0.963	1.340	1.090	0.882
Pd (II)	0.050	0.700	4.000	0.751	2.100	0.600	0.829
Rh (III)	0.096	0.800	2.280	0.949	11.240	1.160	0.881
Ir(III)	0.130	0.813	2.290	0.949	5.380	0.960	0.857

4.5 Adsorption –Desorption Cycles

If a biosorption process is to be used as an alternative to the traditional wastewater treatment schemes, the regeneration of the biosorbent is crucially important for keeping the process costs down (Ahalya, et al 2003). For this purpose, it is desirable

to desorb the sorbed metals and to regenerate the biosorbent material for subsequent cycles of application. The desorption and regeneration processes should: yield the metals in a concentrated form; restore the biosorbent close to the original condition for effective reuse with undiminished metal uptake and without physical changes or damage to the biosorbent (Ahalya, et al 2003).

The desorption of the tested PGMs from the loaded biomass was carried out using different concentrations of HCl (hydrochloric acid), CS $(NH_2)_2$ (thiourea), H_2SO_4 (sulphuric acid) and CS (NH_2)-HCI (hydrochloric + thiourea) solution as shown in Table 4.9.

Table 4.9: desorption data for Au (III), Pd (II), Pt (II), Rh (III) and Ir (III)

Eluant Concentration(M)	Desorption Efficiency (%)				
	Au (III)	Pd (II)	Pt(II)	Rh (III)	Ir (III)
0.1M HCl	1.2	7.5	8.3	3.5	5.9
0.5M HCl	0.6	8.8	9.4	4.4	8
1M HCl	0.4	10.3	8.5	11.4	8.5
0.1M H_2SO_4	0.4	4.0	4.4	22.3	12.7
0.5M H_2SO_4	1.5	6.2	7.0	27.4	15.0
1M H_2SO_4	3.1	8.3	15.9	30.0	25.0
0.1M Thiourea	15.8	17.0	8.1	1.3	3.0
0.5M Thiourea	17.5	30.0	9.4	2.2	4.4
1M Thiourea	17.8	46.1	15.6	3.1	4.4
1M HCl + 0.1M Thiourea	99.5	99.2	97.8	20.0	24.5
1M Thiourea + 0.1M HCl	31.1	72.0	96.0	10.1	9.4

The results show that 0.1M CS $(NH_2)_2$ in 1M HCI solution can effectively desorb Au (III), Pd(II) and Pt (II) metal ions from the yeast biomass. More than 97% of Au (III), Pd (II) and Pt (II) metal ion biosorbed on the yeast was desorbed. However, none of the eluants tested were able to effectively desorb Rh (III) and Ir (III) from the

biomass. Only 20% and 24.5% of biosorbed Rh(III) and Ir (III) respectively was desorbed using 0.1M CS $(NH_2)_2$ in 1M HCI solution. However, 1M H_2SO_4 solution gave the highest desorption of 30% for Rh (III) and 25% for Ir (III). The high percentage desorption for Au(III), Pd(II) and Pt (II) obtained when acidified thiourea was used can be explained as due to both stable complex formation and the electrostatic interaction between Au (III)), Pd(II) and Pt (II) species and charged species from elution. For example, a study made by Lin and Lien, 2013 showed that $AuCl_4^-$ is a strong oxidizing agent that is readily reduced to Au (I) by thiourea according to the equation below:

$$AuCl_4^- + 4CS(NH_2)_2 + H_2O \longrightarrow Au(CS(NH_2)_2)_2^+ + CO(NH_2)_2 + S + 2Cl^- + 2HCl$$

Au (I) may further be reduced to Au (0) under reducing conditions.

$$Au(CS(NH_2)_2)_2^+ + e^- \longrightarrow Au^0 + 2CS(NH_2)_2$$

The differences in the desorption results of Rh (III) and Ir (III) compared to the other tested PGMs can be explained by the kinetic inertness of rhodium and iridium complexes as well as by the stereochemistry of these complexes (Louw, 2008).

The behaviour of the yeast biomass regarding its stability and regeneration was assessed by conducting 5 adsorption-desorption cycles using 0.1M CS $(NH_2)_2$ in 1M HCI and the results are presented in Figure 4.38 and 4.39.

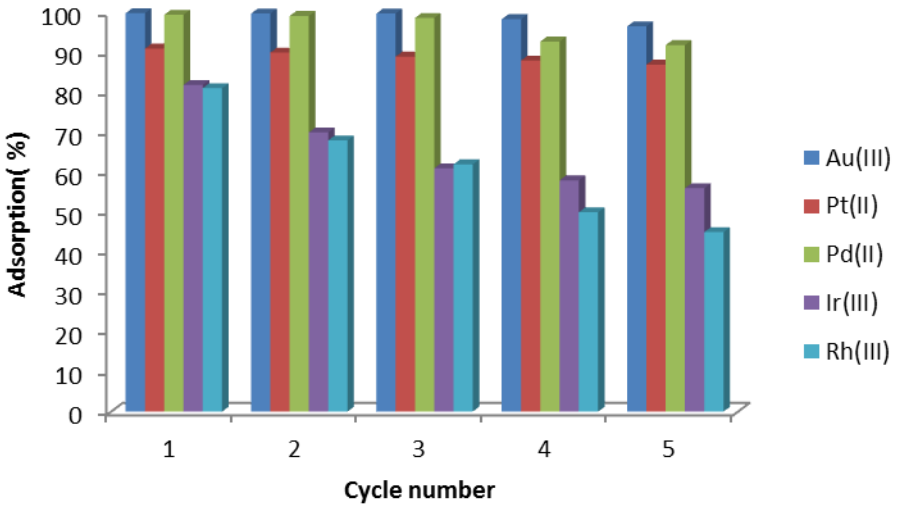


Figure 4.38: Adsorption efficiency cycle of the yeast biomass for Au (III), Pd (II), Pt (II), Ir (III) and Rh (III).

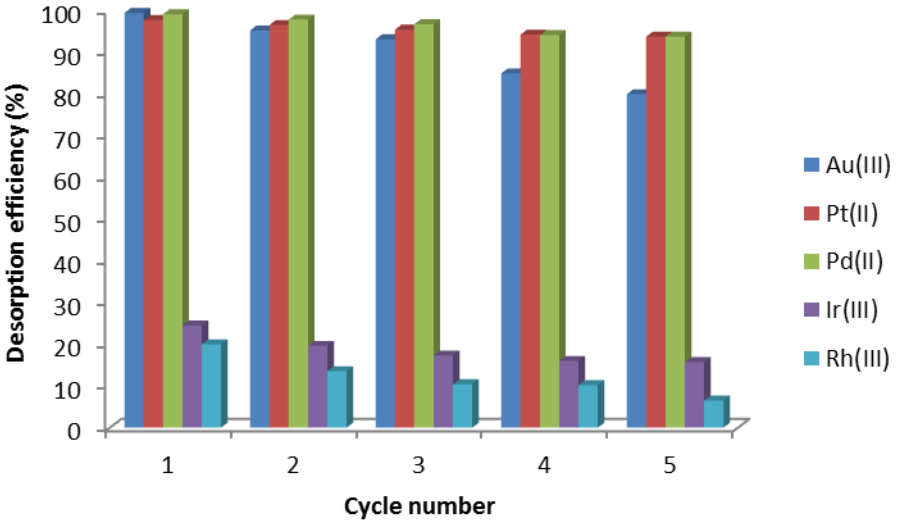


Figure 4.39: Desorption efficiency cycle

As can be seen from Figure 4.38, the adsorption of Au (III), Pd (II) and Pt (II) remained almost constant for the 5 adsorption cycle whereas the adsorption of Ir (III) and Rh (III) decreased from 81.9% and 81.1% to 56% and 45% respectively after 5 adsorption cycles.

Figure 4.39 shows that the desorption of Au (III), Pd (II), Pt (II) decreased slightly as the number of cycles increased, however desorption efficiency of above 80% was still achievable for Au (III), Pd (II), Pt (II) after 5 adsorption desorption cycles. Ir (III) and Rh (III) were not effectively desorbed from the biomass and the desorption efficiency decreased from 24.5% and 20% to 15.7% and 6.5% respectively after 5 adsorption desorption cycles. The adsorption efficiency is in the order of Au (III) >Pd (II) > Pt (II) >Ir (III) > Rh (III). The higher adsorption rate (above 40%) still obtained regardless of the poor desorption of Ir (III) and Rh (III) from the biomass surface may be due to the fact that not all the biomass surface are occupied with metal ion at the initial stage. This is as a result of dilute or low concentration of metals in solution compared to the available binding sites therefore providing binding site for the metal ions at the subsequent cycles. It has been reported that in general, the greater the atomic weight, electro negativity, electrode potential and ionic size, the greater will be the affinity for sorption (Sengil and Ozacar, 2009) Electro negativities and ionic radius of the elements are given in Table 4.9.

Table 4.10: Ionic radius and Electronegativity of the tested PGMs

Ion	Ionic radius (pm)	Electronegativity (Pauling)
Au (III)	85.0	2.54
Pd (II)	86.0	2.20
Pt (II)	80.0	2.28
Ir (III)	68.0	2.20
Rh (III)	66.5	2.28

It is clear that ionic radius is the dominant factor for sorption of the tested PGM ions to the yeast biomass. Although the adsorption percentage removal was lower for Ir (III) and Rh (III) coupled with their smaller ionic radius compared to other PGMs tested, the desorption of these two metals should be easier and higher than that of Au (III),Pd (II) and Pt (II) but the reverse is the case. This may be due to the higher affinity of the desorption agent (acidified thiourea) for Au (III),Pd (II) and Pt (II) which mainly depends on the species of metal ion adsorbed onto the biomass and the

affinity between these species with the charged species from elution as explained with the chemical reaction in section 4.5.

The weight loss of the biomass was in the range of 30-35% after 5 adsorption desorption cycles.

4.6 Column Studies

Continuous mode sorption studies have an important role in evaluating the technical feasibility of a process for industrial treatment systems. Column adsorption tests by ethanol treated yeast immobilized on Plaster of Paris were carried out using PGMs dilute process streams obtained from precious metal refinery section of Impala Platinum, Springs, South Africa. The process used at this plant for PGMs extraction is primarily based on ion exchange technology. An overview of the refining process employed at Impala Refineries in Springs, South Africa, has been presented in Figure 2.4.

After the extraction process, the effluent generated contains PGMs in very low concentrations, base metals (e.g nickel, iron, copper, cobalt etc.) as well as other elements like selenium, Tellurium etc.

4.6.1 Characterisation of PGMs dilutes process streams

Two forms of process effluents are produced in the precious metal refinery section of Impala Platinum, Springs, South Africa namely acidic and alkaline effluents (the process for the generation of these effluents cannot be discussed due to the confidentiality of the information). Characterization of the effluents under study was made by analyzing various parameters viz, COD, metal contents, TS, TSS and TDS as discussed in section 3.4. Table 4.11 gives the summary of the physico-chemical characteristics of the two forms of PGMS effluents.

Table 4.11: Summary of the physico-chemical characterization of the PGMs process streams

Characteristics	Acidic Sample	Alkaline Sample	USEPA limits	DWAF guide line for industrial disposal
pH	1.8	8.5	n/a	5-10
Total conductivity(mS/m)	12,644	15,423	n/a	n/a
colour	Brown	Pale brown/yellow	n/a	n/a
COD (mg/l)	200	221	5	0-75
TSS (mg/l)	1080	1230	4	0-25
TDS (mg/l)	220	304	50	n/a
TS (mg/l)	1300	1534	n/a	0-1600
Chlorides(mg/l)	3497	856	n/a	0-500
Sulphate (SO_4) (mg/l)	10947	70349	5	0-500
t (NH_3)(total ammonia) (mg/l)	79.1	‹2.5	0.01	n/a
Ag (mg/l)	0.004	0.002	n/a	n/a
Au (mg/l)	0.015	‹0.001	0.005	n/a
Pd (mg/l)	0.248	0.215	0.02	n/a
Pt (mg/l)	1.88	2.72	0.1	n/a
Rh (mg/l)	0.065	0.029	0.02	n/a
Ir (mg/l)	8.25	3.8	0.02	n/a
Ru (mg/l)	0.937	5.12	0.1	n/a
Co (mg/l)	0.026	0.947	0.005	n/a
Cu (mg/l)	0.275	0.787	0.005	0.006
Zn (mg/l)	0.077	0.310	0.0002	0.05
Te (mg/l)	1.24	10.1	0.02	n/a
Se (mg/l)	416	1113	0.01	0.05
Fe (mg/l)	1.17	1.10	0.005	0.0 – 10.0
Na (mg/l)	45100	103850	0.1	n/a
Ni(mg/l)	2.08	41.4	0.005	n/a

The high concentration of Sulphate, Sodium and Chlorides contents results in a very high ionic strength water.

4.6.2 Analysis of chemical oxygen demand (COD)

Chemical oxygen demand test is commonly used to indirectly measure amount of organic compounds in water. COD is an indicator of the concentration of organics in the solution. During the adsorption process, the COD analysis of the effluent was carried out at different time intervals. The measured COD decreased from 200mg/l to less than 68mg/l for the acidic sample and from 221mg/l to less than 95mg/l for the alkaline sample after 30minutes which corresponds to the removal efficiency of about

66% and 57% respectively. Beyond this time, there was no significant change in the COD level. The analysis of chemical oxygen demand was based on the column experiments.

4.7 Column Experiments

The results of the column experiments presented here are based on the purification of the PGMs dilute process solution. Since the feed solution to the Impala refinery section also contains base metals, the results presented are therefore focused not only on the platinum group metals but also on the base metals as well as other trace elements present in the dilute solution. The work focused on the removal of metal species with high concentration or those found above their discharge limit (in the case of base metals and the anions) and concentration above 0.1mg/l in the case of PGMs as indicated in Table 4.11. The species of interest includes: Sulphates, Chlorides, Na, Ni, Se, Ru, Pd, Pt, Ir (for acidic sample) and Pd, Pt, Ir, Ru, Ni, Na, Se, Te, Sulphate, Chlorides (for alkaline sample).

For the test works the dilute process streams were conditioned to pH 3 (the optimum pH for PGMs adsorption in the batch studies) and the formation of yellow precipitate was observed in the alkaline solution. XRD analysis of the precipitate showed the presence of Halite (61%), Thernadite (13.4%) and Disodium Sulphate (VI) (25.56%). After the alkaline solution was filtered to remove the precipitate, the solution changed to a very milky/ cloudy yellowish solution and this affected the adsorption of other metals in solution. Therefore, the result presented here focused only on the work conducted on the acidic solution.

From the perspective of dynamic modelling, the dynamic behaviour of a packed column is described in terms of a breakthrough curve. A breakthrough curve is a plot of effluent solute concentration versus time. The breakthrough point is characterised by the beginning of a sharp increase in the outlet concentration and it is the point at which the effluent solute reaches its maximum allowable value.

4.7.1 Effect of flow rates

The effect of flow rates on the biosorption of metals of interest by Plaster of Paris immobilized yeast were studied by varying the flow rate from 0.9 to 2.1ml/s while the bed height was held constant at 13cm. The breakthrough curves were constructed as C/C_o (C is the effluent concentration at time t while C_o is the initial concentration of the influent stream) versus time as presented in Figure 4.40-4.48. Breakthrough in this study is considered to have occurred when there is a sharp increase in the outlet concentration. The breakthrough time is arbitrarily inferred for C/C_o at 0.05 according to literature **(**Oliviera et al., 2011). However, the breakthrough in this study is based on the allowable discharge limits of various metal of interest as outlined by the United State Environmental Protection Agency (2010), as well as the Department of Water Affairs and Forestry (1996). These values are in Table 4.11. In addition, saturation was assumed to have occurred when the effluent concentration was equal to influent concentration generally at 90%- 95% of the influent concentration according to literature (Oliviera et al., 2011). However, by looking at the shape of most of the graphs presented below, it can be concluded that the saturation of the bed was not reached. In addition, the steepness of most of the graphs show that frequent and accurate monitoring of the effluent quality is needed to assure that a high concentration of the contaminant is not allowed to exit the column before the run is terminated (Benjamin and Lawler, 2013). The steepness of the breakthrough curve determines the extent to which the capacity of an adsorbent bed can be utilized.

Figure 4.40 – 4.43 show the breakthrough curves for the effect of flow rate on the adsorption of the platinum group metals found in the dilute process stream under study. Figure 4.40 shows the effect of flow rates on the adsorption of platinum at inlet metal concentration of 1.88mg/l. The results show that as the flow rate increased from 0.9 to 2.1ml/s, the breakthrough time decreased from 20 minutes to 10 minutes. Analysis of this figure shows that the maximum allowable value for platinum was not reached at any of these flow rates. Table 4.12 below gives the allowable discharge limits of various PGMs and base metals in wastewater (United State Environmental Protection Agency, 2010) and the metal concentration at breakthrough point (0.9ml/s and 13cm bed depth). According to Table 4.12, the maximum allowable limit for

platinum is 0.01mg/l which means that breakthrough is considered to have occurred at the normalised concentration $\frac{C}{C_O} = 0.005$, but the figure shows that as the flow rate increased the breakthrough only occurred at $\frac{C}{C_O} = 0.307$, $\frac{C}{C_O} = 0.313$ and $\frac{C}{C_O} = 0.34$ respectively.

Table 4.12: Discharge limits for PGMs and some base metals in wastewater

Component	limit	Concentration at breakthrough point (C_b)
Platinum	0.1mg/l	0.58mg/l
Palladium	0.02mg/l	0.005mg/l
Selenium	0.01mg/l	208mg/l
Tellurium	0.02mg/l	0.025mg/l
Iridium	0.02mg/l	2.64mg/l
Ruthenium	0.1mg/l.	0.38mg/l
Sodium	0.1mg/l	18,085mg/l
Sulphate	5mg/l	2,364mg/l
Nickel	0.005mg/l	0.29mg/l

Furthermore, if the saturation of the bed is considered to have occurred when the effluent concentration equal 0.9Co, Figure 4.40 shows that the saturation of the bed by platinum ion was not reached at any of the flow rate studied. The highest saturation point was observed at the flow rate of 2.1ml/s with the value of $\frac{C}{C_O} = 0.48$ which might be an indication of high affinity of the adsorbent towards platinum ion. However, platinum not being able to reach the allowable limit even at the lowest flow rate may be as a result of competitive adsorption with other metal ions or the inorganic content like sulphate and chloride which have higher affinity for the adsorbent than platinum.

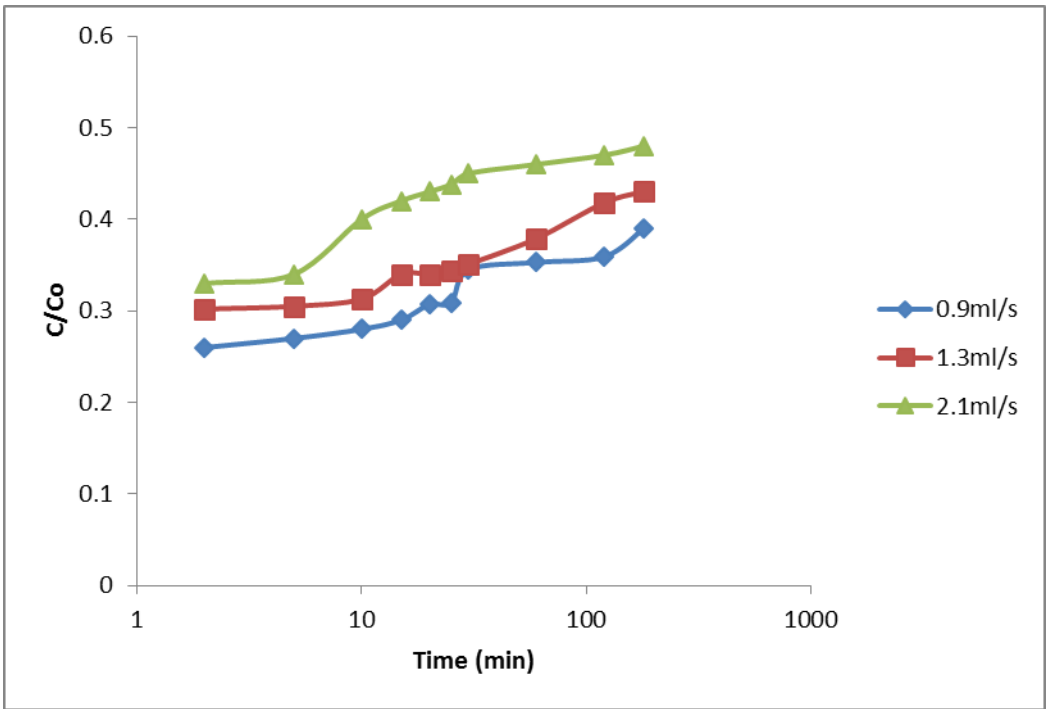


Figure 4.40: Breakthrough curve for platinum adsorption at different flow rates (C_o = 1.88mg/l, bed height = 13cm, temp. = 25˚C).

Figure 4.41 shows the effect of flow rates on the adsorption of palladium at inlet metal concentration of 0.248mg/l. The results show that if the maximum allowable limit for palladium is 0.01mg/l according to Table 4.12, then the breakthrough time only occurred at 180minutes for 0.9ml/s, 120minutes for 1.3ml/s and 60minutes for 2,1ml/s. This indicated that for a sharp breakthrough to occur with the lower flow rates, and for the bed to be saturated with palladium ions the adsorption time must be prolonged beyond 180minutes used. Since a longer breakthrough time imply better adsorption capacity, this means that at the lower flow rates, it would take a longer time for the adsorbent material to be completely saturated with the adsorbate. It can therefore be deducted from the graph that despite the very low concentration of palladium, the sorbent has high affinity for palladium which is in agreement with the results obtained in the batch studies.

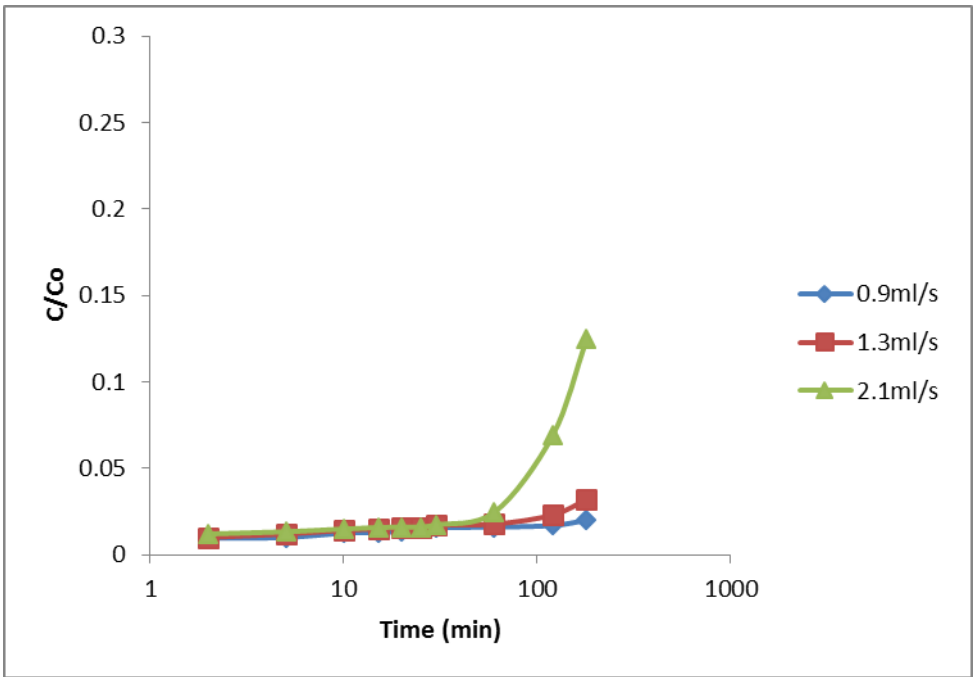


Figure 4.41: Breakthrough curve for palladium adsorption at different flow rates (C_o = 0.248 mg/l, bed height = 13cm, temp. = 25˚C).

Figure 4.42 shows the effect of solution flow rate on the adsorption of iridium at inlet concentration of 8.25mg/l.The figure shows that as the flow rate increased from 0.9ml/s to 2.1 ml/s the breakthrough time decreased from 25minutes to 5minutes respectively. In addition, according to Table 4.12, the maximum allowable limit for iridium was not reached at any of these flow rates. Although, the adsorption capacity of the bed decreased as the flow rate increased, the saturation point of only 0.47Co was obtained at the flow rate of 2.1ml/s which may indicate high affinity for the metal ion but limited by the effect of competitive adsorption.

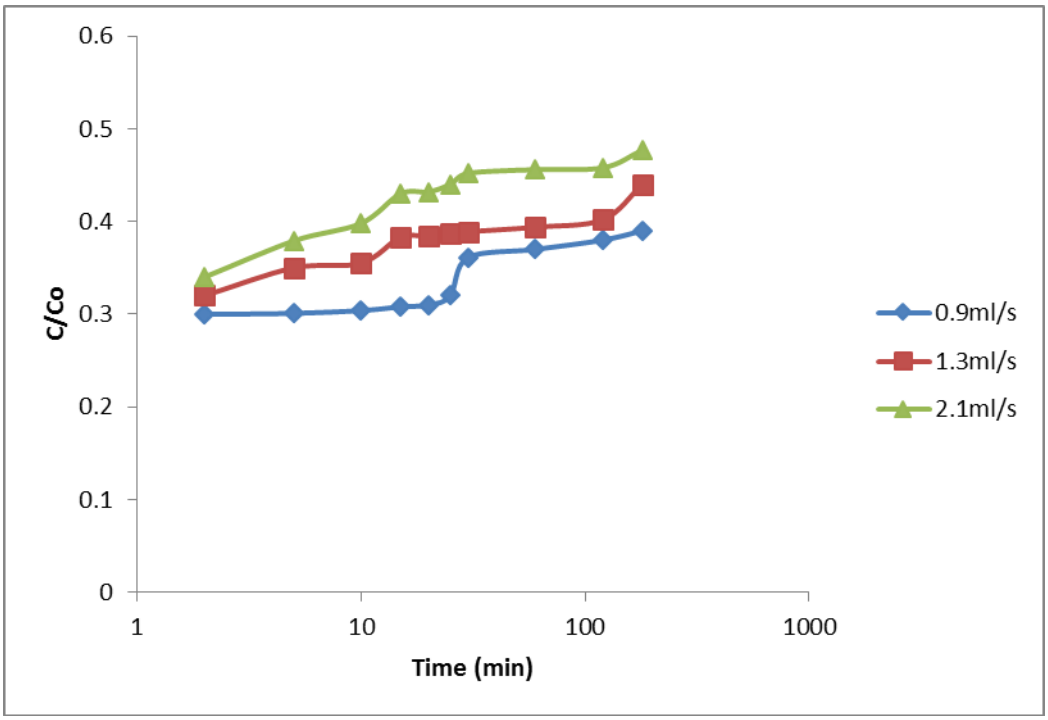


Figure 4.42: Breakthrough curve for iridium adsorption at different flow rates (C_o = 8.25 mg/l, bed height = 13cm, temp. = 25˚C).

Figure 4.43 shows the effect of solution flow rate on the adsorption of ruthenium at inlet concentration of 0.937mg/l. The results indicate that as the flow rate increases there is no significant difference in the breakthrough time between 0.9 and 1.3ml/s which indicates that the adsorption of ruthenium remains almost constant regardless of the flow rate.

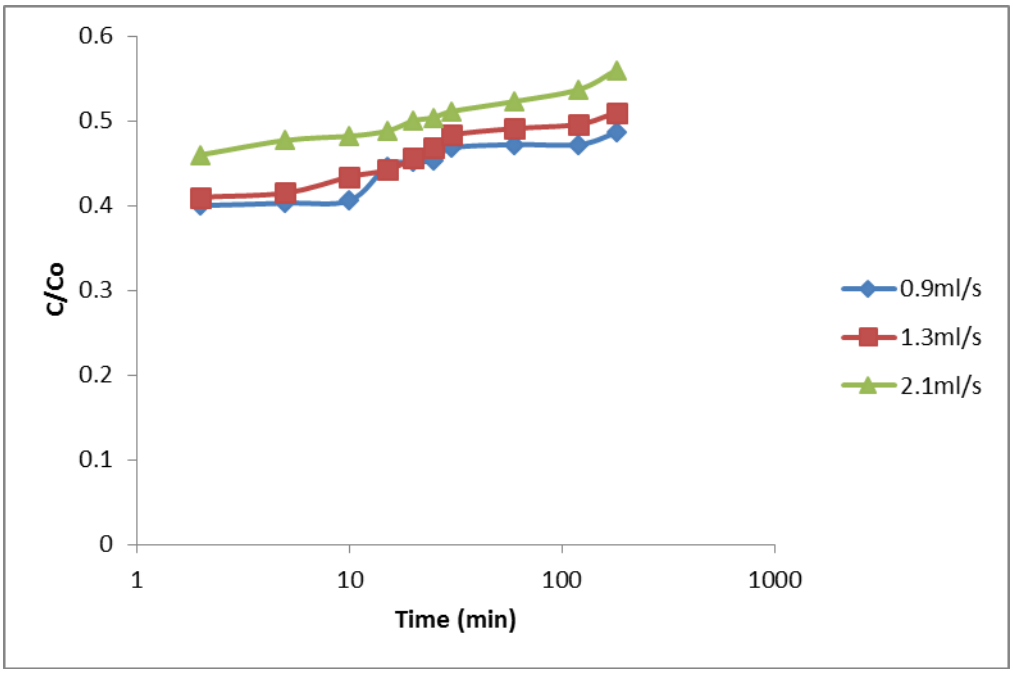


Figure 4.43: Breakthrough curve for ruthenium adsorption at different flow rates (C_o = 0.937mg/l, bed height = 13cm, temp. = 25˚C).

Figure 4.44 – 4.48 show the breakthrough curves for the base metals and other trace elements found in the dilute process stream under study.

Figure 4.44 shows the effect of solution flow rate on the adsorption of nickel at inlet concentration of 2.08mg/l. From the graph, an increase in the flow rate from 0.9ml/s to 2.1ml/s decreased the breakthrough time from 25minutes to 10minutes. In addition, for the column to be saturated with nickel ion, the adsorption time must be prolonged more than 180minutes used due to the low concentration of nickel in solution and this also applied to all other metal ions with low concentrations in the solution like palladium.

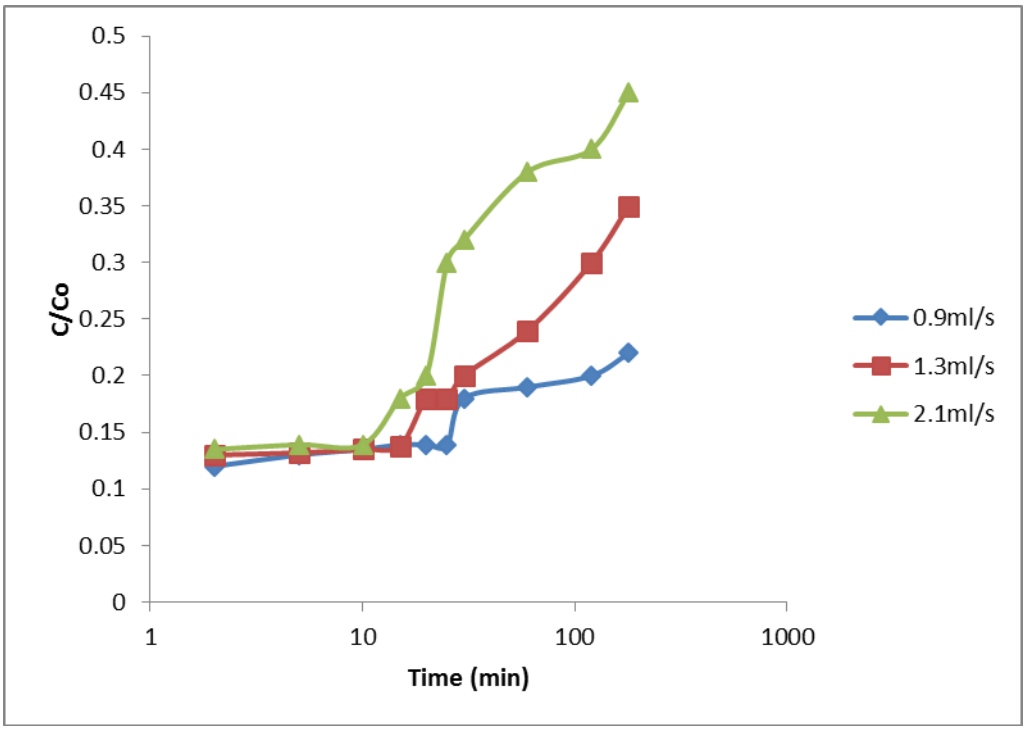


Figure 4.44: Breakthrough curve for nickel adsorption at different flow rates (C_o = 2.08 mg/l, bed height = 13cm, temp. = 25˚C).

Figure 4.45 shows the effect of solution flow rate on the adsorption of selenium at inlet concentration of 416 mg/l. The results show that as the flow rate decreased, the adsorption of selenium slightly increased and saturation was only reached when the flow rate reached 2.1ml/s while at flow rate of 0.9ml/s and 1.3ml/s, the contact time must be prolonged to achieve saturation. In the same way, the allowable discharge limit, if it is considered to be reached when the concentration in the effluent according to Table 4.12 has a value of 0.01mg/l, was not achievable due to a very high concentration of selenium present in the solution thereby leading to early saturation of the column.

Based on the information in Table 4.11, selenium is one of the metals with high concentration in the process stream under study. Therefore , due to a very high concentration of selenium, as the flow rate increased, the saturation of the column is reached more rapidly, especially at high flow rate.

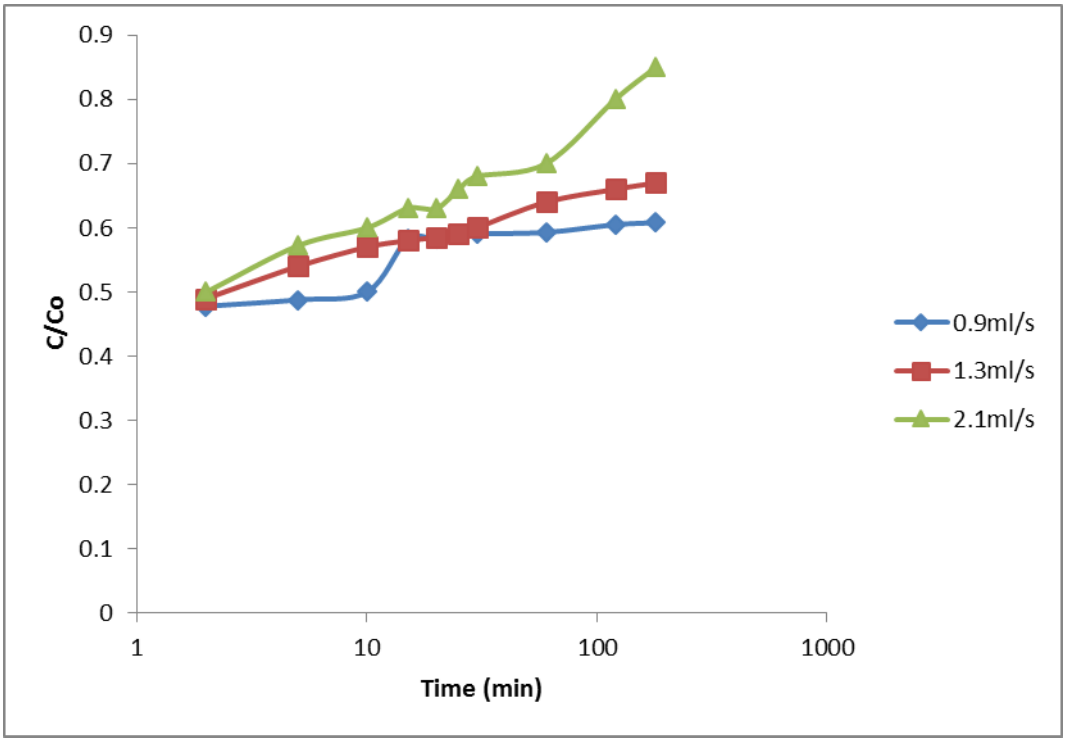


Figure 4.45: Breakthrough curve for selenium adsorption at different flow rates (C_o = 416 mg/l, bed height = 13cm, temp. = 25˚C).

Figure 4.46 shows the effect of solution flow rate on the adsorption of tellurium at inlet concentration of 1.24 mg/l. The results show that the breakthrough time decreased from 30minutes to 10minutes as the flow rate increased from 0.9 to 2.1ml/s. In addition, from the figure the allowable limit (0.02mg/l) for tellurium was only achievable at the flow rate of 0.9ml/s.

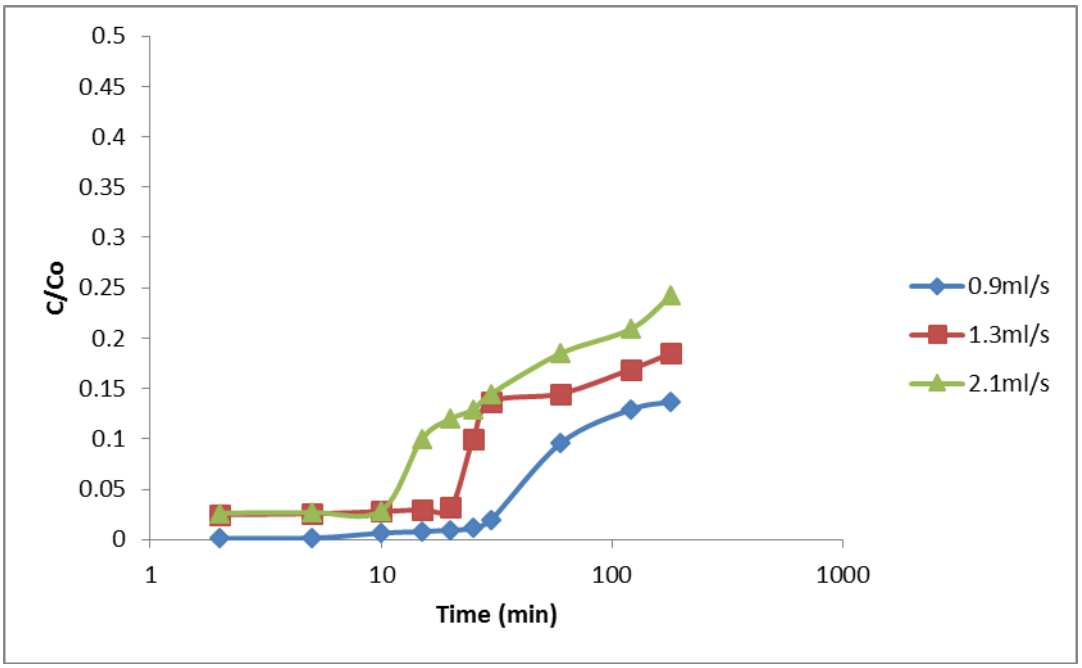


Figure 4.46: Breakthrough curve for tellurium adsorption at different flow rates (C_o = 1.24 mg/l, bed height = 13cm, temp. = 25˚C).

Figure 4.47 shows the effect of solution flow rate on the adsorption of sodium at inlet concentration of 45,100 mg/l. Sodium has the highest concentration in the solution under study therefore as the flow rate increased, the saturation of the column is reached much more rapidly. In addition, the retention of sodium increased as the flow rate decreased and only reached saturation in the column when the flow rate is 2.1ml/s.

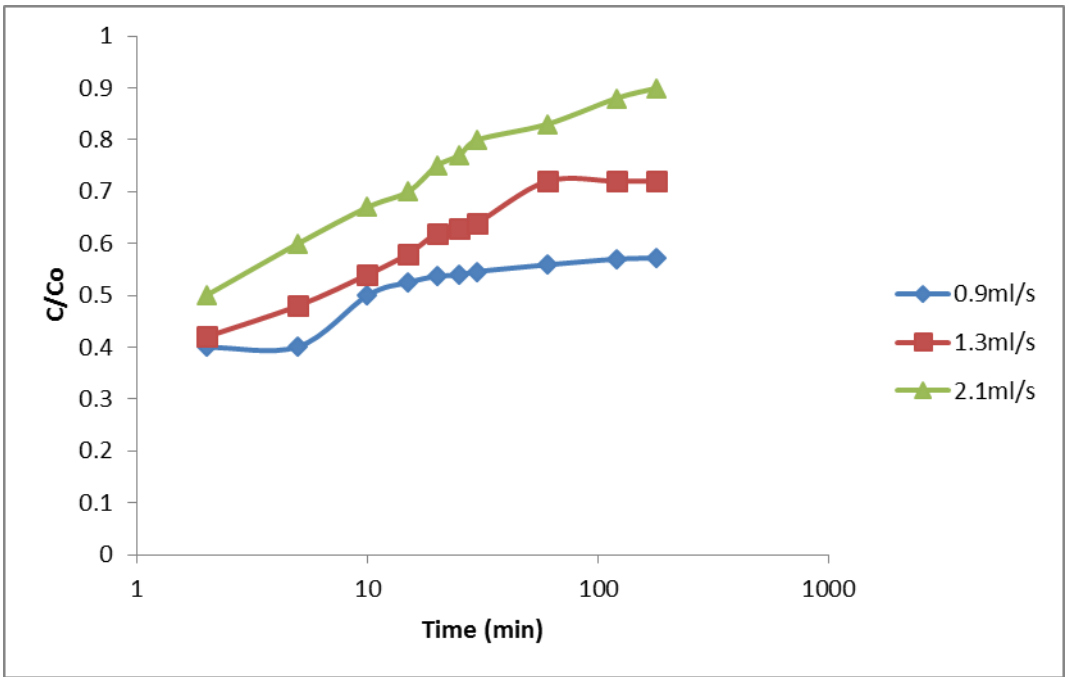


Figure 4.47: Breakthrough curve for sodium adsorption at different flow rates (C_o = 45,100 mg/l, bed height = 13cm, temp. = 25˚C).

Figure 4.48 shows the effect of solution flow rate on the adsorption of sulphate ions at inlet concentration of 10,947 mg/l. Figure 4.48 shows that as flow rate increased, the breakthrough time decreased from 30minutes to 10 minutes respectively. In addition despite the high concentration of sulphate ion in solution, the saturation of the column was not rapid as compared to other metals with high concentration in solution (Se, and Na). This may be explained using the point of zero charge on the yeast. The pHzc of the yeast is 6.31which means at pH lesser than this, the surface of the sorbent will be positively charged which is prone to attracting negatively charged ions. This may be the reason why sulphate ions and metals which formed negative complexes in solution such as platinum and palladium, were easily adsorbed from the solution regardless of their concentration.

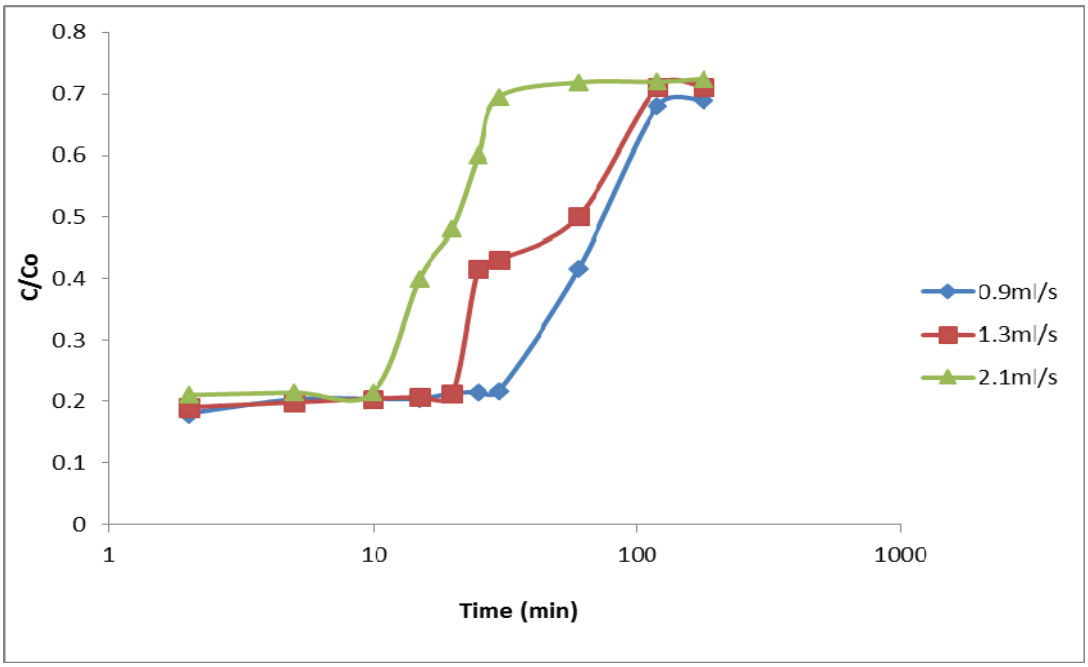


Figure 4.48: Breakthrough curve for sulphate adsorption at different flow rates (C_o = 10,947 mg/l, bed height = 13cm, temp. = 25˚C).

Overall Discussion

The overall results for the effect of flow rate on all the metals of interest show that as the flow rate increased, the breakthrough time as well as the residence time decreased. As a result of the increase in the flow rate, the bed utilization (the manner or extent at which the available binding sites is been used up) as well as the bed adsorption capacity will be reduced. This is due to insufficient residence time of the solute in the column and insufficient diffusion of the solute into the pores of the adsorbent, therefore the solute left the column before equilibrium occurred. It was observed that breakthrough generally occurred faster with higher flow rates. The reason is that at high flow rate, there are more adsorbates per unit time for the available surface, therefore both the breakthrough time and saturation time are achieved faster than in the case of lower flow rate. These results are in agreement with other findings in literature for systems of biosorption in columns for different metals using different sorbent materials (Calero et al., 2009; Danny et al., 2000; Khan et al., 2011). The results indicated that breakthrough generally occurs faster with higher flow rate while at lower flow rate metal ions have more time to contact with the adsorbent resulting in higher removal of metal ions in the column.

For most of the platinum group metals present in the solution under study, regardless of the flow rate investigated, a prolonged time higher than 180minutes was required to reach column saturation which is in agreement with the findings in batch experiments.

Table 4.13 summarised the breakthrough times for different metals studied at different flow rates.

Table 4.13: Breakthrough times at different flow rates

Metal ions	0.9ml/s t_b(min)	1.3ml/s t_b(min)	2.1ml/s t_b(min)
Platinum	25	10	5
Palladium	180	120	60
Iridium	25	10	5
Ruthenium	10	5	2
Selenium	10	2	2
Tellurium	30	20	10
Nickel	25	15	10
Sodium	5	2	2
Sulphate	30	20	10

Based on the information in Table 4.13, the results indicate that a flow rate of 0.9ml/s offers a classic breakthrough curve to work on compared to the other two flow rates tested since a longer breakthrough time indicates higher efficiency of the adsorbent. Therefore, the subsequent experiments were carried out with 0.9ml/s flow rate.

4.7.2 Effect of Bed Depths

The retention of metal ions in a fixed-bed column depends, among other factors, on the quantity of solid sorbent used or, on the bed depth of the column (Calero et al; 2009).The sorption performance of Plaste00r of Paris immobilized yeast was assessed using various bed depths 6.5cm, 8.5cm and 13cm at flow rate of 0.9ml/s. Figure 4.49 – 4.57 shows the breakthrough curves for the metal ions at different bed depths.

Figure 4.49 shows the effect of bed depth on the sorption of platinum. The results show that the breakthrough time increased with increasing bed height. The figure shows that the adsorption of platinum metal remained almost constant at each of the bed depth. However, the saturation of the bed is not reached at any of the bed depth.

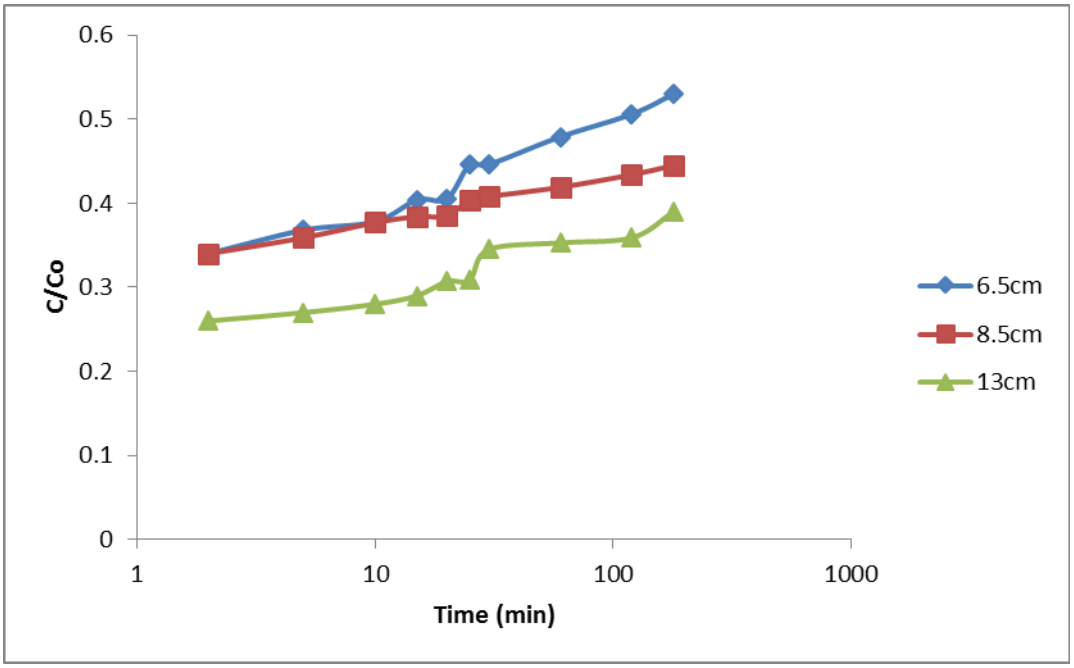


Figure 4.49: Breakthrough curve for platinum at different bed depth (C_o = 1.88mg/l, flow rate = 0.9ml/s, temp. = 25˚C).

Figure 4.50 shows the effect of bed depth on the sorption of palladium. From the figure, as the bed height decreased from 13cm to 6.5cm, the breakthrough time also decreased from 180minutes to 30minutes because at lower bed depth the saturation at the binding sites is faster.

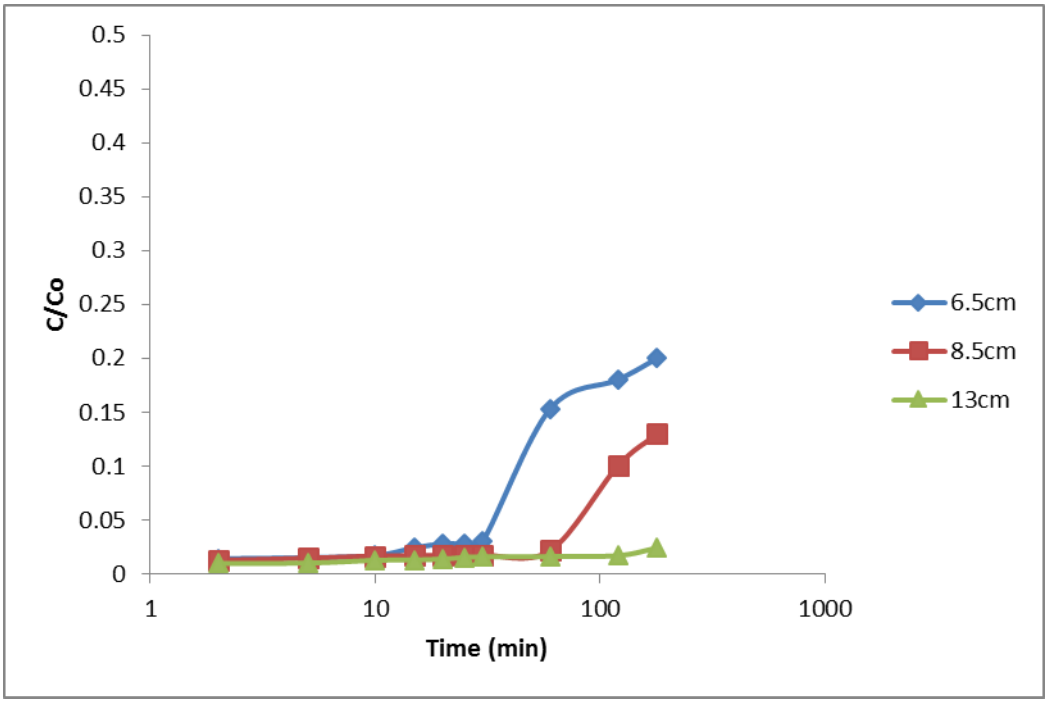


Figure 4.50: Breakthrough curve for palladium at different bed depth (C_o = 0.248mg/l, flow rate = 0.9ml/s, temp. = 25˚C).

Figure 4.51 shows the effect of bed depth on the sorption of iridium. The results show that the saturation of the column with iridium ion was rapid with lower bed heights compared to other Platinum group metals in solution. This is because iridium has the highest concentration in solution compared to other PGMs and as the bed depth increased, the adsorption of iridium increased although not reaching the allowable limit at the highest bed depth according to Table 4.12.

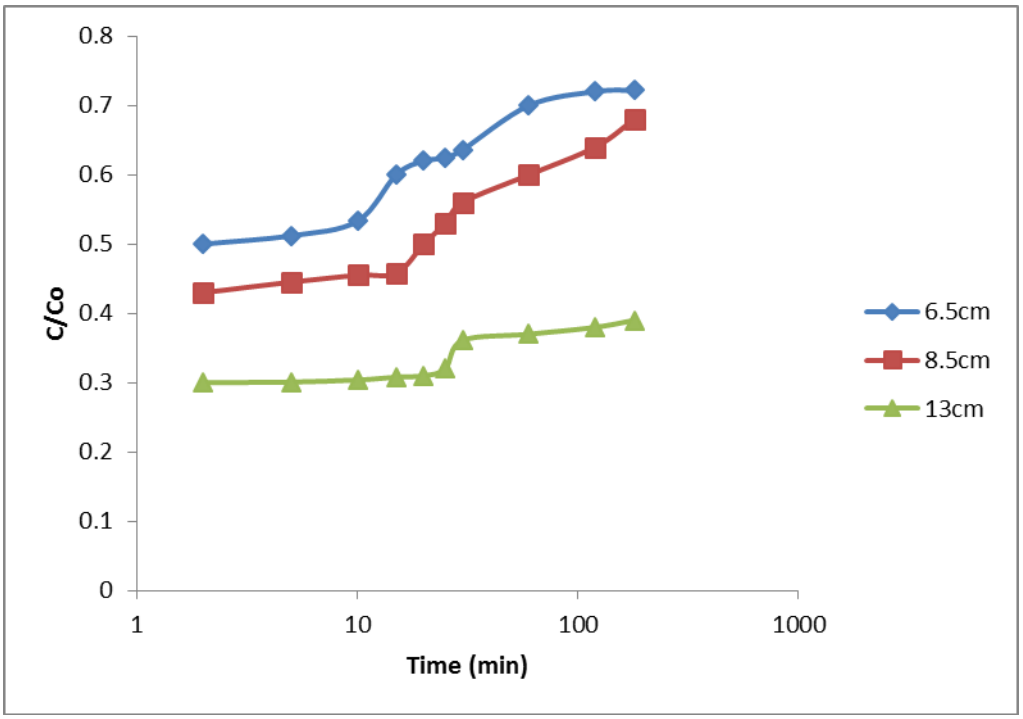


Figure 4.51: Breakthrough curve for iridium at different bed depth (C_o = 8.25mg/l, flow rate = 0.9ml/s, temp. = 25˚C).

Figure 4.52 shows the effect of bed depth on the sorption of ruthenium. The same trend as observed in the case of iridium was noted. The saturation of the column appeared to be very rapid despite the increase in the bed depth. Although ruthenium concentration in the solution is low, it appears as though the affinity for this metal by the adsorbent is low compared to other PGMs with similar concentrations in solution (Ruthenium was not investigated in the batch tests).

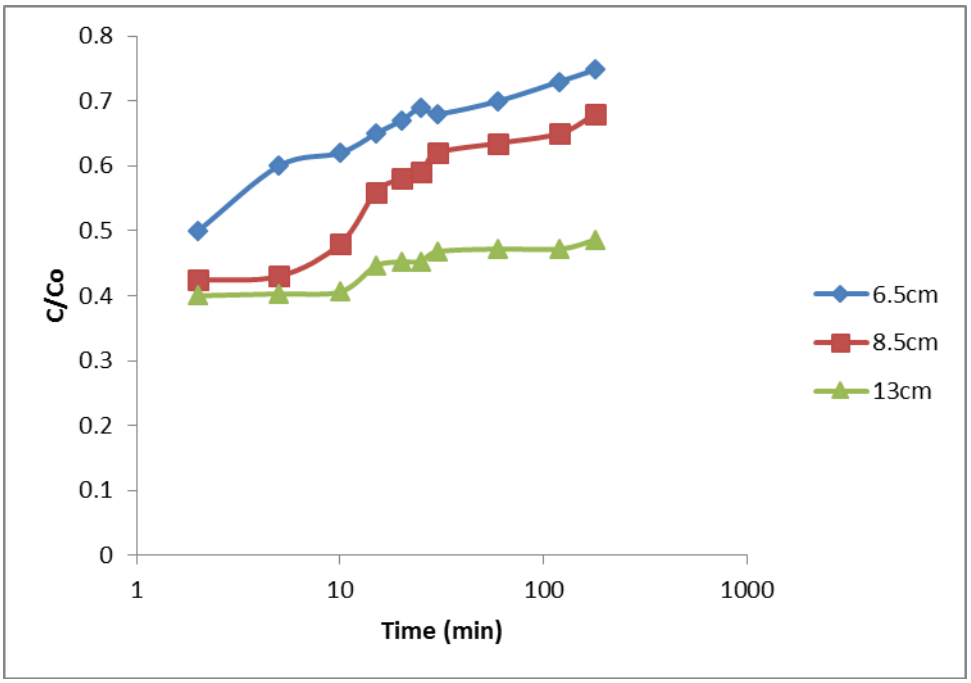


Figure 4.52: Breakthrough curve for ruthenium adsorption at different bed depth (C_o = 0.937mg/l, flow rate = 0.9ml/s, temp. = 25˚C).

Figure 4.53 shows the effect of bed depth on the sorption of nickel. The results show that the breakthrough time increased from 10minutes to 25minutes as bed height increased from 6.5cm to 13cm. The figure also revealed that the adsorbent has a strong affinity for the nickel ion.

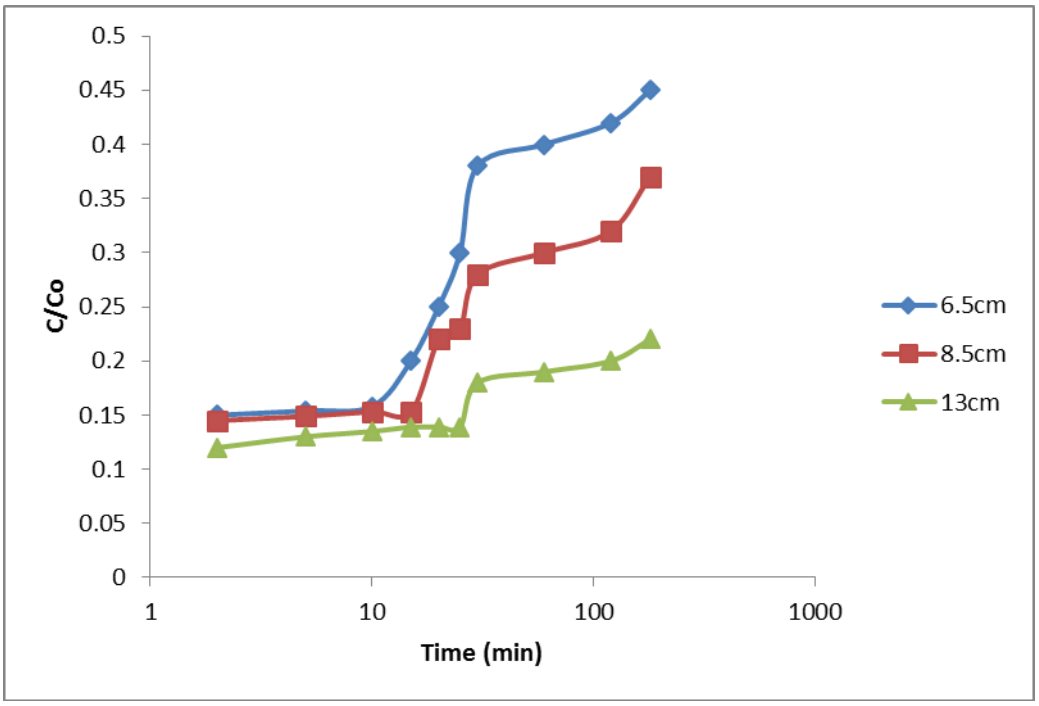


Figure 4.53: Breakthrough curve for nickel adsorption at different bed depth (C_o = 2.08 mg/l, flow rate = 0.9ml/s, temp. = 25˚C).

Figure 4.54 shows the effect of bed depth on the sorption of selenium. From the figure, the adsorption of selenium increased as the bed depth increased from 6.5cm to 13cm due to the availability of more binding sites but the saturation of the column occurred faster due to high concentration of selenium. However, the saturation of the column was only reached at 6.5cm bed depth.

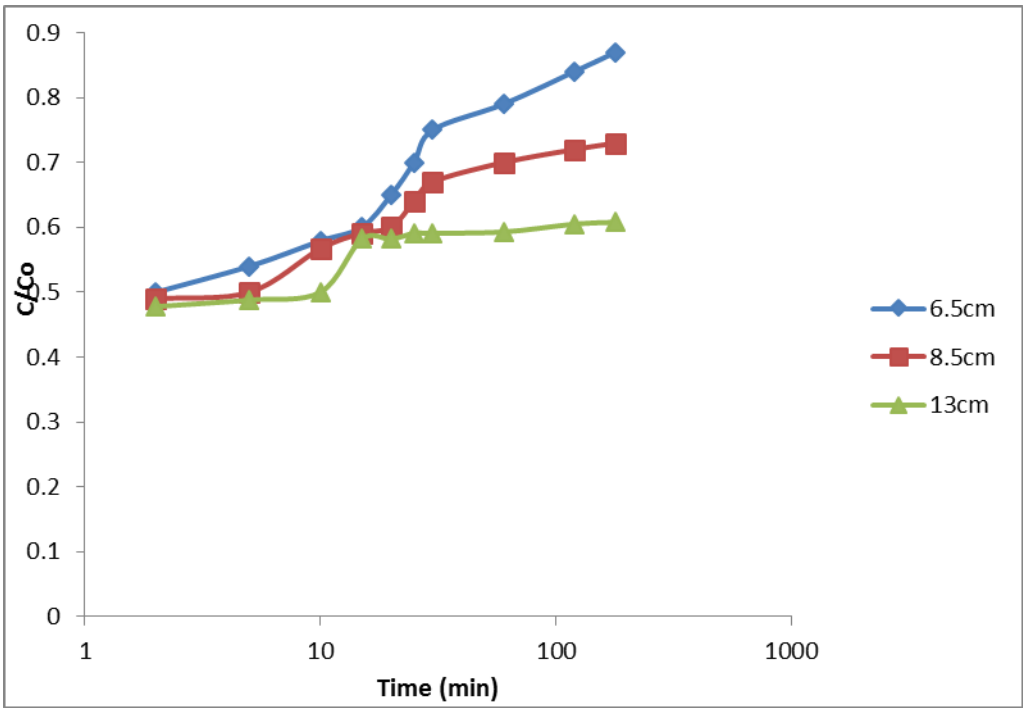


Figure 4.54: Breakthrough curve for selenium adsorption at different bed depth (C_o = 416 mg/l, flow rate = 0.9ml/s, temp. = 25˚C).

Figure 4.55 shows the effect of bed depth on the sorption of tellurium. The figure shows that the breakthrough time increased from 10minutes to 30minutes as the bed depth increased from 6.5cm to 13cm. The results also show that the adsorbent has a high affinity for this metal compared to platinum, ruthenium, and nickel which were also present in lower concentration in the solution.

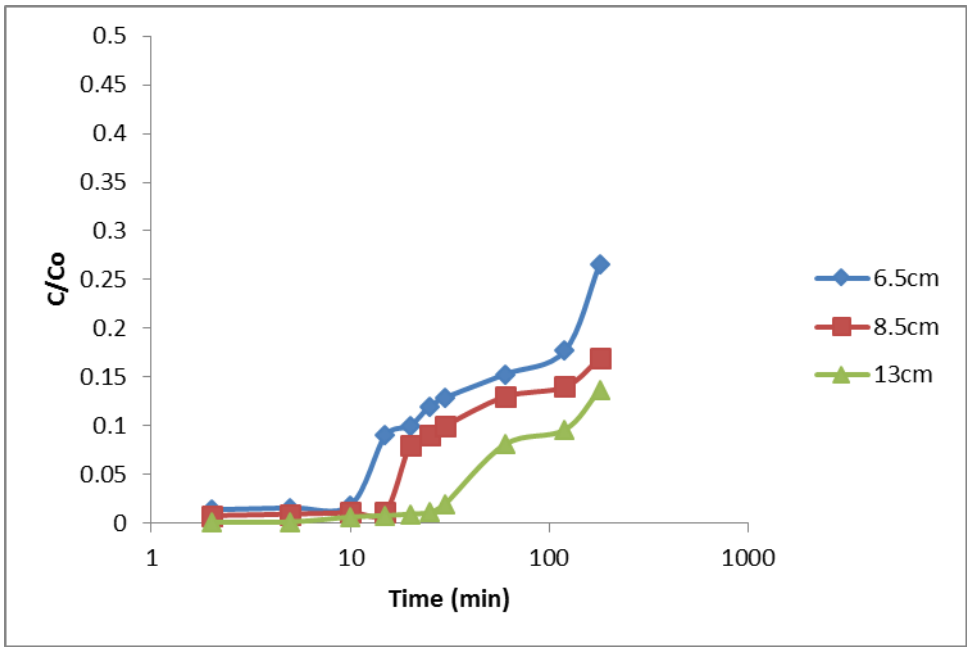


Figure 4.55: Breakthrough curve for tellurium adsorption at different bed depth (C_o = 1.24 mg/l, flow rate = 0.9ml/s, temp. = 25˚C).

Figure 4.56 shows the effect of bed depth on the sorption of sodium. The figure shows that as bed depth decreased from 13cm to 6.5cm, the saturation of the bed became rapid reaching the value of $0.5C_o$, $0.8C_o$ and $0.92C_0$ respectively in 180minutes.

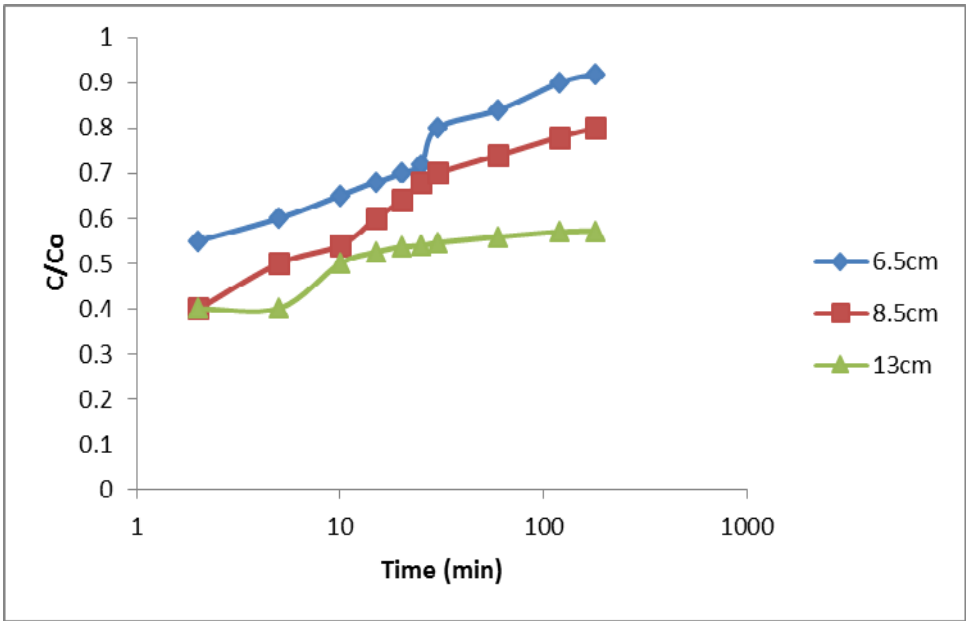


Figure 4.56: Breakthrough curve for sodium adsorption at different bed depth (C_o = 45,100 mg/l, flow rate = 0.9ml/s, temp. = 25˚C).

Figure 4.57 shows the effect of bed depth on the sorption of sulphate ions. The result shows that the breakthrough time increased significantly from 10 minutes to 30 minutes when the bed depth increased from 6.5cm to 13cm. Similarly, the time necessary to reach saturation of the column is higher as the bed depth increased.

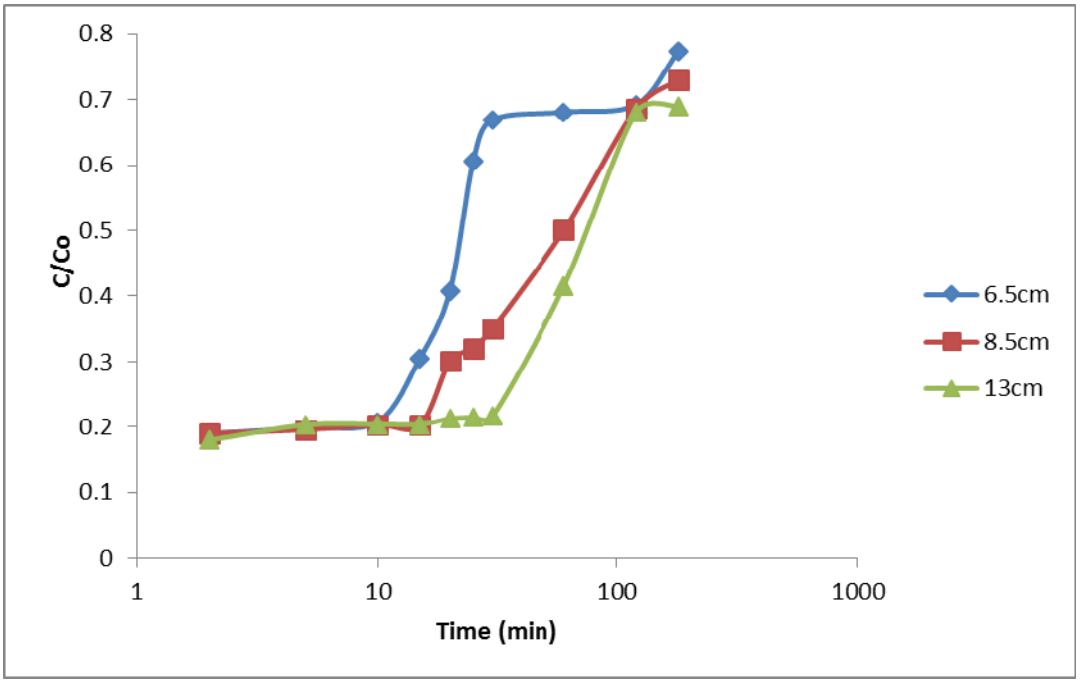


Figure 4.57: Breakthrough curve for sulphate adsorption at different bed depth (C_o = 10,947mg/l, flow rate = 0.9ml/s, temp. = 25˚C).

Overall Discussion

Generally, the effect of bed depth on the metal ions studied shows that the breakthrough time increased as the bed depth increased from 6.5cm to 13cm and the effect is more significant with the higher bed depth. The increase in bed depth resulted in the increase in metal uptake which is as a result of availability of more binding sites for sorption and an increase in the contact time leading to a decrease in the solute concentration in the effluent. On the other hand, when the column is operated at the lowest bed depth, the binding sites available for sorption is limited and the contact time between the sorbent and the solute is reduced. Similarly, the time necessary for saturation of the column is higher as the bed depth is increased, in some cases a time longer than 180minutes used is necessary.

It must be noted that that the mass transfer zone in a packed bed column moves from the entrance of the bed and proceed towards the exit (Chowdhury et al; 2013). Hence, for the same influent concentration in a packed bed system, an increase in bed height would create a longer distance for the mass transfer zone to reach the exit resulting in an extended breakthrough time (Chowdhury et al; 2013). Although an increase in bed depth increased the breakthrough time, a very high bed height is not practical for a single column, instead multiple beds should be designed (Netpradit et al; 2004). This is because by increasing the bed height (the adsorbent dosage) to a certain level, the adsorption density (the amount adsorbed per unit mass) decreases. The decrease in adsorption density with an increase bed depth is mainly due to the unsaturation of the adsorption sites (Dorris et al; 2003)

Table 4.14 summarised the breakthrough time for different metals studied at different bed depths.

Table 4.14: Breakthrough times at different bed depths

Metal ions	6.5cm t_b(min)	8.5cm t_b(min)	13cm t_b(min)
Platinum	10	10	25
Palladium	30	60	180
Iridium	10	15	25
Ruthenium	2	5	10
Selenium	2	5	10
Tellurium	10	15	30
Nickel	10	15	25
Sodium	2	2	5
Sulphate	10	15	30

Based on the information in Tables 4.13 and 4.14, it is evident from the t_b (values at 0.9ml/s and 13cm) that the binding affinity for the PGMs in the solution under study on Plaster of Paris immobilized yeast follows the order $Pd^{2+}>Pt^{2+}>Ir^{3+}>Ru^{3+}$ which is consistent with the batch experimental results for Pd, Pt, and Ir while the binding affinity for other elements in the solution follows the order of $Te^{2+}>SO_4^{2-}>Ni^{2+}>Se^{2+}>Na^{+}$. Generally, the binding affinity for all the elements follows the order $Pd^{2+}> SO_4^{2-}>Te^{2+}>Pt^{2+}>Ir^{3+}>Ni^{2+}>.Ru^{3+}>Se^{2+}> Na^{+}$.

Based on the information in Table 4.12, most of the elements in the solution did not reach their allowable discharge limit even before breakthrough was achieved. Therefore a multiple column should be applied for practical purposes in treating effluents of this nature. As the chloride concentration within the dilute stream represented one of the highest contaminating anion concentrations, the concentration was also monitored. The chloride concentration decreased in the early stage of treatment (at 0.9ml/s and 13cm bed depth), indicating that the column did sorb chloride ions. Within 20 minutes, the chloride concentration had reached 2,098mg/l equivalent to 40% removal. The use of more columns will inevitably continue to decrease the anions and other elements concentration in solution but a decision must be made regarding how many columns would be economically feasible.

Once the breakthrough time was determined, the breakthrough capacity Q_B (The column adsorption capacity at breakthrough point) of the adsorbent was calculated as (Goel et al; 2005):

$$Q_B = \left(\frac{t_b Q_w C_O}{m} \right) \tag{4.9}$$

where t_b is the breakthrough time (min), Q_w is the flow rate of the influent wastewater (l/min), C_o is the inlet concentration (mg/l) and m is the mass (g) of the adsorbent. In addition, the volume of effluent treated (ml) at breakthrough was calculated as:

$$V_{ef} = Qt_B \tag{4.10}$$

where Q is the influent flow rate (ml) and t_B is the breakthrough time (min) and the results are presented in Tables 4.15and 4.16.

The results presented in Tables 4.15 and 4.16 shows that, for all metal ions present in solution, an increase in bed adsorption capacity (Q_b) are noticed at the breakthrough point with the increase in bed depth and decrease in flow rates. However, a slight different trend was observed with nickel, selenium and sodium with regards to the value of Q_b at different flow rate. It was observed from the results that the adsorption capacity (Q_b) at 2.1ml/s for nickel, selenium and sodium are higher than at 1.3ml/s. This is due to the closeness in the breakthrough point for these metals at these two flow rates.

The increase in the bed adsorption capacity (Q_b) with increase in bed depth is due to the increase in the specific surface of the adsorbent which supplies more fixation binding sites (Taty-Costodes et al., 2005). Furthermore, the results showed that an increase in the bed depth with a decrease in flow rate increased the volume of effluent that could be treated effectively before breakthrough. Since effluent from industries contain more than one metal ion present in solution, calculating the volume of effluent treated at breakthrough point will give an indication of the volume of solution that can be treated for each of the metal to reach its allowable limit i.e. if the breakthrough time for each metal present in the effluent is known, then the volume of effluent that can be treated effectively can be determined.

Table 4.15: Adsorption breakthrough data at different flow rates

Metal ions	Q (ml/s)	Q_b (mg/g)	V_{ef} (ml)
Platinum	0.9	0.058	1350
	1.3	0.034	780
	2.1	0.027	630
Palladium	0.9	0.056	9720
	1.3	0.053	9360
	2.1	0.043	7560
Iridium	0.9	0.258	1350
	1.3	0.149	780
	2.1	0.12	630
Ruthenium	0.9	0.012	540
	1.3	0.008	390
	2.1	0.005	252
Nickel	0.9	0.065	1350
	1.3	0.056	11790
	2.1	0.060	1260
Selenium	0.9	5.212	540
	1.3	1.500	156
	2.1	2.432	252
Tellurium	0.9	0.046	1620
	1.3	0.044	1560
	2.1	0.036	1260
Sodium	0.9	282.5000	270
	1.3	163.230	156
	2.1	263.690	252
Sulphate	0.9	411.460	1620
	1.3	396.220	1560
	2.1	320.020	1260

Table 4.16: Adsorption breakthrough data at different bed depth

Metal ions	Z (cm)	Q_b (mg/g)	V_{ef} (ml)
Platinum	6.5	0.045	540
	8.5	0.037	540
	13.0	0.058	1350
Palladium	6.5	0.018	1620
	8.5	0.029	3240
	13.0	0.056	9720
Iridium	6.5	0.198	540
	8.5	0.245	810
	13.0	0.258	1350
Ruthenium	6.5	0.004	108
	8.5	0.009	270
	13.0	0.012	540
Nickel	6.5	0.050	540
	8.5	0.061	810
	13.0	0.065	1350
Selenium	6.5	2.000	108
	8.5	4.120	270
	13.0	5.212	540
Tellurium	6.5	0.029	540
	8.5	0.037	810
	13.0	0.046	1620
Sodium	6.5	217.350	108
	8.5	178.650	108
	13.0	282.530	270
Sulphate	6.5	263.780	540
	8.5	325.240	810
	13.0	411.460	1620

4.7.3 Evaluation of kinetic models

Adam-Bohart model

The Adam-Bohart model was applied to the experimental data for the description of the initial part of the breakthrough curve using the equation below:

$$\ln\left(\frac{C_t}{C_o}\right) = K_{AB}C_o t - K_{AB}N_o\frac{Z}{U_o} \tag{4.11}$$

The values of K_{AB} and N_o at different bed depth and flow rates for each metal were calculated and presented in Table 4.17 and 4.18 respectively.

Table 4.17 shows the linear regression analysis at different bed depth. The results show that the adsorption capacity of the adsorbent (N_o) increased with an increase in the bed height for all the metals in solution and the mass transfer coefficient (K_{AB}) decreased with an increase in the bed height. Furthermore, the trend observed in Table 4.17 shows that for the metals which have high concentration in the solution, the value of N_o was found to be very high while the value of the kinetic coefficient K_{AB} was found to be very low compare to those metals with lower concentration in the solution. This shows that the overall system kinetics was dominated by external mass transfer in the initial part of the column. This finding is in agreement with other studies in literature (Chowdhury et al., 2013; Saadi et al., 2013).

Table 4.17: Adam-Bohart model parameters at different bed depth.

Metal ion	Z(cm)	C_o(mg/l)	K_{AB} (mL/min.mg)	N_o (mg/l)	R^2
Platinum	6.5	1.88	0.0290000	253.00	0.94
	8.5	1.88	0.0230000	301.43	0.91
	13.0	1.88	0.0166000	425.00	0.99
Palladium	6.5	0.248	0.3520000	14.80	0.90
	8.5	0.248	0.2760000	18.82	0.93
	13.0	0.248	0.2120000	25.19	0.91
Iridium	6.5	8.25	0.0170000	1070.89	0.97
	8.5	8.25	0.0094000	1268.50	0.93
	13.0	8.25	0.0050000	1591.95	0.97
Ruthenium	6.5	0.937	0.1220000	116.66	0.94
	8.5	0.937	0.0900000	120.30	0.92
	13.0	0.937	0.0600000	221.66	0.86
Nickel	6.5	2.08	0.0200000	155.66	0.84
	8.5	2.08	0.0170000	242.88	0.86
	13.0	2.08	0.0160000	307.67	0.91
Selenium	6.5	416	0.0002500	53471.00	0.65
	8.5	416	0.0002400	61497.00	0.94
	13.0	416	0.0001800	87026.45	0.88
Tellurium	6.5	1.24	0.0590000	100.30	0.98
	8.5	1.24	0.0387000	141.65	0.98
	13.0	1.24	0.0380000	144.48	0.73
Sodium	6.5	45,100	0.0000017	4023766.10	0.88
	8.5	45,100	0.0000016	778,4044.70	0.90
	13.0	45,100	0.0000014	100,466685.34	0.84
Sulphate	6.5	10,947	0.0000019	1123441.70	0.86
	8.5	10,947	0.0000012	4682261.20	0.84
	13.0	10,947	0.0000008	9241402.10	0.87

Table 4.18 shows the Adam-Bohart parameters at different flow rates. The results show that due to more saturation of the adsorbent sites, the adsorption capacity of the adsorbent (N_o) decreased with an increase in flow rate while the kinetic constant of the model (K_{AB}) increased with an increase in flow rate. This showed that the overall system kinetics was dominated by external mass transfer. The trends observed in Table 4.17 and 4.18 is in agreement with other studies in literature (Chowdhury et al., 2013; Saadi et al., 2013; Danny et al., 2000; Khan et al., 2011).

Table 4.18: Adam-Bohart model parameters at different flow rates

Metal ion	Q (ml/s)	C_o(mg/l)	K_{AB} (mL/min.mg)	N_o (mg/l)	R^2
Platinum	0.9	1.88	0.0167000	483.00	0.99
	1.3	1.88	0.0260000	421.84	0.97
	2.1	1.88	0.0300000	317.50	0.90
Palladium	0.9	0.248	0.1290000	30.50	0.91
	1.3	0.248	0.1780000	20.69	0.90
	2.1	0.248	0.3250000	14.80	0.96
Iridium	0.9	8.25	0.0048000	2095.00	0.97
	1.3	8.25	0.0050000	1450.00	0.98
	2.1	8.25	0.0050000	1070.89	0.89
Ruthenium	0.9	0.937	0.0580000	276.78	0.86
	1.3	0.937	0.0600000	143.27	0.86
	2.1	0.937	0.0670000	120.30	0.95
Nickel	0.9	2.08	0.0057000	601.25	0.91
	1.3	2.08	0.0100000	286.62	0.91
	2.1	2.08	0.0177000	155.66	0.90
Selenium	0.9	416	0.0001100	153,681.80	0.88
	1.3	416	0.0001620	74434.25	0.94
	2.1	416	0.0001800	53471.48	0.88
Tellurium	0.9	1.24	0.0270000	184.62	0.73
	1.3	1.24	0.0310000	133.02	0.89
	2.1	1.24	0.0388000	100.30	0.95
Sodium	0.9	45,100	0.0000013	14035576.92	0.84
	1.3	45,100	0.0000013	7306856.50	0.92
	2.1	45,100	0.0000037	4023766.10	0.90
Sulphate	0.9	10,947	0.0000009	9241402.10	0.80
	1.3	10,947	0.0000025	4324159.00	0.96
	2.1	10,947	0.0000037	388513.50	0.74

The correlation coefficient R^2 values ranged from 0.75 to 0.99. Although the Adam-Bohart model provides a simple comprehensive approach to evaluating sorption column tests, its validity is limited to the range of conditions used (Patel and Vashi, 2012).

The Thomas Model

The Thomas model is suitable for an adsorption process where the external and internal diffusion will not be the limiting step (Yahaya et al., 2011). The experimental data were fitted to the Thomas model to determine the rate constant (K_{Th}) and maximum solid-phase concentration (q_o) using equation the below:

$$\ln\left(\frac{C_t}{C_o}\right) = K_{AB}C_o t - K_{AB}N_o\frac{Z}{U_o} \tag{4.12}$$

Thomas model parameters for the adsorption process at different flow rate and bed depth are presented in Table 4.19 and Table 4.20.

The results show that as the bed height increased, the rate constant (K_{Th}) and the maximum solid – phase concentration (q_o) also increased. Furthermore, as the flow rate increased, the value of q_o decreased while the value of K_{Th} increased. The decrease in q_o with an increase in flow rate may be attributed to lower residence time and premature saturation of the active sites. Based on Table 4.19 and 4.20, an increase in K_{Th} with an increase in flow rate as well as bed height is in agreement with the studies by Chowdhury et al. (2013) but contradicts the findings by Yahaya et al. (2011) who observed a decrease in K_{Th} with an increase in flow rate as well as bed height. These differences may be as a result of the assumption by Thomas model that adsorption is limited by chemical reaction kinetics (Yahaya et al., 2011). The values of R^2 ranged from 0.72 to 0.903. From the low values of the regression coefficient (R^2) in Tables 4.19 and 4.20, it can be concluded that the experimental data did not fit well with the Thomas model.

Table 4.19: Thomas model parameters at different bed depth.

Metal ion	Z(cm)	C_o(mg/l)	q_o (mg/g)	K_{Th}(mL/min.mg)	R^2
Platinum	6.5	1.88	0.309	2.00×10^{-4}	0.723
	8.5	1.88	0.420	2.70×10^{-4}	0.760
	13.0	1.88	0.520	4.80×10^{-4}	0.830
Palladium	6.5	0.248	0.055	4.75×10^{-3}	0.728
	8.5	0.248	0.087	4.95×10^{-3}	0.750
	13.0	0.248	0.105	7.17×10^{-3}	0.890
Iridium	6.5	8.25	1.340	4.96×10^{-5}	0.698
	8.5	8.25	1.632	6.90×10^{-5}	0.734
	13.0	8.25	1.749	9.80×10^{-5}	0.798
Ruthenium	6.5	0.937	0.126	4.90×10^{-4}	0.820
	8.5	0.937	0.185	5.30×10^{-4}	0.790
	13.0	0.937	0.199	6.00×10^{-4}	0.856
Nickel	6.5	2.08	0.407	1.40×10^{-4}	0.890
	8.5	2.08	0.630	1.80×10^{-4}	0.889
	13.0	2.08	0.760	2.06×10^{-4}	0.931
Selenium	6.5	416	45.030	7.20×10^{-7}	0.783
	8.5	416	63.770	1.25×10^{-6}	0.825
	13.0	416	78.120	1.27×10^{-5}	0.892
Tellurium	6.5	1.24	0.278	1.40×10^{-3}	0.759
	8.5	1.24	0.437	1.85×10^{-3}	0.825
	13.0	1.24	0.520	2.4×10^{-3}	0.838
Sodium	6.5	45,100	5909.300	1.00×10^{-9}	0.732
	8.5	45,100	8036.470	8.00×10^{-9}	0.746
	13.0	45,100	10152.390	1.80×10^{-7}	0.780
Sulphate	6.5	10,947	1997.250	7.00×10^{-9}	0.773
	8.5	10,947	3,122.300	5.80×10^{-8}	0.862
	13.0	10,947	3727.250	1.57×10^{-7}	0.903

Table 4.20: Thomas model parameters at different flow rates

Metal ion	Q (ml/s)	C_o(mg/l)	q_o (mg/g)	K_{Th}(mL/min.mg)	R^2
Platinum	0.9	1.88	0.520	5.00×10^{-4}	0.830
	1.3	1.88	0.425	3.00×10^{-3}	0.783
	2.1	1.88	0.309	2.00×10^{-3}	0.772
Palladium	0.9	0.248	0.105	7.20×10^{-3}	0.890
	1.3	0.248	0.079	7.80×10^{-3}	0.870
	2.1	0.248	0.055	8.00×10^{-3}	0.814
Iridium	0.9	8.25	1.750	1.00×10^{-4}	0.798
	1.3	8.25	1.730	4.00×10^{-4}	0.826
	2.1	8.25	1.340	7.00×10^{-4}	0.741
Ruthenium	0.9	0.937	0.199	6.00×10^{-4}	0.856
	1.3	0.937	0.178	9.00×10^{-4}	0.794
	2.1	0.937	0.152	12.00×10^{-2}	0.781
Nickel	0.9	2.08	0.760	2.00×10^{-4}	0.931
	1.3	2.08	0.587	1.00×10^{-3}	0.901
	2.1	2.08	0.407	1.40×10^{-2}	0.896
Selenium	0.9	416	78.100	1.27×10^{-6}	0.892
	1.3	416	68.000	4.00×10^{-6}	0.800
	2.1	416	57.900	6.49×10^{-6}	0.769
Tellurium	0.9	1.24	0.520	2.40×10^{-3}	0.838
	1.3	1.24	0.390	2.80×10^{-3}	0.849
	2.1	1.24	0.250	3.10×10^{-3}	0.807
Sodium	0.9	45,100	1015.400	1.80×10^{-8}	0.780
	1.3	45,100	6963.700	8.80×10^{-8}	0.820
	2.1	45,100	6007.800	9.90×10^{-8}	0.781
Sulphate	0.9	10,947	3727.300	1.57×10^{-7}	0.903
	1.3	10,947	2842.100	2.83×10^{-7}	0.891
	2.1	10,947	1009.400	1.5000×10^{-6}	0.800

4.7.4 Summary

The overall aim of this study is to look at the possibility of purifying platinum group metals dilute process stream (both synthetic and real effluent from industry) using waste yeast of Saccharomyces Cerevisiae. Saccharomyces Cerevisiae waste yeast biomass was pretreated with ethanol and sodium hydroxide in order to improve the adsorption capacity of the biomass. Ethanol treated biomass exhibited a far higher removal efficiency than the untreated and sodium hydroxide treated biomass under the same condition. This was due to the biomass protein been denatured and the yeast cell walls destroyed. Thus the permeability within the internal structure of the yeast

improved. The summary of the metal uptake by the untreated, ethanol treated and sodium hydroxide treated is given in the table below

Table 4.21: Summary of the effect of biomass pre-treatment on the adsorption of Pt (II), Au (III), Pd (II), Ir (III) and Rh (III).

Metal ions	Untreated yeast metal uptake (%)	Ethanol treated yeast metal uptake (%)	NaOH treated yeast metal uptake (%)
Au (III)	66.3	86.0	28.5
Pt (II)	77.3	88.4	36.3
Pd (II)	77.2	81.3	70.3
Ir (III)	9.0	15.7	8.0
Rh (III)	35.0	41.3	26.7

The area of greatest weight lost was the sodium hydroxide treatment, in which a large proportion of lipids and proteins were lost and these base soluble materials also have metal binding capacity. This account for the low metal uptake removal by the sodium hydroxide treated biomass.

A thorough evaluation of sorption performance is usually based on a combination of both kinetics and equilibrium parameters (Mack, 2008). Both have been investigated here in order to understand the mechanisms of sorption of the tested PGMs onto the sorbent. The adsorption kinetics of the tested PGMs indicated a rapid uptake of above 70% for Pt (II), Au (III), Pd (II) within the first 30 minutes while for Ir (III) and Rh (III), the uptake only reached 9.9% and 30.1% respectively in the first 30 minutes and this is due to the slow kinetic properties of these two metals. This rapid uptake is the major indicator of passive adsorption to the cell surface i.e. biosorption. The isotherm data were also fitted into Langmuir and Freundlich isotherm models. The isotherm data indicated that the experimental data fitted well with Langmuir isotherm.

The purpose of the diagnostic two-level full factorial design presented was to establish which experimental factors have significant effect on the adsorption of PGMs in dilute stream and whether these effects are positive or negative. The factors investigated included temperature, pH, initial metal ion concentration and biomass dosage. Factors were studied at their low and high levels. The experimental results

were analyzed statistically for the significance of factors using the normal probability plots. The results obtained revealed that only the solution pH and initial metal ion concentration are most significant for adsorption of the tested PGMs while temperature and biomass dosage are statistically insignificant.

Efficient desorption of bound metal ions is important in an adsorption operation. The desorption of the tested PGMs from the loaded biomass was carried out using different concentrations of hydrochloric acid, sulphuric acid, thiourea and hydrochloric – thiourea solution. All the mineral acids tested proved ineffective for the desorption of all the tested PGMs. A combination of a complexing ligand and a decrease in pH (acidified thiourea) proved effective for the desorption of Au (III), Pt (II), and Pd(II) while it was ineffective for the desorption of Rh (III) and Ir (III) from the sorbent.

The sorption of Platinum group metals as well as other trace elements present in real dilute process streams was investigated in a fixed bed column using ethanol treated biomass immobilized on Plaster of Paris. From the physical and chemical properties of the dilute process stream, the presence of high concentration of chloride, sulphate and sodium in the process stream resulted in wastewater with high ionic strength. The metal uptake was favored at lower influent flow rate and higher bed height. In addition, it was revealed that for the bed to reach saturation for most of the metals the adsorption time must be prolonged beyond 180minutes used. The result obtained revealed that palladium sorption was favored compared to every other PGMs present in the dilute solution.

CHAPTER FIVE

CONCLUSIONS AND RECOMMENDATIONS

5.1 Conclusions

5.1.1 Introduction

Conventional methods for the removal of low metal ion concentration from wastewater have been found to possess significant disadvantages. However, a review of literature suggested that employing materials of biological origin allows the application of the knowledge available to the development of technology to treat dilute metal and organic containing solutions. Therefore, the main objective of this work was to investigate the possibility of using a material of biological origin which is also a byproduct of a fermentation process for the purification of platinum group metals effluent from both synthetic and real dilute solution from industry.

In order to investigate this possibility, the objectives of the study were defined as:

- To investigate the use of Saccharomyces cerevisiae biomass for the purification of PGM wastewater stream in batch and continuous process.
- To establish the process parameters and operating conditions such as temperature, pH, residence time and biomass dosage required for the optimum purification efficiency.
- To evaluate the process efficiency in terms of metal removal, chemical oxygen demand, etc. of the waste stream.
- To analyse the effect of chemical pretreatment on the adsorption capacity of the biomass
- To establish an adsorption kinetic model for the process under study.
- To establish the possibility of regeneration and re-use or beneficial disposal of the biomass

5.1.2 Effect of chemical pretreatment

The pretreatment of biosorbent before use in biosorption process is primarily carried out to improve their functional group thereby increase their binding capacities. Whether the pretreatment method will increase or decrease the binding capacity of a particular biomass depends on the functional group present on the biosorbent and the type of metal species to be sorbed from solution. The results presented in this study have shown that chemical pretreatment of the waste yeast with 70g/l ethanol increased the adsorption capacity of the yeast while treatment with 0.1M NaOH reduced the adsorption capacity of the yeast biomass as a result of the loss of some functional groups on the biomass when treated with sodium hydroxide. For example, the percentage adsorption of the yeast biomass for the uptake of Au (III) increased by 19.7% after treatment with ethanol while the uptake of Au (III) decreased by 37.8% after treatment with sodium hydroxide.

The surface area, pore volume and the pore size of both the ethanol treated and the sodium hydroxide treated yeast increased after pretreatment which validates that the reduction in the adsorption capacity of the sodium hydroxide treated biomass was due to the loss of some functional groups on the biomass.

5.1.3 Identification of Influential Factor Tests

The purpose of the diagnostic two-level full factorial design presented was to establish which experimental factors have significant effect on the adsorption of PGMs in dilute stream and whether these effects are positive or negative. The factors investigated included temperature, pH, initial metal ion concentration and biomass dosage. Factors were studied at their low and high levels. The experimental results were analyzed statistically for the significance of factors using the normal probability plot and the percentage of PGMs adsorbed from the synthetic solution was taken as measured response. The design of experiment (DOE) approach was able to determine statistically significant and insignificant factors.

For the PGMs tested, only the solution pH and initial metal ion concentration appeared to be the most significant factors for adsorption while temperature and biomass dosage were found to be statistically insignificant. This means that

temperature and biomass dosage do not significantly influence the adsorption process while the solution pH and initial metal ion concentration have significant effect on the adsorption process. Under the ranges studied, the interaction between most of the variables was found to be statistically insignificant, except that between pH and metal concentration which showed a marked influence only on Pd (II) and Au (III) adsorption.

The results also showed that to achieve optimal adsorption of the tested PGMs, pH and initial metal ion concentration must be kept at high factor level. However, the effect of pH was found to be negative on the adsorption of Pt (II).Therefore to verify the effect of pH on the adsorption of the tested PGMs, confirmatory runs were carried out and it was discovered that the maximum adsorption for all the tested PGMs occurred at pH 3.The results showed that above 70% adsorption was still obtainable at pH above 3 for Au (III), Pd (II), Ir (III) and Rh (III) while for Pt (II), the adsorption reduced from 90.4% at pH 3 to 41.9% at pH higher than 3 which validates that the effect of pH was negative on Pt (II).

5.1.4 Kinetic Studies

In order to evaluate the kinetic mechanism that controlled the adsorption process under study, pseudo-first order, pseudo-second order, and Intra-particle diffusion models were employed to interpret the experimental data. The kinetic information gathered in chapter 4 indicated that the reaction kinetics for all the tested PGMs is pseudo-second order, i.e. limited by a chemical sorption mechanism. The involvement of the chemical mechanism is further validated by information from the Elovich model which was also used to describe second order kinetic assuming that the actual solid surfaces are energetically heterogeneous. There is also some evidence regarding the possible involvement of ion exchange in the sorption of the PGMs tested onto the waste yeast biomass. The fit of the isotherm data to the Langmuir model has been accepted as an indication of ion exchange based on the model assumption that metal binding occurs within a monolayer only (Schneider et al., 2001), although this has been challenged by some authors (Schiewer, 1999; Mack, 2008; Barrera et al., 2006). In this study it is also challenged by the SEM images obtained (Figure 4.7d) that show the rough and patchy of the PGMs onto the sorbent surface, which would not have

occurred if ion exchange were occurring. The high value of b which represents the affinity between sorbent and sorbate in Langmuir isotherm (the higher the value of b, the higher the affinity of the sorbent for the sorbate), suggests a strong binding between the ions and the biomass surface, indicating a chemisorption of metal ions at the surface of the waste yeast biomass. In addition, the R_L (dimensionless parameter used to judge the feasibility of a given adsorption process) showed that in all cases the sorption reaction was favourable (R_L lies between 0 and 1).

5.1.5 Adsorption – Desorption Cycles

Desorption studies on synthetic solution showed that by using thiourea acidified in hydrochloric acid, it is possible to effectively remove Au (III), Pd (II) and Pt (II) metal ions bound to the yeast biomass and to regenerate the biomass allowing for its successive use. Although it was concluded from the kinetic studies that chemical sorption was involved in the sorption of the tested PGMs to the biomass surface, the stable complex formation and the electrostatic interaction between Au (III), Pd (II) and Pt (II) and charged species from elution may have resulted in high desorption of these three PGMs. However, the inability of Rh (III) and Ir (III) to be desorbed effectively from the biomass is due to the kinetic inertness and the stereochemistry of these two metals. Although the acidified thiourea could not effectively desorb Rh (III) and Ir (III) from the sorbent, higher desorption could be obtained by adjusting the concentration of the eluent solution. Investigation of other chelators and ligands may also yield a highly efficient rhodium and iridium desorption The biomass was successfully used for five cycles which is a good indication of S.cerevisiae waste yeast as a potential biomass material giving an opportunity for real decontamination of effluents at minimal cost. For adsorption, the percentage sorption obtained at the initial cycle are 99.9% for Au (III), 91% for Pt (II), 99.5% for Pd (II), 81.9% for Ir (III) and 81.1% for Rh (III) while after 5 cycles, the percentage of metal sorbed were 96.6% for Au (III),87% for Pt (II),91.9% for Pd (II), 56% for Ir (III) and 45% for Rh (III). For desorption, the percentage of metals desorbed at the initial cycle are 99.5% for Au (III), 97.8% for Pt (II), 99.2 for Pd (II), 24.5% for Ir (III) and 20% for Rh (III) while after 5cycles, the percentage of metal desorbed from the biomass were 80% for Au (III), 93.8% for Pt (II), 93% for Pd (II), 15.7% for Ir (III) and 6.5% for Rh (III).

5.1.6 Column Study

The purpose of dynamic/column study was to investigate the removal efficiency of PGMs as well as other trace elements found in real dilute PGMs solution. Effluent generated in industry after PGMs refining contain PGMs in very low concentrations as well as base metals and other trace elements. Plaster of Paris was successfully used as a supportive material for the immobilization of the yeast and its effectiveness in the purification of real effluents was investigated in a packed column. The performance of the bed was analyzed using effluent concentration versus time curves. Dynamic adsorption conditions such as bed height (Z), metal concentration (C_o) and solution flow rate (Q) influenced the purification process. The packed bed column was found to perform better with lower influent rate and higher bed depth. An increase in bed height of the column from 6.5cm to 13cm increased the apparent uptake capacity of the sorbent which implies that the increase in the bed height will increase the contact time between the sorbates and sorbent thus resulted in an increase in uptake capacity.

Generally, the binding affinity for the metals studied on POP immobilized yeast followed the order Pd^{2+}> SO_4^{2-}>Te^{2+}>Pt^{2+}>Ir^{3+}>Ni^{2+}>Cl^->.Ru^{3+}>Se^{2+}> Na^+.

. This is as a result of the protonation of the biomass surface at the pH used which favored the sorption of negatively charged ions and metals which form chloro anionic species in solution. Although the sorbent show a greater affinity for most of the PGMs and other elements present in the dilute solution, the presence of high concentration of the other contaminants like sulphate, chloride and sodium affected the sorption of other metals in solution as most of these metals did not reach their allowable discharge limit according to United State Environmental Protection Agency (USEPA, 2010). Therefore, multiple columns are recommended in treating effluents of this nature with the aim that repeated treatment of a volume of wastewater may remove the organic contaminants and the metal ions to the desired limit.

The column data fitted well with Adam –Bohart model than with Thomas model for all the condition tested. The results gathered from the model indicated that the higher the bed height, the higher the adsorption capacity N_o of the adsorbent and the lower the mass transfer coefficient K_{AB} which showed that the overall system kinetics was

dominated by external mass transfer in the initial part of the column. Although this model is used to describe the initial part of the breakthrough curve, it provides a simple comprehensive approach to evaluating sorption in column tests and its validity is limited to the range of conditions used.

Summary

S.cerevisiae waste yeast biomass was successfully used for the removal of Platinum group metals tested especially from synthetic solution. About 80% removal of all the tested PGMs was achieved from synthetic solution while the presence of other element and the complexity nature of real solution affect the percentage removal in the real industrial effluent. In general, this study is based on the purification of the PGMs dilute stream for the purpose of recovering the valuable metals and water reclamation. Although, the reclamation of waste water is of secondary importance compared to the recovery of the PGMs and other valuable metals present in the solution, it has been observed from this study especially from the trend of adsorption in the fixed bed column that the use of multiple fixed bed column in treating a volume of solution can help in recovering all the valuable metals present in the solution as well as reduce the concentration of other contaminants like sulphate, chloride and sodium to meet the guidelines for industrial water reuse by the Department of Water Affairs and Forestry (1996) as given in Table 4.11. If the dilute process stream can be treated to meet these guidelines, it may be used in tasks such as dust suppression, firefighting, ash quenching and irrigation (Mack, 2005).

5.2 Recommendations

Based on the knowledge gained from this work, the following recommendations are proposed for future studies:

- The choice of biosorbents and the pretreatment method require optimization. The concentration of chemical used for pretreatment in the study can be optimized to see the effect on the uptake efficiency. In addition, other forms of pretreatment such as heat, acid and surfactant which, according to literature,

also increase biomass uptake efficiency can also be investigated on the adsorption of Platinum group metals.

- The cost analysis of the whole process should also be investigated since cost is an important parameter in the choice of adsorbent. This should include the cost of the biomass; the cost of pretreatment and the cost of immobilization. Other aspects to explore include the issue of process design i.e. batch versus continuous treatment modes and process control parameters, incineration versus desorption from the biosorbent, scale – up analysis and an overall cost benefit analysis

- Besides a 2^4 full – factorial design used in this study, other design of experiments such as Response surface methodology (RSM), central composite design (CCD) and the Box- Behnken design must be explored. In addition, a 2^4 full – factorial design with centre points can also be investigated to optimize the operating parameters

- Full characterization of the Platinum group metal wastewater as well as thorough investigation on the speciation of these metals in PGMs wastewater is required. A lack of knowledge regarding the speciation of PGMs in the wastewater solution continues to affect the optimization of a suitable sorption process for the recovery of precious metals from PGMs wastewater.

- Due to the formation of Halite, Thernadite and Disodium sulphate (VI) precipitate which affected the adsorption of the metals in the alkaline solution sample when the solution was conditioned to pH 3, further research could be carried out without changing the pH of the alkaline solution sample.

- Contact time for the column study should be increased in the future studies in order to achieve a clear saturation point.

- The effect of using the mixture of thiourea and sulphuric acid as well as sulphuric acid and hydrochloric acid in adsorption – desorption cycle can be investigated in the future studies.

REFERENCES

Ahalya, N., Ramachandra, T.V., Kanamadi, R.D., 2003. Biosorption of Heavy Metals. Research Journal of Chemistry and Environment 7, 71-79.

Ahluwalia, S.S., Goyal, D., 2007. Microbial and plant derived biomass for removal of heavy metals from wastewater. Bioresource Technology 98, 2243-2257.

Akar, T., Divriklioglu, M., 2010. Biosorption application of modified fungal biomass for decolonization of reactive red 2 contaminated solutions: Batch and dynamics flow mode studies. Bioresource Technology 101, 7271-7277.

Aksu, Z., 2005. Application of biosorption for the removal of organic pollutants: A review. Process biochemistry journal 40, 997-1026.

Alluri, H. K., Ronda, S.R., Settalluri, V.S., Bondili, J.S., Suryanarayana, V., Venkateshwar, P., 2007. Biosorption: An eco – friendly alternative for heavy metals removal. African Journal of Biotechnology 6, 2924-2931.

Alva-Argaez, A., Kokossis, A.C., Smith, R., 1998. Waste water minimization of industrial systems using an integrated approach. Computers and Chemical Engineering 22, 5741-5744.

Atkinson, B.W., Bux, F., Kasan, H.C., 1998. Consideration for application of biosorption technology to remediate metal-contaminated industrial effluents. Water SA 24, 129-135.

Avery, S.V., Tobin, J.M., 1993. Mechanism of adsorption of hard and soft metal ions to Saccharomyces cerevisiae and influence of hard and soft anions. Applied and Environmental Microbiology 59(9), 2851-2856.

Ajaykumar, A.V., Darwish, N.A., Hilal, N., (2009). Study of various parametres in the biosorption of heavy metals on activated sludge. World Applied Sciences Journal 5, 32-40.

Bai, R.S; Abraham, T.E., 2002. Studies on enhancement of Cr (VI) biosorption by chemically modified biomass of Rhizopus nigricans. Water Research 36, 1224-1236.

Bai, R.S., Abraham, T.E., 2003. Studies on chromium (VI) adsorption-desorption using immobilized fungal biomass. Bioresource Technolology 87, 17-26.

Barrera, H., Urena-Nunez, F., Bilyeu, B., Barrera-Diaz, C., 2006. Removal of chromium and toxic ions presents in mine drainage by Ectodermis of Opuntia. Journal of Hazardous Materials B136, 846-853.

Benguerel, E., Demopoulos, G.P., Harris, G.B., 1996. Speciation and separation of rhodium (III) from chloride solutions: a critical review. Hydrometallurgy 40, 135-152.

Benjamin, M.M., Lawler, D.F., 2013. Water quality Engineering: physical/chemical treatment processes. John Wiley and Sons, New Jersey.

Bernadis, F.L., Grant, R.A., Sherrington, D.C., 2005. A review of methods of separation of the platinum-group metals through their chloro-complexes. Reactive and functional polymers 65, 205-217.

Beveridge, T.J., 1990. Interactions of metal ions with components of bacterial cell walls and their biomineralization. In: Poole, R.K, Gadd, G.M (Eds). Metal-microbe interactions. IRL Press, Oxford, 65-83.

Bohart, G.S., Adams, E.Q., 1920. Behavior of charcoal towards chlorine. Journal of Chemical Society 42, 523-529

Box, G.E.P., Hunter W.G., Hunter, J.S., 1978. Statistics for Experiment: An Introduction to Design, Data Analysis and Model Building. John Wiley and Sons, New York.

Brierley, C.L., 1990. Metal immobilization using bacteria. In: Biosorbents for metal ions. Wase, J., Forster, C., (Eds) Taylor and Francis, London, UK, .37-39

Brunauer, S., Emmett, P. H., Teller, E. J., 1938. Journal American Chemical Society 60, 309 – 319.

Calero, M., Hernainz, F., Blazquez, G., Tenorio, G., Martin-lara, M.A., 2009. Study of Cr (III) biosorption in a fixed bed column. Journal of hazardous material 171, 886-893.

Chien, S.H., Clayton, W.R., 1980. Application of Elovich Equation to the kinetics of phosphate release and sorption in soils. Soil Science Society of America Journal 44(2), 265-268.

Chowdhury, Z., Zain, S., Rashid, A., Rafique, R., Khalid, K., 2013. Breakthrough curve analysis for column dynamics sorption of Mn (II) ions from wastewater by using mangostana garcinia-peel based granular-activated carbon. Journal of Chemistry. DOI 10.1155/2013/959761.

Chu, K., Hashim, M.A., 2004. Quantitative analysis of copper biosorption by the microalga Chlorella vulgaris. Environmental Engineering Science 21, 139-147.

Cortina, J.L., Meinhardt, E., Roijals, O., Marti, V., 1998. Modification and preparation of polymeric adsorbents for precious-metal extraction in hydrometallurgical processes. Reactive and Functional Polymers 36, 149-165.

Cowan, J.A.C., 1998. The development of management strategies and recovery systems for heavy metal wastes. Report No.5889/1/98. Water Research Commission, Pretoria, South Africa.

Crundwell, K.F., Moats, S.M., Ramachandran, V., Robinson, G.T., Davenport, W.G., 2011. Extractive metallurgy of Nickel, Cobalt and Platinum-group metals. Elsevier, Netherlands.

Daniel, C., 1959. Use of Half Normal plots in interpreting Factorial Two Level Experiments. Techno metrics 1(4), 311-341.

Danny, C.K., Porter, J.F., McKay, G., 2000. Optimised correlations for the fixed-bed adsorption of metal ions on bone char. Chemical Engineering Science 55, 5819-5829.

Das Saha, P., Chakraborty. S., Chowdhurry, S., 2012. Batch and continuous (fixed-bed column) Biosorption of crystal violet by Artocarpus heterophyllus (Jackfruit) leaf powder. Bio interfaces 92, 262-270.

Department of Water Affairs and Forestry. 1996. South African Water Quality Guidelines (2nd Edition). Volume 3: Industrial Use.

Department of Water Affairs and Forestry. 2005. A draft position paper for Water Allocation Reform in South Africa. Towards a framework for water allocation planning. Discussion Document. Pretoria, South Africa.

De Rome, L., Gadd, G., 1987. Copper adsorption by Rhizopus arrhizus, Cladosporium resinae and Penicillium italicum. Applied Microbiology Biotechnology 26. 84-90.

Dhankar, R., Guriyan, R.B., 2011. International journal of Advanced Science and Technology 2 (6), 103-128.

Diels, L., Van Roys, S., Mergeay, M., Doyen, W., Taghavi, S., Leyson, R., 1993. Immobilization of bacteria in composite membranes and development of tubular membranes reactors for heavy metal recuperation. 3rd International Conference on Effective Membrane Processes-New perspectives. Mechanical Engineering Publications Limited. UK.

Dobson, S.R., Burgess, E.J., 2007. Biological treatment of precious metal refinery wastewater: A review. Mineral Engineering 20, 519-532.

Dorris, K.L., YuL, J., Shukla S.S., Shukla A., Margrave J.L., 2003. Adsorption of Chromium from aqueous solutions by Maple Sawdust. Journal of Hazardous Material B100, .3-63.

Dula, T., Siraj, K., Kitte, S.A., 2014. Adsorption off hexavalent chromium from aqueous solution using chemically activated carbon prepared from locally available waste of bamboo (Oxytenanthera abyssinica). Environmental Chemistry 2014, 1-9.

Eccles, H., 1999. Treatment of metal-contaminated wastes: why select a biological process? Trends in Biotechnology, 17, 462-465.

Els, E.R., Lorenzen, L., Aldrich, C., 1997. Technical Note: The recovery of palladium with the use of ion exchange resins. Minerals Engineering 10(10), 1177-1181.

Environmental Potential Atlas. 2001. Availability of water per capital in South Africa.

Environmental Protection Agency. 1980. Development document for effluent limitation guidelines and standards for the inorganic chemicals manufacturing point source category, USEPA, Effluent Guidelines Division, Office of Water and Waste Management, Washington, DC.

Ferreira, I.M.P.L.V.O., Pinho, O., Vieira, E., Tavarela, J.G., 2010. Brewer's saccharomyces yeast biomass: characteristics and potential application. Trends in food science and technology 21, 77-84.

Frazzoli, C., Dragone, R., Mantovani, A., Massimi, C., Campanella, L., 2007. Functional toxicity and tolerance patterns of bioavailable Pd (ll), Pt. (ll), and Rh (ll) on suspended saccharomyces cerevisiae. Anal bio anal chemistry 389, 2185-2194.

Gadd, G.M., White, C., DeRome, L., 1988. Heavy metal and radionuceotide uptake by fungi and yeasts. In: Norri, R.., Kelly, D.P., (Eds.), Biohydrometallurgy. Chippenham, Wilts, UK.

Gadd, G. M., 2009. Biosorption: critical review of scientific rationale, environmental importance and significance for pollution treatment. Journal of Chemical Technology & Biotechnology 84(1), 13-28.

Ghosh, G., 1988. Immobilization of Baker's yeast using Plaster of Paris. Biotechnology Techniques 2(3), 217-219.

Gianadda, P., Brouckaert, C.J., Sayer, R., Buckley, C.A., 2002. The application of pinch analysis to water. Regent and effluent management in a chlor-alkali facility. Water Science and Technology, 46(9), 21-28.

Glaister, B.J., Mudd, G.M., 2010. The environmental costs of platinum-PGM mining and sustainability: is the glass half-full or half-empty? Mineral Engineering 23, 438-450.

Godlewska-Zylkiewicz, B., 2003. Biosorption of Platinum and Palladium for their separation/preconcentration prior to graphite furnace atomic absorption spectrometric determination. Spectrochimica Acta Part B 58, 1531-1540

Godlewska-Zylkiewicz, B., Kozlowska, M., 2005. Solid phase extraction using immobilized yeast saccharomyces cerevisiae for determination of palladium in road dust.Analytical Chimica Acta 539, 61-67.

Godlewska-Zylkiewicz, B., Malejko, J., Lesniewska, B., Kojlo, A., 2008. Assessment of immobilized yeast for the separation and determination of platinum in environmental samples by flow-injection chemilumnescence and electro-thermal atomic absorption spectrometry. Microchim Acta 163, 327-334.

Goel, J., Krishna, K., Chira, R., Vinod, K., 2005. Removal of lead (II) by adsorption using treated granular activated carbon and column studies. Journal of Hazardous Material 125, 211-220.

Goksungur, Y., Uren, S., Guvenc, U., 2002. Biosorption of Copper Ions by caustic treated waste baker's yeast biomass. Turk J Biol. 27, 23-29.

Holan, Z.R., Volesky, B., Prasetyo, I., 1993. Biosorption of cadium by biomass of marine-algae. Biotechnology Bioengineering 41, 819-825.

Holtzhausen, L., 2002. The war for water, fighting the battle for the last drop. Water Sewage and Effluent 22 (2), 26-29.

Hu, M.Z.C., Reeves, M., 1997. Biosorption of Uranium by Psedomonas aeruginosa strain CSU immobilized in a novel matrix. Biotechnology progress 13, 60-70.

Hussain, A.A., Mohammed, S.R., Nallu, M., Arivoli, S., 2012. Kinetics and thermodynamics studies of copper (II) ions from aqueous solution by activated granite. International journal of advanced scientific research and technology 2(3), 69-78.

Inglezakis, V.J., Zorpas, A., 2012. Ion exchange technology 1: Theory and Materials. In: Inamuddin, Luqman, M., (Eds). Springer Heidelberg New York, London.

http://www.halwachs.de/pgm-refining.htm. Accessed August 2012.

Johnson- Matthey 2003. Platinum Today. www.platinum. matthey.com

Kapoor, A., Viraraghavan, T., 1995. Fungal biosorption- an alternative treatment option for heavy metal bearing wastewaters: a review. Bioresource Technology 53, 195-206.

Kentish, S.E., Stevens, G.W., 2001. Innovations in separations technology for the recycling and re-use of liquid waste streams. Chemical Engineering Journal 84, 149-159.

Khan, F.R., Bury, N.R., Hogstrand, C., 2011. Copper and Zinc detoxification in Gammarux pulex (L.). The Journal of Experimental Biology 215, 822-832.

Kratochvil, D., 1997. Biosorption of heavy metals by Sargassum seaweed biomass, ph.D,thesis, Chemical Engineering, McGill University, Montreal, Canada.

Lagergren, S., 1898. About the theory of so-called adsorption of soluble substances. Kungliga SvenskaVetenskapsakademiens. Handlingar 24(4), 1-39.

Langmuir, I., 1916. The Constitution and fundamental properties of solids and liquids: Part 1. Journal of American chemical society, 2221-2295.

Lin, T., Lien, H., 2013. Effective and Selective Recovery of Precious Metals by Thiourea Modified Magnetic Nanoparticles. International journal of molecular sciences14, 9834-9847.

Louw, T., 2008. The Separation of Platinum and Gold from an Industrial Feed Solution. PhD Thesis. Nelson Mandela Metropolitan University, South Africa.

Lu, Y., Wilkins E., 1996. Heavy metal removal by caustic-treated yeast immobilized in alginate. Journal of hazardous materials 49, 165-179.

Luef, E., Prey, T., Kubicek, C.P., 1991. Biosorption of Zinc by fungal mycelial wastes. Applied Microbiology Biotechnology 34, 688-692.

Machado, M.D., Soares, E.V., Soares, H.M.V.M., 2010. Removal of heavy metals using a brewer's yeast strain of Saccharomyces cerevisiae: application to the treatment of real electroplating effluents containing multielements. J Chem Tech Biotechnol.85, 1353-1360.

Mack, C., Wilhelmi, B., Duncan, J.R., Burgess, J.E., 2008. A kinetic study of the recovery of platinum ions from an artificial aqueous solution by immobilized saccharomyces cerevisiae biomass. Mineral Engineering 21, 31-37.

Mack, C., Wilhelmi, B., Duncan, J.R., Burgess, J.E., 2007. Biosorption of Precious metals. Biotechnology Advances 25(3), 264-271.

Mack, C.L., 2005. Screening of technologies for the recovery of rhodium (III) metal ions from a precious metal refinery wastewater. Master Thesis. Rhodes University, South Africa.

Mack, C.L., 2008. Biosorption of Precious metals from Synthetic and refinery wastewaters by immobilized Saccharomyces Cerevisiae. Ph.D Thesis. Rhodes University, South Africa.

Madrid, Y., Camara, C., 1997. Biological Substrates for metal preconcentration and speciation. Trends in Analytical Chemistry 16(1), 36-44.

Mao, J., Lees, Won, S.W., Yun, Y., 2010. Surface modified bacteria biosorbent with poly (allylaminehydrochloride): Development using response surface methodology and use for recovery of hexachloroplatinate (IV) from aqueous solution. Water research. 44, 5919-5928.

Mohamed, N. S., Krim, L., 2010. Kinetic Analysis of Trivalent Chromium biosorption by Dead Strep-tomyces Rimosus Biomass, The Arabian Journal for Science and Engineering 35, 69-80

Montgomery, D.C., 2005. Design and Analysis of Experiments. John Wiley and Sons, New Jersey

Musapatika, E.T., Onyango, M.S., Aoyi, O., 2010. Cobalt (II) removal from synthetic wastewater by adsorption on South African coal fly ash. South African journal of science 106, 1-7.

Naddafi, K., Nabizadeh, R., Saeedi, R., Mahvi, A.H., Vaezi, F., Yaghmaeian, K., Ghasri, A., Nazmara, S., 2007. Biosorption of Lead (II) and cadmium (II) by protonated Sargassum glaucescens biomass in a continuous packed bed column. Journal of hazardous material 147, 785-791.

Netpradit, S., Thiravetyan, P., Towprayoon, S., 2004. Evaluation of metal hydroxide sludge for reactive dye adsorption in a fixed-bed column system. Water Research 38, 71-78.

Nilanjana, D., 2010. Recovery of precious metals through Biosorption. Hydrometallurgy 103, 180-189.

Nilanjana, D., Vimala, R., Karthikam, P., 2008. Biosorption of heavy metals- An overview. Indian Journal of Biotechnology 7, 159-169.

Niu, H., Volesky, B., 2003. Characteristics of anionic metal species biosorption with waste crab shells. Hydrometallurgy 71, 209-215.

Oliveira, R. C., Jouannin, C., Guibal, E., Garcia Jr, O., 2011. Samarium (III) and praseodymium(III) biosorption on Sargassum sp: Batch study. Process Biochemistry 46(3), 736-744.

Oliveira, R. C., Palmieri, M .C., Oswaldo, G., 2011. Biosorption of Metals: State of the Art, General Features, and Potential Applications for Environmental and Technological Processes. Progress in Biomass and Bioenergy Production, Dr. Shahid Shaukat (Ed.), InTech, 8-176.

Onwu, F.K., Ogah, S.P.I., 2010. Studies on the effect of pH on the sorption of cadmium (II), nickel (II), lead (II) and chromium (VI) from aqueous solutions by African white star apple (Chrysophyllum albidium) shell. African journal of biotechnology 9, 7086-7093.

Pagnanelli, F., Petrangeli Papini, M., Toro, L., Trifoni, M., Veglio, P., 2000. Biosorption of metal ions on Arthrobacter sp: Biomass characterization and biosorption modelling. Environmental Science and Technology 34, 2773-2778.

Pagnanelli, F., Esposito, A., Veglio, F., 2002. Multi-metallic modelling for biosorption of binary systems. Water Research 36, 4095-4105.

Park, D., Yun, Y., Kim, J.Y., Park, J.M., 2008. How to study Cr (VI) biosorption: Use of fermentation waste to detoxifying Cr (VI) in aqueous solution. Chemical Engineering Journal 136, 173-179.

Parvathi, K., Nagendran, R., Nareshkumar, R., 2007. Lead biosorption onto waste beer yeast by-product, a means to decontaminate effluent generated from battery manufacturing industry. Environmental Biotechnology 10, 1-11.

Patel, H., Vashi, R.T., 2012. Fixed bed column adsorption of Acid Yellow 17 dye onto Tamarind seed powder. The Canadian Journal of Chemical Engineering 90(1), 180-185.

Pethkar, A.V., Paknikar, K.M., 1998. Recovery of gold from solutions using Cladosporium cladosporioides biomass beads. Journal of Biotechnology 63, 121-136.

Pratibha, P., Arup, R. B., Pranav, K.G., 2010. Polyvinyl alcohol fuller's earth clay nanocomposite films. In Journal of Applied Polymer Science 115 (5), 3005-3012.

Pujol R., Canler, J.P., 1992. Biosorption and dynamics of bacteria populations in activated sludge. Water Resources 26, 209-212.

Ramachandra, T.V., Ahalya, Kanamadi, R.D., 2005. Biosorption: Techniques and Mechanisms. CES Technical Report 110, 1-91

Rao, C. R. M., Reddi, G. S., 2000. "Platinum group metals (PGM); occurrence, use and recent trends in their determination," Trends in Analytical Chemistry19 (9), 565–586.

Redlich, O., Peterson, D.L., 1959. A useful adsorption isotherm. Journal of physical chemistry 63(6), 1024-1024.

Roberts, G., 1992b. Chitin Chemistry, Macmillan, London, 495.

Robinson, D., 2002. Anglo Platinum, Pers.com.

Ruiz, M., Sastre, A.N., Guibal, E., 2000. Palladium biosorption on glutaraldehyde-crosslinked chitosan. Reactive and functional polymers 45, 155-173.

Saadi, Z., Saadi, R., Fazaeli, R., 2013. Fixed – bed adsorption dynamics of Pb (II) adsorption from aqueous solution using nanostructured alumina. Journal of Nanostructure in Chemistry 3(48), 1-8.

Schiewer, S., 1999. Modelling complexation and electrostatic attraction in heavy metal biosorption by Sargassum biomass. Journal of Applied Phycology 11,79-87

Schneider, I.A.H., Rubio, J., Smith, R.W., 2001. Biosorption of metals onto plant biomass: exchange adsorption or surface precipitation? International Journal of Mineral Processing 62, 111-120.

Schutte, C.F., Pretorious, W.A., 1997. Water demand and population growth. Water SA, 23(2).

Sengil, I.A., Ozacar, M., 2009. Competitive biosorption pf Pb^{2+}, Cu^{2+} and Zn^{2+} ions from aqueous solution onto Valonia tanin resin. Journal of hazardous material.

Simate, G.S., Iyuke, S.E., Ndlovu, S., Heydenrych, M., 2012. The heterogeneous and flocculation of brewery wastewater using carbon nanotubes. Water Research 46, 1185-1197.

Singh, V.P., Stapleton R.D. Jr., 2002. Biotransformations: Bioremediation Technology for Health and Environmental Protection, Elsevier, Amsterdam.

Shemi, A., 2012. Extraction of Aluminium from coal fly ash using a double acid leach process. Master Thesis. University of Witwaterstrand. South Africa.

Shen, J., Duvnjak, Z., 2005. Adsorption kinetics of cupric and cadium ions on corncob particles. Process Biochemistry 40, 3446-3454.

Sheng, P.X., Ting, Y.P., Chen, J.P., Hong, L., 2004. Sorption of lead, cadmium, zinc and nickel by marine algal biomass: characterization of biosorptive capacity and investigation of mechanisms. Journal of Colloid and Interface Science 275, 131-141.

Soares, E.V., Soares, H.M.V.M., 2012. Bioremediation of industrial effluents containing heavy metals using brewing cells of saccharomyces cerevisiae as a green technology; A review. Environmental science pollution resources 19, 1066-1083.

Srivastaval, V.C., Swamy, M.M., Mall, I.D., Prasad, B., Mishra, I.M., 2006. Adsorptive removal of phenol by bagasse, fly ash and activated carbon: Equilibrium, kinetics and thermodynamics, colloids and surfaces: Physico-chemical and Engineering Aspects 272, 89-104.

Stanberg, G.W., Shumate, S.E., Parrott, J.R., 1981. Microbial cells as biosorbents for heavy metals: accumulation of Uranium by Saccharomyces cerevisiae and Pseudomonas aeruginosa. Applied Environmental Microbiology 41, 237-245.

Stumm, W., Morgan, J.J., 1996b. Aquatic Chemistry. Wiley, New York. 49-51.

Sulka, G.D., Jaskula, M., 2003. Study of the kinetics of silver ions cementation onto copper from sulphuric acid solution. Hydrometallurgy 70(1-3), 185-196.

Tangaromsuk, J., Pokethitiyook, P., Kruatrachue, M., Upatham, E.S., 2002. Cadmium biosorption by Sphingomonas paucimobilis biomass. Bioresource Technology 85, 103-105.

Taty-Costodes, V.C., Faudet, H., Porte, C., Ho, Y.S., 2005 .Removal of lead (II) ions from synthetic and real effluents using immobilized pinus sylvestris sawdust: adsorption on a fixed-bed column. Journal of Hazardous Material 123, 135-144.

Thomas, H.C., 1944. Heterogeneous ion exchange in a flowing system. Journal of American Chemical Society 66, 1466–1664

Torapava, N., 2011. Hydration, Solvation and Hydrolysis of Multicharged metal ions. Phd Thesis. Swedish University of Agricultural Sciences. Uppsalia.

Tsezos, M., 1990. Engineering aspects of metal binding by biomass. Microbial mineral recovery, H.L. Ehrlich and C.L. Brierley (Editors), McGraw-Hill, New York, 325-340.

Urrutia, M.M., 1997. General bacteria sorption processes. In: Biosorbents for metal ions. Wase, J. and Forster, C. (Eds) Taylor and Francis, London, UK. 39-66

United State Environmental Protection Agency, 2010. Permit Guidance.

University of Washington (n.d). Adsorption Equilibria. Accessed on 4th April 2013, from www. Faculty.washington.edu.

Vargas, I., Macaskie, L.E., Guibal, E., 2004. Biosorption of Palladium and Platinum by sulfate-reducing bacteria. Chem Techol Biotechnol 79, 49-56.

Vijayaraghavan, K., Yun, Y.S., 2007. Chemical modification and immobilization of Corynebacte-rium glutamicum for biosorption of Reactive Black 5 from aqueous solution. Industrial Engineering Chemical Research 46, 608-617.

Volesky, B., 1987. Biosorbents for metal recovery. Trends in Biotechnology 5, 96-101

Volesky, B., 1990. Biosorption and biosorbents. In: Biosorption of heavy metals. Volesky, B. (Ed.), CRC press. Boca Rotan, Florida.

Volesky, B., 2001. Detoxification of metal-bearing effluents: biosorption for the next century. Hydrometallurgy 59, 203-216.

Volesky, B., 2003. Biosorption process simulation tools. Hydrometallurgy 71, 179-190.

Wang, J., Chen, C., 2006. Biosorption of heavy metals by Saccharomyces cerevisiae: A review. Biotechnology Advances.24, 427-421.

Wilhelmi, B.S., Duncan, J.R., 1996. Reusability of immobilized Saccharomyces cerevisiae with successive copper adsorption-desorption cycles. Biotechnology Letters 18(5), 531-536.

Wright, K.A., Xu, Y., 2000. A water balance approach to the sustainable management of groundwater in South Africa. Water SA 26(2), 167-170.

Xiong, Y., Adhikari, C.R., Kawakita, H., Ohto, k., Inove, K., Harada, H., 2009. Selective recovery of precious metals by persimmon waste chemically modified with dimethylamine. Bioresource Technology 100, 4083–4089

Yahaya, N., Abustana, I., Latiffa, M.F.P.M., Bello, O.S., Ahmad, M.A., 2011. Fixed bed column study for Cu (II) removal from aqueous solution using rice husk based activated carbon. International Journal of Engineering and Technology 11, 248-252.

Yan, G., Allen. D. G., 1994. Biosorption of high molecular weight organochlorines in pulp mill effluent. Water research. 28, 1933-1941.

Yoon, Y.H., Nelson, J.H., 1984. Application of gas adsorption kinetics. Part 1. A theoretical model for respirator cartridge service time. Journal of American Industrial Hygiene Association 45,509–516

Zhang, Y., Liu, W., Xu, M., Zheng, F., Zhao, M., 2010. Study of the mechanisms of Cu^{2+} biosorption by ethanol/caustic – pretreated baker's yeast biomass, Journal of Hazardous Material178, 1085-1093.

Zhelev, T.K., Bhaw, N., 2000. Combined water-oxygen pinch analysis for better wastewater treatment management. Waste management 20, 665-670.

Zhou, L., Liu, J., Liu, Z., 2009. Adsorption of platinum (IV) and palladium (II) from aqueous solution by thiourea-modified chitosan microspheres. Journal of hazardous materials 172, 439-446.

Zhou, J.L., Kiff, R.J., 1991. The uptake of copper from aqueous solution by immobilized fungal biomass. Journal of Chemical Technology and Biotechnology 52, 317-330.

APPENDIX A

Data for determining point of Zero charge

Table A1: Data for the determination of point of zero charge for untreated yeast

Mass of adsorbent	pH 3	pH 6	pH 11
0	3.00	6.00	11.00
0.05	3.57	6.58	7.07
0.10	3.94	6.54	6.99
0.50	4.30	6.34	6.78
1.00	5.39	6.24	6.58
5.00	5.97	5.98	5.99
10.00	5.79	5.80	5.82

Table A2: Data for the determination of point of zero charge for ethanol treated yeast

Mass of adsorbent	pH 3	pH 6	pH 11
0	3.00	6.00	11.00
0.05	3.23	6.77	7.91
0.10	3.61	6.68	7.50
0.50	5.95	6.66	6.93
1.00	6.21	6.36	6.79
5.00	6.42	6.12	6.48
10.00	6.34	6.11	6.43

% Adsorption

The amount of metal adsorbed from the dilute stream to the biomass surface (%) was calculated using equation 3.2 as specified in section 3.1

Example

The amount of platinum adsorbed unto the untreated yeast biomass surface from the dilute stream at 10 min is given as:

$$\theta = \frac{\left(C_i - C_f\right)100}{\left(C_i\right)} \qquad \text{(A1)}$$

C_i = 10mg/l

After 10 min, C_f = 4.79mg/l

$$\theta = \frac{\left(10 - 4.79\right)100}{10} = 52.1\%$$

Table A3: Data for the effect of biomass pretreatment on the adsorption of Pt (II)

Time (min)	Untreated yeast Adsorption (%)	Ethanol treated yeast. Adsorption (%)	NaOH treated yeast. Adsorption (%)
0	0	0	0
10	52.1	56.0	27.8
20	58.4	64.0	26.1
30	58.7	70.8	26.3
60	67.4	78.6	27.0
120	74.8	86.0	28.3
180	77.3	88.4	28.5

Table A4: Data for the effect of biomass pretreatment on the adsorption of Pd (II)

Time (min)	Untreated yeast Adsorption (%)	Ethanol treated yeast. Adsorption (%)	NaOH treated yeast. Adsorption (%)
0	0	0	0
10	75.6	75.2	59.4
20	75.8	77.5	63.0
30	75.9	77.9	67.7
60	76.2	78.7	67.8
120	76.7	78.7	69.6
180	77.2	81.3	70.3

Table A5: Data for the effect of biomass pretreatment on the adsorption of Au (III)

Time (min)	Untreated yeast Adsorption (%)	Ethanol treated yeast. Adsorption (%)	NaOH treated yeast. Adsorption (%)
0	0	0	0
10	48.7	78.5	18.6
20	49.3	82.0	23.9
30	60.0	84.6	29.3
60	61.3	84.6	30.2
120	62.0	85.5	34.3
180	66.3	86.0	36.2

Table A6: Data for the effect of biomass pretreatment on the adsorption of Ir (III)

Time (min)	Untreated yeast Adsorption (%)	Ethanol treated yeast. Adsorption (%)	NaOH treated yeast. Adsorption (%)
0	0	0	0
10	3.0	6.7	0.4
20	5.0	7.7	4.0
30	6.0	9.9	4.8
60	7.0	11.0	4.9
120	7.0	14.9	5.5
180	9.0	15.7	8.0

Table A7: Data for the effect of biomass pretreatment on the adsorption of Rh (III)

Time (min)	Untreated yeast Adsorption (%)	Ethanoltreated yeast. Adsorption (%)	NaOHtreated yeast. Adsorption (%)
0	0	0	0
10	9.1	28.7	5.0
20	26.4	29.7	9.4
30	26.9	30.1	9.7
60	29.2	30.9	13.2
120	29.8	34.6	18.9
180	35.0	41.9	26.7

APPENDIX B

Adsorption Kinetics data

Table B1: Data for Lagergren Pseudo-first-order kinetics model for Pt (II), Pd (II), Au (III), Rh (III) and Ir (III).

Time (min)	$\log(q_e - q_t)$				
	Pt (II)	Pd (II)	Au (III)	Rh (III)	Ir (III)
0	0.2475	0.1970	0.2355	0.0767	-0.5031
10	-0.1884	-1.1540	-0.8340	-0.5783	-0.7447
20	-0.3116	-1.6198	-1.0969	-0.6126	-0.7959
30	-0.4535	-1.7959	-1.5528	-0.6271	-0.9355
60	-0.7077		-1.5528	-0.6576	-1.0269
120	-1.4949		-2.0000	-0.8356	-1.7959
180					

Table B2: Data for Pseudo-second-order kinetics model for Pt (II), Pd (II), Au (III), Rh (III) and Ir (III).

Time (min)	$\frac{t}{q_t}$				
	Pt (II)	Pd (II)	Au (III)	Rh(III)	Ir (III)
0	0	0	0	0	0
10	8.93	6.65	6.37	17.42	74.63
20	15.62	12.90	12.19	33.67	129.87
30	21.18	19.26	17.73	49.84	151.52
60	38.16	38.12	17.73	97.08	272.73
120	69.12	38.12	70.18	173.41	400.00
180	101.81	110.70	104.65	214.80	573.25

Table B3: Data for Intraparticle diffusion model for Pt (II), Pd (II), Au (III), Rh (III) and Ir (III).

$t^{1/2}(\text{min})^{1/2}$	q_t (mg/g)				
	Pt (II)	Pd (II)	Au (III)	Rh (III)	Ir (III)
0	0	0	0	0	0
3.16	1.12	1.50	1.57	0.57	0.13
4.47	1.28	1.55	1.64	0.59	0.15
5.48	1.41	1.56	1.69	0.60	0.19
7.75	1.57	1.57	1.69	0.62	0.22
10.96	1.73	1.57	1.71	0.69	0.30
13.42	1.76	1.63	1.72	0.84	0.31

Table B4: Data for Elovich model for Pt (II), Pd (II), Au (III), Rh (III) and Ir (III).

ln t	q_t (mg/g)				
	Pt (II)	Pd (II)	Au (III)	Ir (III)	Rh (III)
2.30	1.120	1.504	1.570	0.134	0.574
2.99	1.280	1.550	1.640	0.154	0.594
3.40	1.420	1.558	1.692	0.198	0.602
4.09	1.570	1.574	1.692	0.220	0.618
4.79	1.740	1.574	1.710	0.300	0.692
5.19	1.770	1.626	1.720	0.314	0.838

APPENDIX C

Design of Experiments

Main Effects

An effect is the difference in response averages that are applicable to the levels of the factor. The effect of a factor on the response can be obtained by taking the difference between the average response when the factor is high and the average response when the factor is low.

Effect of factor **A** = Average response at $\mathbf{A}_{high}$ – Average response at $\mathbf{A}_{low}$ (C1)

Example

From Table 4.5, section 4.3, using Platinum as an example,

Average response at $\mathbf{A}_{high}$, is given by averaging the results obtained running experiments 2, 4, 6,8,10, 12, 14 and 16, and average response at A_{low} by averaging the results obtained from running experiments 1, 3, 5, 7,9, 11, 13 and 15

Average adsorption of platinum at A_{high}=

(32.3+21+87.6+67.9+50.3+33+89.1+66.6)/8 = 55.9

Average adsorption of platinum at $\mathbf{A}_{low}$ =

(49.28+27+86.6+66.5+32.3+9+89.5+66.5)/8 = 53.3

Difference = 55.9 – 53.3 = 2.6

: Effect of factor A on platinum adsorption = 2.6

Effect of factor A is also referred to as a main factor

Interaction Effect

An interaction of factors is a relationship where the effect that a factor has on the product or process is altered due to the presence of one or more factor. An interaction is a product of two or more factors. A cross product of factor **A** and factor **B** yields a

two factor interaction **AB**. An interactive effect of interaction **AB** on the response can be obtained by taking the difference between the average response when **AB** is high and average response when **AB** is low.

Effect of interaction AB = Average response at AB_{high} - AB_{low} (C2)

From Table 4.4, using platinum as example,

Average response at $\mathbf{AB}_{high}$, is given by averaging the results obtained running experiments 1, 4, 5,8,9, 12, 13 and 16, and average response at A_{low} by averaging the results obtained from running experiments 2, 3, 6, 7,10, 11, 14 and 15.

Average adsorption of platinum at AB_{high} =
(49.28+21+86.6+67.9+32.3+33+89.5+66.6)/8= 55.7

Average adsorption of platinum at $\mathbf{AB}_{low}$ =
(32.3+27+87.6+66.5+50.3+9+89.1+66.5)/8= 53.5

Difference = 55.7- 53.5= 2.2

: Effect of interaction AB on platinum adsorption = 0.825.

Applying the same approach as above to the rest of the factorial design in Table 4.5, the main and interactive effects are calculated and arranged in ascending order of magnitude as shown in the Tables below for all the five PGMs tested.

Table C1: Main and interactive effects for Pt (II)

Order Number i	1	2	3	4	5	6	7	8	9	10	11	12	13	14	15
Effect	-19.9	-8.4	-2.1	-2	-1.6	-1.4	-0.6	-0.2	0.1	0.6	1.0	2.2	2.6	7.8	45.7
Identity of effect	B	ACD	AC	ABC	BD	BC	ABD	D	BCD	ABCD	CD	AB	A	AD	C

Table C2: Main and interactive effects for Au (III)

Order Number i	1	2	3	4	5	6	7	8	9	10	11	12	13	14	15
Effect	-22.6	-7.2	-6.6	-5.6	-1.2	-0.8	-0.4	0.3	0.8	1	6	6.6	7.5	31.8	56.2
Identity of effect	BC	ABC	CD	AC	ABD	ACD	D	BCD	AD	ABCD	AB	BD	A	B	C

Table C3: Main and interactive effects for Pd (II)

Order Number i	1	2	3	4	5	6	7	8	9	10	11	12	13	14	15
Effect	-19.1	-8.1	-5.4	-4.1	-1.8	-0.8	1.43	1.45	2.1	3.6	4.8	5.5	5.6	28.8	43.1
Identity of effect	BC	CD	ACD	AC	ABCD	BD	ABD	BCD	ABC	A	AD	D	AB	B	C

Table C4: Main and interactive effects for Ir (III)

Order Number i	1	2	3	4	5	6	7	8	9	10	11	12	13	14	15
Effect	-6.1	-3.2	-2.3	-1.1	-1	-0.9	-0.5	0.36	0.86	1.16	1.36	1.56	3.9	20	47.5
Identity of effect	BCD	BC	ACD	ABD	A	CD	AC	ABC	ABCD	AD	AB	D	BD	B	C

Table C5: Main and interactive effects for Rh (III)

Order Number i	1	2	3	4	5	6	7	8	9	10	11	12	13	14	15
Effect	-6.0	-4.9	-3.4	-2.4	-0.7	2.35	2.37	3.52	3.75	4.3	4.4	8.77	10.5	20.0	36.9
Identity of effect	ABD	BCD	AD	ACD	BC	ACD	D	ABC	AC	ABCD	BD	AB	A	B	C

Normal Probability Plots

Normal probability plots are a plot of probability

$$p = \left(i - \frac{1}{2} \right) \times \frac{100}{m} = \left(i - \frac{1}{2} \right) \times \frac{100}{15} \qquad \text{(C3)}$$

for i = 1,2,3,4.....m where m = the number of effects under consideration on the y-axis against effects in Table C1- C5 on the X-axis.

Computing $p = \frac{100(i-0.5)}{15}$ for $i =$ 1, 2, 3....15and adding the obtained values to Tables C1-C5 gives the effects for normal probability plots as shown in Tables C6-C10

Table C6: Normal probability plot for Pt (II)

Order Number i	1	2	3	4	*5*	6	7	8	9	10	11	12	13	14	15
Effect	-19.9	-8.4	-2.1	-2	*-1.6*	-1.4	-0.6	-0.2	0.1	0.6	1.0	2.2	2.6	7.8	45.7
Identity of effect	B	ACD	AC	ABC	*BD*	BC	ABD	D	BCD	AB CD	CD	AB	A	AD	C
$p = \frac{100(i-0.}{15}$	3.3	10	16.7	23.3	30	36	43.3	50	56	63	70	76	83	90	96.7

Table C7: Normal probability plot for Au (III)

Order Number i	1	2	3	4	5	6	7	8	9	10	11	12	13	14	15
Effect	-22.6	-7.2	-6.6	-5.6	-1.2	-0.8	-0.4	0.3	0.8	1	6	6.6	7.5	31.8	56.2
Identity of effect	BC	ABC	CD	AC	ABD	ACD	D	BCD	AD	ABCD	AB	BD	A	B	C
$p = \frac{100(i-0.5}{15}$	3.33	10	17.7	23.3	30	36.6	43.3	50	56	63.33	70	76	83	90	96.7

Table C8: Normal probability plot for Pd (II)

Order Number i	1	2	3	4	5	6	7	8	9	10	11	12	13	14	15
Effect	-19.1	-8.1	-5.4	-4.1	-1.8	-0.8	1.43	1.45	2.1	3.6	4.8	5.5	5.6	28.8	43.1
Identity of effect	BC	CD	ACD	AC	ABCD	BD	ABD	BCD	ABC	A	AD	D	AB	B	C
$p=\frac{100(i-0.5)}{15}$	3.33	10	17.7	23.3	30	36.6	43.3	50	56	63.3	70	76	83	90	96.7

Table C9: Normal probability plot for Ir (III)

Order Number i	1	2	3	4	5	6	7	8	9	10	11	12	13	14	15
Effect	-6.1	-3.2	-2.3	-1.1	-1	-0.9	-0.5	0.36	0.86	1.16	1.36	1.56	3.9	20	47.5
Identity of effect	BCD	BC	ACD	ABD	A	CD	AC	ABC	ABCD	AD	AB	D	BD	B	C
$p=\frac{100(i-0.5)}{15}$	3.33	10	17.7	23.3	30	36.6	43.3	50	56	63.3	70	76	83	90	96.7

Table C10: Normal probability plot for Rh (III)

Order Number i	1	2	3	4	5	6	7	8	9	10	11	12	13	14	15
Effect	-6.0	-4.9	-3.4	-2.4	-0.7	2.35	2.37	3.52	3.75	4.3	4.4	8.77	10.5	20.0	36.9
Identity of effect	ABD	BCD	AD	ACD	BC	ACD	D	ABC	AC	ABCD	BD	AB	A	B	C
$p=\frac{100(i-0.5)}{15}$	3.33	10	17.7	23.3	30	36.6	43.3	50	56	63.3	70	76	83	90	96.7

Modeling the significant effects for adsorption prediction

Beginning with effects with magnitudes close to zero (using Au (III) as an example), 12 of the estimates fit well on a straight line. Those corresponding to B, C and BC do not fit on the straight line. It can therefore be concluded that the effects B, C and BC are not easily explained as chance occurrences. This suggests that all effects with the exception of the average adsorption 63.99, B = 31.8, C = 56.2 and BC = -22.6 can be explained by noise.

Therefore, Adsorption, $Y=\overline{Y}+\left(\frac{B}{2}\right)X_B+\left(\frac{C}{2}\right)X_C-\left(\frac{BC}{2}\right)X_{BC}$ (C4)

Where, $\overline{Y}$ represents the average of all the data for the runs (i.e., average of all adsorptions) and X_B, X_C and X_{BC} are the predictor variables (i.e., +1 or -1), B and C are main effects while BC is interaction effects.

Therefore,

Predicted adsorption,

$$Y=63.99+\frac{31.8}{2}X_B+\frac{56.2}{2}X_C-\frac{22.6}{2}X_{BC} \quad \text{(C5)}$$

$$Y=63.99+16.54X_B+28.11X_C-11.33X_{BC} \quad \text{(C6)}$$

The predicted extraction is calculated by substituting an appropriate variable in a particular run.

Example (Using Data for Au (III))

From Table 4.5

In run 1, the predictor variables are $X_B = -1$, $X_C = -1$ and $X_{BC} = +1$

Predicted adsorption = 63.99 – 16.54 – 28.11 – 11.33 = 8%

In run 8, the predictor variables are $X_B = +1$, $X_C = +1$ and $X_{BC} = +1$

Predicted adsorption = 63.99 +16.54 + 28.11 – 11.33 = 97.3%

The positive signs of the variables of the prediction model equation for Au (III) indicate that in order to maximize the adsorption of Au (III), these factors must be kept in high levels.

Residuals

This is the difference between the actual adsorption and the predicted extraction for each runs. From Table 4.5, using Run 8 for Au (III).

Actual adsorption = 97.8, Predicted adsorption = 97.3

Residual = 97.8-97.3= 0.5.

Graphical Residual analysis

Normal plotting of residuals provides a diagnostic check for any tentatively entertained model (Box et al; 1978).The normal probability plots of the residuals tests the theory that the residuals have a normal distribution. This should be a straight line if the residuals have a normal distribution. In addition, a plot of residuals versus the predicted values (fitted model values) is a test of the theory that the variations are the same in each group.

Example

The normal plot of residuals and the plot of residuals versus predicted adsorption for Au (III) are presented in Figures C1 and C2 respectively. Figure C1 is a normal plot of residuals for Au (III). The Figure shows that all residues lie on a straight line with a linear correlation coefficient of 94.72%, which shows that the residuals were normally distributed.

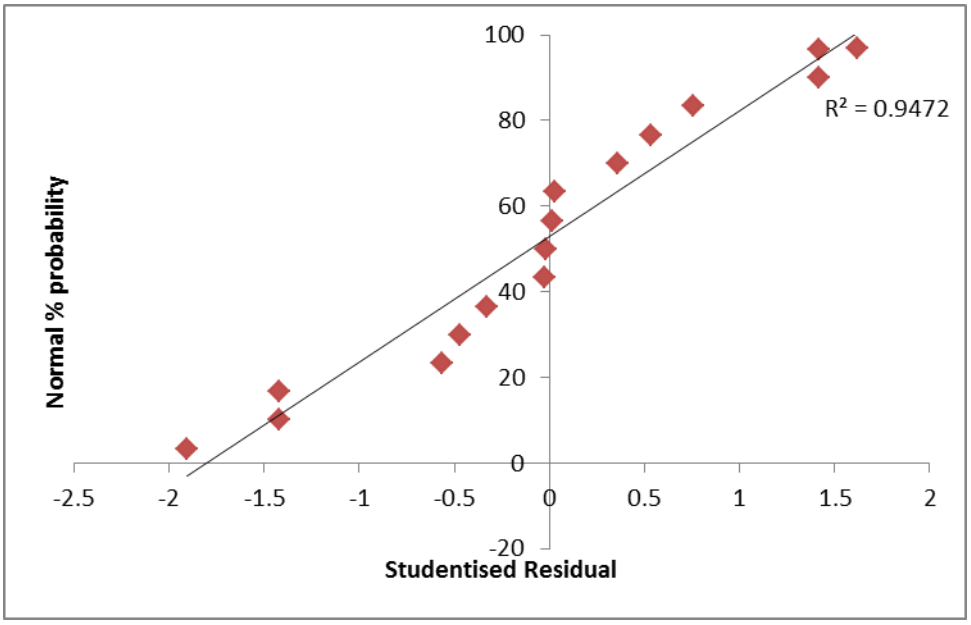


Figure C1: Normal plot of residuals for Au (III)

Figure C2 shows the plot of residuals versus predicted adsorption for Au (III). The Figure indicates that all residuals were distributed between -2 and +1.6. Since the residuals were distributed normally as illustrated in Figure C1 and Figure C2, it can be concluded that the predicated adsorption model equation for Au (III):

$Y = 63.99 + 16.54X_B + 28.11X_C - 11.33X_{BC}$ fitted the experimental data well.

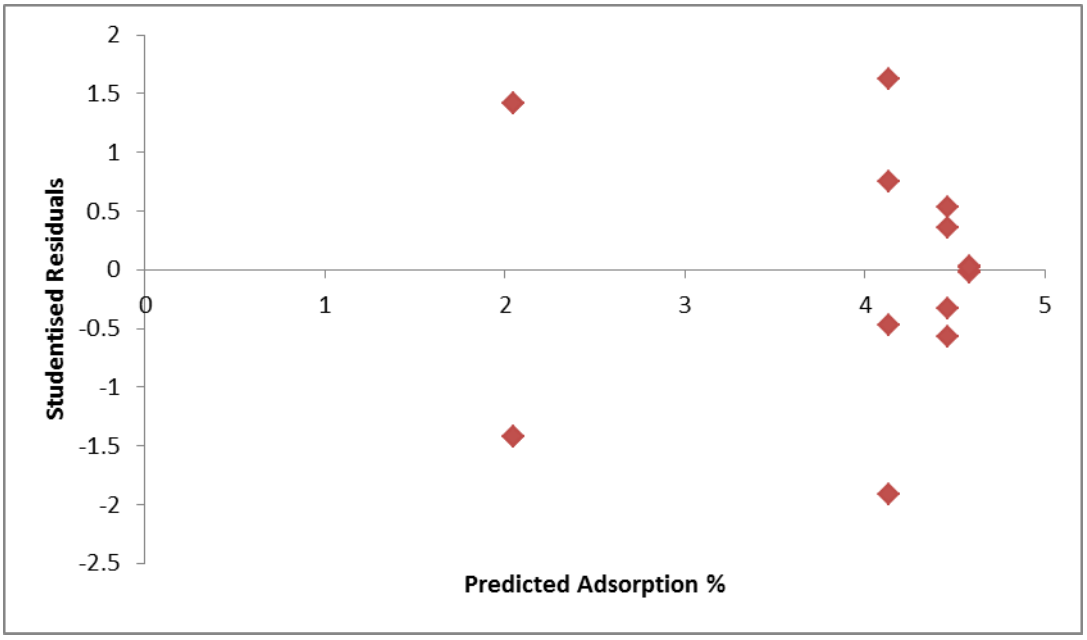
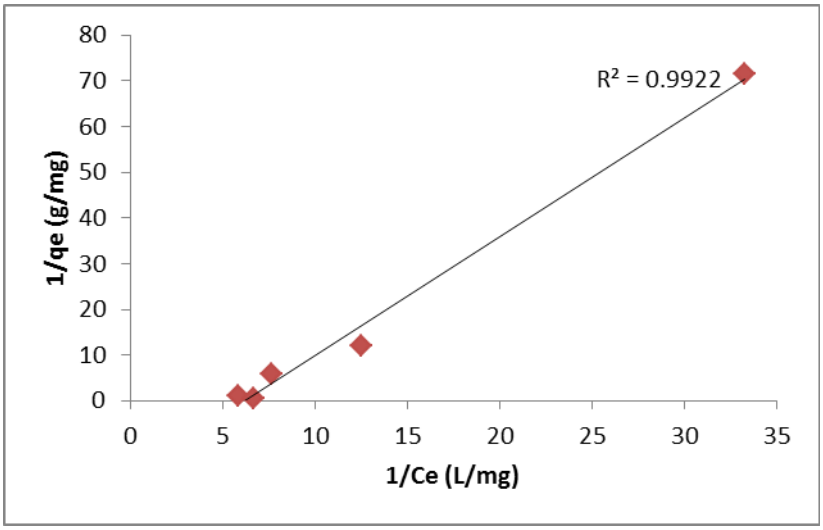


Figure C2: Plot of residuals versus predicted adsorption Au (III)

APPENDIX D

Adsorption Isotherm data

(a)



(b)

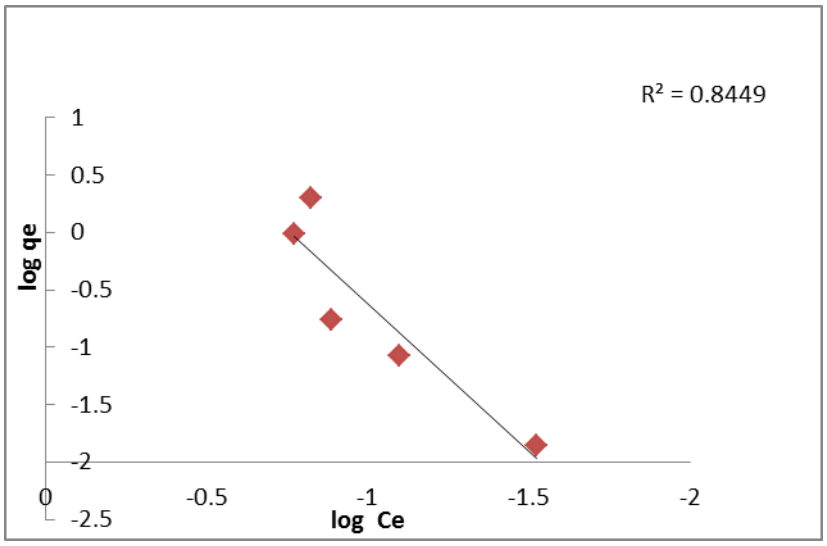
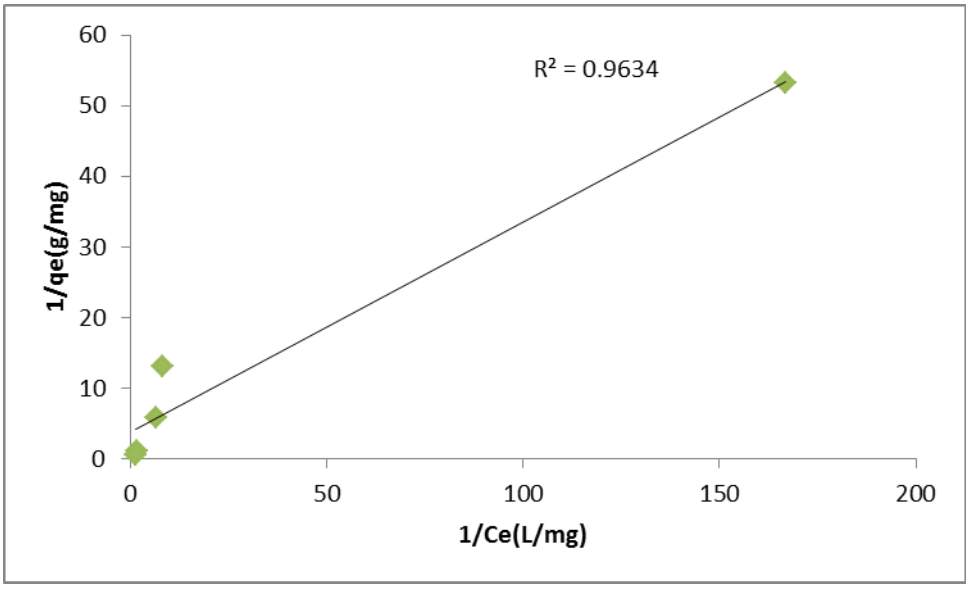


Figure D1: Linear regression analysis For Au (III) (a) Langmuir (b) Freundlich.

(a)



(b)

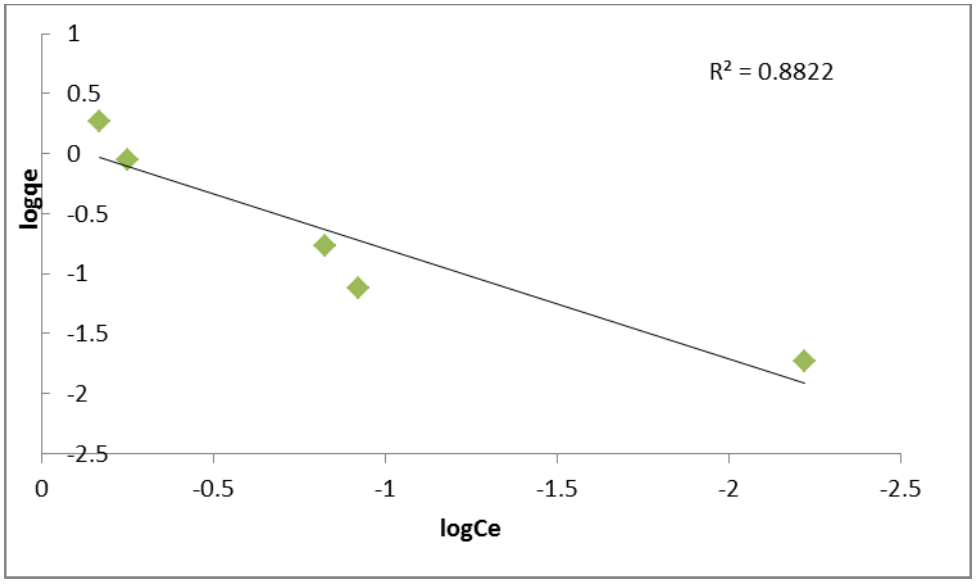
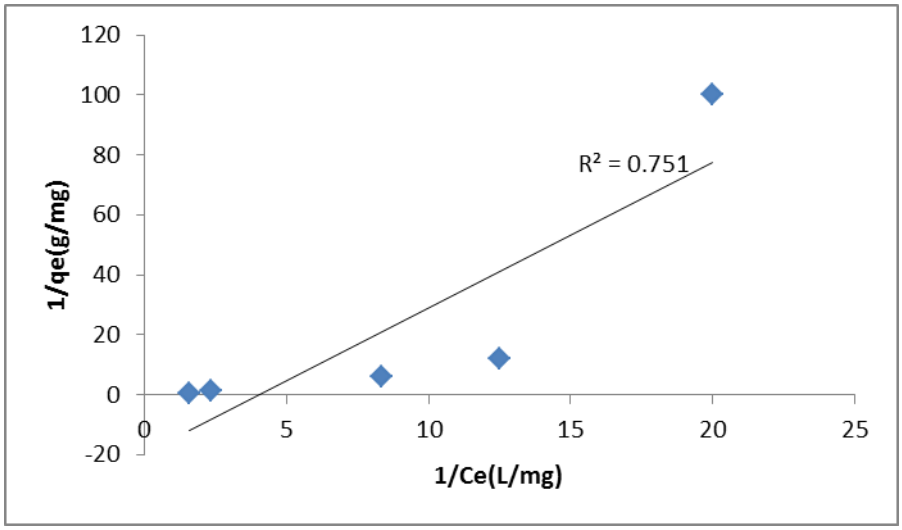


Figure D2: Linear regression analysis For Pt (II) (a) Langmuir (b) Freundlich.

(a)



(b)

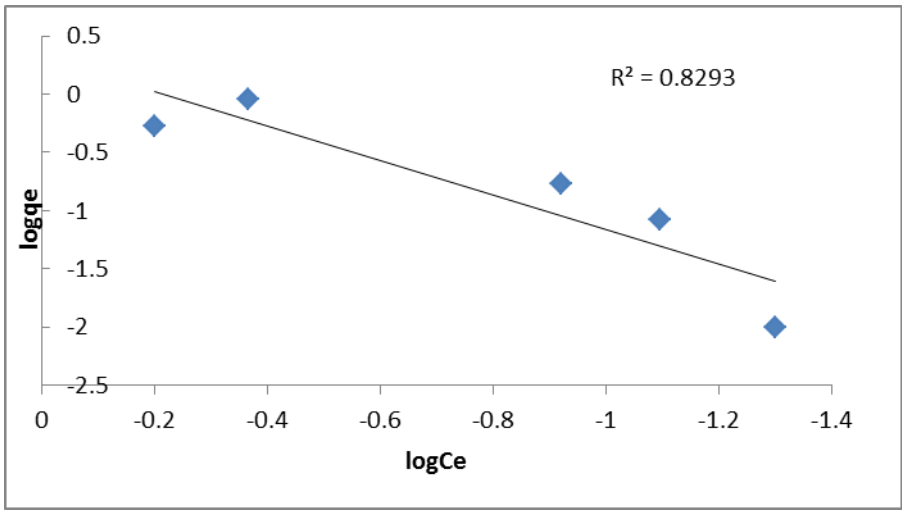
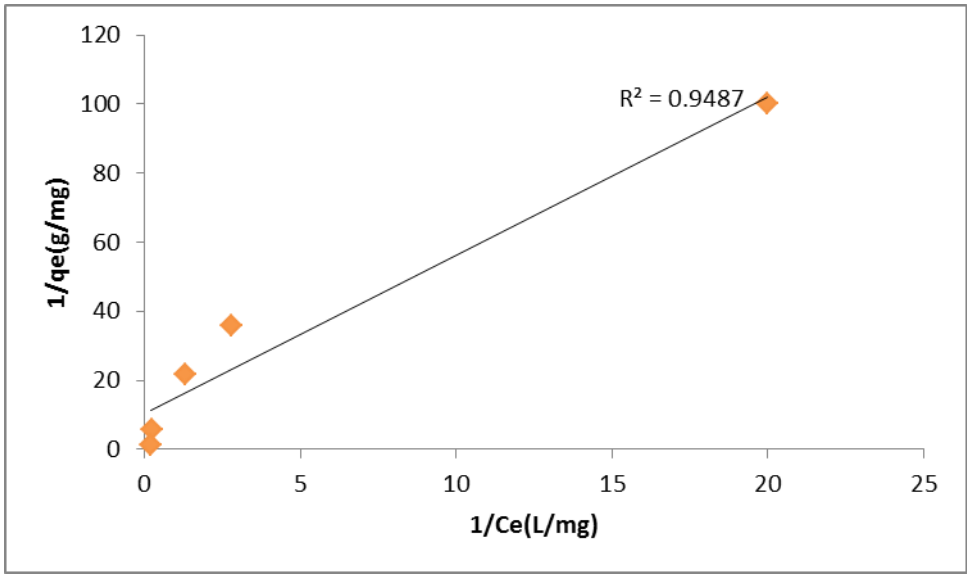


Figure D3: Linear regression analysis For Pd (II) (a) Langmuir (b) Freundlich.

(a)



(b)

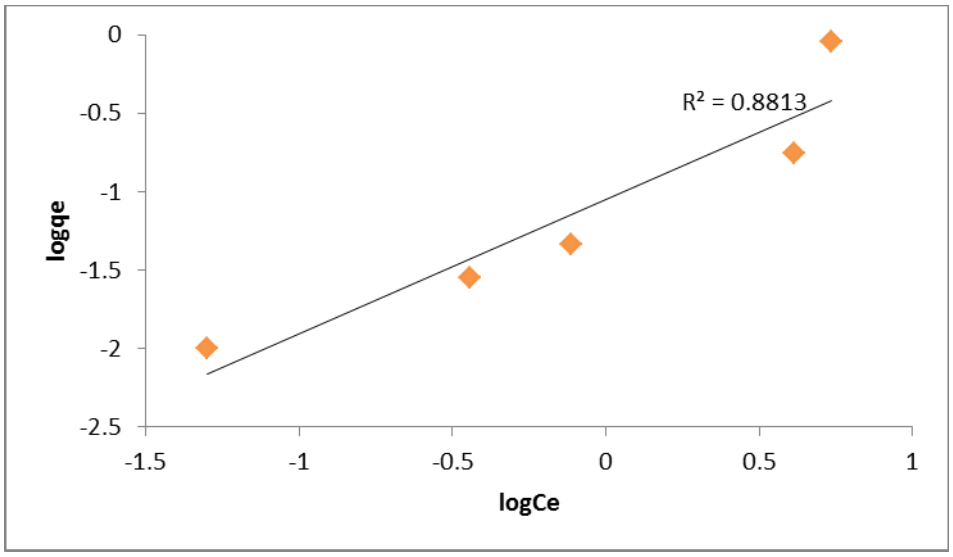
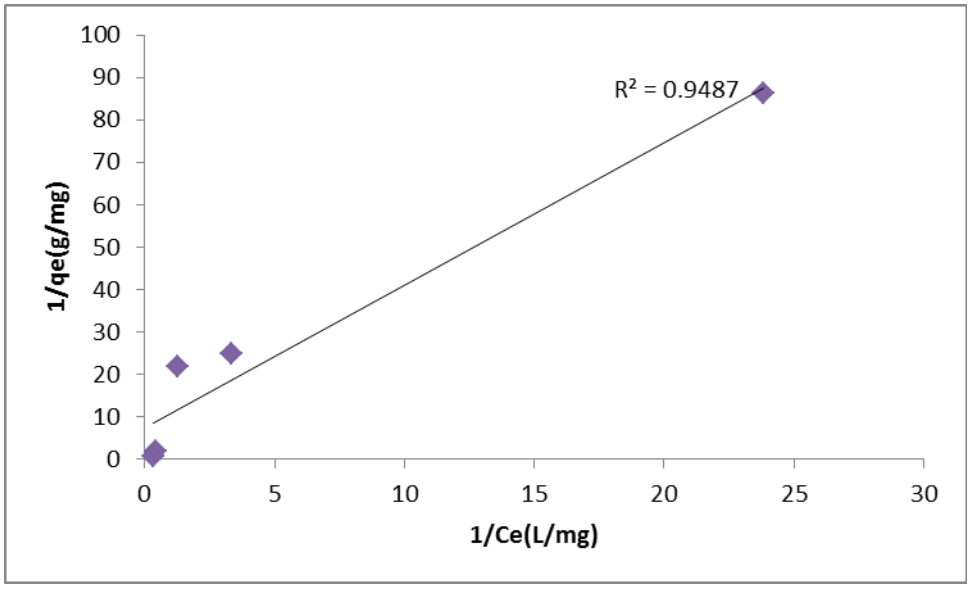


Figure D4: Linear regression analysis For Rh (III) (a) Langmuir (b) Freundlich.

(a)



(b)

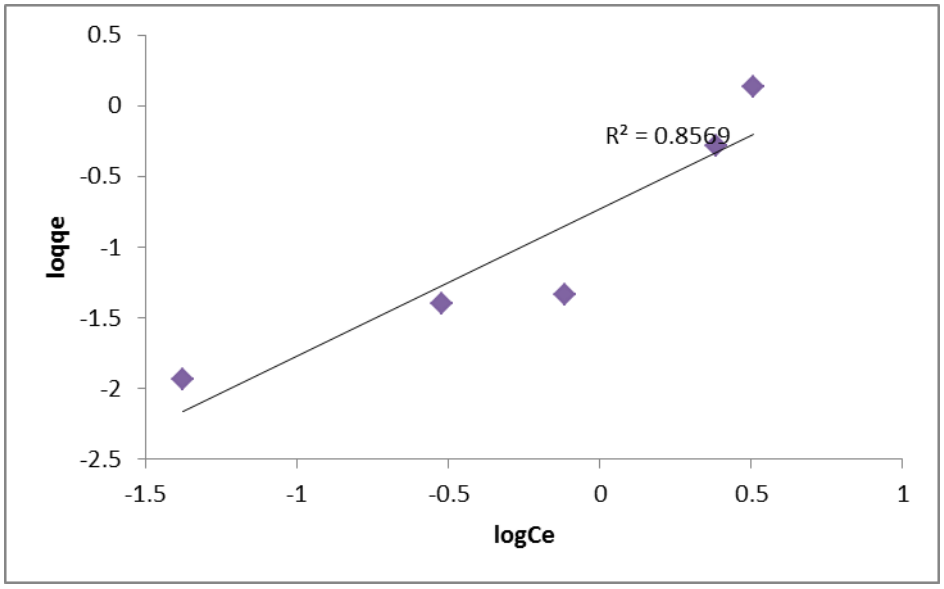


Figure D5: Linear regression analysis For Ir (III) (a) Langmuir (b) Freundlich.

Table D1: Langmuir and Freundlich adsorption isotherm data for Au (III)

C_o (mg/l)	C_e (mg/l)	q_e (mglg)	log q_e	Log C_e	$1/C_e$ (l/mg)	$1/q_e$ (g/mg)
0.1	0.030	0.014	-1.854	-1.523	33.300	71.430
0.5	0.080	0.084	-1.076	-1.097	12.500	11.910
1.0	0.130	0.174	-0.759	-0.886	7.690	5.750
5.0	0.170	0.966	-0.015	-0.770	5.880	1.035
10.0	0.150	1.969	0.295	-0.824	6.670	0.508

Table D2: Langmuir and Freundlich adsorption isotherm data for Pt (II)

C_o (mg/l)	C_e (mg/l)	q_e (mglg)	log q_e	Log C_e	$1/C_e$ (l/mg)	$1/q_e$ (g/mg)
0.1	0.010	0.020	-1.726	-2.220	166.670	53.190
0.5	0.120	0.080	-1.119	-0.921	8.330	13.160
1.0	0.150	0.170	-0.770	-0.824	6.660	5.880
5.0	0.560	0.890	-0.052	-0.252	1.786	1.130
10.0	0.680	1.860	0.270	-0.168	1.471	0.540

Table D3: Langmuir and Freundlich adsorption isotherm data for Pd (II)

C_o (mg/l)	C_e (mg/l)	q_e (mglg)	log q_e	Log C_e	$1/C_e$ (l/mg)	$1/q_e$ (g/mg)
0.1	0.050	0.010	-2.000	-1.300	20.000	100.000
0.5	0.080	0.084	-1.076	-1.097	12.500	11.900
1.0	0.120	0.170	-0.770	-0.921	8.330	5.880
5.0	0.430	0.914	-0.039	-0.367	2.330	1.094
10.0	0.630	1.872	-0.273	-0.201	1.590	0.534

Table D4: Langmuir and Freundlich adsorption isotherm data for Rh (III)

C_o (mg/l)	C_e (mg/l)	q_e (mglg)	log q_e	Log C_e	$1/C_e$ (l/mg)	$1/q_e$ (g/mg)
0.1	0.050	0.010	-2.000	-1.300	20.000	100.000
0.5	0.360	0.028	-1.553	-0.444	2.780	35.7000
1.0	0.770	0.046	-1.337	-0.114	1.299	21.730
5.0	4.120	0.176	-0.755	0.615	0.243	5.680
10.0	5.460	0.908	-0.042	0.737	0.183	1.100

Table D5: Langmuir and Freundlich adsorption isotherm data for Ir (III)

C_o (mg/l)	C_e (mg/l)	q_e (mglg)	log q_e	Log C_e	$1/C_e$ (l/mg)	$1/q_e$ (g/mg)
0.1	0.042	0.012	-1.936	-1.377	23.810	86.210
0.5	0.300	0.040	-1.398	-0.523	3.330	25.000
1.0	0.775	0.046	-1.337	-0.114	1.290	21.740
5.0	2.410	0.512	-0.286	0.382	0.415	1.930
10.0	3.210	1.351	0.133	0.507	0.312	0.740

APPENDIX E

Adsorption Desorption data

Table E1: Adsorption data for Pt (II), Pd (II), Au (III), Rh (III) and Ir (III)

	Adsorption Cycles				
Metal Ions	Cycle 1	Cycle 2	Cycle 3	Cycle 4	Cycle 5
Au(III)	99.9	99.8	99.8	98.4	96.6
Pt (II)	91.0	90.0	89.0	88.0	87.0
Pd (II)	99.5	99.2	98.7	92.8	91.9
Ir (III)	81.9	70.0	61.0	58.0	56.0
Rh (III)	81.1	68.0	62.0	50.0	45.0

Table E2: Desorption data for Pt (II), Pd (II), Au (III), Rh (III) and Ir (III)

	Desorption Cycles				
Metal Ions	Cycle 1	Cycle 2	Cycle 3	Cycle 4	Cycle 5
Au(III)	99.5	95.3	93.2	85.0	80.0
Pt (II)	97.8	96.6	95.5	94.3	93.8
Pd (II)	99.2	97.9	96.8	94.2	93.8
Ir (III)	24.5	19.6	17.3	16.0	15.7
Rh (III)	20.0	13.5	10.4	10.2	6.5

APPENDIX F

Data for column studies

Table F1: Data for platinum breakthrough curve using Plaster of Paris immobilized yeast at 13cm bed depth and different flow rates

	C_e/C_o		
Time (min)	0.9ml/s	1.3ml/s	2.1ml/s
2	0.260	0.302	0.330
5	0.270	0.305	0.340
10	0.280	0.313	0.400
15	0.290	0.340	0.420
20	0.307	0.340	0.430
25	0.309	0.344	0.438
30	0.345	0.351	0.450
60	0.353	0.379	0.460
120	0.359	0.418	0.470
180	0.390	0.430	0.480

Table F2: Data for palladium breakthrough curve using Plaster of Paris immobilized yeast at 13cm bed depth and different flow rates

	C_e/C_o		
Time (min)	0.9ml/s	1.3ml/s	2.1ml/s
2	0.0095	0.0100	0.0120
5	0.0100	0.0120	0.0133
10	0.0125	0.0141	0.0149
15	0.0129	0.0149	0.0157
20	0.0137	0.0157	0.0160
25	0.0153	0.0157	0.0160
30	0.0157	0.0173	0.0173
60	0.0160	0.0177	0.0246
120	0.0169	0.0230	0.0690
180	0.0200	0.0320	0.1250

Table F3: Data for iridium breakthrough curve using Plaster of Paris immobilized yeast at 13cm bed depth and different flow rates

	C_e/C_o		
Time (min)	0.9ml/s	1.3ml/s	2.1ml/s
2	0.300	0.320	0.340
5	0.301	0.350	0.379
10	0.304	0.355	0.398
15	0.308	0.383	0.430
20	0.310	0.384	0.432
25	0.320	0.387	0.440
30	0.361	0.389	0.452
60	0.370	0.394	0.456
120	0.380	0.402	0.458
180	0.400	0.440	0.477

Table F4: Data for ruthenium breakthrough curve using Plaster of Paris immobilized yeast at 13cm bed depth and different flow rates

	C_e/C_o		
Time (min)	0.9ml/s	1.3ml/s	2.1ml/s
2	0.400	0.410	0.460
5	0.403	0.415	0.477
10	0.406	0.434	0.482
15	0.446	0.442	0.488
20	0.452	0.456	0.500
25	0.453	0.469	0.504
30	0.468	0.483	0.511
60	0.472	0.491	0.523
120	0.472	0.496	0.537
180	0.486	0.510	0.560

Table F5: Data for selenium breakthrough curve using Plaster of Paris immobilized yeast at 13cm bed depth and different flow rates

	C_e/C_o		
Time (min)	0.9ml/s	1.3ml/s	2.1ml/s
2	0.478	0.49	0.50
5	0.488	0.54	0.57
10	0.500	0.57	0.60
15	0.582	0.58	0.63
20	0.582	0.58	0.63
25	0.591	0.58	0.66
30	0.591	0.62	0.68
60	0.593	0.64	0.70
120	0.605	0.66	0.80
180	0.608	0.67	0.85

Table F6: Data for sodium breakthrough curve using Plaster of Paris immobilized yeast at 13cm bed depth and different flow rates

	C_e/C_o		
Time (min)	0.9ml/s	1.3ml/s	2.1ml/s
2	0.400	0.42	0.50
5	0.401	0.48	0.60
10	0.500	0.54	0.67
15	0.525	0.58	0.70
20	0.537	0.62	0.75
25	0.539	0.63	0.77
30	0.546	0.64	0.80
60	0.559	0.72	0.83
120	0.570	0.72	0.88
180	0.572	0.72	0.90

Table F7: Data for sulphate breakthrough curve using Plaster of Paris immobilized yeast at 13cm bed depth and different flow rates

	C_e/C_o		
Time (min)	0.9ml/s	1.3ml/s	2.1ml/s
2	0.180	0.190	0.210
5	0.203	0.198	0.214
10	0.204	0.204	0.215
15	0.204	0.207	0.400
20	0.213	0.212	0.480
25	0.215	0.415	0.600
30	0.216	0.430	0.695
60	0.415	0.500	0.719
120	0.680	0.712	0.720
180	0.690	0.712	0.725

Table F8: Data for tellurium breakthrough curve using Plaster of Paris immobilized yeast at 13cm bed depth and different flow rates

	C_e/C_o		
Time (min)	0.9ml/s	1.3ml/s	2.1ml/s
2	0.0014	0.0250	0.0260
5	0.0016	0.0260	0.0270
10	0.0065	0.0280	0.0290
15	0.0081	0.0300	0.1000
20	0.0096	0.0320	0.1200
25	0.0110	0.1000	0.1290
30	0.0200	0.1370	0.1450
60	0.0960	0.1450	0.1850
120	0.1290	0.1690	0.2090
180	0.1370	0.1850	0.2420

Table F9: Data for nickel breakthrough curve using Plaster of Paris immobilized yeast at 13cm bed depth and different flow rates

	C_e/C_o		
Time (min)	0.9ml/s	1.3ml/s	2.1ml/s
2	0.120	0.130	0.135
5	0.130	0.132	0.139
10	0.135	0.135	0.139
15	0.139	0.138	0.180
20	0.139	0.180	0.200
25	0.139	0.180	0.300
30	0.180	0.200	0.320
60	0.190	0.240	0.380
120	0.200	0.300	0.400
180	0.220	0.350	0.450

Table F10: Data for platinum breakthrough curve using Plaster of Paris immobilized yeast at 0.9ml/s flow rate and different bed depths

	C_e/C_o		
Time (min)	6.5cm	8.5cm	13cm
2	0.340	0.340	0.260
5	0.368	0.359	0.270
10	0.378	0.377	0.280
15	0.404	0.385	0.290
20	0.405	0.404	0.307
25	0.446	0.408	0.309
30	0.446	0.408	0.345
60	0.479	0.419	0.353
120	0.506	0.434	0.359
180	0.530	0.445	0.390

Table F11: Data for palladium breakthrough curve using Plaster of Paris immobilized yeast at 0.9ml/s flow rate and different bed depths

	C_e/C_o		
Time (min)	6.5cm	8.5cm	13cm
2	0.0140	0.0125	0.0095
5	0.0150	0.0145	0.0100
10	0.0169	0.0165	0.0125
15	0.0242	0.0169	0.0129
20	0.0278	0.0173	0.0137
25	0.0278	0.0177	0.0153
30	0.0298	0.0177	0.0157
60	0.1530	0.0214	0.0160
120	0.1800	0.1000	0.0169
180	0.2000	0.1300	0.0240

Table F12: Data for iridium breakthrough curve using Plaster of Paris immobilized yeast at 0.9ml/s flow rate and different bed depths

	C_e/C_o		
Time (min)	6.5cm	8.5cm	13cm
2	0.500	0.430	0.300
5	0.512	0.445	0.301
10	0.533	0.455	0.304
15	0.600	0.458	0.308
20	0.620	0.500	0.310
25	0.624	0.530	0.320
30	0.636	0.560	0.361
60	0.700	0.600	0.370
120	0.720	0.640	0.380
180	0.722	0.680	0.400

Table F13: Data for ruthenium breakthrough curve using Plaster of Paris immobilized yeast at 0.9ml/s flow rate and different bed depths

	C_e/C_o		
Time (min)	6.5cm	8.5cm	13cm
2	0.500	0.420	0.400
5	0.600	0.430	0.403
10	0.620	0.480	0.406
15	0.650	0.560	0.446
20	0.670	0.580	0.452
25	0.690	0.590	0.458
30	0.680	0.620	0.468
60	0.700	0.630	0.472
120	0.730	0.650	0.472
180	0.748	0.680	0.486

Table F14: Data for selenium breakthrough curve using Plaster of Paris immobilized yeast at 0.9ml/s flow rate and different bed depths

	C_e/C_o		
Time (min)	6.5cm	8.5cm	13cm
2	0.500	0.490	0.478
5	0.540	0.500	0.488
10	0.579	0.567	0.5
15	0.600	0.591	0.582
20	0.650	0.600	0.582
25	0.700	0.640	0.591
30	0.750	0.670	0.591
60	0.790	0.700	0.593
120	0.840	0.720	0.605
180	0.870	0.730	0.608

Table F15: Data for sodium breakthrough curve using Plaster of Paris immobilized yeast at 0.9ml/s flow rate and different bed depths

	C_e/C_o		
Time (min)	6.5cm	8.5cm	13cm
2	0.550	0.400	0.400
5	0.600	0.500	0.401
10	0.650	0.540	0.500
15	0.680	0.600	0.525
20	0.700	0.640	0.537
25	0.720	0.680	0.539
30	0.800	0.700	0.546
60	0.840	0.740	0.559
120	0.900	0.780	0.570
180	0.920	0.800	0.572

Table F16: Data for sulphate breakthrough curve using Plaster of Paris immobilized yeast at 0.9ml/s flow rate and different bed depths

	C_e/C_o		
Time (min)	6.5cm	8.5cm	13cm
2	0.190	0.190	0.180
5	0.199	0.196	0.203
10	0.208	0.203	0.204
15	0.305	0.203	0.204
20	0.408	0.300	0.213
25	0.606	0.320	0.215
30	0.669	0.350	0.216
60	0.681	0.500	0.415
120	0.692	0.685	0.680
180	0.773	0.730	0.690

Table F17: Data for tellurium breakthrough curve using Plaster of Paris immobilized yeast at 0.9ml/s flow rate and different bed depths

	C_e/C_o		
Time (min)	6.5cm	8.5cm	13cm
2	0.014	0.008	0.0014
5	0.016	0.009	0.0016
10	0.018	0.011	0.0065
15	0.090	0.012	0.0081
20	0.100	0.080	0.0096
25	0.120	0.090	0.0113
30	0.129	0.100	0.0200
60	0.153	0.130	0.0810
120	0.177	0.140	0.0960
180	0.266	0.169	0.1370

Table F18: Data for nickel breakthrough curve using Plaster of Paris immobilized yeast at 0.9ml/s flow rate and different bed depths

	C_e/C_o		
Time (min)	6.5cm	8.5cm	13cm
2	0.150	0.145	0.120
5	0.154	0.149	0.130
10	0.158	0.153	0.135
15	0.200	0.153	0.139
20	0.250	0.220	0.139
25	0.300	0.230	0.139
30	0.380	0.280	0.180
60	0.400	0.300	0.1900
120	0.420	0.320	0.200
180	0.450	0.370	0.220